สารที่มีฤทธิ์ทางชีวภาพจากกระต่ายทะเล *BURSATELLA LEACHII* ของไทย

นางสาว สุชาดา สุนทรชัชเวช

วิทยานิพนธ์นี้เป็นส่วนหนึ่งของการศึกษาตามหลักสูตรปริญญาวิทยาศาสตรดุษฎีบัณฑิต

สาขาวิชาเภสัชเคมีและผลิตภัณฑ์ธรรมชาติ

คณะเภสัชศาสตร์ จุฬาลงกรณ์มหาวิทยาลัย

ปีการศึกษา 2547

ISBN 974-53-2126-5

ลิขสิทธิ์ของจุฬาลงกรณ์มหาวิทยาลัย

BIOACTIVE COMPOUNDS FROM THE THAI SEA HARE, *BURSATELLA LEACHII*

Miss Suchada Suntornchashwej

สถาบันวิทยบริการ
จุฬาลงกรณ์มหาวิทยาลัย

A Dissertation Submitted in Partial Fulfillment of the Requirements
for the Degree of Doctor of Philosophy in Pharmaceutical Chemistry and Natural Products
Faculty of Pharmaceutical Sciences
Chulalongkorn University
Academic year 2004

ISBN 974-53-2126-5

Thesis Title	Bioactive compounds from the Thai sea hare, *Bursatella leachii*
By	Miss Suchada Suntornchashwej
Field of Study	Pharmaceutical Chemistry and Natural Products
Thesis Advisor	Khanit Suwanborirux, Ph.D.

Accepted by the Faculty of Pharmaceutical Sciences, Chulalongkorn University in Parital Fulfillment of the Requirements for the Doctor's Degree

..... Dean of the Faculty of Pharmaceutical Sciences

(Associate Professor Boonyong Tantisira, Ph.D.)

THESIS COMMITTEE

.....Chairman

(Associate Professor Sumphan Wongseripipatana, Ph.D.)

.....Thesis Advisor

(Khanit Suwanborirux, Ph.D.)

.....Member

(Professor Minoru Isobe, Ph.D.)

.....Member

(Associate Professor Rutt Suttisri, Ph.D.)

.....Member

(Assistant Professor Chamnan Patarapanich, Ph.D.)

สุชาดา สุนทรชัชเวช : สารที่มีฤทธิ์ทางชีวภาพจากกระต่ายทะเล *Bursatella leachii* ของไทย (BIOACTIVE COMPOUNDS FROM THE THAI SEA HARE, *BURSATELLA LEACHII*) อ. ที่ปรึกษา : อ. ดร. คณิต สุวรรณบริรักษ์, 184 หน้า. ISBN 974-53-2126-5.

จากการศึกษาทางเคมีของกระต่ายทะเล *Bursatella leachii* ของไทย (family Aplysiidae, phylum Mollusca) โดยการแยกสกัดให้ได้สารบริสุทธิ์ด้วยวิธีทางโครมาโตกราฟี ควบคู่กับการทดสอบฤทธิ์ทางชีวภาพ สามารถแยกสาร malyngamide X ซึ่งเป็น malyngamide ชนิดแรก ที่มี tripeptide เป็นส่วนประกอบในโมเลกุล ได้เป็นปริมาณ 0.71% โดยน้ำหนักสิ่งสกัดหยาบ จากการศึกษาทางเคมีของกระต่ายทะเลที่เก็บใหม่ สามารถแยกสารที่มีรายงานว่ามีฤทธิ์กระตุ้นการเกิด actin assembly อย่างแรง คือ สาร hectochlorin และสารชนิดใหม่เพิ่มอีกสองชนิด ประกอบด้วย สารอนุพันธ์ของ hectochlorin คือ deacetylhectochlorin และสารที่มีโครงสร้างทางเคมีแตกต่างจากสาร hectochlorin คือสาร *syn*-3-isopropyl-6-(4-methoxy-benzyl)-4-methyl-morpholine-2,5-dione ได้เป็นปริมาณ 0.25, 0.08 และ 0.007% โดยน้ำหนักสิ่งสกัดหยาบ ตามลำดับ สาร malyngamide X แสดงฤทธิ์ทางชีวภาพอย่างปานกลาง ได้แก่ ฤทธิ์ความเป็นพิษต่อเซลล์มะเร็งชนิด KB, NCI-H187 และ BC โดยมีค่า ED_{50} 8.20, 4.12 และ 7.03 μM ตามลำดับ ฤทธิ์ต้านมาลาเรีย โดยมีค่า ED_{50} 5.44 μM และ ฤทธิ์ต้านวัณโรค โดยมีค่า MIC 50 μg/ml สาร hectochlorin แสดงฤทธิ์ความเป็นพิษอย่างแรงต่อเซลล์มะเร็งชนิด KB และ NCI-H187 โดยมีค่า ED_{50} 0.86 และ 1.20 μM สาร deacetylhectochlorin แสดงฤทธิ์ความเป็นพิษต่อเซลล์มะเร็งสองชนิดนี้แรงกว่าสาร hectochlorin โดยมีค่า ED_{50} 0.31 และ 0.32 μM ตามลำดับ สำหรับสารอนุพันธ์ชนิดใหม่ morpholine-2,5-dione ไม่ได้ทำการทดสอบฤทธิ์ทางชีวภาพเนื่องจากปริมาณสารมีจำกัด

การกำหนดลักษณะสเตริโอเคมีของสาร malyngamide X ได้เป็น 2(*S*), 5(*S*), 7(*S*), 8(*R*), 14(*S*), และ 7'(*S*) ทำโดยวิธี non-hydrolytic degradation method ซึ่งเป็นการวิเคราะห์ข้อมูลที่ได้จาก วิธี NMR chiral solvation โดยใช้สาร 2,2,2-trifluoro-1-(9-anthryl)ethanol (TFAE หรือ Pirkle's alcohol) วิธี modified Mosher's method การทดลอง NOEs และ conformation calculations ร่วมกับข้อมูลทางชีวสังเคราะห์ของสารกลุ่ม malyngamide นอกจากนี้ได้นำเสนอแบบจำลอง solvation model แสดงความสัมพันธ์ระหว่างลักษณะทางสเตริโอเคมีกับค่า chemical shift ของโปรตอน ของสาร malyngamide X และสารแบบจำลองที่ได้สังเคราะห์ขึ้นบางชนิด ได้แก่สารที่ได้จากปฏิกิริยาการทำให้ tautomycin แตกสลายด้วยด่าง และสารอนุพันธ์ enantiomer ของ Δ^3-pyrrolin-2-one ชนิดต่างๆ เมื่อเกิดเป็นสารประกอบเชิงซ้อนกับ TFAE ข้อมูลที่ได้จะเป็นประโยชน์ในการประยุกต์ใช้เพื่อกำหนดลักษณะทางสเตริโอเคมีของสารจากธรรมชาติชนิดอื่นโดยไม่มีการดัดแปลงโครงสร้างทางเคมีของสารที่มีอยู่

สาขาวิชาเภสัชเคมีและผลิตภัณฑ์ธรรมชาติ	ลายมือชื่อนิสิต.....
ปีการศึกษา 2547	ลายมือชื่ออาจารย์ที่ปรึกษา.....

4476971433 : MAJOR PHARMACEUTICAL CHEMISTRY AND NATURAL PRODUCTS

KEY WORDS: SEA HARE / *BURSATELLA LEACHII* / NON-HYDROLYTIC DEGRADATION METHODS/ ABSOLUTE STEREOCHEMISTRY / BIOACTIVITY

SUCHADA SUNTORNCHASHWEJ : BIOACTIVE COMPOUNDS FROM THE THAI SEA HARE, *BURSATELLA LEACHII*. THESIS ADVISOR: KHANIT SUWANBORIRUX, Ph.D., 184 pp. ISBN 974-53-2126-5.

Chemical investigation of the extract from the Thai sea hare, *Bursatella leachii* (family Aplysiidae, phylum Mollusca), led to the isolation of one known and three new compounds. Bioassay-guided isolation from the first collection of the sea hare afforded a new malyngamide X, the first tripeptide malyngamide (0.71% yield of the crude extract). The second collection of the sea hare provided a potent stimulator of actin assembly, hectochlorin, and its new derivative, deacetylhectochlorin, together with a new structurally unrelated molecule, *syn*-3-isopropyl-6-(4-methoxy-benzyl)-4-methyl-morpholine-2,5-dione, in 0.25, 0.08, and 0.007% yield of the crude extract, respectively. Malyngamide X exhibited moderate cytotoxicity against KB, NCI-H187, and BC cancer cell lines with ED_{50}'s of 8.20, 4.12, and 7.03 μM, respectively; anitimalaria with ED_{50}'s of 5.44 μM; and antituberculosis with MIC's of 50 μg/ml. Hectochlorin showed strong cytotoxicity against KB and NCI-H187 with ED_{50}'s of 0.86 and 1.20 μM, while deacetylhectochlorin exhibited more potent cytotoxicity with ED_{50}'s of 0.31 and 0.32 μM, respectively. However, the small amount of the new morpholine-2,5-dione derivative precluded biological evaluation.

Non-hydrolytic degradation methods were developed as an exemplary study for assigning absolute stereochemistry of malyngamide X having conformationally flexible system as 2(*S*), 5(*S*), 7(*S*), 8(*R*), 14(*S*), and 7'(*S*). The current strategy comprised of the NMR applications of the NMR chiral solvating agent (CSA) employing 2,2,2-trifluoro-1-(9-anthryl)ethanol (TFAE, Pirkle's alcohol), the modified Mosher's method, and partly NOEs correlations in conjunction with the conformational calculations and the biogenetic considerations. In addition, we have demonstrated the proposed solvation models that lead to stereochemical determination at some chiral carbons within the molecules of malyngamide X and several synthetic model compounds including alkaline degradation product of tautomycin and enantiomers of Δ^3-pyrrolin-2-one derivatives. The solvation models extend the use of TFAE and allow one to employ the current strategy to other natural compounds without chemical modification of the compounds as well.

Field of study Pharmaceutical Chemistry and Natural Products Student's signature.....

Academic year 2004 Advisor's signature.....

ACKNOWLEDGEMENTS

I would like to express my appreciation to my thesis advisor, Dr. Khanit Suwanborirux and my Japanese teacher, Prof. Minoru Isobe, than whom no-one could have been more helpful and courteous, for their valuable advice and continual guidance throughout this research study.

I am grateful to Assoc. Prof. Narongsak Chaichit of Thammasart University, Dr. Prasat Kittakoop of the National Center for Genetic Engineering and Biotechnology (BIOTEC), Dr. Suthasinee Pichayawasin of Khon Kaen University and Dr. Boonchoo Sritulaluk of Chulalongkorn University for providing X-ray crystallography, ESITOF MS data, and CD spectra, respectively. My appreciations are extended to Prof. Naoki Saito, Mejii Pharmaceutical University and Mr. Kazushi Koga, Nogoya University for assistance in EIMS, FABMS and 600 MHz NMR spectral data. The corrections and improvements by all of my thesis committee are gratefully acknowledged.

Gratitude is due to the Pharmaceutical Research Instrument Center, Faculty of Pharmaceutical Sciences for providing 300 MHz NMR spectrometer and other scientific equipments; the Scientific and Technological Research Equipment Center, Chulalongkorn University for recording 500 MHz NMR spectrometer; the Laboratory of Organic Chemistry, Graduate School of Bioagricultural Science, Nagoya University, for providing 400, 600 MHz NMR and Q-TOF mass spectrometer, and BIOTEC, Thailand for providing biological assays.

The Bioactive Marine Natural Product Chemistry Research Unit (BMNCU) is supported by a grant for centers of excellence, Chulalongkorn University. This research was partially supported by the Thailand Research Fund for the 2000 Royal Golden Jubilee Ph.D. Program Scholarship (PHD/ 0204/ 2543), the Association of International Education (AIEJ), Japan and Grant-in-Aid for Specials Promotion from MEXT, Japan (16002007).

On the personal side, my sincere appreciation is conveyed to Assoc. Prof. Surattana Amnuoypol, Mrs. Kiyoko Isobe, Mr. Phongsin Kaewrattanasripho, and all my friends at Chulalongkorn Univeristy and Nagoya University who have shared happy time together

Finally, I would like to express my special and deepest appreciation to my family, for their love, understanding and encouragement.

CONTENTS

	Page
ABSTRACT (Thai)	iv
ABSTRACT (English)	v
ACKNOWLEDGEMENTS	vi
CONTENTS	vii
LIST OF FIGURES	xii
LIST OF SCHEMES	xxi
LIST OF TABLES	xxii
ABBREVIATION	xxiii
CHAPTER	
I. INTRODUCTION	1
II. HISTORICAL	3
1. Characteristics of sea hares	3
2. Secondary metabolites from sea hares	6
2.1.Peptides	6
2.2.Polyketides	11
2.3.Terpenes	14
2.4.Other types of compounds	14
3. Malyngamide-type natural products	24
4. Hectochlorin and structurally related compounds	30
5. NMR chiral derivatizing agents (CDA) and NMR chiral solvating agents (CSA)	34
5.1. NMR chiral derivatizing agent (CDA)	35
5.2. NMR chiral solvating agent (CSA)	38
III EXPERIMENTAL	45
1. Animal materials	45
2. Identification and characterization of the sea hare, *Bursatella leachii*	45
3. Chemical reagents	47
4. General experimental procedures	47
4.1. Analytical thin-layer chromatography (TLC)	47
4.2. Preparative thin-layer chromatography	48

Page

4.3. Column chromatography..... 48
4.3.1. Vacuum liquid and flash column chromatography..... 48
4.3.2. Gel filtration chromatography..... 48
4.3.3. High pressure liquid chromatography (HPLC)..... 49
4.4. Spectroscopy..... 49
4.4.1. Ultraviolet (UV) absorption spectra..... 49
4.4.2. Infrared (IR) absorption spectra..... 49
4.4.3. Mass spectra..... 50
4.4.4. Proton and carbon-13 nuclear magnetic resonance (^{1}H and ^{13}C-NMR) spectra..... 50
4.5. Physical properties..... 50
4.5.1. Optical rotations..... 50
4.5.2. Circular dichroism (CD) spectra..... 51
4.6. Crystallization technique..... 51
4.7. X-ray crystallography..... 51
4.8. Solvents..... 51
5. Extraction and isolation..... 51
5.1. The sea hare collected in 2000..... 51
5.1.1. Extraction..... 51
5.1.2. Isolation of malyngamide X [**SHO-27**]..... 52
5.2. The sea hare collected in 2002..... 53
5.2.1. Extraction..... 53
5.2.2. Isolation of hectochlorin [**SHOII-28**], deacetylhectochlorin [**SHOII-51**], and *syn*-3-isopropyl-6-(4-methoxy-benzyl)-4-methyl- morpholine-2,5-dione [**SHOII-76**]..... 54
6. Physical and spectral data of the isolated compounds..... 56
6.1. Malyngamide X [**SHO-27**]..... 56
6.2. Hectochlorin [**SHOII-28**]..... 56
6.3. Deacetylhectochlorin [**SHOII-51**]..... 57
6.4. *syn*-3-Isopropyl-6-(4-methoxy-benzyl)-4-methyl-morpholine-2,5-dione [**SHOII-76**]..... 57

Page

7. Preparation of deacetylhectochlorin from hectochlorin..... 58
8. Preparation of 7-*O*-(*R*)-(+)-MTPA and 7-*O*-(*S*)-(−)-MTPA esters of malyngamide X 58
8.1. Preparation of 7-*O*-(*R*)-(+)-MTPA ester of malyngamide X [**SHO27a**]..... 58
8.2. Preparation of 7-*O*-(*S*)-(−)-MTPA ester of malyngamide X [**SHO27b**]..... 59
9. Preparations of model compounds for NMR chiral solvation experiments..... 59
9.1. Preparation of alkaline degradation product from tautomycin [**M1**]..... 59
9.2. Preparation of 5-acyl meldrum's acid derivative [**142**]..... 60
9.2.1. Method A using isopropenyl chloroformate (IPCF) as a condensing agent..... 60
9.2.2. Method B using 2-chloro-1,3-dimethyl-2-imidazolinium hexafluoro phosphate (CIP) as a condensing agent..... 61
9.3. Preparation of *N*-Boc-5(*S*)-isopropyl-4-hydroxy-Δ^3-pyrrolin-2-one [**143**]..... 61
9.4. Preparation of *N*-Boc-5(*S*)-isopropyl-4-methoxy-Δ^3-pyrrolin-2-one [**M2**]..... 62
9.5. Preparation of 5(*S*)-isopropyl-4-methoxy-Δ^3-pyrrolin-2-one [**M3**]..... 63
9.6. Preparation of 5(*S*)-Isopropyl-4-methoxy-1-propionyl-Δ^3 pyrrolin-2-one [**M4**]..... 64
9.7. Preparation of *N*-Boc-5(*R*)-isopropyl-4-hydroxy-Δ^3-pyrrolin-2-one [**144**]..... 64
9.8. Preparation of *N*-Boc-5(*R*)-isopropyl-4-methoxy-Δ^3-pyrrolin-2-one [**M5**]..... 65
9.9. Preparation of 5(*R*)-isopropyl-4-methoxy-Δ^3-pyrrolin-2-one [**M6**]..... 65

Page

9.10. Preparation of 5(*R*)-Isopropyl-4-methoxy-1-propionyl-Δ^3-pyrrolin-2-one [**M7**]..... 65
10. Preparation of samples for NMR chiral solvation measurements..... 66
11. Conformational calculations at the C-2 epimers of malyngamide X [**SHO-27**]..... 66
12. Biological testings of the isolated compounds..... 66
12.1. Cytotoxicity test..... 66
12.2. Antimalarial test..... 66
12.3. Antituberculous test..... 67
IV RESULTS AND DISCUSSION..... 68
1. Structure elucidation of the isolated compounds..... 69
1.1. Structure Elucidation of Malyngamide X [**SHO27**]..... 69
1.2. Identification of Hectochlorin [**SHOII-28**]..... 74
1.3. Structure Elucidation of Deacetylhectochlorin [**SHOII-51**]..... 78
1.4. Structure Elucidation of s*yn*-3-Isopropyl-6-(4-methoxy-benzyl)-4-methyl-morpholine-2,5-dione [**SHOII-76**]..... 83
2. Non-hydrolytic degradation method for absolute configurational assignment: application to malyngamide X..... 86
2.1. Determination of absolute configuration at C-7'..... 87
2.2. Determination of absolute configuration at C-5, C-7, and C-8..... 93
2.3. Determination of absolute configuration at C-14..... 98
2.4. Determination of absolute configuration at C-2..... 101
3. Biological activity of the isolated compounds..... 105
4. Preparation of model compounds for the NMR chiral solvation experiments..... 105
4.1. Alkaline degradation product of tautomycin..... 105
4.2. The enantiomers of 5-isopropyl-4-methoxy-Δ^3-pyrrolin-2-ones 107
4.2.1. Step I: formation of *N*-Boc-5(*S*)-isopropyl-4-hydroxy-Δ^3-pyrrolin-2-one..... 107

Page

4.2.2. Step II: *O*-methylation..... 112
4.2.3. Step III: deprotection..... 113
4.2.4. Step IV: *N*-propionylation..... 113
4.2.5. Spectroscopic data of model analogues **M2**–**M7**..... 114
V CONCLUSION..... 116
REFERENCES..... 119
APPENDIX 131
VITA..... 184

สถาบันวิทยบริการ
จุฬาลงกรณ์มหาวิทยาลัย

LIST OF FIGURES

Figure		Page
1	The structures of peptide-derived dolastatins.....	7
2	The structures of auristatin PE [**19**] and cemadotin [**20**].....	10
3	The structures of macrolides isolated from sea hares.....	11
4	(A) The structure-cytotoxicity and (B) the structure–actin-depolymerizing activity relationships of aplyronine A.....	12
5	The structures of aplyolide A–E.....	13
6	The structures of terpenes isolated from sea hares.....	15
7	The structures of alkaloids and malyngamides isolated from sea hares	16
8	Structures and cell adhesion inhibitor of the macrosphelides.....	20
9	Structures of cyanobacterial-derived dolastatins.....	22
10	Malyngamides with 7(*S*)-methoxydodec-4(*E*)-enoic acid.....	27
11	Malyngamides with 7(*S*)-methoxytetradec-4(*E*)-enoic acid.....	28
12	Malyngamides with 7-methoxy-9-methylhexadec-4(*E*)-enoic acid.....	29
13	Malyngamides with 7(*S*)-methoxyeicos-4(*E*)-enoic acid.....	29
14	Hectochlorin and its structurally related compounds.....	31
15	Structures of some natural products containing chlorinated fatty acid	33
16	(A) Determination of the absolute configuration of cholesterol and the signs of $\Delta\delta$ values of its MTPA esters. (B) Configurational correlation model for the (*R*)-MTPA derivative and the (*S*)-MTPA derivative. (C) Configurational correlation model for (*R*)-2NMA and (*S*)-2NMA derivative.....	36
17	Common chiral derivatizing agents for ^{1}H NMR analysis.....	37
18	Common chiral solvating agents.....	39
19	Proposed solvation model between (A) (*R*)-lacinilene C methyl ether (*R*-**134)** and (B) (*S*)-lacinilene C methyl ether (*S*-**134**) and (*S*)-TFAE.....	41
20	A) Association of racemic lactones with TFAE as proposed by Pirkle. (B) Proposed solvation model between (*R*)- and (*S*)-TFAE and (*S*)-**135**	42
21	The observed chemical shift non-equivalence (ppm) and the assigned absolute configuration at C-5 of butenolide moiety.....	43

Figure **Page**

22 (A) The sea hare *Bursatella leachii* collected from Sichang Marine Sciences Research and Training Center, Thailand, and (B) purple ink secretion..... 46

23 (A) Structure of janolusimide showing numbering system (B) Partial structures of malyngamide X [**SHO27**] showing H,H COSY correlations and important HMBC correlations..... 70

24 The structures of 4-amino-3-hydroxy-2-methylpentanoic acid-containing natural products..... 72

25 Partial structures of hectochlorin [**SHOII-28**] showing H,H COSY correlations and important HMBC correlations..... 75

26 ORTEP plot of hectochlorin [**SHOII-28**]..... 76

27 Partial structures of deacetylhectochlorin [**SHOII-51**] showing H,H COSY correlations and important HMBC correlations..... 78

28 Hydrazine hydrolysis of hectochlorin and key ^{1}H NMR signals..... 80

29 ^{1}H NMR spectra ($CDCl_3$, 300 MHz) of natural and transformed deacetylhectochlorin..... 82

30 (A) Structure of s*yn*-3-isopropyl-6-(4-methoxy-benzyl)-4-methyl-morpholine-2,5-dione [**SHO-II 76**] showing (B) H,H COSY correlations and important HMBC correlations..... 83

31 Selected NOESY correlations and the *J* values observed in *syn*-3-isopropyl-6-(4-methoxy-benzyl)-4-methyl-morpholine-2,5-dione [**SHOII-76**]..... 85

32 The structure of ergosecaline, the first example of morpholine 2,5-dione containing natural product..... 86

33 The sequence of non-hydrolytic degradation methods for determining absolute stereochemistry of malyngamide X [**SHO27**] 88

34 Proposed solvation model between (A) chiral methyl homoallyl ether or chiral allyl ether with both enantiomer of TFAE, and (B) (*R*) and (*S*) chiral allyl ether with (*R*)-TFAE by Pirkle and Boeder 90

Figure **Page**

35 The 500 MHz ^{1}H NMR spectra at 273 °K (3.10 - 3.60 ppm) of the alkaline degradation product of tautomycin [**M1**] having 6 equiv. of (*R*)- and (*S*)-TFAE and the solvation model..... 91

36 The 500 MHz ^{1}H NMR spectra at 273 °K (3.05 - 3.45 ppm) of malyngamide X [**SHO27**] having 5 equiv. of (*R*)- and (*S*)-TFAE and the solvation model..... 93

37 Preparation of MTPA esters **SHO27a** and **SHO27b**..... 94

38 $\Delta\delta_{SR}$ ($\delta_{\mathbf{SHO27b}} - \delta_{\mathbf{SHO27a}}$) values for the MTPA esters of malyngamide X ($CDCl_3$, 600 MHz) and the absolute configurational assignment at C-7(*S*) 96

39 The ^{1}H and $^3J_{H,H}$ values in the 4(*S*)-amino-3(*S*)-hydroxy-2(*R*)-methylpentanoic acid containing **SHO27**, janolusimide, and bleomycin A_2..... 97

40 Possible rotamers of the four diastereotopic orientations (**A**) 5(*S*), 7(*S*), 8(*R*); (**B**) 5(*R*), 7(S), 8(*R*); (**C**) 5(*S*), 7(*S*), 8(*S*); and (**D**) 5(*R*), 7(S), 8(*S*) of malyngamide X [**SHO27**] with dihedral angles between H^7–C–C–H^8 approximately 180°..... 98

41 (A) Experimental $\Delta\delta_{RS} = \delta_R - \delta_S$ values observed for H-5 of compounds **M2**–**M7** ($CDCl_3$, 274° K, 600 MHz) and the proposed solvation model. (B) ^{1}H NMR spectra between 4.40 and 4.60 ppm of malyngamide X [**SHO27**] having 5 equiv. of (*R*)- and (*S*)-TFAE (274 K, $CDCl_3$, 600 MHz)..... 100

42 Stereoview of the lowest-energy conformations for malyngamide x [**SHO27**] with two possible absolute configurations at C-2, (A) 2(*R*) and (B) 2(*S*)-epimer..... 103

43 (A) The proposed biosynthesis of malyngamide X [**SHO27**] (B) Selected glycine- or *β*-alanine derived malyngamides..... 104

44 The UV spectrum of malyngamide X [**SHO27**] in methanol..... 132

45 The IR spectrum (Film) of malyngamide X [**SHO27**..... 132

46 The FAB MS spectrum of malyngamdie X [**SHO27**]..... 133

47 The 500 MHz ^{1}H NMR spectrum of malyngamide X [**SHO27**] in $CDCl_3$ and in C_6D_6 (expanded δ_H 1.9 – 2.6 ppm)..... 133

Figure **Page**

48 The 500 MHz coupling patterns of malyngamide X [**SHO27**] in $CDCl_3$ (expanded δ_H 0.60–1.50 ppm)..... 134

49 The 500 MHz coupling patterns of malyngamide X [**SHO27**] in $CDCl_3$ (expanded δ_H 2.00–3.50 ppm)..... 134

50 The 500 MHz coupling patterns of malyngamide X [**SHO27**] in $CDCl_3$ (expanded δ_H 3.60–6.50 ppm)..... 135

51 The 300 MHz ^{1}H NMR spectrum of malyngamide X [**SHO27**] in D_2O exchangeable experiment showing $^3J_{H\text{-}7,H\text{-}8}$ = 8.9 Hz and $^3J_{H\text{-}7,H\text{-}5}$ = 2.6 Hz..... 135

52 The 75 MHz (A) DEPT-90, (B) DEPT-135, and (C) ^{13}C NMR spectrum of malyngamide X [**SHO27**] in $CDCl_3$..... 136

53 The 300 MHz H, H COSY spectrum of malyngamide X [**SHO27**] in $CDCl_3$..... 137

54 The 300 MHz HMQC spectrum of malyngamide X [**SHO27**] in $CDCl_3$ 137

55 The 300 MHz HMBC spectrum ($^nJ_{CH}$ = 8 Hz) of malyngamide X [**SHO27**] in $CDCl_3$..... 138

56 The 300 MHz HMBC spectrum ($^nJ_{CH}$ = 8 Hz) of malyngamide X [**SHO27**] in $CDCl_3$ (expanded δ_H 3.60–6.50 ppm. and δ_C 15.0–85.0)..... 139

57 The 300 MHz HMBC spectrum ($^nJ_{CH}$ = 4 Hz) of malyngamide X [**SHO27**] in $CDCl_3$..... 139

58 The 500 MHz NOESY spectrum of malyngamide X [**SHO27**] in $CDCl_3$ 140

59 The ESITOF MS spectrum of 7-*O*-(*R*)-(+)-MTPA ester of malyngamide X [**SHO27a**] in $CDCl_3$..... 141

60 The 600 MHz ^{1}H NMR spectrum of 7-*O*-(*R*)-(+)-MTPA ester of malyngamide X [**SHO27a**] in $CDCl_3$..... 141

61 The ESITOF MS spectrum of 7-*O*-(*S*)-(–)-MTPA ester of malyngamide X [**SHO27b**] in $CDCl_3$..... 142

62 The 600 MHz ^{1}H NMR spectrum of 7-*O*-(*S*)-(–)-MTPA ester of malyngamide X [**SHO27b**] in $CDCl_3$..... 142

63 Overlaid H,H COSY spectra of 7-*O*-(*R*)-(+)-MTPA ester **SHO27a** (black) and 7-*O*-(*S*)-(–)-MTPA ester **SHO27b** (red) in $CDCl_3$..... 143

Figure **Page**

64 The 600 MHz ^{1}H NMR spectrum of malyngamide X in $CDCl_3$ at 274 °K..... 144

65 The 600 MHz ^{1}H NMR spectrum of malyngamide X [**SHO27**] plus 5 equiv. of (*R*)-2,2,2-trifuluoro-1-(9-anthryl)-ethanol (*R*-TFAE) in $CDCl_3$ at 274 °K..... 145

66 The 600 MHz ^{1}H NMR spectrum of malyngamide X [**SHO27**] plus 5 equiv. of (*S*)-2,2,2-trifuluoro-1-(9-anthryl)-ethanol (*S*-TFAE) in $CDCl_3$ at 274 °K..... 146

67 Variation of chemical shift non-equivalence ($\Delta\delta_{RS} = \delta_R - \delta_S$) with temperature for the methoxyl protons at C-7' of malyngamide X [**SHO27**] in the presence of 20 equiv. (*R*)-TFAE (solid line) and (*S*)-TFAE (dashed line) ($CDCl_3$, 600 MHz..... 147

68 The 600 MHz H, H COSY spectrum of malyngamide X [**SHO27**] plus 5 equiv. (*R*)-TFAE in $CDCl_3$ at 274 °K..... 148

69 The 600 MHz H, H COSY spectrum of malyngamide X [**SHO27**] plus 5 equiv. (*S*)-TFAE in $CDCl_3$ at 274 °K..... 148

70 The circular dichroism spectrum of hectochlorin [**SHOII-28**] in methanol..... 149

71 The UV spectrum of hectochlorin [**SHOII-28**] in MeOH..... 149

72 The IR spectrum (Film) of hectochlorin [**SHOII-28**] 150

73 The EIMS mass spectrum of hectochlorin [**SHOII-28**]..... 150

74 The 300 MHz ^{1}H NMR spectrum of hectochlorin [**SHOII-28**] in $CDCl_3$ 151

75 The 75 MHz ^{13}C NMR spectrum of hectochlorin [**SHOII-28**] in $CDCl_3$ 151

76 The 75 MHz (A) DEPT-135 and (B) ^{13}C NMR spectrum of hectochlorin [**SHOII-28**] in $CDCl_3$..... 152

77 The 300 MHz H,H COSY spectrum of hectochlorin [**SHOII-28**] in $CDCl_3$..... 152

78 The 300 MHz HMQC spectrum of hectochlorin [**SHOII-28**] in $CDCl_3$ 153

79 The 300 MHz HMQC spectrum of hectochlorin [**SHOII-28**] in $CDCl_3$ (expanded δ_H 1.0–2.5 ppm and δ_C 10.0–55.0 ppm)..... 154

80 The 300 MHz HMBC spectrum ($^{n}J_{CH}$ = 8 Hz) of hectochlorin [**SHOII-28**] in $CDCl_3$..... 154

Figure **Page**

81 The 300 MHz HMBC spectrum ($^{n}J_{CH}$ = 8 Hz) of hectochlorin [**SHOII-28**] in $CDCl_3$ (expanded δ_H 1.0–2.5 ppm and δ_C 15.0–95.0 ppm) 155

82 The 300 MHz HMBC spectrum ($^{n}J_{CH}$ = 8 Hz) of hectochlorin [**SHOII-28**] in $CDCl_3$ (expanded δ_H 1.0–9.0 ppm and δ_C 120.0–180.0 ppm)..... 155

83 The 300 MHz HMBC spectrum ($^{n}J_{CH}$ = 4 Hz) of hectochlorin [**SHOII-28**] in $CDCl_3$..... 156

84 The circular dichroism spectrum of deacetylhectochlorin [**SHOII-51**] in methanol..... 157

85 The UV spectrum of deacetylhectochlorin [**SHOII-51**] in MeOH..... 157

86 The IR spectrum (Film) of deacetylhectochlorin [**SHOII-51**]..... 158

87 The EIMS mass spectrum of deacetylhectochlorin [**SHOII-51**]..... 158

88 The 300 MHz ^{1}H NMR spectrum of deacetylhectochlorin [**SHOII-51**] in $CDCl_3$..... 159

89 The 75 MHz ^{13}C NMR spectrum of deacetylhectochlorin [**SHOII-51**] in $CDCl_3$..... 159

90 The 75 MHz (A) DEPT-135 and (B) ^{13}C NMR spectrum of deacetylhectochlorin [**SHOII-51**] in $CDCl_3$..... 160

91 The 300 MHz H,H COSY spectrum of deacetylhectochlorin [**SHOII-51**] in $CDCl_3$..... 160

92 The 300 MHz HMQC spectrum of deacetylhectochlorin [**SHOII-51**] in $CDCl_3$..... 161

93 The 300 MHz HMBC spectrum ($^{n}J_{CH}$ = 8 Hz) of deacetylhectochlorin [**SHOII-51**] in $CDCl_3$..... 162

94 The 300 MHz HMBC spectrum ($^{n}J_{CH}$ = 4 Hz) of deacetylhectochlorin [**SHOII-51**] in $CDCl_3$..... 163

95 The circular dichroism in MeOH of (A) hectochlorin [**SHOII-28**], (B) natural deacetylhectochlorin [**SHOII-51**] and [C] transformed deacetylhectochlorin obtained by deacetylation of hectochlorin..... 164

Figure **Page**

96 The 300 MHz ^{1}H NMR spectrum in $CDCl_3$ of (A) hectochlorin [**SHOII-28**], (B) natural deacetylhectochlorin [**SHOII-51**], and (C) transformed deacetylhectochlorin..... 165

97 The UV spectrum of *syn*-3-isopropyl-6-(4-methoxy-benzyl)-4-methyl-morpholine-2,5-dione [**SHOII-76**] in MeOH..... 166

98 The IR spectrum (Film) of *syn*-3-isopropyl-6-(4-methoxy-benzyl)-4-methyl-morpholine-2,5-dione [**SHOII-76**]..... 166

99 The ESITOF MS mass spectrum of *syn*-3-isopropyl-6-(4-methoxy-benzyl)-4-methyl-morpholine-2,5-dione [**SHOII-76**]..... 167

100 The 600 MHz ^{1}H NMR spectrum of *syn*-3-isopropyl-6-(4-methoxy-benzyl)-4-methyl-morpholine-2,5-dione [**SHOII-76**] in $CDCl_3$..... 167

101 The 600 MHz ^{1}H coupling patterns of *syn*-3-isopropyl-6-(4-methoxy-benzyl)-4-methyl-morpholine-2,5-dione [**SHOII-76**] in $CDCl_3$..... 168

102 The 150 MHz ^{13}C NMR spectrum of *syn*-3-isopropyl-6-(4-methoxy-benzyl)-4-methyl-morpholine-2,5-dione [**SHOII-76**] in $CDCl_3$..... 168

103 The 600 MHz H,H COSY spectrum of *syn*-3-isopropyl-6-(4-methoxy-benzyl)-4-methyl-morpholine-2,5-dione [**SHOII-76**] in $CDCl_3$..... 169

104 The 600 MHz HMQC spectrum of *syn*-3-isopropyl-6-(4-methoxy-benzyl)-4-methyl-morpholine-2,5-dione [**SHOII-76**] in $CDCl_3$..... 169

105 The 600 MHz HMBC spectrum ($^{n}J_{CH}$ = 8 Hz) of *syn*-3-isopropyl-6-(4-methoxy-benzyl)-4-methyl-morpholine-2,5-dione [**SHOII-76**] in $CDCl_3$ 170

106 The 600 MHz NOESY spectrum of *syn*-3-isopropyl-6-(4-methoxy-benzyl)-4-methyl-morpholine-2,5-dione [**SHOII-76**] in $CDCl_3$..... 171

107 The 600 MHz ^{1}H NMR spectrum of alkaline degradation product of tautomycin **M1** in the presence of (*R*)-TFAE (upper) and (*S*)-TFAE (lower) in $CDCl_3$ at 274 °K..... 172

108 The 400 MHz NMR spectrum of *N*-Boc-L-valine in $CDCl_3$..... 173

109 The 400 MHz ^{1}H NMR spectrum of Meldrum's acid in $CDCl_3$..... 173

110 The 400 MHz ^{1}H NMR spectrum of crude product of Meldrum acid's derivative **142** in $CDCl_3$..... 174

111 The 400 MHz NMR spectrum of crude product of *N*-Boc-5(*S*)-isopropyl-4-hydroxy-Δ^3-pyrrolin-2-one [**143**] in $CDCl_3$..... 174

Figure **Page**

112 The ESITOF MS spectrum of *N*-Boc-5(*S*)-isopropyl-4-methoxy-Δ^3-pyrrolin-2-one [**M2**] in $CDCl_3$..... 175
113 The 400 MHz ^{1}H NMR spectrum of *N*-Boc-5(*S*)-isopropyl-4-methoxy-Δ^3-pyrrolin-2-one [**M2**] in $CDCl_3$..... 175
114 The ESITOF MS spectrum of 5(*S*)-isopropyl-4-methoxy-Δ^3-pyrrolin-2-one [**M3**] in $CDCl_3$..... 176
115 The 400 MHz ^{1}H NMR spectrum of 5(*S*)-isopropyl-4-methoxy-Δ^3-pyrrolin-2-one [**M3**] in $CDCl_3$..... 176
116 The ESITOF MS spectrum of 5(*S*)-isopropyl-4-methoxy-1-propionyl-Δ^3-pyrrolin-2-one [**M4**] in $CDCl_3$..... 177
117 The 400 MHz 1H NMR spectrum of 5(*S*)-isopropyl-4-methoxy-1-propionyl-Δ^3-pyrrolin-2-one [**M4**] in $CDCl_3$..... 177
118 The ESITOF MS spectrum of *N*-Boc-5(*R*)-isopropyl-4-methoxy-Δ^3-pyrrolin-2-one [**M5**] in $CDCl_3$..... 178
119 The 400 MHz ^{1}H NMR spectrum of *N*-Boc-5(*R*)-isopropyl-4-methoxy-Δ^3-pyrrolin-2-one [**M5**] in $CDCl_3$..... 178
120 The ESITOF MS spectrum of 5(*R*)-isopropyl-4-methoxy-Δ^3-pyrrolin-2-one [**M6**] in $CDCl_3$..... 179
121 The 400 MHz ^{1}H NMR spectrum of 5(*R*)-isopropyl-4-methoxy-Δ^3-pyrrolin-2-one [**M6**] in $CDCl_3$..... 179
122 The ESITOF MS spectrum of 5(*R*)-isopropyl-4-methoxy-1-propionyl-Δ^3-pyrrolin-2-one [**M7**] in $CDCl_3$..... 180
123 The 400 MHz ^{1}H NMR spectrum of 5(*R*)-isopropyl-4-methoxy-1-propionyl-Δ^3-pyrrolin-2-one [**M7**] in $CDCl_3$..... 180
124 The 600 MHz ^{1}H NMR spectra of *N*-Boc-5(*S*)-isopropyl-4-methoxy-Δ^3-pyrrolin-2-one [**M2**] in the presence of 10 equiv. (*R*)-TFAE (upper) and (*S*)-TFAE (lower) in $CDCl_3$ at 274 °K..... 181
125 The 600 MHz ^{1}H NMR spectra of *N*-Boc-5(*S*)-isopropyl-4-methoxy-Δ^3-pyrrolin-2-one [**M3**] in the presence of 10 equiv. (*R*)-TFAE (upper) and (*S*)-TFAE (lower) in $CDCl_3$ at 274 °K..... 181

Figure **Page**

126 The 600 MHz ^{1}H NMR spectra of 5(*S*)-isopropyl-4-methoxy-1-propionyl-Δ^3-pyrrolin-2-one [**M4**] in the presence of 10 equiv. (*R*)-TFAE (upper) and (*S*)-TFAE (lower) in $CDCl_3$ at 274 °K..... 182

127 The 600 MHz ^{1}H NMR spectra of *N*-Boc-5(*R*)-isopropyl-4-methoxy-Δ^3-pyrrolin-2-one [**M5**] in the presence of 10 equiv. (*R*)-TFAE (upper) and (*S*)-TFAE (lower) in $CDCl_3$ at 274 °K..... 182

128 The 600 MHz ^{1}H NMR spectra of 5(*R*)-isopropyl-4-methoxy-Δ^3-pyrrolin-2-one [**M6**] in the presence of 10 equiv. (*R*)-TFAE (upper) and (*S*)-TFAE (lower) in $CDCl_3$ at 274 °K..... 183

129 The 600 MHz ^{1}H NMR spectra of 5(*R*)-isopropyl-4-methoxy-1-propionyl-Δ^3-pyrrolin-2-one [**M7**] in the presence of 10 equiv. (*R*)-TFAE (upper) and (*S*)-TFAE (lower) in $CDCl_3$ at 274 °K..... 183

สถาบันวิทยบริการ
จุฬาลงกรณ์มหาวิทยาลัย

LIST OF SCHEMES

Scheme		Page
1	Taxonomy of the sea hare, *Bursatella leachii*.....	4
2	Determination of the absolute configuration of chiral carboxylic acid using PGME esters.....	38
3	Extraction of the sea hare collected 2000.....	52
4	Isolation of malyngamide X [**SHO27**].....	53
5	Extraction of the sea hare collected 2002.....	53
6	Isolation of hectochlorin [**SHOII-28**], deacetylhectochlorin [**SHOII-51**], and *syn*-3isopropyl-6-(4-methoxy-benzyl)- 4-methyl-morpholine-2,5-dione [**SHOII-76**].....	55
7	Preparation of the alkali degradation product of tautomycin.....	106
8	Proposed *trans*-esterification and elimination mechanism on alkali degradation of tautomycin by Sugiyama and colleagues (1996).....	106
9	Preparation of of 5(*S*)-isopropyl-4-methoxy-Δ^3-pyrrolin-2-one derivatives **M2** to **M4** and its enantiomers **M5** to **M7**.....	108
10	Preparation of *N*-Boc-5(*S*)-isopropyl-4-hydroxy-Δ^3-pyrrolin-2-one [**143**] employing IPCF (method A) or CIP (method B) as a condensing agent, and keys ^{1}H signals.....	109
11	Proposed acylation mechanism of Meldrum's acid utilizing (Method A) isopropenyl chloroformate, IPCF or (Method B) 2-chloro-1,3-dimethyl-2-imidazolinium hexafluorophosphate, CIP as a condensing agent.....	110
12	Proposed intramolecular cyclization mechanism of Meldrum's derivative [**142**] in refluxing EtOAc.....	111
13	(A) *O*-methylation *via* Mitsunobu reaction, and (B) the proposed *O*-methylation mechanism of *N*-Boc-5(*S*)-isopropyl-4-hydroxy-Δ^3-pyrrolin-2-one [**143**].....	112
14	Deprotection reaction of 5(*S*)-isopropyl-4-methoxy-Δ^3-pyrrolin-2-one [**M3**].....	113
15	(A) *N*-propionyl reaction, and (B) the proposed reaction mechanism	114

LIST OF TABLES

Table		Page
1	Compounds isolated from sea hares.....	17
2	Cyanobacterial origins of the dolastatins originally isolated from sea hares.....	21
3	Malyngamide-type natural products.....	25
4	Biological activities of hectochlorin and its structurally related compounds.....	32
5	^{1}H and ^{13}C NMR spectral data of malyngamide X [**SHO27**] recorded in $CDCl_3$.....	73
6	^{1}H and ^{13}C NMR spectral data of hectochlorin and **SHOII-28** recorded in $CDCl_3$.....	77
7	^{1}H and ^{13}C NMR spectral data of hectochlorin [**SHOII-28**] and deacetylhectochlorin [**SHOII-51**] recorded in $CDCl_3$.....	81
8	^{1}H and ^{13}C NMR spectral data of *syn*-3-isopropyl-6-(4-methoxy-benzyl)-4-methyl-morpholine-2,5-dione [**SHOII-76**] recorded in $CDCl_3$.....	85
9	^{1}H NMR data ($CDCl_3$, 600 MHz) of malyngamide X [**SHO27**], (*R*)-MTPA ester of malyngamide X [**SHO27a**], (*S*)-MTPA ester of malyngamide X [**SHO27b**] and difference in chemical shift ($\Delta\delta_{SR} = \delta_{\mathbf{SHO27b}} - \delta_{\mathbf{SHO27a}}$).....	95
10	Physicochemical properties and spectroscopic data of model compounds **M2**–**M7**.....	115

ABBREVIATIONS

%	=	percent or part per hundred
Å	=	Armstrong
°C	=	degree Celcius
°K	=	degree Kelvin
$\Delta\delta$	=	chemical shift non-equivalence
δ	=	chemical shift
ε	=	molar absorptivity
μg	=	microgram
μl	=	microliter
μM	=	micromole
λ_{max}	=	wave length at maximum absorption
ν_{max}	=	wave number at maximum absorption
$[\alpha]^{20}_{D}$	=	specific rotation at 20 °C and sodium D line (589 nm)
amu	=	atomic mass unit
BC	=	human breast cancer cell line
br s	=	broad singlet
c	=	concentration
calc	=	calculated
^{13}C NMR	=	carbon-13 nuclear magnetic resonance
CD	=	circular dichroism
C_6D_6	=	deuterated benzene
CDA	=	chiral derivatizing agent
$CDCl_3$	=	deuterated chloroform
CH_2Cl_2	=	dichloromethane
CIP	=	2-chloro-1,3-dimethyl-2-imidazolinium hexafluorophosphate
CSA	=	chiral solvating agent
d	=	doublet
dd	=	doublet of doublets
DEAD	=	diethyl azodicarboxylate
DIEA	=	*N*,*N*-diisopropylethylamine

DMAP	=	dimethylaminopyridine
dq	=	doublet of quartets
ED_{50}	=	50% effective dose
EIMS	=	electron impact mass spectrometry
ESI MS	=	electrospray ionization mass spectrometry
EtOAc	=	ethyl acetate
Et_2O	=	diethyl ether
FAB MS	=	fast atom bombardment mass spectrometry
h	=	hour
H,H COSY	=	$^1H,^1H$ correlation spectroscopy
HMBC	=	^1H-detected heteronuclear multiple bond correlation
HMQC	=	^1H-detected heteronuclear multiple quantum coherence
^1H NMR	=	proton nuclear magnetic resonance
HPLC	=	high-pressure liquid chromatography
Hz	=	hertz
IPCF	=	isopropenyl chloroformate
IR	=	infrared
J	=	coupling constant
KB	=	human epidermoid carcinoma cells of the nasopharynx
m	=	multiplet
M	=	molar
M^+	=	molecular ion
$[M + H]^+$	=	protonated molecular ion
$[M + K]^+$	=	the peak 39 mass unit above the molecular ion peak
$[M + Na]^+$	=	the peak 23 mass unit above the molecular ion peak
MHz	=	megahertz
MIC	=	minimum inhibition concentration
MTPA-Cl	=	α-methoxy-α-(trifluoromethyl)phenylacetyl chloride
m/z	=	mass to charge ratio
NCI-H187	=	human lung carcinoma cell line
NOESY	=	nuclear Overhauser and exchange spectroscopy
nm	=	nanometer
NMR	=	nuclear magnetic resonance
ppm	=	part per million

q	=	quartet
quin	=	quintet
s	=	singlet
sext	=	sextet
t	=	triplet
TFA	=	trifluoroacetic acid
TFAE	=	2,2,2-trifluoro-1-(9-anthryl)ethanol
TLC	=	thin layer chromatography
TMS	=	tetramethylsilane
UV	=	ultraviolet

สถาบันวิทยบริการ
จุฬาลงกรณ์มหาวิทยาลัย

CHAPTER I

INTRODUCTION

During extensive investigations for bioactive secondary metabolites from Thai marine organisms by our laboratory, a wealth of novel compounds has been discovered. For instance, the chemical study of Thai marine sponge in the genus *Xestospongia* has afforded a series of new renieramycin derivatives (Amnouypol et al., 2004). Meanwhile, two new nitrogenous germacrane sesquiterpenes have been isolated from the Thai sponge *Axinyssa* n. sp. which exhibited strong antimicrobial activity (Satitpatipan and Suwanborirux, 2004). Chemical investigation of the Thai tunicate *Ecteinascidia thurstoni* has resulted in the isolation of potent antitumor substances ecteinascidins 770 and 786 (Suwanborirux et al., 2002). To date, renieramycins and ecteinascidins are very interesting compounds, both for developing as new anticancer drug candidates (National Cancer Institute PDQ Clinical Trials Database, n. d.). In addition to the marine macroorganisms, two new bioactive macrolactins have been obtained from a culture strain of the marine bacterium *Bacillus* sp. Sc026 isolated from the sediment collected from Sichang Island, Thailand (Jaruchoktaweechai et al., 2000). This series of papers strongly supports Thai marine organisms as a challenging source of novel bioactive compounds. We then paid particular attention to the Thai sea hare (กระต่ายทะเล, order Anaspidea, subclass Opisthobranch, phylum Mollusca) collected from the Gulf of Thailand of which its chemical study has not yet been reported.

The ability of the sea hares to concentrate defensive metabolites from several different algae species makes these molluscs attractive for marine natural product chemists (McPhail et al, 1999; Burja et al, 2001). Over the past 30 years, numerous bioactive secondary metabolites, particularly cytotoxic compounds, have been discovered from various collections of sea hares worldwide including the antitumor peptides, dolastatins, from the Indian Ocean sea hare, *Dolabella auricularia* (Pettit et al., 1993); the antitumor macrolides, aplyronines, from the Japanese sea hare, *Aplysia kurodai* (Kigoshi et al., 1996); the cytotoxic terpenoid, auriculol, from

the Japanese sea hare, *D. auricularia* (Kigoshi et al., 2001); the cytotoxic alkaloid, makalikone ester, from the Hawaiian sea hare, *Stylocheilus longicauda* (Gallimore et al., 2000); and the cytotoxic lipopeptide, malyngamide S, from the New Zealander sea hare, *Bursatella leahii* (Appleton et al., 2002). Recently, two new cytotoxic compounds, auriride and dolastatin 19, have been isolated from the sea hare *D. auricularia* collected from the coast of the Shima Peninsula (Suenaga et al., 2004) and the Gulf of California (Pettit et al., 2004), respectively. As the secondary metabolite content of the sea hare is dependent on the site and time of collection (Pawlik, 1993; Wessels, Kong, and Wright, 2000), the sea hares continue to dominate as a marine source of new biologically active compounds.

Biological evaluation from the first collection of the Thai sea hare, identified as *Bursatella leachii* mainly on the basis of its morphological characteristics, showed antimalarial activity with ED_{50} of 2.4 μg/ml, antituberculous activity at MIC of 50 μg/ml, and cytotoxicity against Vero cell line, KB and BC cancer cell lines with EDs_{50} of 16.2, 7.2 and 6.6 μg/ml, respectively. This primary screening led us to make a second collection of the molluscs and perform the isolation, purification and structure elucidation of the secondary metabolites from each collection.

We also experimented with NMR chiral solvating agent (CSA) in combination with the usual procedures for determining absolute stereochemistry without hydrolytic degradation of the natural compound. The application of NMR chiral solvation method has many advantages since there is no degradation or modification of the natural compound (for reviews see: Parker, 1991; Mander, 1994; Wenzel and Wilcox, 2003). Additionally, the solvate complexes with CSA are non-covalent bonding, thus allowing complete recovery of the original natural compound. Our achievement in applying the current strategy for the assignment of absolute configuration at some stereogenic centers of a multifunctional lipopeptide isolated from the sea hare is a good starting point in employing this strategy with other natural compounds as well.

CHAPTER II

HISTORICAL

1. Characteristics of Sea Hares

Sea hares are shell-less molluscs belonging to family Aplysiidae, subclass Opisthobranchia, phylum Mollusca. Members of the subclass Opisthobranchia are almost all marine organisms, which include the sea hares (กระต่ายทะเล, order Anaspidea); the nudibranches (ทากเปลือย, order Nudibranchia); the cell suckers (order Sacoglossa or Ascoglossa). Sea hares are the largest group of the opisthobranches but are often very cryptic due to the green mottled color patterns of most species. Often their presence is only observed if they are inadvertently stepped on or disturbed in some way, when they secrete large amounts of reddish-purple dye. Most sea hares have large parapodia (= อวัยวะที่ใช้ในการว่ายน้ำ) that fold over the mantle cavity (= ช่องแมนเทิล มีเหงือกบรรจุอยู่ภายใน) on the back of the animal, and have a small internal shell. Despite their large parapodia, most sea hares cannot swim. They are herbivorous, feeding on a variety of algae. Sea hares, like all other opisthobranches, are hermaphrodites with fully functional male and female reproductive organs. They produce enormous numbers of eggs. These are laid under coral slabs and consist of long strings of eggs clumped together in a tangled, spaghetti-like mass and are usually olive green or pale brown (สุชาติ อุปถัมป์, 2538; Pechenik, 1993; Sea Slugs Forum Database, n.d.). A number of reviews discussing naturally occurring bioactive compounds have been mainly reported in 4 genera of sea hares including *Aplysia*, *Dolabella*, *Bursatella*, and *Stylocheilus*. The characterization of sea hares presented below will emphasize on these 4 genera (Scheme 1).

Among 10 genera of sea hares, the genus *Aplysia* is commonly known as sea hares because of their large scrolled rhinophores (= ระยางค์ส่วนหัว ทำหน้าที่รับกลิ่นและสารเคมี) which are thought to superficially resemble the prominent ears of rabbits. It has high parapodia that join low down posteriorly near the tail, and there is

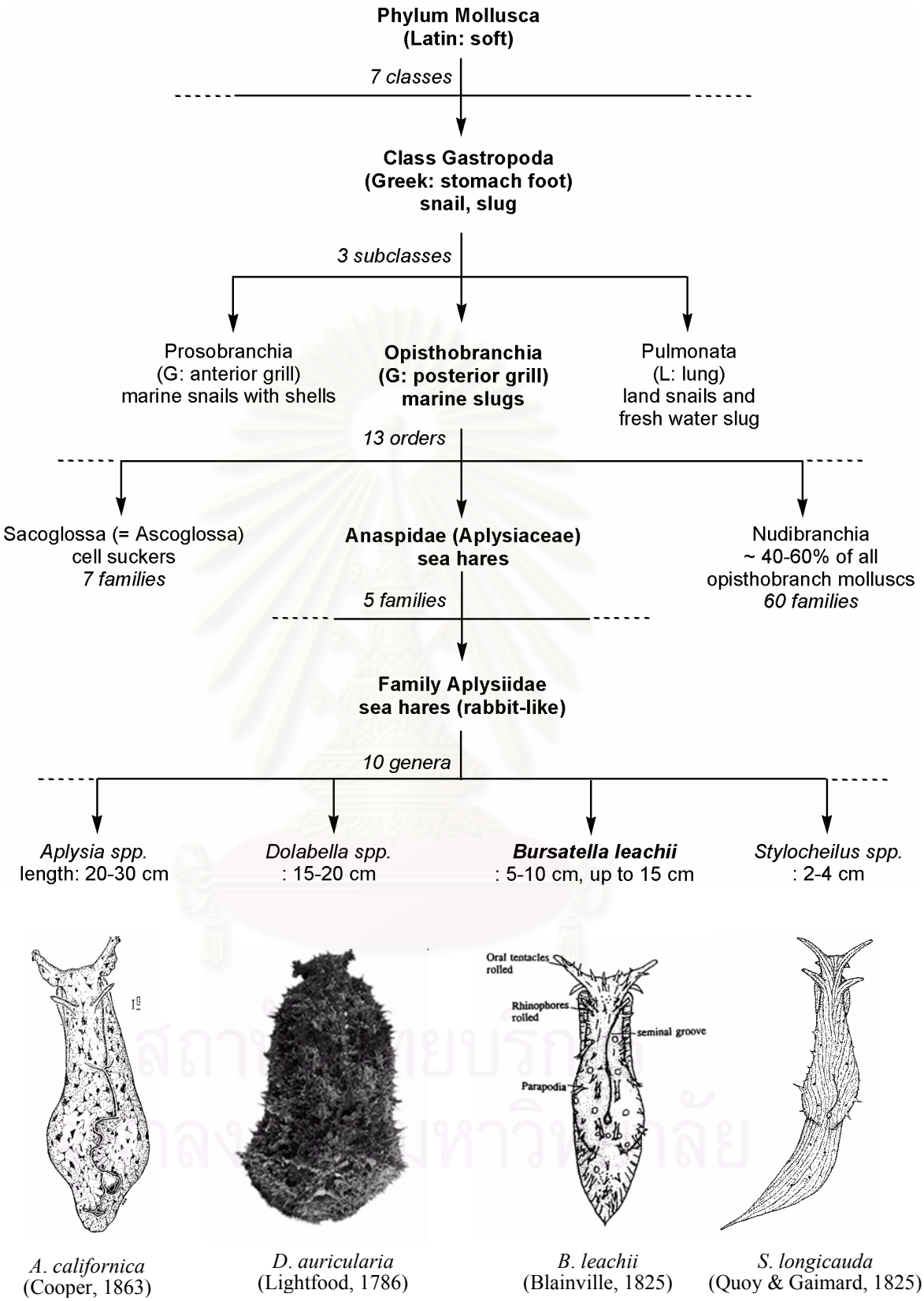

Scheme 1. Taxonomy of the sea hare, *Bursatella leachii*

a prominent black spot on its short tail. The *Dolabella* species of sea hares have attracted the interest of many researchers in the isolation of its biologically active substances (Cimino et al., 2001). This sea hare differs in shape from species of *Aplysia*, and is immediately recognizable as its sloping back end looks as if it has been cut off. It has a small, narrow head and its body increases in width and height to just over two-thirds of the length of the animal where it ends abruptly and slopes sharply down. The ragged sea hare *Bursatella* is of a single species worldwide, that is, *Bursatella leachii*. It has numerous, long, branched, filamentous simple and compound villi (papillae) covering its body. The genus *Stylocheilus* is one of the smallest groups of sea hares. Its general body color is light brown with numerous thin, longitudinal maroon to dark brown stripes running parallel to the parapodial margins and extending at least partway up the rhinophores and oral tentacles (= อวัยวะคล้ายหนวด ทำหน้าที่รับสัมผัส). The papillae are thin, usually simple, scattered over the entire surface (Sea Slug Furum Database, n.d.; Jensen, 1998a; 1998b).

Sea hares have no external defense; a vestigial shell is concealed within the mantle (= ผิวหนังที่ปกคลุมอวัยวะภายในของหอย), leaving the soft body exposed to possible predators. Defensive roles have been assigned to two of their chemical secretions, as well as to the general toxicity of sea hares themselves (Stallard and Faulkner, 1974; Pennings, 1994; Cimino et al., 2001).

(a) A purple fluid is expelled from purple gland on the upper mantle when sea hares are disturbed. This secretion has been suggested to contain substances capable of immobilizing the chemosensory apparatus of predators. Chemical characterization of the purple fluid yielded a characteristic fluid derived from pigments of dietary Rhodophyta algae such as phycoerythrobilin, γ-phycoerythrin (Prince, Nolen, and Coelno, 1998), and cytolytic proteins including dolabellanins and aplysianins (Yamazaki et al., 1989).

(b) A milky white fluid is discharged by sea hares from the opaline gland located on the lower mantle as a bitter-tasting irritant and can cause muscular paralysis followed by death to some marine organisms.

(c) The most toxic organ of sea hares has invariably proved to be the digestive (midgut) gland. Chemical studies of the compounds found in the digestive glands of sea hares revealed typical algal metabolites of their diet.

The poisonous properties of sea hares and their use of toxic materials were already known in pre-Christian times. Despite its toxicity, the Californian sea hare, *Aplysia californica*, when dried, was used medicinally by coastal Chinese physicians (Cimino et al., 2001).

2. Secondary Metabolites from Sea Hares

Sea hares of the genera *Aplysia*, *Dolabella*, *Bursatella* and *Stylocheilus* have been known to be rich sources of biologically active compounds, particularly cytotoxic substances (Cimino et al., 2001). Virtually, most of the metabolites from sea hares have been isolated from whole animal or their digestive gland, which show convincing links to the animal's algal diet (Burja et al., 2001). The secondary metabolites from sea hares can be classified as: peptides, polyketides, terpenes, and others as shown in Table 1.

2.1. Peptides

Chemical investigations of sea hares have attracted natural product researchers since the discovery of the antineoplastic peptides, the dolastatins 1–9, from the Indian Ocean sea hare *Dolabella auricularia* (Pettit et al., 1981; 1982). However, only the chemical structure of dolastatin 3 [**1**] could be established due to the small amounts available (about 1 mg each from 100 kg of animal) and sensitivity to decomposition. Larger recollection of the sea hare (1,600 kg) led to isolation of the new dolastatins 10 to 15 [**2-7**] (Pettit et al., 1987; 1989; 1993). Dolastatins 16 [**8**] to 18 [**10**] (Pettit, Xu, Hogans et al., 1997; Pettit, Xu, Williams et al, 1997; Pettit, Xu et al., 1998) were additionally discovered from Papua New Guinea specimens of the mollusces. Recently, Pettit's group has contributed a new dolastatin 19 [**27**] (Pettit et al., 2004) structurally unrelated to other dolastatins from the Gulf of Californian sea hare *D. auricularia*. Furthermore, Yamada and colleagues have reported the isolation of dolastatins C [**11**] to E [**13**], dolastatin G [**14**], nordolastatin G [**15**], dolastatin H [**16**], isodolastatin H [**17**], and dolastatin I [**18**] from the Japanese *D. auricularia*

(Sone, Nemoto, Ishiwata et al., 1993; Sone, Nemoto, Ojika et al., 1993; Ojika, Nagoya and Yamada, 1995; Mutou et al., 1996; Sone, Shibata et al., 1996; Sone, Kigoshi and Yamda, 1997). The chemical structures of the peptide-derived dolastatins are shown in Figure 1.

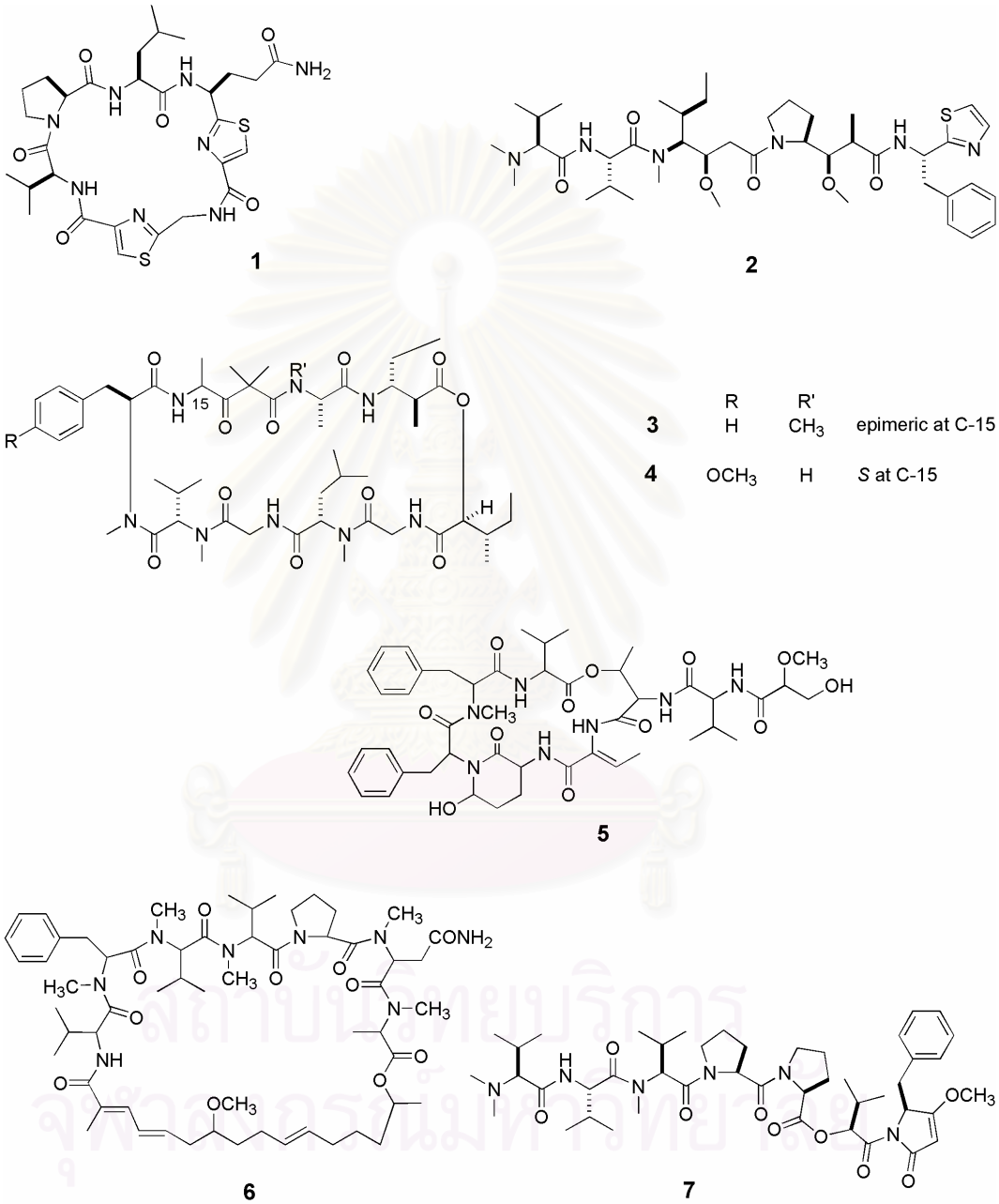

1	Dolastatin 3	**5**	Dolastatin 13
2	Dolastatin 10	**6**	Dolastatin 14
3	Dolastatin 11	**7**	Dolastatin 15
4	Dolasatin 12		

Figure 1. The structures of peptide-derived dolastatins.

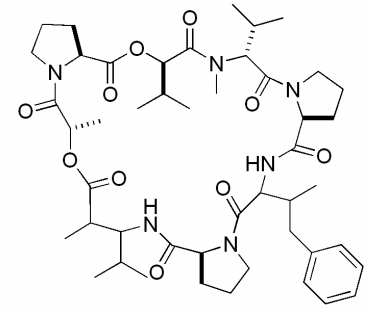

8

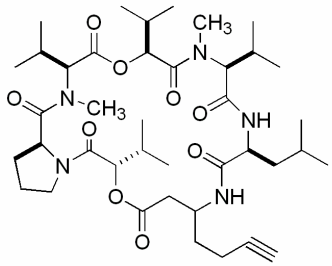

9

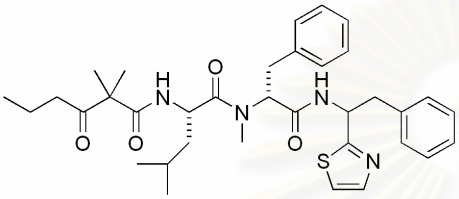

10

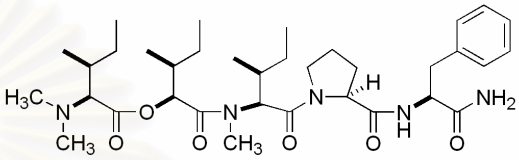

11

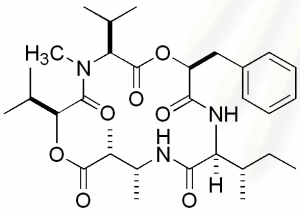

12

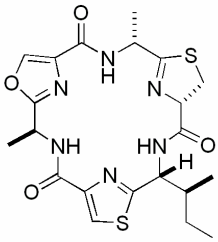

13

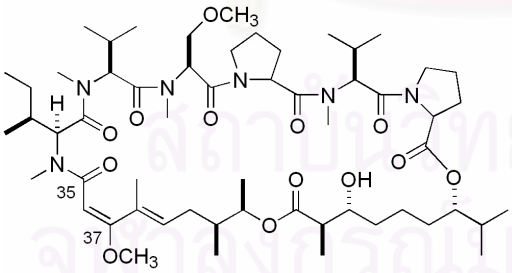

14

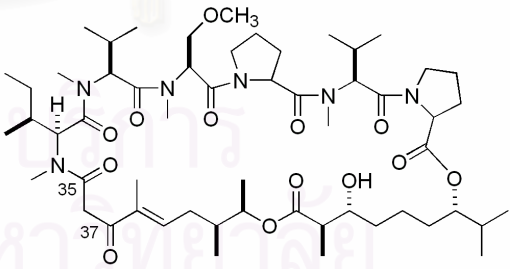

15

8	Dolastatin 16	**12**	Dolastatin D
9	Dolastatin 17	**13**	Dolastatin E
10	Dolastatin 18	**14**	Dolastatin G
11	Dolastatin C	**15**	Nordolastatin G

Figure 1. (*Continued*)

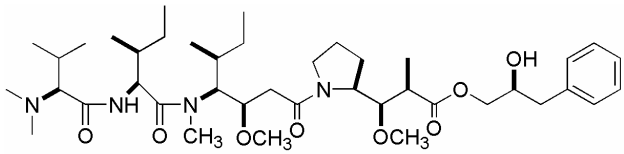

16

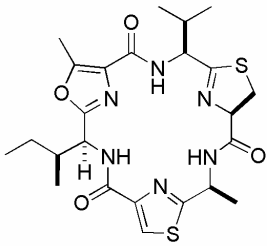

18

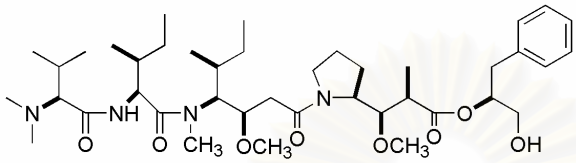

17

16 Dolastatin H
17 Isodolastatin H
18 Dolastatin I

Figure 1. (*Continued*)

Among them, dolastatins 10 [**2**], 11 [**3**], and 15 [**7**] are very valuable in medical research. Dolasatins 10 and 15 showed the most interesting cytotoxicity with GI_{50} to NCI's 60 human tumor cell lines of 0.1 and 1.0 nM, respectively (Pettit et al., 1993). The antitumor activities of dolastatins 10 and 15 were proved to be tubulin polymerization inhibition, thereby interfering with cell division (Jordan et al., 1998; Poncet et al., 1998; Pettit, Srianngam et al., 1998; Pettit, Flahive et al., 1998). Currently, dolastatin 10 (NSc 376128), its synthetic analogues (auristatin PE or TZT-1027) [**19**] and dolastatin 15 analogue (cemadotin or LU-103793) [**20**] have advanced to phase II clinical trials as promising cancer chemotherapeutic agents (Hoffmann, Blessing, and Lentz, 2003; Kerbrat et al., 2003; National Cancer Institute PDQ Clinical Trials Database, n. d.). The structures of these synthetic analogues are shown in Figure 2. Dolastatin 11 [**3**] is now a candidate as a pharmacological agent in cancer chemotherapy. The antitumor activity of **3** is proved to be anti-actin. Actin is one of the most abundant and common proteins in the cytoskeleton and regulates various cell functions, such as muscle contraction, cell motility, and cell division. Dolastatin 11 was shown to arrest cytokinesis *in vivo* and to increase the amount of F-actin to stabilize F-actin in *vitro*. Interestingly, dolastatin 11 binds at a different site in F-actin

from those of jasplakinolide and phalloidin, two anti-actin lead compounds (Oda et al., 2003).

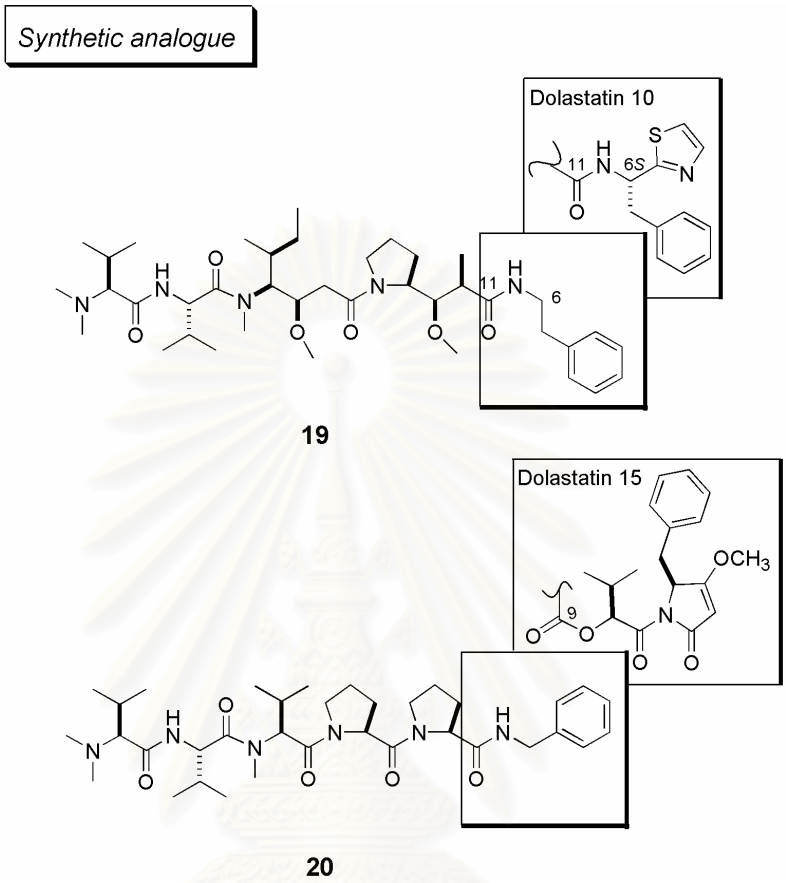

Figure 2. The structures of auristatin PE [**19**] and cemadotin [**20**].

In addition to the dolastatins, a cytotoxic depsipeptide named aurilide [**21**] was recently isolated from the Japanese sea hare *Dolabella auricularia* by Yamada's group (Suenaga et al., 2004). Aurilide showed both strong antitumor activity in the NCI 60 cell lines and microtuble stabilizing property.

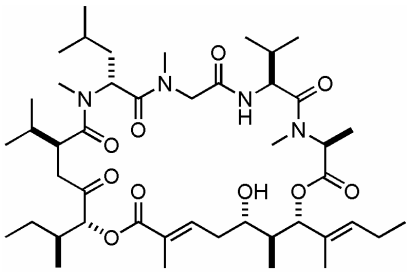

21 Aurilide

2.2. Polyketides

Polyketides from the sea hares are usually complex macrolides of relatively large oxygen-containing heterocycles such as the aplyronines [**22-24**], aurisides [**25-26**], dolastatin 19 [**27**], and dolabelides [**28-31**] shown in Figure 3. Compared to the peptides, the macrolides from sea hares are quite rare.

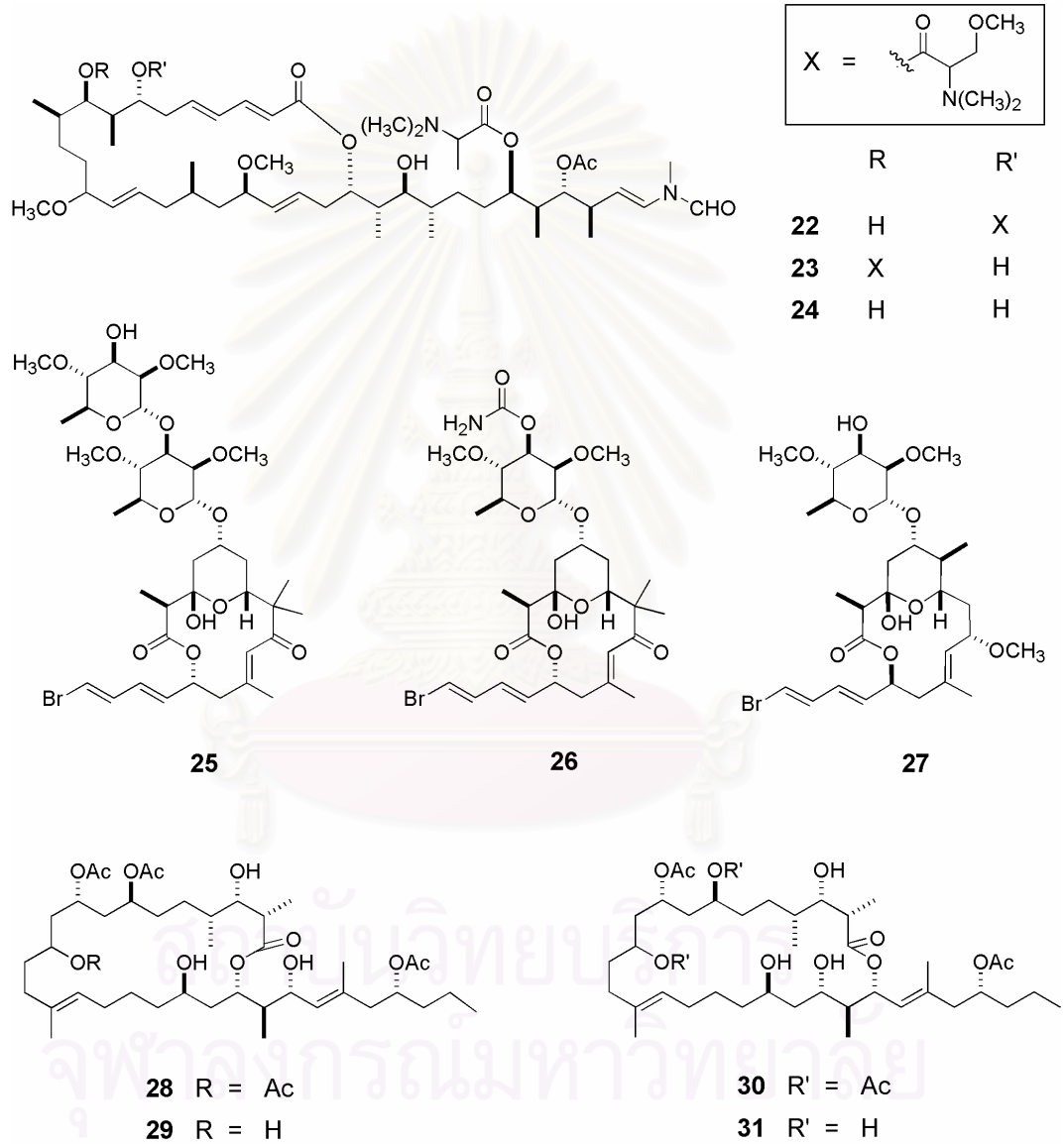

22	Aplyronine A	**27**	Dolastatin 19
23	Aplyronine B	**28**	Dolabelide A
24	Aplyronine C	**29**	Dolabelide B
25	Auriside A	**30**	Dolabelide C
26	Auriside B	**31**	Dolabelide D

Figure 3. The structures of macrolides isolated from sea hares.

Among these, aplyronine A is an interesting antitumor macrolide. The antitumor aplyronines A [**22**], B [**23**], and C [**24**] were isolated from the Japanese sea hare *Aplysia kurodai* by Yamada and colleagues (1993). Aplyronine A exhibited exceedingly potent antitumor activities with various human cancer cell lines. The target biomolecule of aplyronine A is actin (Kigoshi et al., 2002). Aplyronine A inhibits the polymerization of G-actin to F-actin and depolymerizes F-actin to G-actin by severing. Thus, this compound is considered a new type of antitumor substance from the standpoint to its mode of action. The structure-cytotoxicity (Kigoshi et al., 1996) and structure–actin-depolymerizing activity relationships (Kigoshi et al., 2002) of aplyronine A are summarized in Figure 4.

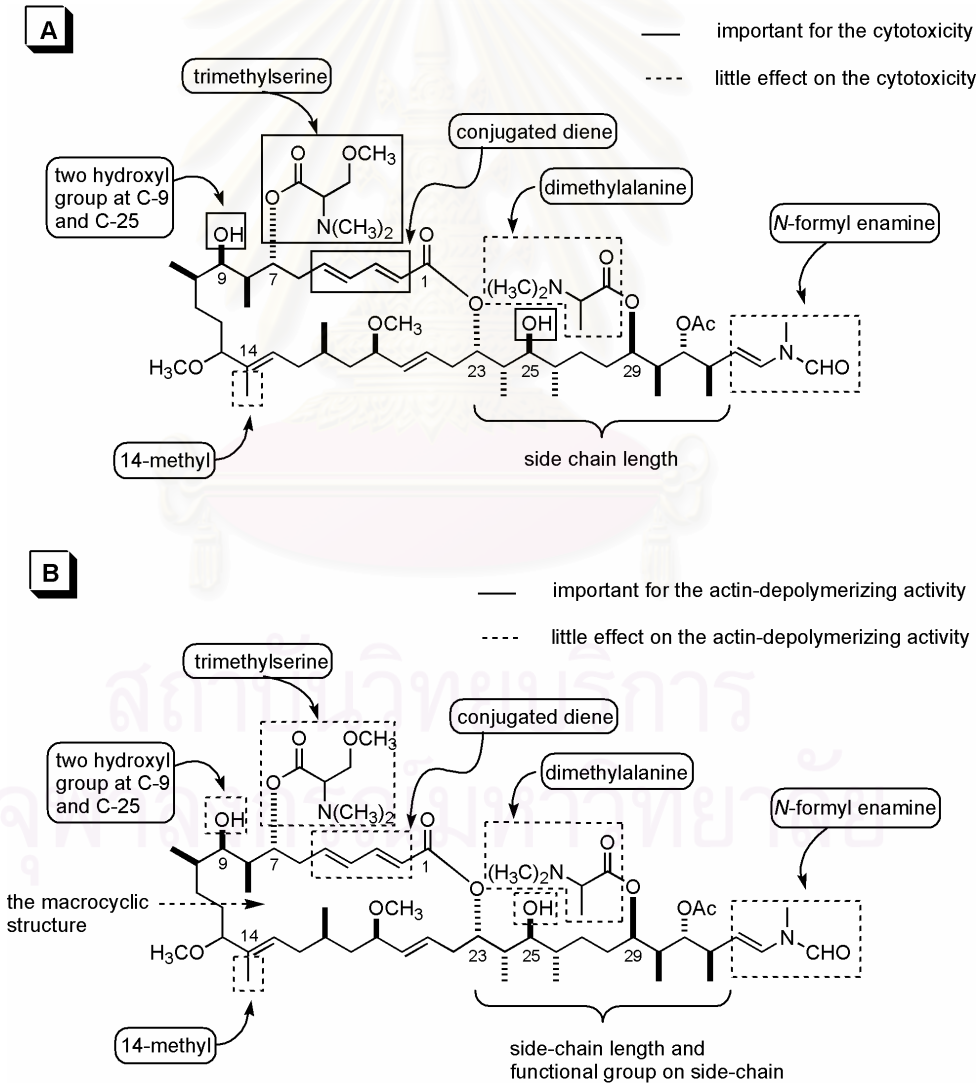

Figure 4. (A) The structure-cytotoxicity and (B) the structure–actin-depolymerizing activity relationships of aplyronine A.

The macrocyclic lactone dolastatin 19 [**27**] (0.5 mg from 600 kg wet wt of sea hare) was recently isolated from the sea hare *Dolabella auricularia* collected from the Gulf of California (Pettit et al., 2004). The overall structure of dolastatin 19 was a 14-membered macrolide glycoside with a hemiketal-bearing ring. It structure differed from other reported dolastatins (see heading 2.1) but closured to aurisides A [**25**] and B [**26**] isolated from the same species collected in Japan (Sone, Kigoshi and Yamada, 1996). The cytotoxicities of dolastatin 19 and aurisides are shown in Table 1.

Focusing on the external body parts of the animal, Spinella and colleagues (1997) reported the isolation of the ichthyotoxic macrolactones aplyolides A [**32**] to E [**36**] from skin of the sea hare *Aplysia kurodai*. The structures of aplyolides are shown in Figure 5. Aplyolides belong to a small group of hydroxy fatty acid lactones isolated from marine organisms. The authors proposed the *de novo* biosynthetic pathway by the molluscs to construct these unusual hydroxy fatty acid lactones. The anatomical localization of the aplyolides suggested their potential biological role as defensive substances.

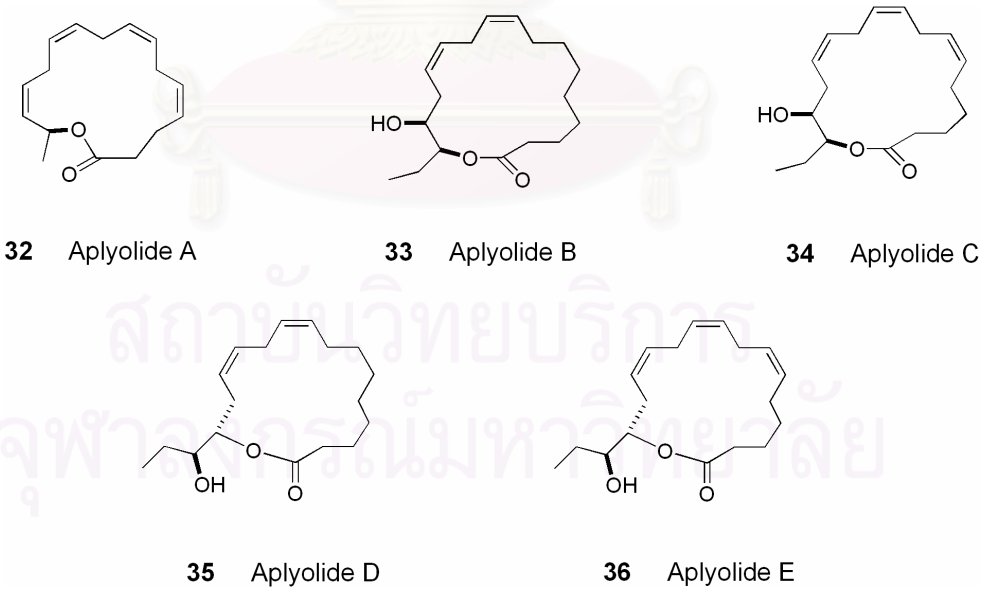

Figure 5. The structures of aplyolide A–E.

2.3. Terpenes

The terpenes isolated from sea hares are almost all halogenated mono-, sesqui-, di-, and tri-terpenoids (Figure 6 and Table 1). They are generally derived from algae on which sea hares feed on and used as chemical protection for the molluscs (McPhail et al., 1999; Wessels et al, 2000; Cimino et al., 2001). The biological significance of natural polyhalogenated terpenoids has been studied as antitumor, particularly for solid tumors (Fuller et al., 1992). However, none of these polyhalogenated terpenoids has been developed as anticancer agents. Some novel terpenoid skeletons have been discovered such as aplydactone [**47**] from the sea hare *Aplysia dactylomela* (Fedorov et al., 2001).

2.4. Other types of compounds

A small number of alkaloid-type metabolites have been discovered from sea hares in the genera *Stylocheilus* and *Aplysia* (Figure 7 and Table 1). Two proline esters named makalika ester [**51**] and makalikone ester [**52**], and a tryptophan peptide, lyngbyatoxin A acetate [**53**] were isolated from Hawaiian collection of the sea hare *Stylocheilus logicauda* (Gallimore, Galario et al., 2000). Additionally, two tryptophan-derived peptides named dactylamides A [**54**] and B [**55**] were discovered from the sea hare *Aplysia dactylomela* (Appleton, Babcock and Copp, 2001). The biosynthesis pathway for compounds **51** and **52** has been proposed to involve the esterification between *N*-methylprolines and *tert*-butyl residue which is further connected to chloro-substituted octatrienol. The presence of *tert*-butyl functionality has been found in metabolites of the cyanobacteria *Lyngbya majuscula*. As the sea hare *Stylocheilus* is known to feed on *L. majuscula* (Burja et al., 2001), the true origin of these isolated compounds should be the algal diet. Lynbyatoxin A was originally isolated from the cyanobacteria *L. majuscula* (Cardellina, Marner and Moore, 1979). Therefore, the occurrence of lynbyatoxin A acetate [**53**] suggested some modification by the mollusc as previously described for laurenisol and allolaurinterol acetates from the sea hare *Aplysia dactylomela* (Appleton et al, 2001). The malyngamides O [**56**], P [**57**], and S [**58**] were amide of methoxylated fatty acid isolated from two genera of sea hares (Figure 7 and Table 1). The details of this class of compound will be discussed in section 3.

Monoterpenes

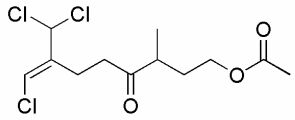

37

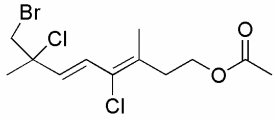

38

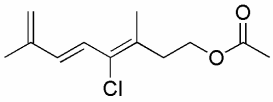

39

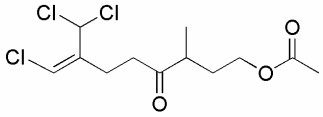

40

Sesquiterpenes

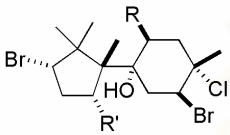

	R	R
41	OAc	OH
42	H	OH
43	H	H

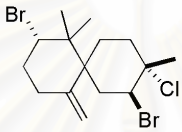

44

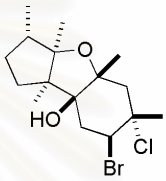

45

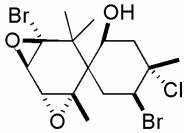

46

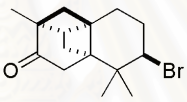

47 Aplydactone

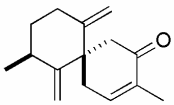

48

Triterpenes

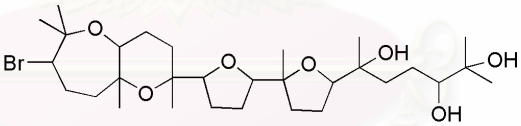

49 Aurirol

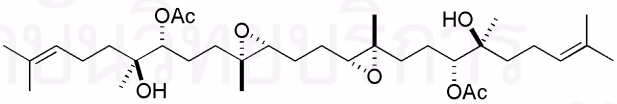

50 Auriculol

Figure 6. The structures of terpenes isolated from sea hares.

Alkaloids

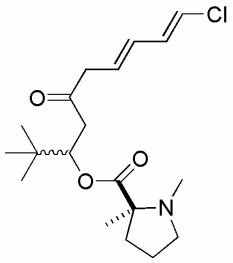

51 Makalika ester

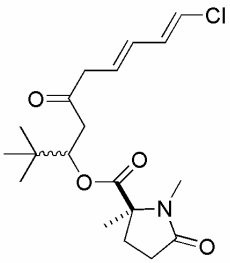

52 Makalikone ester

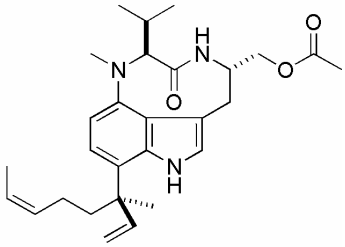

53 Lyngbyatoxin A acetate

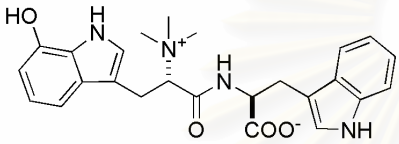

54 Dactylamide A

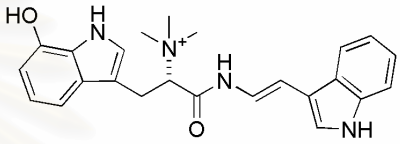

55 Dactylamide B

Malyngamides

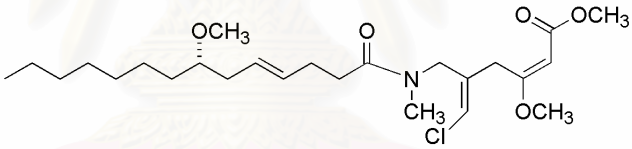

56 Malyngamide O

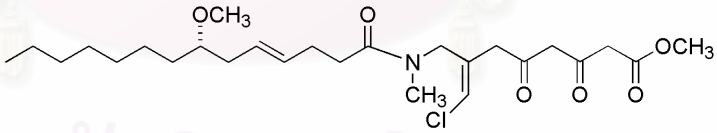

57 Malyngamide P

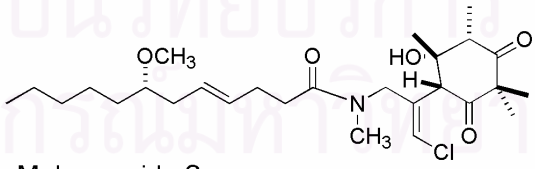

58 Malyngamide S

Figure 7. The structures of alkaloids and malyngamides isolated from sea hares.

Table 1. Compounds isolated from sea hares (January 1995 – March 2005)

Compound	Sea hare	Bioactivity[a]	References
1. Peptides			
1.1) Dolastatin 16 [**8**]	*Dolabella auricularia* (Papua New Guinea)	Cytotoxic to NCI human tumor cell lines, GI_{50} = 0.25 μM	Pettit, Xu, Hogans et al, 1997
1.2) Dolastatin 17 [**9**]	*D. auricularia* (Papua New Guinea)	Cytotoxic to NCI human tumor cell lines, GI_{50} = 0.58–0.10 μM range	Pettit, Xu et al., 1998
1.3) Dolastatin 18 [**10**]	*D. auricularia* (Japan)	Cytotoxic to NCI human tumor cell lines, GI_{50} = 0.63 μM	Pettit, Xu, Williams et al., 1997
1.4) Dolastatin E [**13**]	*D. auricularia* (Japan)	Cytotoxic to HeLa-S_3 cells, IC_{50} = 45–52 μM range	Ojika, Nagoya et al., 1995
1.5) Dolastatin G [**14**] and Nordolastatin G [**15**]	*D. auricularia* (Japan)	Cytotoxic with IC_{50} = 0.93 (**14**) and 5.0 (**15**) μM against HeLa-S_3 cells	Mutou et al., 1996
1.6) Dolastatin H [**16**] and Isodolastatin H [**17**]	*D. auricularia* (Japan)	17 showed *in vivo* antitumor activity to murine P388 leukemia with a T/C = 141% at dose of 6 μg/kg/day	Sone, Shibata et al., 1996
1.7) Dolastatin I [**18**]	*D. auricularia* (Japan)	Cytotoxic to HeLa-S_3 cells, IC_{50} = 23 μM	Sone, Kigoshi, and Yamada, 1997
1.8) Auriride [**21**]	*D. auricularia* (Japan)	Cytotoxic to NCI 60 cell lines, GI_{50} 0.14 μM with microtubule stabilization properties	Suenaga et al., 2004
2. Polyketides			
2.1) Aplyronines A [**22**], B [**23**] and C [**24**]	*Aplysia kurodai* (Japan)	Cytotoxic with IC_{50} = 0.036 (**22**), 4.08 (**23**), and 168 (**24**) nM against HeLa-S_3 cells	Kigoshi et al., 1996
2.2) Dolastatin 19 [**27**]	*D. auricularia* (Gulf of California)	Cytotoxic with IC_{50} = 1.14, and 1.20 μM against MCF-7 and KM20L2 cells, respectively	Pettit et al., 2004

Table 1. (*Continued*)

Compound	Sea hare	Bioactivity[a]	References
2.3) Dolabelides C [**30**] and D [**31**]	*D. auricularia* (Japan)	Cytotoxic with IC_{50} = 2.41 (**30**) and 2.41 (**31**) μM against HeLa-S_3 cells	Seenaga et al., 1997
2.4) Aplyolides A [**32**] to E [**36**]	*A. kurodai* (Australia)	All showed ichthyotoxic to the mosquito fish *Gambusia affinis* at 10 ppm	Spinella et al., 1997
3. Terpenes			
3.1) Monoterpenes [**37**] to [**40**]	*A. punctata* (Spain)	**37**, **38**, and **40** showed cytotoxic with ED_{50} 2.5, 2.5 and 1.5 μg/ml against P-388, A-549, HT-29, and MEL-28 cells, respectively	Ortega, Zubía, and Salvá, 1997
3.2) Sesquiterpenes [**41**] to [**46**]	*A. dactylomela* (South Africa)	-	McPhail and Gerwick, 1999
3.3) Aplydactone [**47**]	*A. dactylomela* (Madagascar)	-	Fedorov et al, 2001
3.4) Chamigrain [**48**]	*Aplysia* sp. (Madagascar)	-	Fedorov et al., 2000
3.5) Aurirol [**49**]	*D. auricularia* (Indian Ocean)	Cytotoxic to HeLa-S_3 cells, IC_{50} = 11 μM	Suenaga et al,, 1998
3.6) Auriculol [**50**]	*D. auricularia* (Japan)	Cytotoxic to HeLa-S_3 cells, IC_{50} = 7 μM	Kigoshi et al., 2001
4. Others			
4.1) Makalika ester [**51**], Makalikone ester [**52**]	*Stylocheilus longicauda* (Hawaii)	**52** showed cytotoxic against P-388, A-H549, and HTB38 cells, IC_{50} = 7–14 μM range	Gallimore, Galario et al, 2000
4.2) Lyngbyatoxin A acetate [**53**]	*S. longicauda* (Hawaii)	cytotoxic against P-388, A-H549, and HTB38 cells, IC_{50} = 0.10 μM	Gallimore, Galario et al, 2000
4.3) Dactylamides A [**54**] and B [**55**]	*A. dactylomela* (New Zealand)	No activity	Appleton, Babcock, and Copp, 2001
4.4) Malyngamides O [**56**] and P [**57**]	*S. longicauda* (Hawaii)	**56** showed cytotoxicity with IC_{50} = 4 μM against P-388, A-549, and HT-29 cells	Gallimore and Scheuer, 2000

Table 1. (*Continued*)

Compound	Sea hare	Bioactivity[a]	References
4.5) Malyngamide S [**58**]	*Bursatella leachii* (New Zealand)	Cytotoxic to NCI human tumor cell lines, GI_{50} = 34 μM	Appleton et al., 2002

[a] HeLa-S_3: human epitheloid carcinoma NCI-H40: non-small cell lung cancer, P-388: mice lymphoma, A-549: human lung carcinoma, HT-29: human colon carcinoma, MEL-28: human melanoma, HTB-38: human colon carcinoma, HL-60: human leukemic carcinoma, MCF-7: human breast cancer, KM20L2: human colon carcinoma

There is an interesting review for bioactive materials isolated from microorganisms inhabiting with sea hares. The fungal strain *Periconia byssoides*, isolated from gastrointestinal tract of the sea hare *Aplysia kurodai*, yielded 16 membered macrosphelides A [**59**], C [**61**], and E [**62**]–I [**66**] (Yamada et al., 2001). The macrosphelides A–D were originally isolated from the culture broth of a microbial, *Macrosphaeropsis* sp. (Hayashi et al., 1995) in which macrosphelide B [**60**] acted as the strongest cell-adhesion inhibitor with ED_{50} = 3.5 μM. The macrosphelides A, C and E–H inhibited the adhesion of human-leukemia HL-60 cells to human-umbilical-vein endothelial cells (HUVEC) with IC_{50} ranging from 8.6–27.2 μM which were more potent than herbimycin A (IC_{50} = 38 μM), a standard sample in the adhesion-assay system. Cytotoxicity of these macrosphelides against P388 lymphocytic leukaemia cells and HL-60 cells was also examined. Macrosphelide H exhibited the highest potent cytotoxicity to P388 cells with ED_{50} = 54 μM, consistent with its potent inhibitory activity in cell-adhesion assay. Structures and cell adhesion inhibitory activity of macrosphelide B isolated from *Macrosphaeropsis* sp., and macrosphelides A, C and E–I isolated from the sea hare *A. kurodai* are shown in Figure 8.

The origins of secondary metabolites from sea hares relating to the dietary algae have been reviewed (Wessels, Kong and Wright, 2000; Burja et al., 2001). For instance, the promising anticancer drug candidate dolastatin 10 [**2**] was first isolated from the Indian Ocean sea hare *Dolabella auricularia* in very low yield (10^{-6} to 10^{-7}% wet weight). However, the true origin of dolastatin 10 has

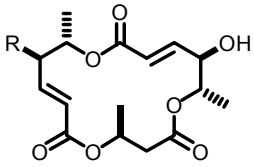

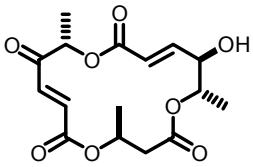

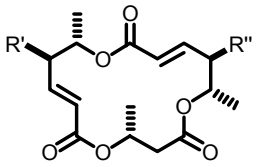

	R'	R''
62	H	H
63	H	OH
64	OH	H

59 R =OH
61 R = H

60

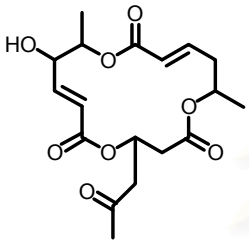

65

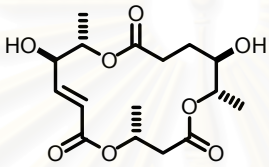

66

Inhibitory activity on cell adhesion

Compound		IC_{50} μM
Macrosphelide A	**59**	18.7
B	**60**	3.5
C	**61**	36.5
E	**62**	19.5
F	**63**	27.2
G	**64**	22.5
H	**65**	8.6
I	**66**	> 100
Herbimycin A		38.0

Figure 8. Structures and cell adhesion inhibitory activity of the macrosphelides.

been recently demonstrated to be the cyanobacterium *Symploca* sp. VP642 of from which dolastatin 10 could be isolated in 10^{-2}% dry weight (Luesch et al., 2001). Discovery of other dolastatin 10 analogues, termed symplostatin 1 [**67**] (Harrigan, Luesch et al., 1998) and symplostatin 3 [**68**] (Luesch, Yoshida, Moore, Paul, Mooberry et al., 2002) have been reported from the cyanobacterium *Symploca hydnoides* and *Symploca* sp. VP452, respectively. Several other dolastatin analogues have recently been isolated as cyanobacterial metabolites. These are summarized in Table 2 and Figure 9.

Table 2. Cyanobacterial origins of the dolastatins originally isolated from sea hares

Compound	Cyanobacteria	Comment	References
1. Dolastatin 10 and analogues			
1.1) Dolastatin 10 [**2**]	*Symploca* sp. VP642 (Palau)	**2** was originally isolated from *Dolabella auricularia*	Luesch et al., 2001
1.2) Symplostatin 1 [**67**]	*Symploca hydnoides* (Guam)	Analogue of dolastatin 10	Harrigan, Luesch et al., 1998
1.3) Symplostatin 3 [**68**]	*Symploca* sp. VP452 (Hawaii)	Analogue of dolastatin 10	Luesch, Yoshida, Moore, Paul, Mooberry et al., 2002
2. Dolastatin 12 and analogues of dolastatins 11 and 12			
2.1) Dolastatin 12 [**4**] 2.2) Lyngbyastatin 1 [**69**]	*Lyngbya majuscula* and *Schizothrix calcicola* assemblages (Guam)	**70** is an analogue of dolastatins 11 [**3**] and 12 [**4**], originally isolated from *D. auricularia*	Harrigan, Yoshida et al., 1998b
2.3) Lyngbyastatin 3 [**70**]	*L. majuscula* (Guam)	Analogue of dolastatins 11 and 12	Williams, Moore, and Paul, 2003
3. Analogues of dolastatin 13			
3.1) Symplostatin 2 [**71**]	*S. hydnoides* (Guam)	Analogue of dolastatin 13 [5], originally isolated from *D. auricularia*	Harrigan et al., 1999
3.2) Somamides A [**72**] and B [73]	*L. majuscula* and *Schizothrix* sp. assemblages (Fiji)	Analogue of dolasatin 13	Nogle, Williamson, and Gerwick, 2001
4. Dolastatin 16 and analogues			
4.1) Dolastatin 16 [**8**]	*L. majuscula* (Madagasca)	**8** was originally isolated from *D. auricularia*	Nogle and Gerwick, 2002
4.2) Homodolastatin 16 [**74**]	*L. majuscula* (Kenya)	Analogue of dolastatin 16	Davies-Coleman et al., 2003

Table 2. (*Continued*)

Compound	Cyanobacteria	Comment	References
5. Others			
5.1) Lyngbyastatin 2 [**75**] and Norlyngbyastatin 2 [**76**]	*L. majuscula* (Guam)	Analogues of dolastatin G [**14**] and nordolastatin G [**15**], respectively, originally were isolated from *D. auricularia*	Luesch et al., 1999
5.2) Mevalonide D [**77**]	*S. hydnoides* (Hawaii)	Analogue of isodolastatin H [**17**], originally isolated from *D. auricularia*	Horgen et al., 2002

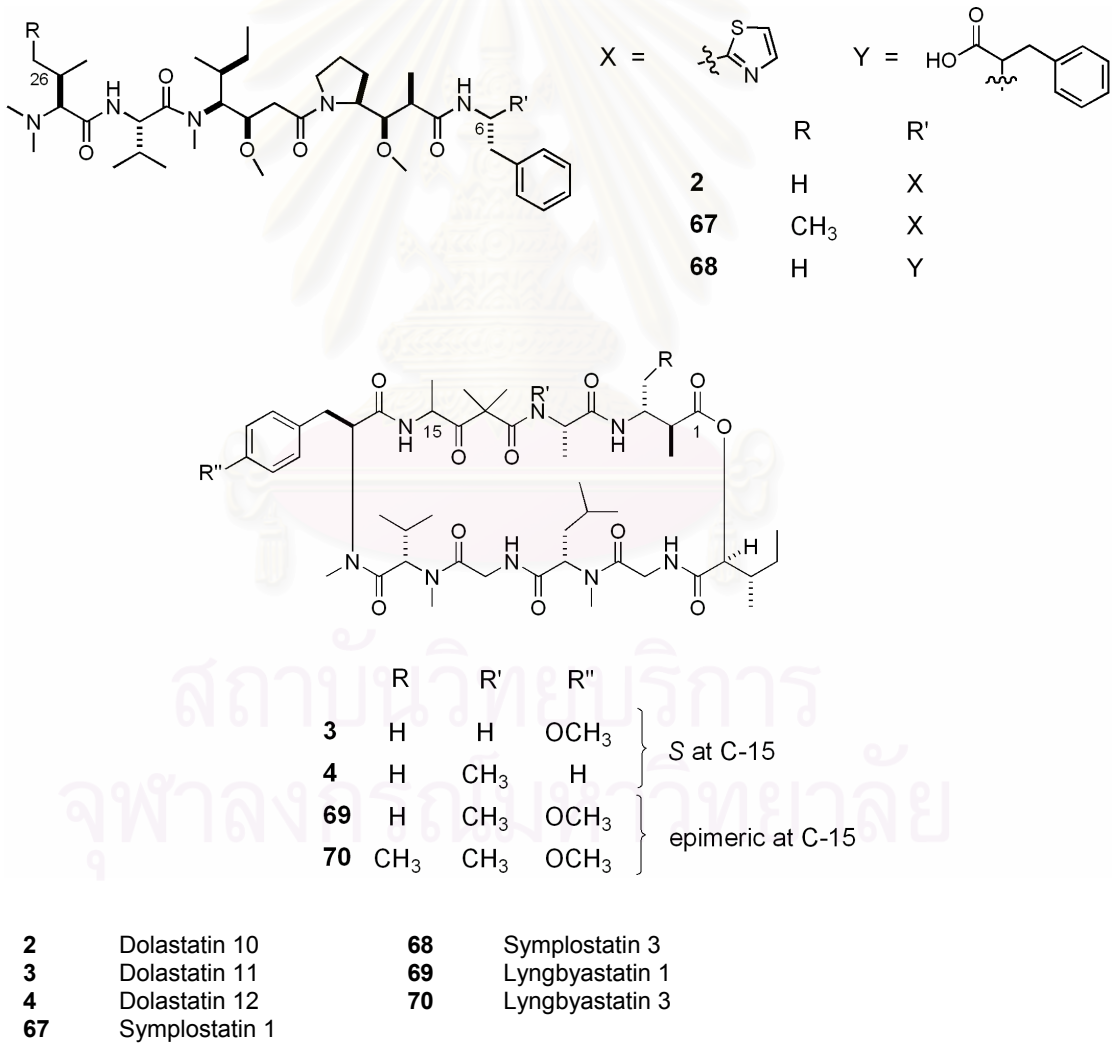

Figure 9. Structures of cyanobacterial-derived dolastatins.

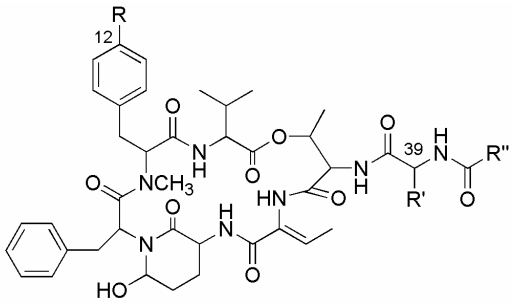

	R	R'	R''
5	H	$CH(CH_3)_2$	$CH(OCH_3)CH_2OH$
73	H	CH_3	H

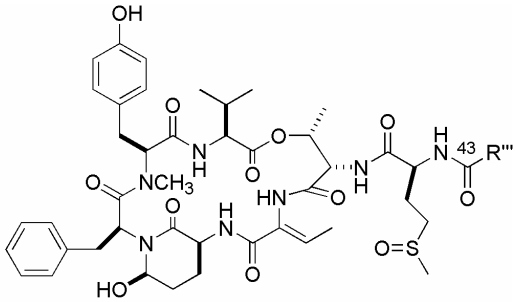

71 R''' = 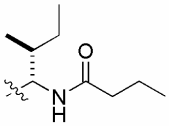

72 R''' = C_5H_{11}

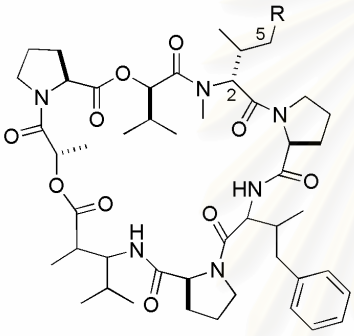

8 R = H

74 R = CH_3

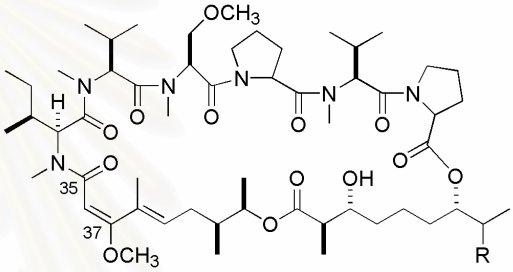

14 R = CH_3

75 R = H

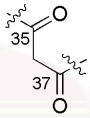

15 R = CH_3

70 R = H

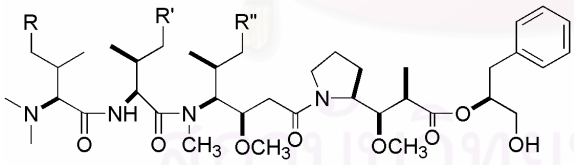

	R	R'	R''
17	H	CH_3	CH_3
77	CH_3	H	H

5	Dolastatin 13	**72**	Somamide A
8	Dolastatin 16	**73**	Somamide B
14	Dolastatin G	**74**	Homodolastatin 16
15	Nordolastatin G	**75**	Lyngbyastatin 2
17	Isodolastatin H	**76**	Norlyngbyastatin 2
71	Symplostatin 2	**77**	Mevalonide D

Figure 9. (*Continued*)

3. Malyngamide-type Natural Products

The malyngamides are a structurally intriguing class of secondary metabolites, which occur in nearly all tropical marine collections of the cyanobacterium *Lyngbya majuscula* as listed in Table 3. All malyngamides are *N*-substituted amides of methoxylated fatty acids. The majority of the fatty acid substructure in malyngamides is 7(*S*)-methoxytetradec-4(*E*)-enoic acid (= lyngbic acid, Figure 10) whereas the 7(*S*)-methoxydodec-4(*E*)-enoic acid (Figure 11), 7-methoxy-9-methylhexadec-4(*E*)-enoic acid (Figure 12), and 7(*S*)-methoxyeicos-4(*E*)-enoic acid (Figure 13) are rarely reported. To date, more than 30 structures of malyngamides have been reported in the literature (Table 3). These compounds showed such biological properties as ichthyotoxicity (malyngamide H [**87**]), brine shrimp toxicity (malyngamides K [**91**]) and cytotoxicity to mouse neuroblastoma cells (malyngamide N [**94**]). Among them, malyngamide J [**90**] has been selected for *in vivo* evaluation by the NCI because of its unusual cytotoxicity profile in the 60 cell line *in vitro* assay and its structural novelty (Wu, Milligan and Gerwick, 1997). While almost all malyngamides have been discovered from the collection of *L. majuscula*, malyngamides O [**56**] and P [**57**] (Gallimore and Scheuer, 2000), and malyngamide S [**58**] (Appleton et al., 2002) were isolated from the sea hares *Stylocheilus logicuada*, and *Bursatella leachii,* respectively. However, the true producers of these malyngamides have been suggested to be the cyanobacteria fed on by the molluscs (Burja et al, 2001).

The amine-derived portion of the malyngamides, though justly complex and variable, is assumed to be of amino acid origins. The amino acid glycine (or in some cases i.e. malyngamides H and J, β-alanine) has been proposed to be the first extension unit of an initial polyketide chain, which then undergoes further polyketide extensions (McPhail and Gerwick, 2003). The C-1 in the glycine-derived residue is usually reduced to a chloromethylene moiety (malyngamides O, S, and M), while in some cases to a methoxy (malyngamides U, V, and W) or hydroxy (malyngamides D and E) group.

Table 3. Malyngamide-type natural products

Compound[a]	Source of compound	Bioactivity[e]	References
Malyngamides A [**78**], B [**79**]and C [**80**]	*Lyngbya majuscula* (Hawaii)	-	Cardellina II et al., 1978; Hannak and Bayer, 1979; Ainslie et al., 1985
Malyngamides D [**81**][d] and E [**82**][d]	*L. majuscula* (Marshall Islands)	-	Mynderse and Moore, 1978
Malyngamides D [**83**][d] and its acetate [**84**][d]	*L. majuscula* (Puerto Rico shore)	**83** exhibited cytotoxic to KB cells (ED_{50} 68 μM)	Gerwick, Reyes, and Alvarado, 1987
Malyngamide F [**85**]	*L. majuscula*	-	Cited in Burja et al., 2001
Malyngamide G [**86**][b]	*L. majuscula* (French coast)	Potent immunosuppressive property (ED_{50} = 16 μM)	Praud et al., 1993; Mesguiche et al., 1999
Malyngamide H [**87**]	*L. majuscula* (shallow water, Netherlands)	Ichthyotoxic to gold fish (LC_{50} = 12 μM, EC_{50} = 5 μM)	Orjala, Nagle, and Gerwick, 1995
Malyngamides I [**88**] and its acetate [**89**]	*L. majuscula* (on a reef, Japan)	**88** was toxic to brine shrimp (LD_{50} =73 μM), gold fish (LD_{50} < 20 μM); **89** exhibited cytotoxic to Neuro-2a neuroblastoma (IC_{50} = 12 μM)	Todd and Gerwick, 1995
Malyngamides J [**90**], K [**91**] and L [**92**]	*L. majuscula* (Scuba diving, Curacao)	-Toxic to goldfish with LC_{50} 66, 14 and 17 μM, respectively -Toxic to brine shrimp with LC_{50} 30, 17 and 32 μM, respectively	Wu, Milligan, and Gerwick, 1997
Malyngamides M [**93**] and N [**94**]	Red alga *Gracilaria coronopifolia* (Maui)	Cytotoxic to Neuro-2a mouse neuroblastoma cells with IC_{50} > 20 and 12 μM, respectively	Kan et al., 1998
Serinol-derived malyngamides A [**95**][c] and B [**96**][c]	Unidentified blue-green alga (river, Australia)	-	Wan and Erickson, 1999
Malyngamides O [**56**] and P [**57**]	sea hare, *Stylocheilus longicauda* (Scuba diving, Hawaii)	**56** was cytotoxic to P-388, A-549, and HT-29, all with IC_{50} 4 μM	Gallimore and Scheuer, 2000

Table 3. (*Continued*)

Compound[a]	Source of compound	Bioactivity[e]	References
Malyngamides Q [**97**] and R [**98**]	*L. majuscula* (shallow water, Madagascar)	**98** was toxic to brine shrimp (LD_{50} 18 ppm)	Milligan, Márquez, Willamson, Davies-Coleman et al., 2000
Isomalyngamides A [**99**] and B [**100**]	*L. majuscula* (Kahala beach, Hawaii)	Toxic to crayfish with LD_{50} 450 and 900 μM, respectively	Kan et al., 2000
Hermitamides A [**101**] and B [**102**]	*L. majuscula* (shallow water, Papua New Guinea)	-Toxic to brine shrimp with LD_{50} 14 and 45 μM, respectively -Cytotoxic to Neuro-2a mouse neuroblastoma cells with IC_{50} 6 and 14 μM, respectively -Only 101 showed ichthyotoxicity to gold fish with LD_{50} 53 μM	Tan, Okino, and Gerwick, 2000
Malyngamide S[b] [**58**]	Sea hare, *Bursatella leachii* (New Zealand)	Cytotoxicity to HL-60, P-388, BSC-1, and NCI human tumor activity	Appleton et al., 2002
Malyngamide T [**103**]	*L. majuscula* (shallow water, Puerto Rican)	-	Nogle and Gerwick, 2003
Malyngamides U [**104**][b], V [**105**][b] and W [**106**][b]	*L. majuscula* (shallow water, New Geinea)	In active in brine shrimp toxicity assay	McPhail and Gerwick, 2003

[a] If not indicated otherwise, malyngamides with 7(*S*)-methoxytetradec-4(*E*)-enoic acid

[b] malyngamides with 7(*S*)-methoxydodec-4(*E*)-enoic acid

[c] Malyngamides with 7-methoxy-9-methylhexadec-4(*E*)-enoic acid

[d] Malyngamdies with 7(*S*)-methoxyeicos-4(*E*)-enoic acid

[e] P-388: mice lymphoma, A-549: human lung carcinoma, HT-29: human colon carcinoma, HL-60: human leukemic, KB: human epidermoid carcinoma of nasopharynx

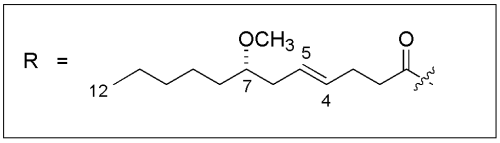

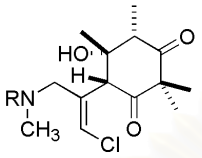

58 Malyngamide S

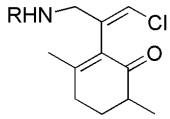

86 Malyngamide G

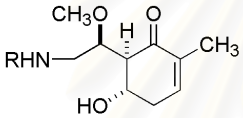

104 Malyngamide U

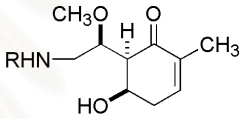

105 Malyngamide V

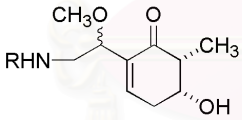

106 Malyngamide W

Figure 10. Malyngamides with 7(*S*)-methoxydodec-4(*E*)-enoic acid.

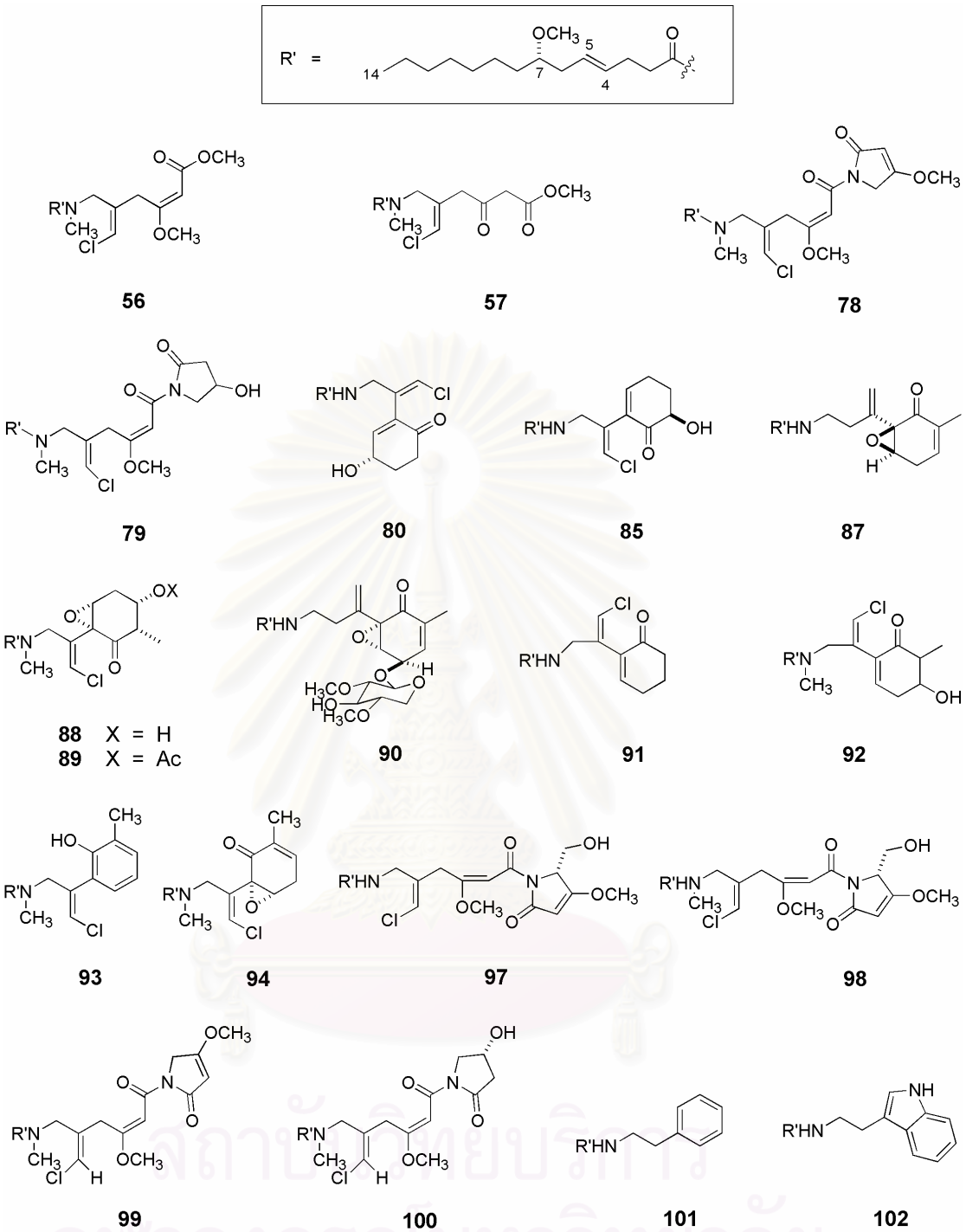

56	Malyngamide O	**88**	Malyngamide I	**97**	Malyngamide Q
57	.....P	**89**	.....I acetate	**98**	Malyngamide R
78	.....A	**90**	.....J	**99**	Isomalyngamide A
79	.....B	**91**	.....K	**100**	Isomalyngamide B
80	C	**92**	L	**101**	Hermitamide A
85	.....F	**93**	.....M	**102**	Hermitamide B
87	.....H	**94**	.....N		

Figure 11. Malyngamides with 7(*S*)-methoxytetradec-4(*E*)-enoic acid.

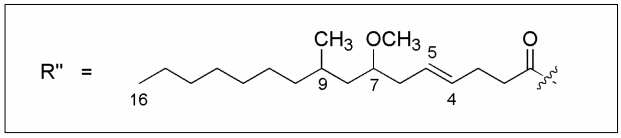

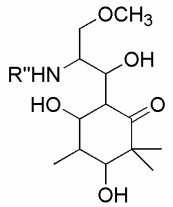

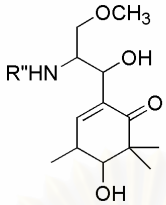

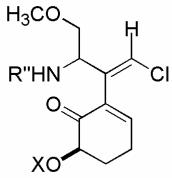

81 Malyngamide D **82** Malyngamide E **83** Malyngamide D X = H

84 Malyngamide D acetate X = Ac

Figure 12. Malyngamides with 7-methoxy-9-methylhexadec-4(*E*)-enoic acid.

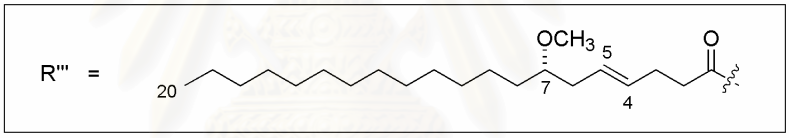

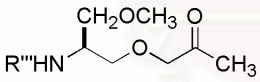

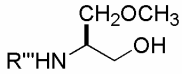

95 Serinol-derived malyngamide A **96** Serinol-derived malyngamide B

Figure 13. Malyngamides with 7(*S*)-methoxyeicos-4(*E*)-enoic acid.

4. Hectochlorin and Structurally Related Compounds

These compounds are characterized by the presence of a dichlorinated *β*-hydroxy octanoic acid unit and two thiazole hydroxy acid units. Currently, a small number of compounds structurally related to hectochlorin [**107**] has been found in nature, including dolabellin [**108**] and a series of lyngbyabellins [**109**]–[**112**]. Structures and biological activities of these compounds are shown in Figure 14 and Table 4, respectively. Dolabellin, originally isolated from the sea hare *Dolabella auricularia*, is the first example of this structural class and is the first natural product containing a thiazole hydroxy acid residue (Sone et al., 1995). Since then, they were discovered from various strains of the cyanobacterium *Lyngbya majuscula*. These includes hectochlorin (Marquez et al., 2002) and a series of lyngbyabellins (Luesch, Yoshida, Moore, and Paul, 2000; Luesch, Yoshida, Moore, Paul, and Mooberry, 2000; Luesch, Yoshida, Moore, and Paul, 2002; Milligan, Márquez, Williamson, and Gerwick, 2000; Williams, Yoshida et al., 2003). These findings strongly support a cyanobacterial origin for dolabellin, which is consistent with previous findings about the origin of dolastatins and malyngamides O, P and S.

Hectochlorin [**107**] was first isolated from the Jamaican cyanobacterium *L. majuscula* (Marquez et al., 2002). **107** has been shown to be a potent stimulator of actin assembly, and exhibit inhibitory activities toward the NCI 60-cell line assay with an average GI_{50} of 5.1 μM and the fungus *Candida albicans* causing 11 mm zone of inhibition at 10 μg/disc (disc diameter, 6 mm). The hyperpolymerization effect on the protein actin of **107** is as potent as the standard sample jasplakinolide. The EC_{50} values for the two compounds were 20 $\pm$ 0.6 and 19 $\pm$ 0.5 μM, respectively. Stereostructure of **107** was determined through single X-ray crystallography as several heavy atoms (chlorine and sulfur) are within the molecule. When hectochlorin was subjected to recrystallization in a mixture of MeOH and water, hectochlorin hydrate, with one molecule of water, cocrystallized with the compound (Marquez et al., 2002). This molecule of water occupies the central cavity, forming hydrogen bonds to the two imino nitrogens in both thiazole rings. A total synthesis of **107** was achieved by Cetusic and colleagues (2002).

A series of lyngbyabellins [**109**]–[**112**] were isolated from particular strains of *L. majuscula* found in Palau and Guam (Table 4). The compounds are either cyclic [**109**]–[**111**] or acyclic [**112**] with a variety of stereochemical configurations. Comparing their cytotoxicity against human epidermoid carcinoma of nasopharynx (KB), **109** exhibited strongest activity with IC_{50} = 0.04 μM whereas **110–112** showed IC_{50} in the 0.1–2.1 μM range (Table 4). Therefore, two thiazole rings and isoleucine-derived unit at C-15 are considered to be important for cytotoxic activity. However, the macrocyclic structure has little effect on cytotoxicity as the acyclic lyngbyabellin D [**112**] was as potent as the cyclic lyngbyabellins B [**110**] and C [**111**].

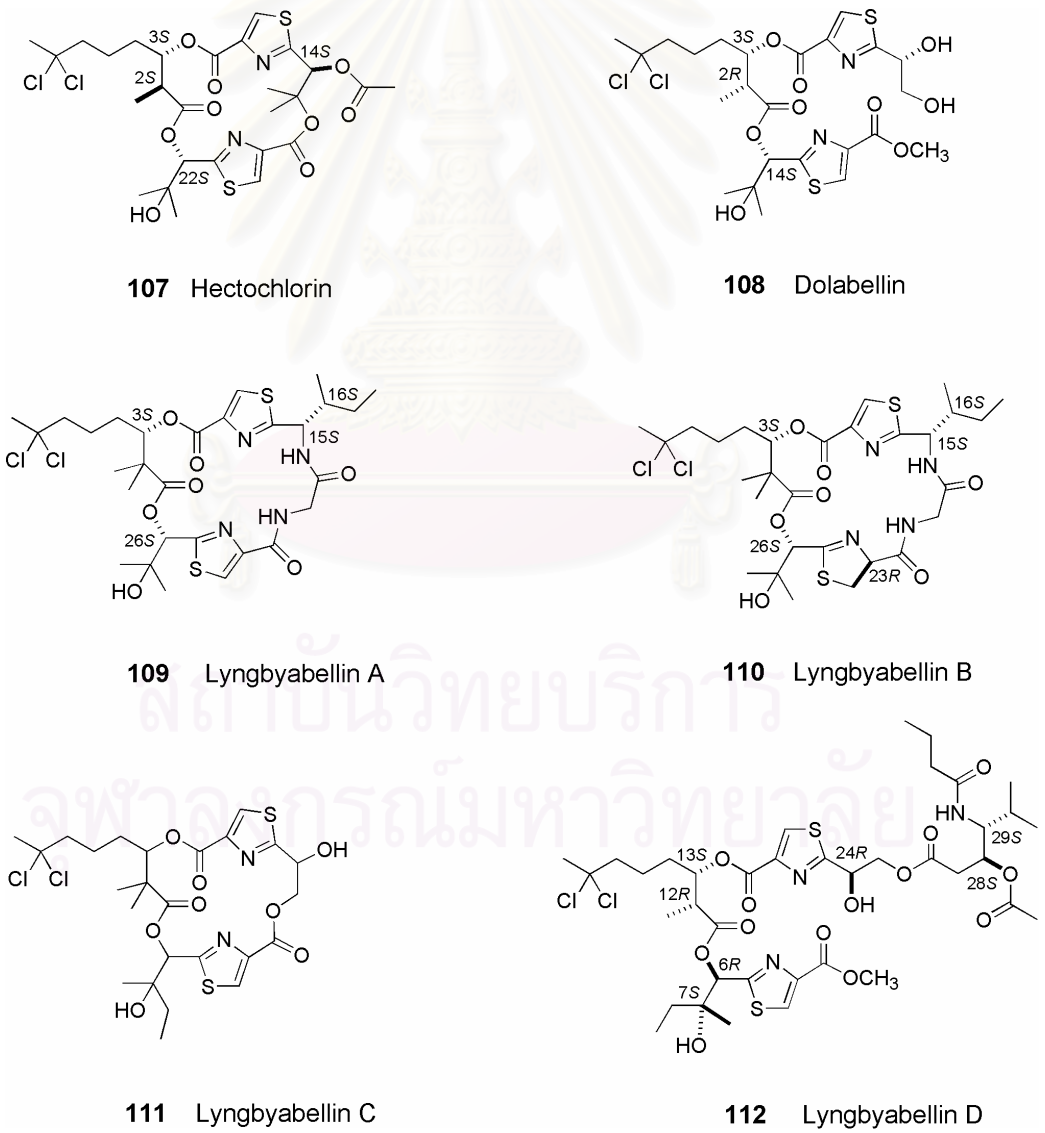

Figure 14. Hectochlorin and its structurally related compounds.

Table 4. Biological activities of hectochlorin and its structurally related compounds

Compound	Source	Bioactivity[a]	References
Hectochlorin [**107**]	Cyanobacterium, *Lyngbya majuscula* collected from Jamaica and Panama	- Fungicide with 16 mm zone of inhibition at 100 μg/6 mm disk - Cytotoxic to NCI human tumor cell lines, GI_{50} = 5.1 μM - Stimulator of actin assembly, EC_{50} = 20 μM	Marquez et al., 2002
Dolabellin [**108**]	Indian Ocean sea hare, *Dolabella auricularia*	Biological testing is not performed due to limit amount of compound	Sone et al., 1995
Lyngbyabellin A [**109**]	Guamanian strain of cyanobacterium *L. majuscula*	- Cytotoxic with IC_{50} 0.04 and 0.7 μM against KB and LoVo cells, respectively - Toxic to mice: LD_{50} 2.4–8.0 mg/kg - Cytoskeleton-disrupting effect to A-10 cells at 0.01–5.0 μg/ml	Luesch, Yoshida, Moore, Paul, and Mooberry, 2000
Lyngbyabellin B [**110**]	Guamanian strain of cyanobacterium *L. majuscula*	- Cytotoxic with IC_{50} 0.1 and 1.22 μM against KB and LoVo cells, respectively - Toxic to brine shrimp: LD_{50} 3.0 ppm - Fungicide with 10.5 mm zone at 100 μg/ 6 mm disk - Stimulator of actin assembly, EC_{50} > 50 μM	Luesch, Yoshida, Moore, and Paul, 2000; Milligan, Marquez, Williamson, and Gerwick, 2000
Lyngbyabellin C [**111**]	Palauan strain of cyanobacterium *L. majuscula*	- Cytotoxic with IC_{50} 2.1 and 5.3 μM against KB and LoVo cells, respectively	Luesch et al., 2002
Lyngbyabellin D [**112**]	Recollection of Guamanian strain of cyanobacterium *L. majuscula*	- Cytotoxic with IC_{50} 0.1 μM against KB cells	Williams, Yoshida et al., 2003

[a] KB: human epidermoid carcinoma of nasopharynx, LoVo cells: human colon adenocarcinoma cell line

The natural chlorinated carboxylic acids have been found as the major constituents among organohalogen compounds in fish, mollusces, and some other invertebrates and sea weed (Dembitsky and Srebnik, 2002). Chlorinated fatty acids could be incorporated into the natural peptides (dolabellin [**107**] and hectochlorin [**108**]), alkaloids (alkaloid [**113**]); and as chlorinated derivatives of fatty acid amides (mirabimide E [**114**]) as shown in Figure 15.

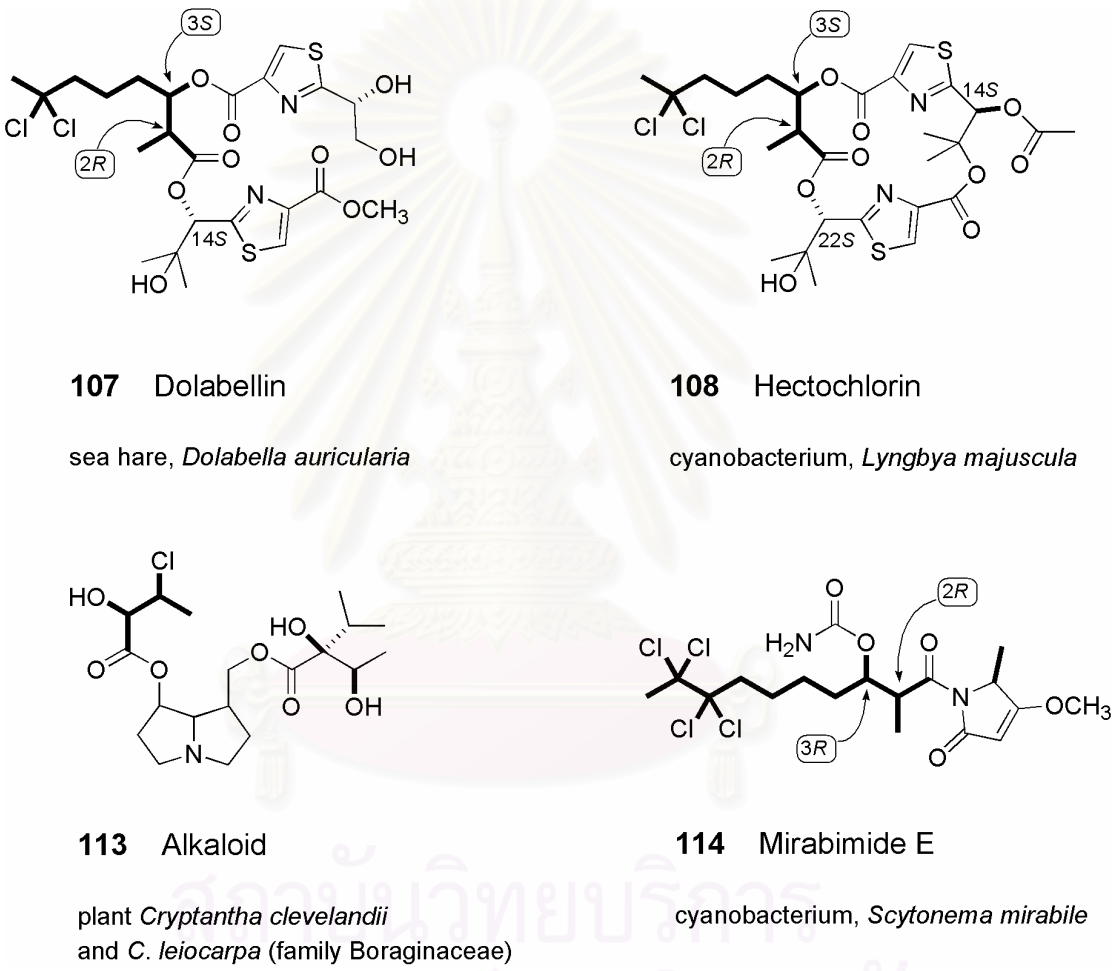

Figure 15. Structures of some natural products containing chlorinated fatty acid.

5. NMR Chiral Derivatizing Agents (CDA) and NMR Chiral Solvating Agents (CSA)

Assignment of the absolute configuration is an important aspect of the stereostructure determination process for both synthetic and natural compounds. Many methods for absolute configuration assignment are known which involve (chiral) chromatographic techniques, X-ray diffraction analysis, CD spectroscopy and NMR methods (Neri and Tringali, 2001). Of the various options available for this task, the use of chromatographic techniques involved with simple or chiral GC or HPLC are widely employed in determining the absolute configuration of amino acid composition of the naturally occurring peptides. The method is used to deduce the stereochemistry of amino acid in two steps. First, acid/alkaline hydrolysis of the peptides affords amino acids hydrolysate. Second, the hydrolysate is subjected to chiral chromatographic column and the retention times were analyzed in comparison with those of authentic standards (see for instance, Williams, Luesch et al, 2003). In the alternative way, the hydrolysate is subjected to derivatization with Marfey's reagent prior to HPLC analysis (or HPLC-MS analysis in advanced Marfey's method, see: Fujii et al., 1998) and comparing the retention times to Marfey's derivatives of authentic standards (see for instance, MacMillan et al, 2002; Davies-Coleman et al, 2003). However, application of this hydrolytic degradation method to natural products is diminished with the amount of the natural material, the availability of the authentic standards, and the racemization or instability of amino acid hydrolysate under ordinary hydrolysis conditions (Fujii et al, 2002). In some cases the application of the crystallographic methods utilizing heavy atom derivatives is useful for absolute configuration assignment of natural products (see for instance, Marquez et al, 2002). However, the availability of a suitable crystal places a serious limitation on the method. The NMR spectroscopy utilizing chiral derivatizing agents (CDA) and chiral solvating agents (CSA) are the alternative methods for direct assignment of absolute configuration. These methods make use of chemical shift differences between esters (or amides) derived from both enantiomers of chiral derivatizing agent, or solvate complexes formed between the compound and enantiomers of chiral solvating agent.

5.1. NMR chiral derivatizing agent (CDA)

The most widely used NMR chiral derivatizing technique is the Kakisawa–Kashman modification (Ohtani et al.,1991) of the Mosher method (Dale and Mosher, 1968) using 2-methoxy-2-phenyl-2-(trifluoromethyl)acetic acid (MTPA, **115**) as CDA. This useful technique, generally known as the modified Mosher's method, analyses the absolute stereochemistry of secondary alcohols (and primary amines) using the differences between the chemical shifts of the protons arising from the shielding influence of the aromatic ring of (*R*)- and (*S*)-MTPA esters as depicted in Figures 16**A** and **B**. In the MTPA esters, the $\Delta\delta$ values ($\delta_S - \delta_R$) for protons adjacent to the secondary alcohol are negative for the protons oriented on the left-hand side of the MTPA plane (L^3), but for those located on the right side (L^2) the values are positive. These rules rely on the ester or amide taking up the ideal geometry proposed by Mosher in which the carbinyl proton and ester carbonyl and trifluoromethyl groups of the MTPA moiety lie in the same plane.

Another popular CDA in the absolute configuration assignment of alcohols is methoxy-(2-naphthyl)acetic acid (2NMA, **116**) because of the greater anisotropic effect of the 2-naphthyl group compared to the benzene ring of MTPA. Conversely, in NMA esters, the conformational model retains with the α-methoxy group near coplanar with the carbonyl as reported for esters of *O*-methoxy mandelic acid (MPA) (Takahashi, Kato et al., 1999; Takahashi, Iwashima and Iguchi, 1999, Porto et al., 2003). The conformational correlation model for NMA esters have been proposed as depicted in Figure 16**C** and the chemical shift differences are defined as $\Delta\delta = \delta_R - \delta_S$. Therefore, protons on the right side of the NMA plane must have positive values ($\Delta\delta > 0$) and protons on the left side of the plane must have negative values ($\Delta\delta < 0$) in agreement with configurational correlation model for the MTPA esters shown in Figure 16**B**.

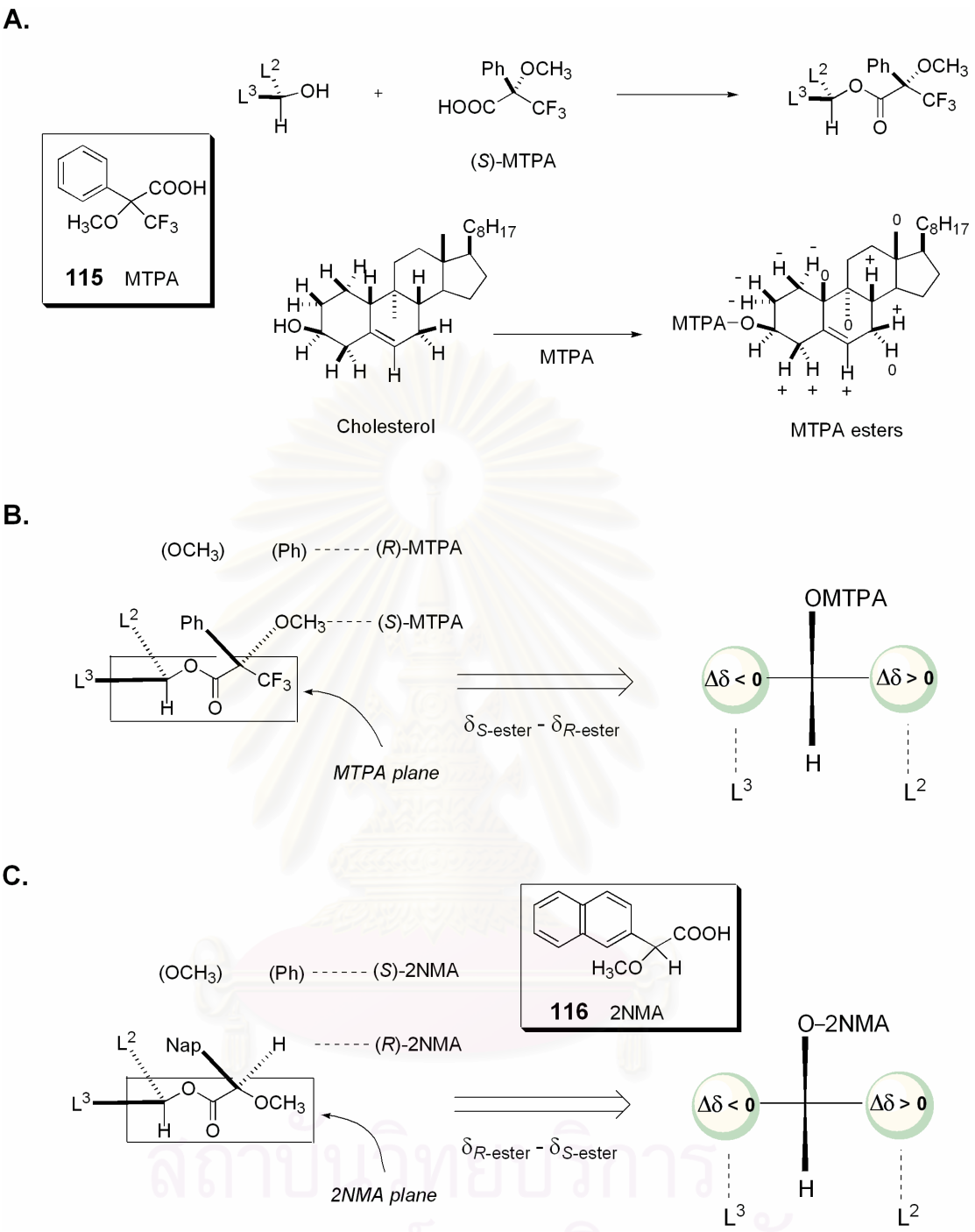

Figure 16. (A) Determination of the absolute configuration of cholesterol and the signs of $\Delta\delta$ values of its MTPA esters (Othani et al., 1991). (B) Configurational correlation model for (*R*)-MTPA derivative and (*S*)-MTPA derivative. (C) Configurational correlation model for (*R*)-2NMA and (*S*)-2NMA derivative.

Other than MTPA, a variety of new and efficient auxiliaries have been developed (Figure 17) that can be applied to diverse monofunctional compounds such as secondary and primary alcohols, amines or carboxylic acids, and polyfunctional compounds (ie. diols) (for reviews see: Parker, 1991; Morris, 2001; Seco, Quiñoá and Riguera, 2001; Wenzel and Wilcox, 2003).

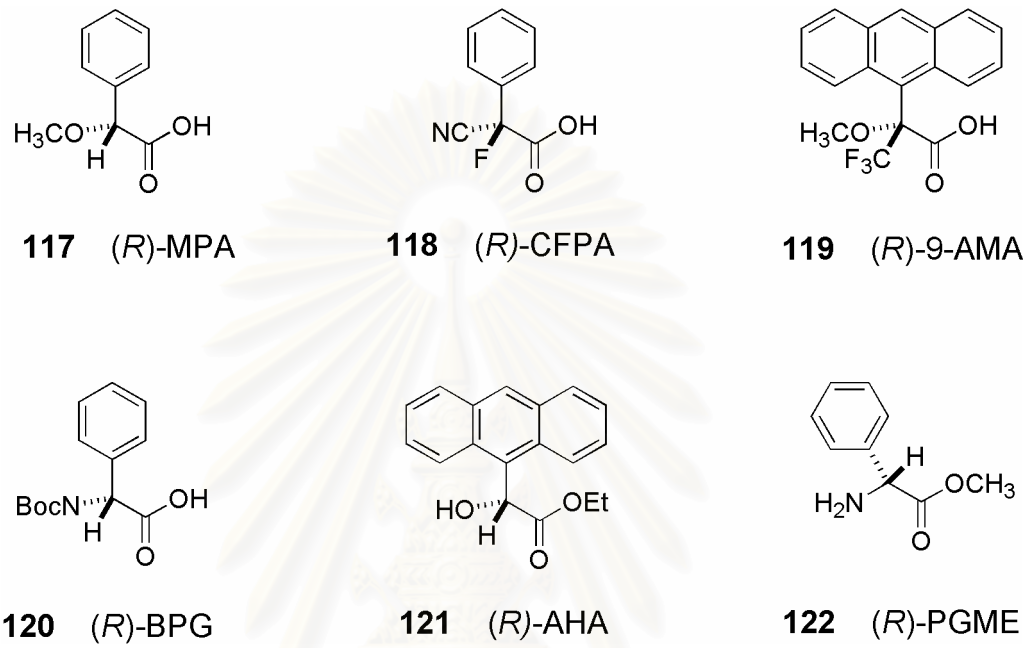

Figure 17. Common chiral derivatizing agents for ^{1}H NMR analysis.

The high reactivity and resolution efficiency CDA α–cyano–α–fluorophenylacetic acid (CFPA, **118**) has been synthesized for application with hindered secondary alcohols and primary amines (Takeuchi, Itoh and Koizumi, 1992; Takeuchi et al., 1998). However, the use of this reagent is limited by its commercial unavailability and difficulty of synthesis method in optically pure form. The choice of three fused aromatic substituent in 2-Anthracen-9-yl-3,3,3-trifluoro-2-methoxy-propionic acid (9-AMA, **119**) is made on the basis of the greater anisotropy of the aromatic ring relative to phenyl ring of MTPA [**115**] and MPA [**117**] (Seco, Quiñoá and Riguera, 1999a). This reagent is advocated when the application of MTPA gives identical signs for Δδ. Boc-phenylglycine (BPG, **120**) is suitable for determining absolute configuration of chiral amines because its amide derivatives have been shown to provide much greater enantiomeric distinction than when observed with the corresponding MTPA and MPA (Seco, Quiñoá and Riguera,

1999b). New CDAs such as anthracen-9-yl-hydroxy-acetic acid ethyl ester (AHA, **121**) (Ferreiro et al., 2000) and phenylglycine methyl ester (PGME, **122**) (Yabuchi and Kusumi, 2000) have been designed for determining absolute configuration of chiral carboxylic acids (Scheme 2).

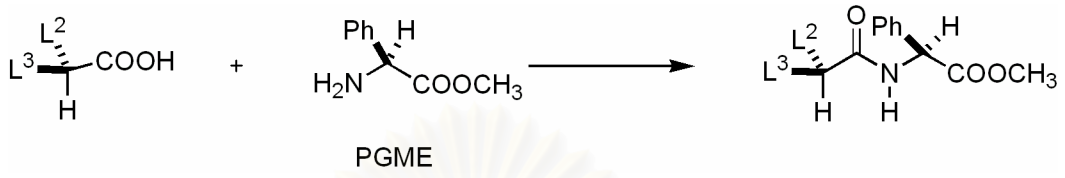

Scheme 2. Determination of the absolute configuration of chiral carboxylic acid using PGME esters.

In addition, for secondary alcohols and primary amines, the procedures for the determination of their absolute stereochemistry have been simplified to the use of only one CDA enantiomer (Seco, Quiñá and Riguera, 2001). The method is based on selective modification of the conformational equilibrium by lowering the temperature of the NMR probe.

5.2. NMR chiral solvating agent (CSA)

NMR chiral solvating agents (CSA) are optically pure compounds that bind *in situ* to the substrate through non-covalent, intermolecular forces (Wenzel and Wilcox, 2003). They are widely applied in the analysis of enantiomeric excess by recording the ^{19}F or ^{1}H NMR spectrum of diastereomers forming by the associated complexes of a pair of enantiomers with a CSA. This application pioneered by Pirkle and Beare (1969) has recently been reviewed by Parker (1991), and by Wenzel and Wilcox (2003). Analysis in the presence of CSA has also been carried out for the assignment of absolute configuration. The latter use follows from the possibility of relating the sense of chemical shift non-equivalence (upfield *vs*. downfield of a signal) for one enantiomer of a compound dissolved in a given CSA, to the configuration of that enantiomer (for reviews see: Parker, 1991; Morris, 2001; Wenzel and Wilcox, 2003). The most frequently used CSAs are shown in Figure 18.

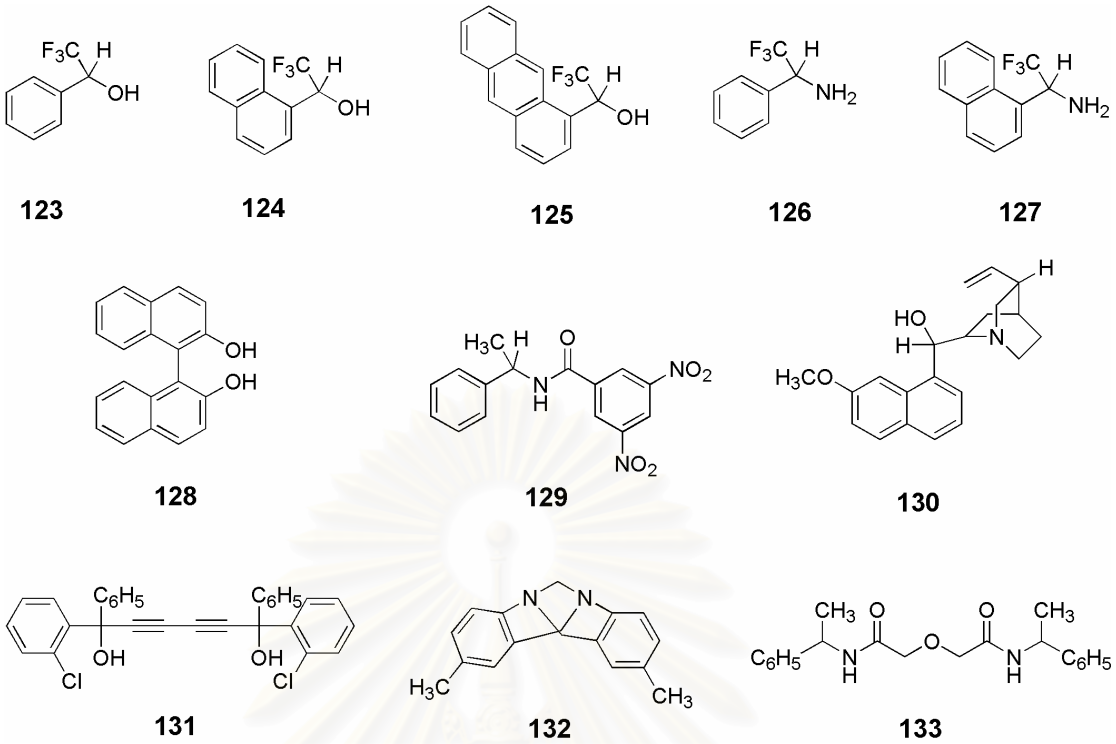

123 2,2,2-trifluoro-1-phenylethanol
124 2,2,2-trifluoro-1-naphthylethanol
125 2,2,2-trifluoro-1-(9-anthrylethanol), TFAE
126 2,2,2-Trifluoro-1-phenyl-ethylamine
127 2,2,2-Trifluoro-1-naphthalen-1-yl-ethylamine
128 1,1'-binaphthalenyl-2,2'-diol
129 *N*-(3,5-dinitrobenzoyl)-α-methylbenzylamine
130 quinine
131 1,6-Bis-(2-chloro-phenyl)-1,6- diphenyl-hexa-2,4-diyne-1,6-diol
132 Tröger's base
133 *N*-(1-Phenyl-ethyl)-2-[(1-phenyl-ethylcarbamoyl) -methoxy]-acetamide

Figure 18. Common chiral solvating agents (Parker, 1991; Morris, 2001).

Wenzel and Wilcox (2003) divided CSAs into two groups based on their interaction (complexation) with substrates. The first group is called "host-guest system" CSAs. The most often studied hosts are crown ethers and cyclodextrins. The ion-pairing interaction that occurs in these systems enhances the enantiomeric discrimination of substrates. The cationic cyclodextrins such as protonated amine (Kitae, Takashima and Kano, 1999) is useful for anionic substrates. Similarly, anionic cyclodextrins such as sulfobutylether (Owens et al., 2000) and carboxymethylthio derivatives (Kano and Hasegawa, 2001; Kano, Hasegawa and Miyamura, 2001) are useful for cationic substrates. The second group is called "donor-acceptor system" CSAs. Donor-acceptor CSAs incorporate sites for hydrogen

bonding or other dipole-dipole interactions, either electron-rich or electron-deficient aromatic rings for π-π interactions, or groups that may sterically hinder association of one configuration of a pair of enantiomers. The classic example of a donor-acceptor CSA is trifluoromethyl-1-aryl ethanol derivatives such as compounds **123**–**127**. Among these, the enantiomers of TFAE [**125**] have been used to determine the absolute configurations of both synthetic and natural compounds which include cyclic α-hydroxy carbonyl compound, lacinilene C methyl ether (Stipanovic et al., 1986), and annonaceous butenolides (Latypov et al., 2002; Jullian et al., 2003).

The phytoalexin lacinilene C methyl ether [**134**] has been isolated from foliar cotton plant tissue. The absolute configuration of **134** was determined through a combination of CD spectroscopy, chiral chromatography, and NMR chiral solvating agents (Stipanovic et al., 1986). From analysis of the sense of unequivocal shifts which appeared in ^{1}H NMR spectra of synthetic (*S*)- and (*R*)-**134**, the diastereomeric solvation model between both enantiomers of **134** and (*S*)-TFAE has been proposed as shown in Figure 19. The primary interaction occurs between the acidic hydroxyl group of TFAE and a primary basic site, the hydroxyl oxygen in **134**, whereas the secondary interaction occurs between the carbinyl hydrogen (weakly acidic due to the inductive effect of the trifluoromethyl group) and a secondary basic site, the carbonyl oxygen of **134**. The diastereomeric solvation complexes showed NMR discrimination due to the stereochemically dependent shielding exerted by the anthryl substituent of TFAE. The anthryl substituent of (*S*)-TFAE caused the aromatic methyl and methoxyl protons signal of (*S*)-**134** to occur at a lower field than that of (*R*)-**134**. As the natural **134** exhibited the same sense of ^{1}H NMR non-equivalence to that of the synthetic (*S*)-**134**, the (*S*)-configuration was assigned to lacinilene C methyl ether. This assignment was consistent with the results obtained by CD spectroscopy and chiral chromatographic experiments.

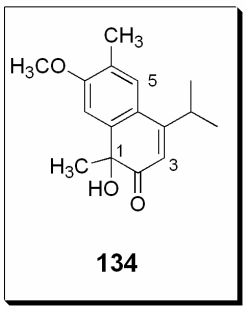

NMR spectral non-equivalence observed for (S)-134 with (S)-TFAE

proton	δ	non-equivalence in ppm (sense)
Ar-OCH_3	3.31	0.044 (H = high field)
Ar-CH_3	2.23	0.025 (H)
C5-H	7.09	0.024 (H)
C3-H	6.04	-

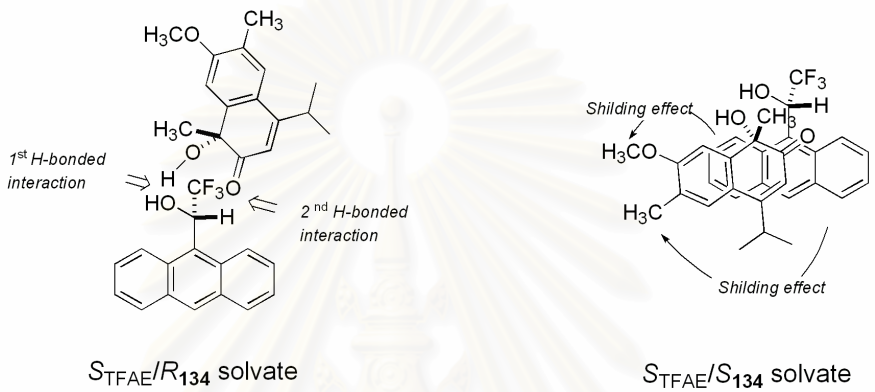

Figure 19. Proposed solvation model between (A) (*R*)-lacinilene C methyl ether (*R*-**134)** and (B) (*S*)-lacinilene C methyl ether (*S*-**134**) and (*S*)-TFAE (Stipanovic et al, 1986).

Acetogenins of the Annonaceae are typical examples of compounds bearing 5-methylfuran-2(5*H*)one at one terminus, known as γ-methyl butenolide moiety. Latypov and colleagues (2002) have recently reported their achievement in applying the NMR chiral solvating agents for determining absolute configuration of several annonaceous butenolides without derivatisation or immolation of the compounds. A simple racemic 5-methylfuran-2(5*H*)one [**135**] was synthesized and used to establish the configurational correlations of this compound and the sense of ^{1}H NMR chemical shift non-equivalence. First, the authors reported a "one-point interaction" of the intermolecular hydrogen bonding between carbinol hydrogen of TFAE and carbonyl oxygen of the lactone **135** and the dipole-dipole interaction between the CSA fragment and the substrate moiety to stabilize the CSA-substrate complex (Latypov et al., 2002). However, this was different from model between lactones and TFAE previously proposed by Pirkle (Parker, 1991; Wenzel and Wilcox, 2003) as shown in Figure 20**A**. Later, they proposed "two-point interaction" showing

one hydrogen bond between carbinol hydrogen of TFAE and the lactone carbonyl of **135**, and another hydrogen bond between the carbinyl hydrogen of TFAE and the ring oxygen of the lactone (Jullian, 2003), which was in agreement with Pirkle's model (Figure 20**B**). Therefore, aromatic shielding effect of the anthryl ring should lead to upfield shifts for 5-CH_3 and 5-H protons in $R_{TFAE}S_{135}$ and $S_{TFAE}S_{135}$, respectively, and this can be used to establish the absolute configuration at this chiral center.

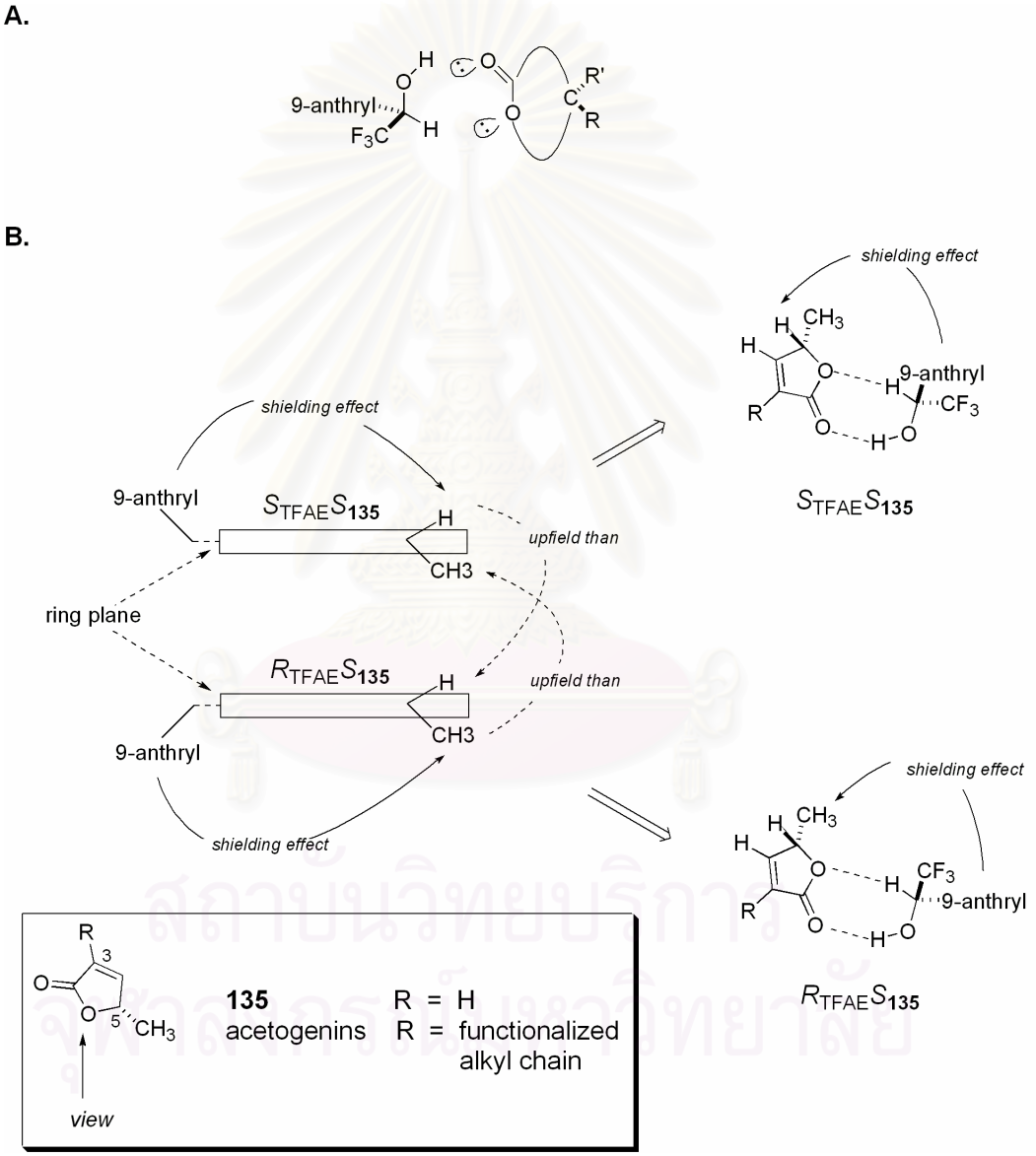

Figure 20. A) Association of racemic lactones with TFAE as proposed by Pirkle (Wenzel and Wilcox, 2003). (B) Proposed solvation model between (*R*)- and (*S*)-TFAE and (*S*)-**135** (Jullian, 2003).

Several natural 5-methylfuran-2(5*H*)ones were analyzed and the absolute configuration of their butenolide moiety could be determined correctly by using the sense of chemical shift non-equivalence referring to the proposed solvation model shown in Figure 20B. Interestingly, the presence of basic sites (i.e. tetrahydrofuran or hydroxyl) did not interfere with the major solvation of the reagent with the lactone moiety. Structures of the annonaceous acetogenins [**136**]–[**139**] and the chemical shift non-equivalence (H-34 or H-36 $\Delta\delta = \delta_R - \delta_S$) are shown in Figure 21.

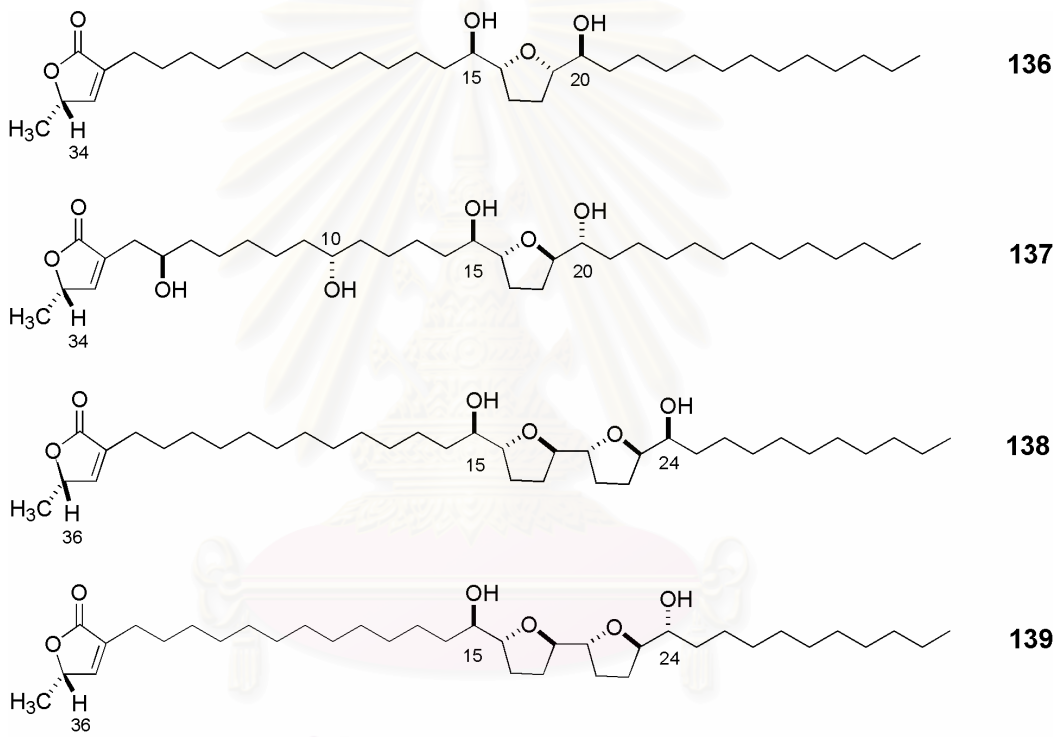

*Chemical shifts of H-34 or H-36 of compounds **136-139** with TFAE at 213° K*

Compound	With (n equiv.) of (*R*)-TFAE	With (n equiv.) of (*S*)-TFAE	$\Delta\delta$ (=$\delta_R - \delta_S$)	absolute configuration at C-5
136	4.995 (20)	4.995 (20)	+ 0.040	*S*
137	4.859 (35)	4.772 (35)	+ 0.087	*S*
138	5.015 (14)	4.949 (14)	+ 0.066	*S*
139	5.012 (9)	4.959 (12)	+ 0.053	*S*

Figure 21. The observed chemical shift non-equivalence (ppm) and the assigned absolute configuration at C-5 of butenolide moiety.

Although this method for configurational assignment is quick and simple to perform, in general, the observed $\Delta\delta$ is typically quite small (0.00-0.10 ppm at room temperature). This drawback is due to the hydrogen bonding between TFAE and substrate, which is not as strong as covalent bond. The observed $\Delta\delta$ is thus the average shifts of diastereomeric complex that forms and rapidly dissociates with bulk of solvent on the NMR time scale (Parker, 1991; Mander, 1994). This can be overcome by increasing solvated formation between the compound and TFAE enantiomers, which originated for the shift nonequivalences in ^{1}H NMR spectrum. Several ways have been proposed as follows (Parker, 1991; Eliel, 1994; Mander, 1994; Wenzel and Wilcox, 2003).

1. Increasing the spectrometer frequency (use high-field NMR instrumentation), the observed $\Delta\delta$ varies with spectrometer frequency. Sharp, well-resolved signals are required, particularly for quantitative work.
2. The association between solute molecules and the chiral solvating agent (CSA), and hence the $\Delta\delta$, are maximized in nonpolar solvents. Polar solvents, such as CH_3OD or DMSO often, but not invariably, interfere with diastereomer solvate formation.
3. Lower the temperature, thereby increasing solvate formation. However, this possibility is limited by solubility.
4. In general, increasing the concentration of both solute and CSA favors the formation of the diastereomeric complex. However, reduction in $\Delta\delta$ due to ion-pair aggregation was noted at high concentrations (> 0.3 M).
5. Stoichiometry between solute and CSA. Nonequivalence in chemical shift reaches a maximum value when diastereomeric complex formation is complete.
6. Addition of achiral shift reagents, for example, $Eu(fod)_3$. Shift reagent molecules can, in some cases, preferentially displace solute molecules from the least stable solvate, thus, enhance the stability of the solute-CSA complex.
7. With racemic CSA, the $\Delta\delta$ disappears altogether, as a consequence of the rapid statistical averaging of solvate formation.

CHAPTER III

EXPERIMENTAL

1. Animal Materials

Two collections of the sea hare *Bursatella leachii* were obtained from the Gulf of Thailand at Sichang Marine Sciences Research and Training Center (SMaRT). Four specimens were collected by hand in October 2000, and eleven specimens in July 2002. The animals were frozen on site before extraction. The voucher specimens and photos of each collection were deposited at the Bioactive Marine Natural Products Chemistry Research Unit–BMNCU, Department of Pharmacognosy, Faculty of Pharmaceutical Sciences, Chulalongkorn University.

2. Identification and Characterization of the Sea Hare *Bursatella leachii*

The identification and characterization of the sea hare as *Bursatella leachii* (family Aplysiidae, order Anaspidea, phylum Mollusca) were conducted mainly by comparison with the photo of sea hares available from Sea Slug Forum Database (http://www.seaslugforum.net), and confirmed with the photo of *Bursatella leachii* Blainville in The Molluscs of the Southern Gulf of Thailand (Swennen, 2001). The pictures of the sea hare and its purple-ink secretion are shown in Figure 22.

Color alive: The general body color is greenish brown with reticulate markings, black spot and clear brighter green areas, each with a peacock-blue ocellus (ocellate spots). Inner edges of the parapodia, mantle cavity and pedal sole are paler in color.

External features: The specimens were between 11 and 20 cm long. The head is short and broad, no shell is present. Numerous simple and compound villi (papillae) of unequal size are scattered over the entire body surface, including the rhinophores and oral tentacles, giving it a ragged appearance. Parapodia are short and not very mobile.

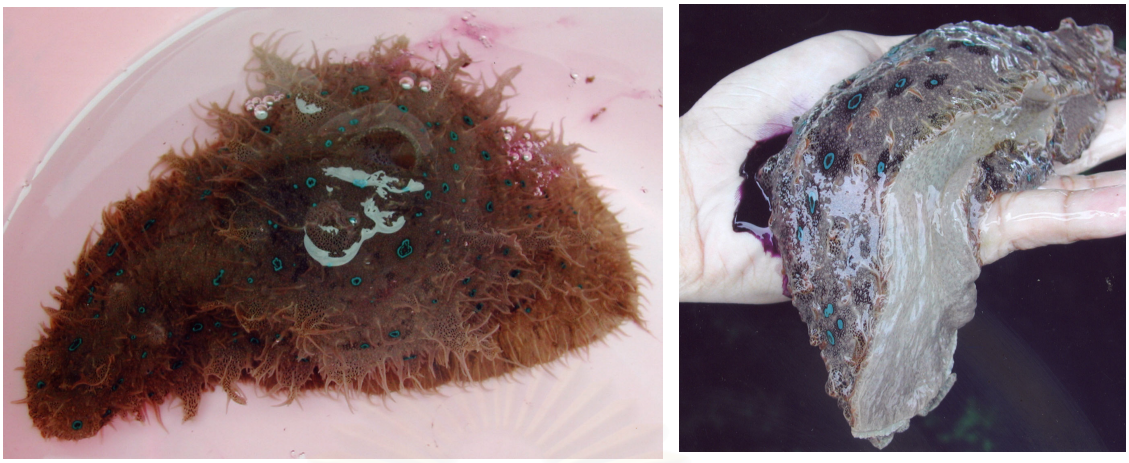

A **B**

Figure 22. (A) The sea hare *Bursatella leachii* collected from Sichang Marine Sciences Research and Training Center, Thailand, and (B) purple ink secretion.

Spawn: The egg mass is of the usual aplyiid shape, i.e. a long, irregularly coiled string, yellow-green in color, adhered to the substratum, containing numerous small eggs.

The genus *Bursatella* is categorized into a single species, *B. leachii*, worldwide, which for convenience is divided into seven or eight several geographical subspecies. It is mainly found in shallow water, on soft bottom of somewhat eutrophic and confined environments, commonly lagoons and in tidal pools. The animals feed on a blue-green algal film that forms on sand grains and other surfaces in the shallow, warm water bays they favor (Sea Slug Forum Database, n.d.).

Jensen (1998a; 1998b) and Swennen (2001) reported their findings of various sea hares from the Gulf of Thailand including *Aplysia euchlora*, *Petalifera petalifera*, *Petalifera petalifera*, and *Bursatella leachii* Blainville.

3. Chemical Reagents

N-Boc-D-valine	(Fluka)
N-Boc-L-valine	(TCI)
2-chloro-1,3-dimethylimidazolinium hexafluorophosphate (CIP)	(TCI)
diethyl azodicarboxylate (DEAD)	(TCI)
N,*N*-diisopropylethylamine (DIEA or Hünig base)	(Ald)
3-(dimethylamino)propylamine	(Aldrich)
4-dimethylaminopyridine (DMAP)	(WAKO)
isopropenylchloroformate (IPCF)	(Aldrich)
Meldrum's acid (2,2-dimethyl-1,3-dioxane-4,6-dione or malonic acid cyclic isopropylidene ester)	(Aldrich)
(*R*)-(−)-α-methoxy-α-(trifluoromethyl)phenylacetyl chloride [(*R*)-MTPA-Cl]	(TCI)
(*S*)-(+)-α-methoxy-α-(trifluoromethyl)phenylacetyl chloride [(*S*)-MTPA-Cl]	(TCI)
propionyl chloride	(WAKO)
trifluoroacetic acid (TFA)	(WAKO)
(*R*)-(−)-2,2,2-trifluoro-1-(9-anthryl)ethanol [(*R*)-TFAE]	(TCI)
(*S*)-(+)-2,2,2-trifluoro-1-(9-anthryl)ethanol [(*S*)-TFAE]	(TCI)

4. General Experimental Procedures

4.1. Analytical thin-layer chromatography (TLC)

Technique : One dimension, ascending

Adsorbent : Si gel $60GF_{254}$ (Merck) precoated on aluminium-backed sheets

Layer Thickness : 0.25 mm

Distance : 6 cm

Temperature : Laboratory temperature

Detection

1. Ultraviolet light (254 and 365 nm)
2. Anisaldehyde spraying reagent and heating at 105 °C for 1–2 min.
3. Dragendorff's spraying reagent and heating at

105 °C for 1–2 min.

4. Molybdenum blue spraying reagent and heating at 105° for 1-2 min.

4.2. Preparative thin-layer chromatography

Technique : One dimension, ascending

Adsorbent : Si gel $60GF_{254}$ (Merck) precoated on glass-plates

Layer Thickness : 1 mm

Distance : 10 cm

Temperature : Laboratory temperature

Detection : Ultraviolet light (254 and 365 nm)

4.3. Column chromatography

4.3.1. Vacuum liquid and flash column chromatography

Adsorbent : Silica gel 60 (No. 7743) particle size 0.063–0.200 nm (70–230 mesh ASTM) (E. Merck)

Packing Method : Wet Packing

Sample Loading : The sample was dissolved in a small amount of organic solvent and then loaded gently on top of the column

Detection : Fractions were examined by TLC observing under UV light (254 and 365 nm)

4.3.2. Gel filtration chromatography

Adsorbent : Sephadex LH-20 (Pharmacia)

Packing Method : Gel filter was suspended in the eluent and left standing to swell for 24 h prior to use. It was then poured into the column and allowed to set tightly.

Sample Loading : The sample was dissolved in a small amount of organic solvent and then loaded gently on top of the column

Detection : Fractions were examined by TLC observing under UV light (254 and 365 nm)

4.3.3. High pressure liquid chromatography (HPLC)

Column	: LiChroCART column (250 X 10 mm)
Flow rate	: 1 ml/min
Mobile phase	1. CH_3CN/MeOH/1% TFA, 2:1:1
	2. MeOH/H_2O, 3:1
Sample preparation	: The sample was dissolved in a small volume of eluant and filtered through millipore filter paper before injection.
Injection volume	: 200 μl
Pump	: ConstaMetric® 4100
Detector	: SpectroMonitor® 4100
Recorder	: Linear®
Temperature	: Laboratory temperature

4.4. Spectroscopy

4.4.1. Ultraviolet (UV) absorption spectra

UV (in MeOH) spectra were obtained on a Milton Roy Spectronic 3000 Array spectrophotometer (Pharmaceutical Research Instrument Center, Faculty of Pharmaceutical Sciences, Chulalongkorn University).

4.4.2. Infrared (IR) absorption spectra

IR spectra (film) were recorded on a Perkin Elmer 2000 FT–IR spectrometer (Pharmaceutical Research Instrument Center, Faculty of Pharmaceutical Sciences, Chulalongkorn University).

4.4.3. Mass spectra

The EIMS and FABMS spectra were obtained with a JEOL JMS–700 mass spectrometer with direct inlet, operating at 10 kV ionization voltages (Meiji Pharmaceutical University).

The ESITOF MS spectra were recorded on a Micromass LCT mass spectrometer (National Center for Genetic Engineering and Biotechnology, National Science and Technology Development Agency) or a Q–TOF Micromass mass

spectrometer equipped with a Z-spray type ESI ion source (Laboratory of Organic Chemistry, Graduate School of Bioagricultural Sciences, Nagoya University).

4.4.4. Proton and Carbon-13 nuclear magnetic resonance (^{1}H and ^{13}C-NMR) spectra

^{1}H (300 MHz) and ^{13}C (75 MHz) NMR spectra were obtained from a Bruker AVANCE DPX–300 FT–NMR spectrometer (Pharmaceutical Research Instrument Center, Faculty of Pharmaceutical Sciences, Chulalongkorn University).

^{1}H (400 MHz) and ^{13}C (100 MHz) NMR spectra were recorded on a Bruker AV400 NMR spectrometer (Laboratory of Organic Chemistry, Graduate School of Bioagricultural Sciences, Nagoya University).

^{1}H (500 MHz) NMR spectrum was obtained from a JEOL JNM–A500 spectrometer (Scientific and Technological Research Equipment Center, Chulalongkorn University).

^{1}H (600 MHz) and ^{13}C (150 MHz) NMR spectra were obtained from a Bruker AMX–600 spectrometer (Laboratory of Organic Chemistry, Graduate School of Bioagricultural Sciences, Nagoya University). The ^{13}C NMR spectrum of 500 μg sample of compound **SHOII-76** was recorded with a 5-mm inverse probe.

Solvent for NMR spectra was deuterated chloroform ($CDCl_3$). Chemical shifts for ^{1}H (300 and 500 MHz) were reported in ppm scale relative to the chemical shift of residual $CHCl_3$ (δ_H 7.24). ^{1}H NMR (400 and 600 MHz) chemical shifts were reported relative to an internal tetramethylsilane (TMS) standard. Chemical shifts for ^{13}C NMR spectra were referenced to the center line $CDCl_3$ at 77.00 ppm.

4.5. Physical properties

4.5.1. Optical rotations

Optical rotations were measured on a Perkin Elmer 341 polarimeter (Pharmaceutical Research Instrument Center, Faculty of Pharmaceutical Sciences,

Chulalongkorn University) or a Perkin Elmer 141 polarimeter (Laboratory of Organic Chemistry, Graduate School of Bioagricultural Sciences, Nagoya University).

4.5.2. Circular dichroism (CD) spectra

CD spectra were recorded on a JASCO J–715 spectropolarimeter (Pharmaceutical Research Instrument Center, Faculty of Pharmaceutical Sciences, Chulalongkorn University).

4.6. Crystallization technique

Compound **SHOII-28** (hectochlorin) was subjected to recrystallization for X-ray crystallography by using a mixture of EtOAc-Hexane (2:1) and the solution was left standing in refrigerator until white-glassy crystals were formed.

4.7. X-ray crystallography

The single crystal X-ray crystallography of compound **SHOII-28** (hectochlorin) was recorded on a SMART CCD 1K Single Crystal Diffractometer (Department of Physics, Faculty of Science, Thammasart University).

4.8. Solvents

Throughout this work, all organic solvents for chromatographic separations were of commercial grade and were redistilled prior to use. Dry solvents for moisture-sensitive reactions were commercially available and used as purchased. Dry CH_2Cl_2 was redistilled from CaH_2 under atmosphere of N_2 before use. The moisture-sensitive reactions were performed under atmosphere of N_2 or Ar.

5. Extraction and Isolation

5.1 The sea hare collected in 2000

5.1.1. Extraction

The internal organs (65 g, wet weight) of the specimens (4 animals) were blended into small pieces and macerated three times with a mixture of EtOH–1-propanol, 1:1 (150 ml, each). The combined extracts were concentrated under

reduced pressure, and the residue was partitioned between EtOAc and H_2O to obtain the crude extract (1.4 g) as a dark green oil. Biological evaluation of the crude extract showed antimalarial activity with ED_{50} of 2.4 μg/ml, antituberculous activity at MIC of 50 μg/ml, and cytotoxicity against KB and BC cancer cell lines with ED_{50} of 7.2 and 6.6 μg/ml, respectively (see Scheme 3).

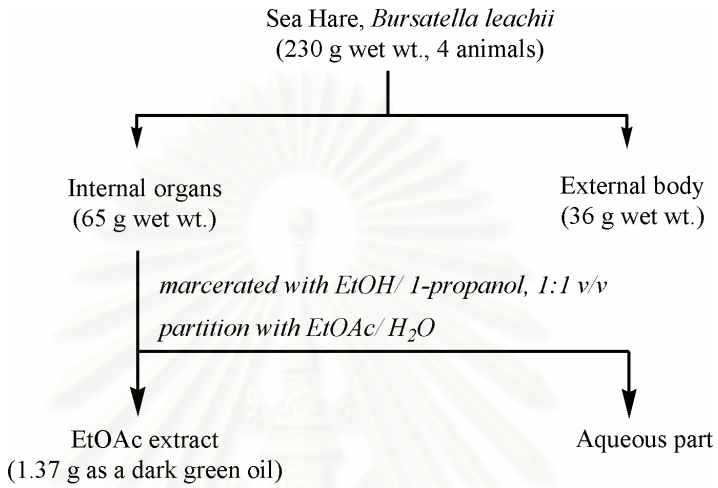

Scheme 3. Extraction of the sea hare collected 2000.

5.1.2. Isolation of malyngamide X [SHO-27]

The EtOAc extract was chromatographed on Si gel flash column chromatography (65 g, 2.5 X 25 cm column) and eluted with gradient of MeOH–$CHCl_3$ (5, 10, 15 ⇝100% MeOH). The fractions were combined according to TLC pattern similarities (solvent system: $CHCl_3$–MeOH = 18:1) to give four pool-fractions, A-3 (389 mg), A-4 (48 mg), A-5 (424 mg), and A-6 (170 mg). The active fraction A-3 having an interesting positive spot to Dragendorff's spraying reagent at R_f 0.34 on Si gel TLC (solvent system: $CHCl_3$–EtOAc–Diethylamine = 1:3:0.05) was further purified by Si gel flash column chromatography (35 g, 3 X 18 cm column; solvent system: 1.5% diethylamine in $CHCl_3$–EtOAC = 1:3) to yield fraction A-26 (135 mg) and fraction A-27 (143 mg). Fraction A-27 was repeatedly chromatographed on Sephadex LH-20 columns (Hexane–$CHCl_3$–MeOH–EtOAc = 20:75:5:20) to afford malyngamide X [**SHO-27**] as a pale yellow oil (10 mg, 0.71% of the crude extract) (see Scheme 4).

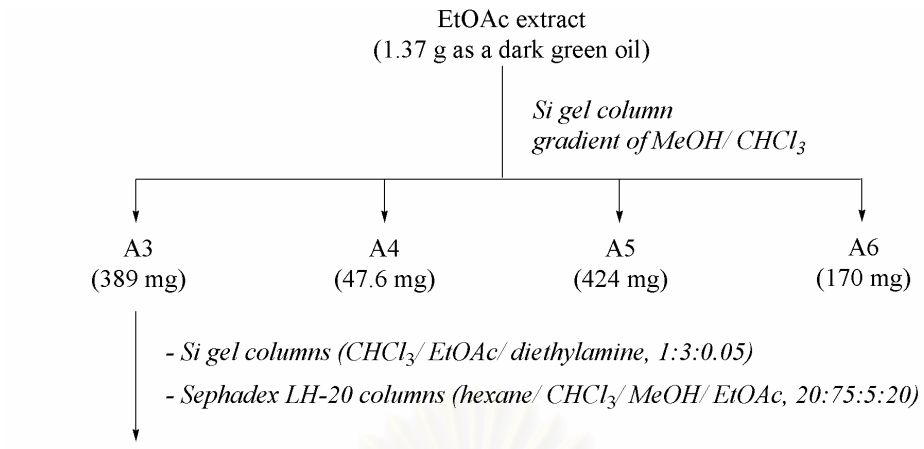

Bioactivity / Fraction	Cytotoxicity (EC_{50}, μg/ml)			Antimalarial (EC_{50}, μg/ml)	Antituberculous (MIC, μg/ml)
	Vero	KB	BC		
External body	-	Neg.	Neg.	Neg.	100
Internal organs	16.15	7.2	6.6	2.4	50
A3	-	Neg.	Neg.	2.9	50
A4	-	Neg.	Neg.	3.2	50
A5	-	Neg.	Neg.	Neg.	Neg.
A6	-	Neg.	Neg.	Neg.	Neg.

Scheme 4. Isolation of malyngamide X [**SHO27**].

5.2. The sea hare collected in 2002

5.2.1. Extraction

The internal organs (440 g, wet weight) of the specimens (11 animals) were blended into small pieces and macerated three times with MeOH (1.5 L, each). The combined MeOH extracts were concentrated under reduced pressure, and then partitioned between EtOAc and H_2O. Concentration of the EtOAc extract yielded a dark green oily residue (6.4 g) (see Scheme 5).

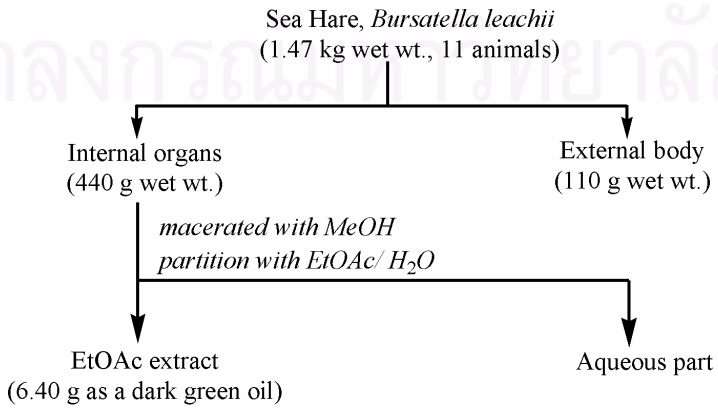

Scheme 5. Extraction of the sea hare collected 2002.

5.2.2. Isolation of hectochlorin [SHOII-28], deacetylhectochlorin [SHOII-51], and *syn*-3-isopropyl-6-(4-methoxy-benzyl)-4-methyl-morpholine-2,5-dione [SHOII-76]

The EtOAc extract was chromatographed on a vacuum liquid column (90 g, 10 X 4 cm) by eluting stepwise with MeOH and CH_2Cl_2 (5, 10, 15 ⇝60% MeOH). The fractions were combined according to their TLC patterns (solvent system: $CHCl_3$–Acetone = 9:1) to give four fractions: B-1 (3 g), B-2 (2.3 g), B-3 (5.7 g), and B-4 (0.3 g). The fraction B-2, eluting with 5-10 % MeOH in CH_2Cl_2, was chromatographed on a vacuum liquid column (20 g, 4.5 X 3.5 cm) using gradient mixtures of acetone-CH_2Cl_2 (5, 10, 15 ⇝100% acetone) to yield five fractions: B-8 (33 mg), B-9 (520 mg), B-10 (470 mg), B-11 (175 mg), and B-12 (317 mg). Fraction B-10, which was eluted with 7-10 % acetone in CH_2Cl_2, showed two interesting positive spots with Dragendorff's spraying reagent at R_f values of 0.50 (**SHOII-28**) and 0.38 (**SHOII-51**) on TLC (solvent system: EtOAc–hexane = 3:1). It was further purified with Si gel flash column chromatography (50 g, 2.5 X 18 cm column; solvent system: EtOAc–hexane = 3:2) to give fractions B-13 (58 mg), B-14 (34 mg), B-15/B-16 (135 mg), and B-17 (88 mg). Fractions B-16 was repeatedly chromatographed on Sephadex LH-20 (solvent system: CH_2Cl_2-EtOAc = 1:1) yielding **SHOII-28** (hectochlorin, 16.2 mg, 0.25 % of the crude extract). Fraction B-17 was subjected to Sephadex LH-20 column (solvent system: CH_2Cl_2–EtOAc = 1:1), followed by C-18 reversed-phase HPLC [LiChroCART column (250 x 10 mm), 1 ml/min, detection at 254 nm] using CH_3C-MeOH-1% TFA in water (2:1:1) as the eluting solvent, yielding fraction B-64 (6.8 mg, t_R 14 min) and compound **SHOII-51** (deacetylhectochlorin, 6.0 mg, t_R 22 min, 0.09 % of the crude extract). Further purification of fraction B-64 with preparative TLC (solvent system: hexane–EtOAc = 1:3) on Si gel, collecting the band with R_f 0.47 to give 0.5 mg (0.007 % of crude extract) of **SHOII-76** (*syn*-3-isopropyl-6-(4-methoxy-benzyl)-4-methyl-morpholine-2,5-dione) as a white solid (see Scheme 6).

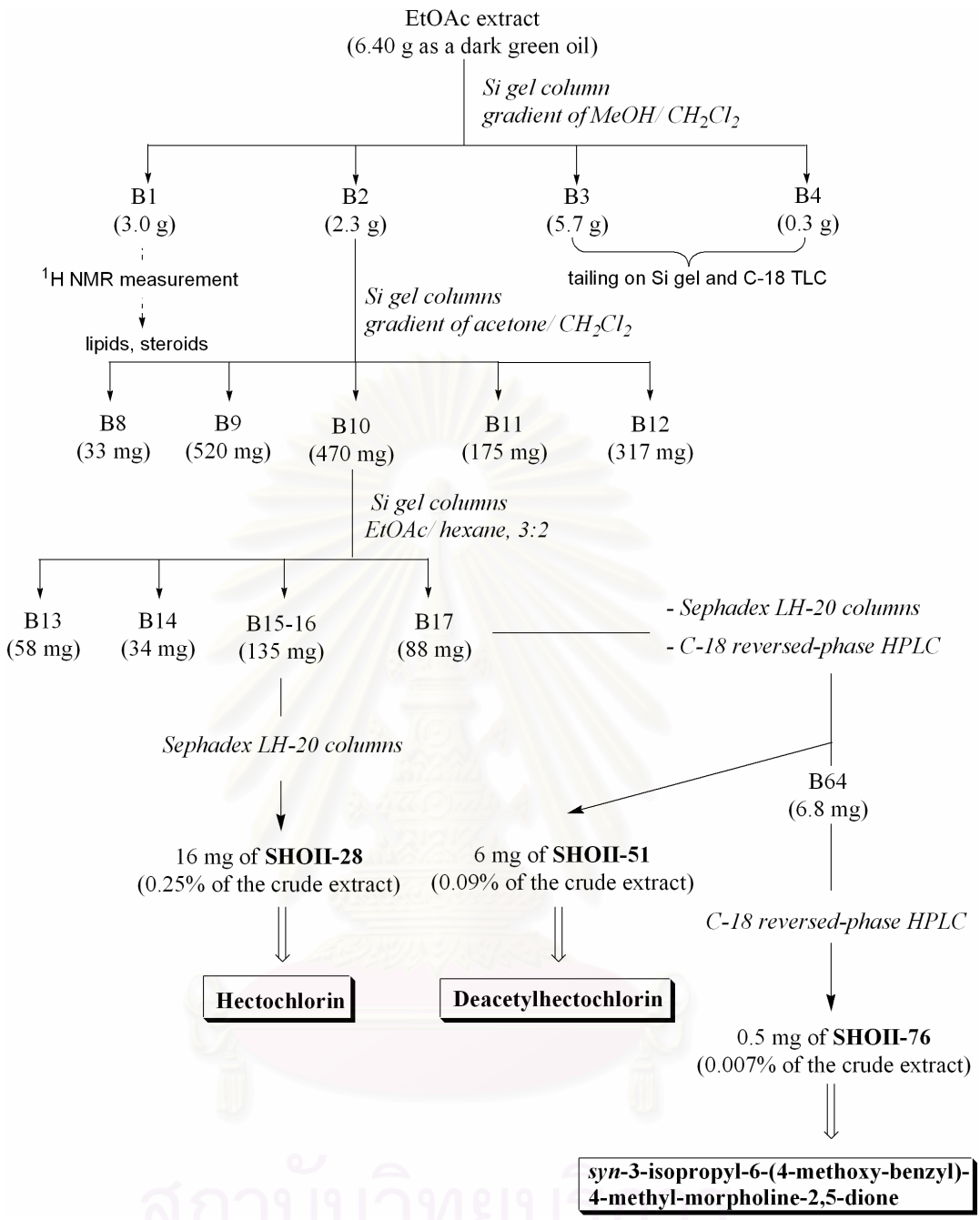

Scheme 6. Isolation of hectochlorin, deacetylhectochlorin, and *syn*-3-isopropyl-6-(4-methoxy-benzyl)-4-methyl-morpholine-2,5-dione.

6. Physical and Spectral Data of the Isolated Compounds

6.1. Malyngamide X [SHO-27]

Malyngamide X was obtained as a pale yellow oil, soluble in $CHCl_3$ (10 mg, 0.71% yield of the crude extract)

$[\alpha]^{20}_D$: −1.81 ° (*c* 0.8, MeOH)

UV : λ_{max} nm (log ε), in methanol; Figure 44
219 (5.11), 241 (5.03)

IR : ν_{max} cm^{-1}, film; Figure 45
3438, 2930, 1722, 1684, 1624, 1460, 1380, 1319, 1247, 1093, 953

HRFABMS : *m/z* (% relative intensity), Figure 46
$[M + K]^+$, 646.4212 (28.94); $[M + H]^+$, 608.4579 (7.04)
calcd. for $C_{33}H_{58}N_3O_7$, 608.4275

^{1}H NMR : δ_H ppm, in $CDCl_3$, 500 MHz; Figures 47, Table 5

^{13}C NMR : δ_C ppm, in $CDCl_3$, 75 MHz; Figure 52, Table 5

6.2. Hectochlorin [SHOII-28]

Hectochlorin was obtained as white crystals, soluble in $CHCl_3$ (16.2 mg, 0.25 % of the crude extract)

$[\alpha]^{20}_D$: −7.47 ° (*c* 0.28, MeOH)

CD : $\Delta\varepsilon_{207}$ −13.7, $\Delta\varepsilon_{230}$ +8.9, $\Delta\varepsilon_{276}$ −0.2 (*c* 0.1, MeOH); Figure 70

UV : λ_{max} nm (log ε), in methanol; Figure 71
239 (3.66)

IR : ν_{max} cm^{-1}, film; Figure 72
3456, 3118, 2983, 2939, 1747, 1692, 1481, 1371, 1314, 1270, 1215, 1149

EIMS : *m/z* (% relative intensity), Figure 73
$[M]^+$, 664 (3.87), $[M + 2]^+$ 666 (3.08); $[M + 4]^+$, 668 (0.81)

^{1}H NMR : δ_H ppm, in $CDCl_3$, 300 MHz; Figure 74, Table 6

^{13}C NMR : δ_C ppm, in $CDCl_3$, 75 MHz; Figure 75, Table 6

6.3. Deacetylhectochlorin [SHOII-51]

Deacetylhectochlorin was obtained as a white solid, soluble in $CHCl_3$ (6.0 mg, 0.09 % of the crude extract)

$[\alpha]^{20}_D$	: −22.78 ° (*c* 0.10, MeOH)
CD	**:** $\Delta\varepsilon_{209}$ −32.6, $\Delta\varepsilon_{228}$ +28.1, $\Delta\varepsilon_{257}$ −18.8 (*c* 0.1, MeOH); Figure 84
UV	: λ_{max} nm (log ε), in methanol; Figure 85 239 (3.83)
IR	: ν_{max} cm^{-1}, film; Figure 86 3391, 3155, 2982, 2939, 1739, 1717, 1479, 1382, 1327, 1241, 1140
EIMS	: *m/z* (% relative intensity), Figure 87 $[M]^+$, 622 (8.36); $[M + 2]^+$, 624 (6.67); $[M+4]^+$, 626 (1.73)
^{1}H NMR	: δ_H ppm, in $CDCl_3$, 300 MHz; Figure 88, Table 7
^{13}C NMR	: δ_C ppm, in $CDCl_3$, 75 MHz; Figure 89, Table 7

6.4. *syn*-3-Isopropyl-6-(4-methoxy-benzyl)-4-methyl-morpholine-2,5-dione [SHOII-76]

syn-3-Isopropyl-6-(4-methoxy-benzyl)-4-methyl-morpholine-2,5-dione was obtained as a white solid, soluble in $CHCl_3$ (0.5 mg, 0.007 % of the crude extract).

$[\alpha]^{20}_D$	: −58.21 ° (*c* 0.05, MeOH)
UV	: λ_{max} nm (log ε), in methanol; Figure 97 223 (2.93), 250 (2.20), 273 (2.08), 281 (1.99)
IR	: ν_{max} cm^{-1}, film; Figure 98 2920, 1744, 1651, 1514, 1249
ESITOF MS	: *m/z* 314.1679 $[M + Na]^+$, 292.1653 $[M + H]^+$, Figure 99
^{1}H NMR	: δ_H ppm, in $CDCl_3$, 600 MHz; Figure 100, Table 8
^{13}C NMR	: δ_C ppm, in $CDCl_3$, 150 MHz; Figure 102, Table 8

7. Preparation of deacetylhectochlorin from hectochlorin

Hectochlorin [**SHOII-28**] 6 mg (9 μmole) was hydrolyzed with 30 μl hydrazine monohydrate and 1 ml MeOH at 0 °C for 2 h. The mixture was twice partitioned between CH_2Cl_2 and water, the organic layers were combined and dried over anhydrous Na_2SO_4, and the solvent was removed under reduced pressure. The extract was purified by C18 reversed-phase HPLC [LiChroCART column, (250 x 10 mm), 2 ml/min, detection at 254 nm] using MeOH and water (3:1) as the eluting solvent to provide 3 mg of deacetylhectochlorin as a white solid (deacetylhectochlorin, t_R 14.1 min).

$[\alpha]^{20}_D$: −26.02 ° (*c* 0.10, MeOH)

CD : $\Delta\varepsilon_{210}$ −25.5, $\Delta\varepsilon_{228}$ +24.6, $\Delta\varepsilon_{268}$ −17.1 (*c* 0.1, MeOH); Figure 95

^{1}H NMR : δ_H ppm, in $CDCl_3$, 300 MHz; Figure 96

8. Preparation of 7-*O*-(*R*)-(+)-MTPA and 7-*O*-(*S*)-(−)-MTPA esters of malyngamide X

8.1. Preparation of 7-*O*-(*R*)-(+)-MTPA ester of malyngamide X [SHO27a]

A solution of malyngamide X [**SHO27**] (0.6 mg, 0.99 μM), (dimethylamino)pyridine (1.22 mg, 10 μM), and triethylamine (100 μl, 720 μM) in 1 ml of CH_2Cl_2 was treated with (+)-(*S*)-MTPA-Cl (30 μl, 160 μM), and the mixture was vigorously stirred at room temperature for 37 h. Then, 3-[(dimethylamino) propyl]amine (20 μl, 160 μM) was added and the residue after removal of the solvent was partitioned (x 3) between 20% aq. MeOH and EtOAc (2:1). The combined EtOAc extract was evaporated and applied to preparative Si gel TLC (solvent system: hexane-EtOAc, 1:3) to give pure 7-*O*-(*R*)-(+)-MTPA ester of malyngamide X (**SHO27a**, R_f 0.3, 0.6 mg, 73% yield).

ESITOF MS : *m/z* 824.5161 $[M + H]^+$, Figure 59

^{1}H NMR : δ_H ppm, in $CDCl_3$, 600 MHz; Figure 60, Table 9

8.2. Preparation of 7-*O*-(*S*)-(−)-MTPA ester of malyngamide X [SHO27b]

In the same manner described for **SHO27a**, (−)-(*R*)-MTPA-Cl was used instead of (+)-(*S*)-MTPA-Cl. The reaction mixture was vigorously stirred at room temperature for 56 h. By using the same work up and purification methods of **SHO27a**, compound 7-*O*-(*S*)-(−)-MTPA ester of malyngamide X was isolated (**SHO27b**, R_f 0.3, 0.6 mg, 73%).

ESITOF MS : *m/z* 824.5154 $[M + H]^+$, Figure 61

^{1}H NMR : δ_H ppm, in $CDCl_3$, 600 MHz; Figure 62, Table 9

9. Preparation of Model Compounds for NMR Chiral Solvation Experiments

9.1. Preparation of alkaline degradation product from tautomycin [M1]

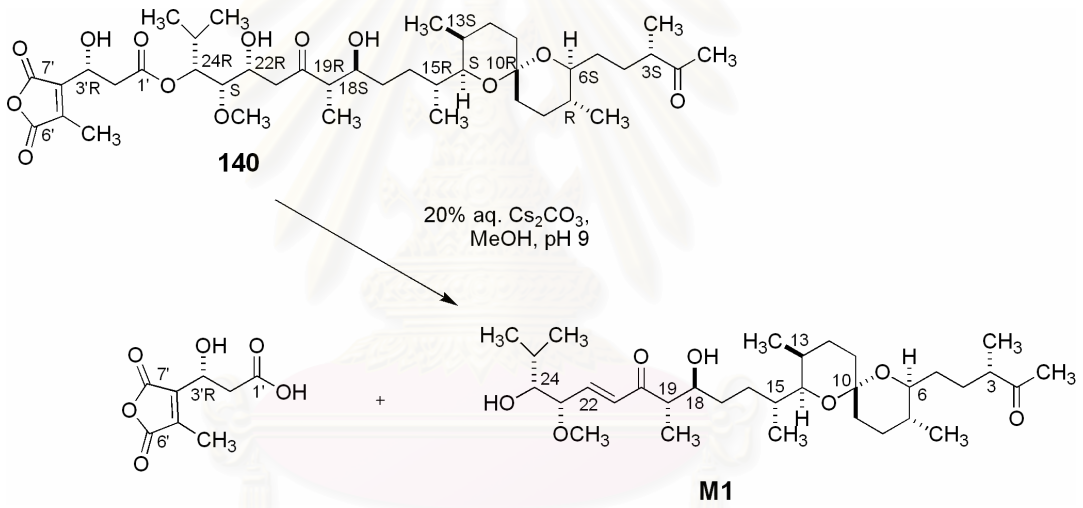

The authentic sample of the alkaline degradation product of tautomycin was obtained from Laboratory of Organic Chemistry, Graduate School of Bioagricultural Sciences, Nagoya University, which was prepared as followings. To a flask containing tautomycin (**140**, 600 mg, 0.78 mmol) and MeOH (20 ml), 20% Cs_2CO_3 in MeOH was carefully added to the solution until pH9, and the solution was stirred at room temperature. While the reaction went on, the solution was kept to pH 9. After 6.5 h, the solution was adjusted to pH 4 with 1 N HCl, and MeOH was evaporated. The resulting mixture was basified with 1 N NaOH to pH 10 and extracted with EtOAc (x 3). The organic layer was dried over anhydrous Na_2SO_4, concentrated on a rotary evaporator to give a brown oil (501 mg), which was further purified by a silica gel column with the solvent system of Et_2O-hexane (4:1) to afford

recovered tautomycin (208 mg, 35%) and the desired product **M1** (279 mg, 63%, corrected yield 97%, yellow oil).

Compound M1. ^{1}H NMR ($CDCl_3$, 400 MHz) δ_H 0.79 (3H, d, J = 6.5 Hz), 0.88 (3H, d, 6), 0.89 (3H, d, 6.5), 0.98 (6H, d, 7.0, 2.0), 1.08 (3H, d, 7.0), 1.17 (3H, d, 7.0), 1.20–1.75 (18H, m), 1.84 (1H, m, H-16), 2.00 (1H, m, H-12), 2.14 (1H, s, H-1), 2.36 (1H, brd, 24-OH), 2.53 (1H, sext, 6.5, H-3), 2.81 (1H, brd, 18-OH), 2.94 (1H, qn, 7.0, H-19), 3.15 (1H, dt, 10.0, 2.0, H-6), 3.25 (1H, dd, 10.0, 2.0, H-14), 3.32 (3H, s, H_3-23), 3.46 (1H, dt, 7.0, 4.0, H-24), 3.68 (1H, m, H-18), 3.81 (1H, dd, 7.0, 4.0, H-23), 6.34 (1H, d, 16.0, H-21), 6.82 (1H, dd, 16.0, 7.0, H-22).

9.2. Preparation of 5-acyl Meldrum's acid derivative [142]

9.2.1. Method A using isopropenyl chloroformate (IPCF) as a condensing agent

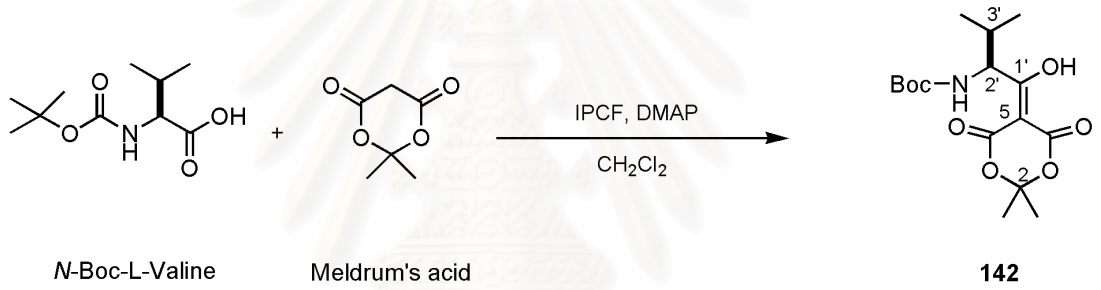

N-Boc-L-valine (500 mg, 2.3 mmol), Meldrum's acid (352 mg, 2.4 mmol), and dimethylaminopyridine (DMAP, 648 mg, 5.3 mmol) were placed in a 50-ml flask using dry CH_2Cl_2 as the solvent. The mixture was left to stir at room temperature and then cooled down to -10 °C with an ice-salt bath. The solution of IPCF was added dropwise during 15 min period. After 2 h stirring at -10 °C, none of *N*-Boc-L-valine was observed at R_f 0.8 on Si gel TLC (solvent system: MeOH-EtOAc-acetic acid = 3:95:2, using molybdenum blue reagent as a spraying reagent) and an additional spot which could be detected with UV 254 nm and molybdenum blue reagent was observed at R_f 0.46. Cold HCl solution (pH 3) was then added to the mixture. After 5 min vigorous stirring, the organic layer was separated and washed with brine, dried on anhydrous Na_2SO_4, and evaporated to dryness, giving the crude compound **142** (1.12 g) as a pale yellow solid (^{1}H NMR spectrum, Figure 110).

9.2.2. Method B using 2-chloro-1,3-dimethyl-2-imidazolinium hexafluoro phosphate (CIP) as a condensing agent

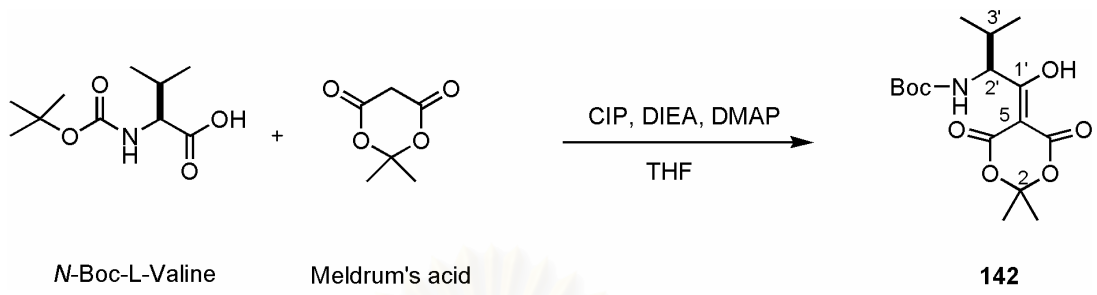

N-Boc-L-valine (7.09 g, 32.63 mmol), Meldrum's acid (5.75 g, 39.16 mmol), and CIP (11 g, 39.16 mmol) were placed in a 300-ml flask using dry THF (140 ml) as the solvent. It was stirred in an ice-water bath for 30 min and diisopropylethylamine (DIEA or Hünig base) (23 ml, 130.52 mmol) was added dropwise. The reaction flask was stirred in an ice-water bath for an additional hour and removed to room temperature (yellowish solution). A solution of DMAP (8 g, 65.26 mmol) in dry CH_2Cl_2 (10 ml) was then added to the flask. During the progression of reaction, the color gradually changed to yellow, orange and deep red. After stirring at room temperature for 1.5 h, none of *N*-Boc-L-valine was observed at R_f 0.8 on Si gel TLC (solvent system: MeOH-EtOAc-acetic acid = 3:95:2, using molybdenum blue reagent as a spraying reagent) and an additional spot, which could be detected with UV 254 nm and molybdenum blue reagent was observed at R_f 0.5. The residue was transferred to a 1-L flask and evaporated to dryness, yielding the crude compounds as a deep red solid.

9.3. Preparation of *N*-Boc-5(*S*)-isopropyl-4-hydroxy-Δ^3-pyrrolin-2-one [143]

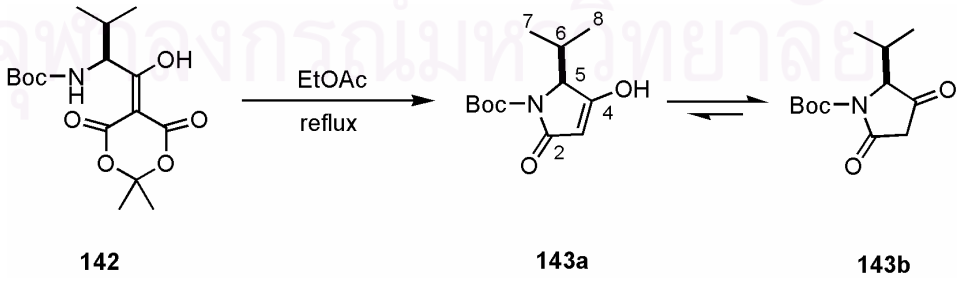

The crude compound **142** obtained from method A or B was refluxed in dry EtOAc until a purple spot with anisaldehyde spraying reagent at R_f 0.46 on Si

gel TLC of **142** (solvent system: MeOH-EtOAc-acetic acid = 3: 95: 2) disappeared and a new, light yellow spot with anisaldehyde spraying reagent at R_f 0.49 was observed. The mixture was concentrated and partitioned twice with 5% aq. $NaHCO_3$ (pH 8) and then EtOAc. The combined aqueous layer containing alkaline salt of compound **143** was acidified to pH 2 with powdered citric acid, and extracted with EtOAc (x 3). Most of compound **143** was found in the EtOAc layer. The combined EtOAc extract was evaporated to dryness, yielding a crude yellow oily residue of the desired product **143**. The ^{1}H NMR spectrum (Figure 112) of the compound showed a mixture of enol [**143a**] and keto [**143b**] forms in 1 to 2 ratio.

Compound 143. ^{1}H NMR ($CDCl_3$, 400 MHz, Figure 111), enol form **143a**: δ_H 0.84 (d, 6.8, H_3-7), 1.13 (d, 6.8, H_3-8), 1.51 (s, H_3-(*tert*)Bu), 2.45 (m, H-6), 4.35 (d, 3.6, H-5), 5.01 (s, H-3); keto form **143b**: δ 0.92 (d, 6.8, H_3-7), 1.12 (d, 6.8, H_3-8), 1.51 (s, H_3-(*tert*)Bu), 2.35 (m, H-6), 3.11 (s, H_2-3), 4.28 (d, 3.6, H-5).

9.4. Preparation of *N*-Boc-5(*S*)-isopropyl-4-methoxy-Δ^3-pyrrolin-2-one [M2]

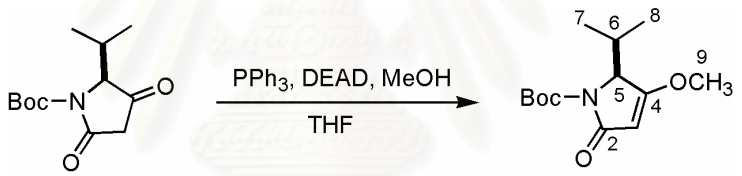

143 **M2**

To a 300-ml flask was added the crude compound **143** (8.56 g, 32.63 mmole) and PPh_3 (12.84 g, 48.95 mmol), fitted with a 3-way valve, and dried with vacuum. Dry THF (150 ml) was then added and the flask was stirred in an ice-water bath. To this stirred solution was added 40% diethyl azodicarboxylate (DEAD) in toluene (9.0 ml, 48.95 mmol). After stirring for 1.5 h, the solution changed into orange suspension. Dry MeOH (2 ml, 48.95 mmole) was then added and color of the solution was changed to red. It was removed to stir at room temperature for an additional hour. Monitoring with Si gel TLC (solvent system: MeOH-EtOAc-Acetic acid, 3:95:2), the reaction mixture showed none of the starting material **145** at R_f 0.5, while a new spot giving light yellow color to anisaldehyde spraying reagent was observed at R_f 0.6. The reaction mixture was concentrated, and absorbed onto a sufficient amount of Si gel powder. It was then placed on the top of Si gel column

using Et_2O as an eluting solvent to give the title compound (**146**) as pale yellow solid (3.7308 g, 44.78% overall yield).

Compound M2. pale yellow solid; $[\alpha]^{28}_D$ = +83.5 ° (*c* 0.20, CH_2Cl_2); ^{1}H NMR ($CDCl_3$, 400 MHz, Figure 113, Table 10) δ_H 0.80 (d, 7.2, H_3-7), 1.09 (d, 7.2, H_3-8), 1.54 (9H, s, H_3-(*tert*)Bu), 2.42 (m, H-6), 3.81 (s, H_3-9), 4.37 (d, 2.4, H-5), 5.06 (s, H-3); ESITOF MS (Figure 112) *m/z* 278.1373 $[M + Na]^+$, calcd for $C_{13}H_{21}NO_4Na$, 278.1368.

9.5. Preparation of 5(*S*)-isopropyl-4-methoxy-Δ^3-pyrrolin-2-one [M3]

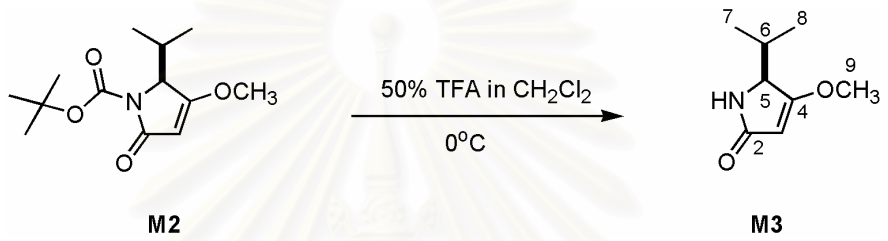

Compound **M2** (6.07 g, 0.02 mole) was stirred with 50% TFA in CH_2Cl_2 (140 ml)) in an ice-water bath for 30 min and then evaporated to dryness. The residual TFA was removed by azeotrope with hexane three times. The residue was added with CH_2Cl_2, and partitioned (x 3) with aqueous $NaHCO_3$ (pH8). The organic layer was combined, dried on anhydrous Na_2SO_4, and evaporated to dryness. The oily crude product was transformed to solid by tritulation with hexane. The precipitate was washed with Et_2O. The mother liquor was concentrated and repeatedly tritulated to give 2.87 g of compound **M3**. Finally, the remaining mother liquor was evaporated to dryness and purified on a Si gel column using EtOAc-Hexane (1:1) as the eluting solvent to give additional compound **M3**. Total amount of compound **M3** was 3.12 g (100.7 % yield).

Compound M3. white solid; $[\alpha]^{28}_D$ = +5.6 ° (*c* 1.00, CH_2Cl_2); ^{1}H NMR ($CDCl_3$, 400 MHz, Figure 115, Table 10) δ_H 0.80 (d, 6.8, H_3-7), 1.00 (d, 6.8, H_3-8), 2.08 (m, H-6), 3.79 (s, H_3-9), 3.98 (dd, 2.8, 1.2, H-5), 5.03 (d, 1.2, H-3), 5.40 (br s, NH); ESITOF MS (Figure 114) *m/z* 156.1016 $[M + H]^+$, calcd for $C_8H_{14}NO_2$, 156.1024.

9.6. Preparation of 5(*S*)-isopropyl-4-methoxy-1-propionyl--Δ^3-pyrrolin-2-one [M4]

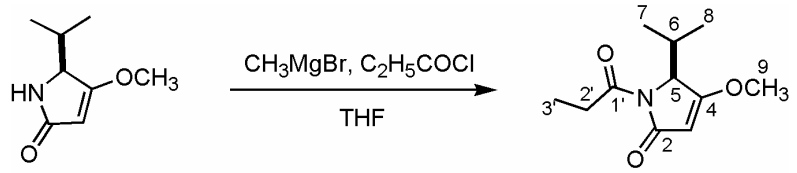

M3 **M4**

Compound **M3** (3.1 g, 0.02 mole) in 50 ml dry THF was added slowly to a stirred solution of DMAP (12 g, 0.1 mole), CH_3MgBr (65 ml, 0.06 mole), and dry THF (150 ml) in an ice-water bath. During this step, some amount of bubble gas (CH_4) was observed. After 30 min, propionyl chloride (7 ml, 0.08 mole) was added dropwise. It was stirred in an ice-water bath for one further hour and then removed to stir at room temperature. The reaction was monitored by using Si gel TLC (solvent system: EtOAc-hexane = 3:1). After stirring for 1 h, none of the starting material (R_f 0.2) was detected and a new spot at R_f 0.8 was observed. The reaction mixture was then worked up by stirring with saturated $NaHCO_3$. The resulting slurry was filtered through a Bushner funnel. The filtrate was evaporated to dryness, extracted with Et_2O and 10% citric acid (x 3), washed with brine (x 2), H_2O (x 1), dried on anhydrous Na_2SO_4, and evaporated to dryness. The crude extract was further purified on a Si gel column using Et_2O: hexane (1:1) as an eluting solvent to give compound **M4** as a yellow solid (3.6 g, 91.29 % yield).

Compound M4. pale yellow solid; $[\alpha]^{28}_D$ = +75.3 ° (*c* 0.60, CH_2Cl_2); ^{1}H NMR ($CDCl_3$, 400 MHz, Figure 117, Table 10) δ_H 0.74 (d, 7.2 Hz, H_3-7), 1.11 (d, 7.2, H_3-8), 1.15 (t, 7.2, H_3-3'), 2.55 (m, H-6), 2.94 (q, 7.2, H_2-2'), 3.83 (s, H_3-9), 4.37 (d, 2.4, H-5), 5.06 (s, H-3); ESITOF MS (Figure 116) *m/z* 234.1108 $[M + Na]^+$, calcd for $C_{11}H_{17}NO_3Na$, 234.1106.

9.7. Preparation of *N*-Boc-5(*R*)-isopropyl-4-hydroxy-Δ^3-pyrrolin-2-one [144]

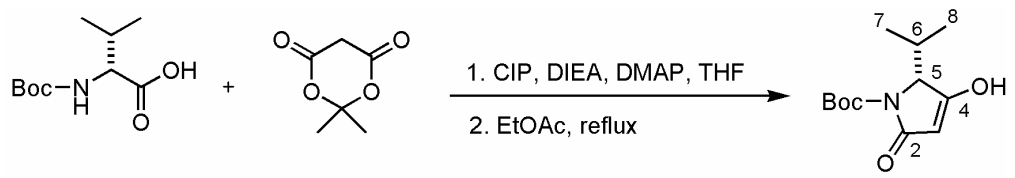

N-Boc-L-Valine Meldrum's acid **144**

In the same manner described for compound **143**, *N*-Boc-D-valine (500 mg, 2.3 mmole) was used instead of *N*-Boc-L-valine. By using the same work up and purification methods, the crude compound **144** having identical ^{1}H NMR spectrum to **143** was obtained as a yellow oily residue.

9.8. Preparation of *N*-Boc-5(*R*)-isopropyl-4-methoxy-Δ^3-pyrrolin-2-one [M5]

In the same manner described for **M2**, **144** was used instead of 2(*S*)-epimer. By using the same work up and purification methods, compound **M5**, having identical ^{1}H NMR spectrum to **M2**, was isolated (60 mg, 10% overall yield).

Compound M5. pale yellow solid; $[\alpha]^{28}_D$ = –77.0 ° (*c* 0.20, CH_2Cl_2); ^{1}H NMR ($CDCl_3$, 400 MHz, Figure 119, Table 10) δ_H 0.80 (d, 7.2, H_3-7), 1.09 (d, 7.2, H_3-8), 1.54 (9H, s, H_3-(*tert*)Bu), 2.42 (m, H-6), 3.81 (s, H_3-9), 4.37 (d, 2.4, H-5), 5.06 (s, H-3). ESITOF MS (Figure 118) *m/z* 278.15 $[M + Na]^+$, calcd for $C_{13}H_{21}NO_4Na$, 278.14.

9.9. Preparation of 5(*R*)-isopropyl-4-methoxy-Δ^3-pyrrolin-2-one [M6]

In the same manner described for **M3**, compound **M5** (50 mg, 0.2 mmol) was used instead of 2(*S*)-epimer. By using the same work up and purification methods, compound **M6**, having identical ^{1}H NMR spectrum to **M3**, was isolated (42 mg, 107 % yield).

Compound M6. white solid; $[\alpha]^{28}_D$ = –6.5 ° (*c* 1.00, CH_2Cl_2); ^{1}H NMR ($CDCl_3$, 400 MHz, Figure 121, Table 10) δ_H 0.80 (d, 6.8, H_3-7), 1.00 (d, 6.8, H_3-8), 2.08 (m, H-6), 3.79 (s, H_3-9), 3.98 (dd, 1.2, 2.8, H-5), 5.03 (d, 1.2, H-3), 5.40 (br s, NH); ESITOF MS (Figure 120) *m/z* 156.44 $[M + H]^+$, calcd for $C_8H_{14}NO_2$, 156.09.

9.10. Preparation of 5(*R*)-isopropyl-4-methoxy-1-propionyl--Δ^3-pyrrolin-2-one [M7]

In the same manner described for **M4**, compound **M6** (15 mg, 0.01 mmol) was used instead of its 5(*S*)-epimer. By using the same work up and purification methods, compound **M7**, having identical ^{1}H NMR spectrum to **M4**, was isolated (14 mg, 67% yield).

Compound M7. pale yellow solid; $[\alpha]^{28}_D$ = –60.9° (*c* 0.60, CH_2Cl_2); ^{1}H NMR ($CDCl_3$, 400 MHz, Figure 123, Table 10) δ_H 0.74 (d, 7.2 Hz, H_3-7), 1.11 (d, 7.2, H_3-8), 1.15 (t, 7.2, H_3-3'), 2.55 (m, H-6), 2.94 (q, 7.2, H_2-2'), 3.83 (s, H_3-9), 4.37 (d, 2.4,

H-5), 5.06 (s, H-3); ESITOF MS (Figure 124) *m/z* 234.51 $[M + Na]^+$, calcd for $C_{11}H_{17}NO_3Na$, 234.11.

10. Preparation of Samples for NMR Chiral Solvation Measurements

Samples for NMR chiral solvation experiments were typically prepared by separately mixing a sample with desired amount of a chiral solvating agent, 2,2,2-trifluoro-1-(9-anthryl)ethanol (TFAE or Pirkle's alcohol), in a very clean NMR tube using $CDCl_3$ as NMR solvent. If not indicated otherwise, the ^1H NMR spectra were recorded at 274 °K with a 600 NMR spectrometer. Chemical shifts were reported in ppm scale relative to the chemical shift of an internal tetramethylsilane (TMS) standard. The chemical shifts of the proton signals were assigned from the H,H COSY data.

11. Conformational Calculations at the C-2 Epimers of Malyngamide X [SHO-27]

Conformational analyses were calculated by the MonteCarlo method using MMFF94S force field, and the calculation of NOE Å by MacroModel were performed on a Power IRIS GTX200BII (Silicongraphics Limited).

12. Biological Testings of the Isolated Compounds

12.1. Cytotoxicity test

The cytotoxicity against breast cancer (BC), oral human epidermoid carcinoma of nasopharynx (KB), and human small cell lung cancer (NCI-H187) cell lines were performed employing the colorimetric method as described by Skehan and co-workers (Skehan, 1990). Ellipticine was used as a reference substance, exhibiting the activity toward BC, KB and NCI-H187 cell lines with the IC_{50} ranges of 0.4 ± 0.1 μg/ml (National Center for Genetic Engineering and Biotechnology, National Science and Technology Development Agency).

12.2. Antimalarial test

The parasite *Plasmodium falciparum* (K1, multidrug resistant strain) was cultured continuously according to the method of Targer and Jensen (1976).

Quantitative assessment of antimalarial activity *in vitro* was determined by means of the microculture radioisotope technique based upon the method described by Desjardins et al (1979). The inhibitory concentration (IC_{50}) represents the concentration that causes 50% reduction in parasite growth as indicated by the *in vitro* uptake of [^{3}H]hypoxanthine by *P. falciparum*. An IC_{50} value of 0.001 μg/ml was observed for the standard sample, artemisinin, in the same test system (National Center for Genetic Engineering and Biotechnology, National Science and Technology Development Agency).

12.3. Antituberculous test

Antimycobacterial activity was assessed against *Mycobacterium tuberculosis* H37Ra using the Microplate Alamar Blue (MABA) (Collins and Franzblau, 1997). The mycobacterium *M. tuberculosis* H37Ra was cultured in Middle-brook 7H9 broth. The standard drugs, isoniazid and kanamycin sulfate, used as reference compounds for the antimycobacterial assay, showed MIC values of 0.040–0.090 and 2.0–5.0 μg/ml, respectively. The MIC values of the reference compounds were determined in the same experiment as experimental samples (National Center for Genetic Engineering and Biotechnology, National Science and Technology Development Agency).

สถาบันวิทยบริการ
จุฬาลงกรณ์มหาวิทยาลัย

CHAPTER IV

RESULTS AND DISCUSSION

The sea hare, *Bursatella leachii* were collected by hand from the Gulf of Thailand. The identification and characterization of the sea hare were conducted mainly on the basis of its morphological characteristics. Regardless of the richness and variety of secondary metabolites from sea hare, our studies have been conducted following the experimental approach for the discovery of active principles, i.e. bioactivity-guided isolation. Bioactivity-guided fractionation from the first collection of the sea hare collected in October 2000 yielded the new and unusual malyngamide type natural product, malyngamide X (**SHO27**, 0.71% yield of the crude extract). Recollection of the mollusc in July 2002 afforded a potent stimulator of actin assembly hectochlorin (**SHOII-28**, 0.25% yield of the crude extract) and its new derivative, deacetylhectochlorin (**SHOII-51** 0.09 yield of the crude extract) together with a new structurally unrelated molecule, *syn*-3-isopropyl-6-(4-methoxy-benzyl)-4-methyl-morpholine-2,5-dione (**SHOII-76**, 0.007% yield of the crude extract).

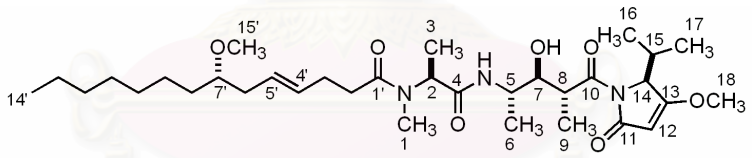

SHO27

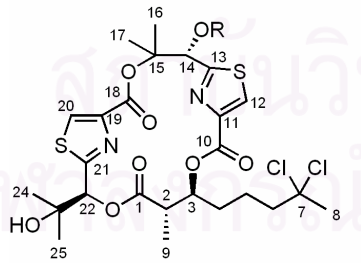

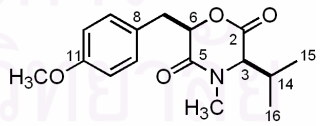

SHOII-28 R = $COCH_3$
SHOII-51 R = H

SHOII-76

Comparison of the structurally unrelated molecules between each collection of the sea hares, it is likely that the sea hares store and enrich secondary metabolites from their diet at different locations before coming back to our collection site. Another explanation may be the varied dietary sources for the sea hares around

the Gulf of Thailand. While the origin of malyngamide-type natural products (i.e. malyngamide X) and hectochlorin have been known to be from cyanobacteria, compound **SHOII-76** has never been reported from any algal species. It is possible that this compound is synthesized by the mollusc itself.

1. Structure Elucidation of the Isolated Compounds

Assignment for determining the gross structures of the three new compounds, **SHOII-27** (malyngamide X), **SHOII-51** (deacetylhectochlorin), and **SHOII-76** (*syn*-3isopropyl-6-(4-methoxy-benzyl)-4-methyl-morpholine-2,5-dione) as well as one known compound, **SHOII-28** (hectochlorin), were mainly accomplished by extensive analysis of 1D-NMR and 2D-NMR measurements of H,H COSY, HMQC, HMBC, and NOESY spectral data in conjunction with the MS data. Stereostructures of the compounds were established with a combination of NMR-based methods, CD spectroscopy, X-ray crystallography, and biogenetic considerations.

1.1. Structure Elucidation of Malyngamide X [SHO27]

Gross structure. Compound **SHO27** was obtained as a pale yellow oil. The molecular formula $C_{33}H_{57}N_3O_7$ of **SHO27** was determined from HRFABMS data (*m/z* 608.4579 $[M + H]^+$, calcd for $C_{33}H_{58}N_3O_7$, 608.4275), and accounting for seven degrees of unsaturation (Figure 46). The IR spectrum (Figure 45) showed absorptions due to free OH or amide NH (3438 cm^{-1}), H-bonded OH or amide NH (broad, 3200–3600 cm^{-1}), amide carbonyl (1624, 1684 and 1722 cm^{-1}) moieties in the molecule. By examination of the ^{13}C NMR spectral data (Figure 52 and Table 5), six degrees of unsaturation accounted for two imide carbonyls (δ_c 170.8 and 175.4), two amide carbonyls (δ_c 173.2 and 171.1), and two carbon–carbon double bonds (δ_c 94.6, 127.1, 130.9 and 179.6). Therefore, compound **SHO27** was a monocylic in nature. According to extensive analyses of 1D, 2D NMR (Table 5) and MS data, the gross structure of **SHO27** was accomplished as a new malyngamide derived from 7-methoxytetradec-4(*E*)-enoic acid (fragment **I**, Figure 23**B**) and a tripeptide constructed from *N*-methylalanine, 4-amino-3-hydroxy-2-methylpentanoic acid, and 5-isopropyl-4-methoxy-Δ^3-pyrrolin-2-one shown as fragments **II**, **III**, and **IV** in

Figure 23**B**, respectively. The amine-derived moiety numbering is based on that of janolusimide (Sodano and Spinella, 1986), a very similar tripeptide (Figure 23**A**).

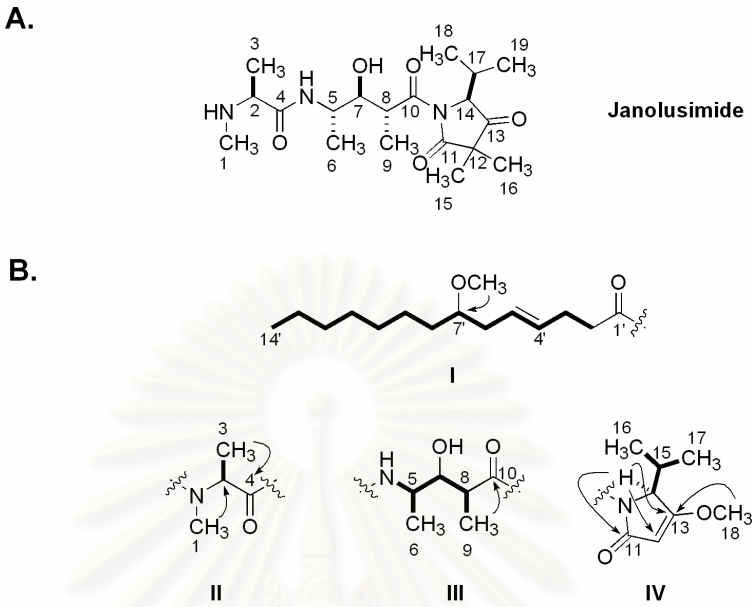

Figure 23. (A) Structure of janolusimide showing numbering system (Sodano and Spinella, 1986). (B) Partial structures of malyngamide X [**SHO27**] showing H,H COSY correlations (▬) and important HMBC correlations (→).

The ^{1}H and ^{13}C NMR spectra (Table 5) of **SHO27** clearly indicated the presence of the characteristic signals for "methoxylated fatty acid" portion of malyngamide-type natural products (Burja et al., 2001 and references cited therein). These signals included a carbonyl carbon at δ_C 173.2 (C-1'); four methylene signals at δ_H 2.38/δ_C 33.9 (C-2'), δ_H 2.34/δ_C 28.2 (C-3'), δ_H 2.16/δ_C 36.5 (C-6'), and δ_H 1.40/δ_C 33.5 (C-8'); a terminal methyl signal at δ_H 0.85/δ_C 14.3 (C-14'); two olefinic signals at δ_H 5.50/δ_C 127.1 (C-4') and δ_H 5.45/δ_C 130.9 (C-5'); a methoxy signal at δ_H 3.30/δ_C 56.5 (OCH_3-15'); and an oxygenated methine signal at δ_H 3.12/δ_C 80.8 (C-7'). Although the aliphatic methylene protons of H_2-9' to H_2-13' in the fatty acid portion appeared as overlapping signals in the δ_H 1.20–1.30 region, their corresponding five carbon signals were all well resolved (δ_C 25.4, 29.4, 29.9, 31.9, and 22.8, respectively). Taken together with the literature precedence, this fatty acyl part (Fragment **I**, Figure 23**B**) was established as 7-methoxytetradec-4(*E*)-enoic acid moiety. The *E*-geometry of the $\Delta^{4'}$ olefin was determined by the H-4'/H-5' coupling constant of 15.3 Hz. The methylene protons H_2-2', which resonated together in

$CDCl_3$, were resolved in C_6D_6 (Figure 47) as a pair of multiplet ($\delta_{H-2'a}$ 2.10 and $\delta_{H-2'b}$ 2.30).

The three partial structures (fragments **II**–**IV**) in the amine-derived portion of the molecule were established by analyses of the H,H COSY, HMQC, HMBC, and 2D NOESY spectra (Table 5, Figure 23**B**). The CH_3–CH(X)–residue in the *N*-methylalanine fragment (fragment **II**) was delineated by the H,H COSY cross-peak between methyl protons at δ_H 1.32 (H_3-3) and down field methine proton at δ_H 5.20 (H-2). The fragment was further confirmed by HMBC correlations of the *N*-methyl protons signal at δ_H 2.93 (H_3-1) to C-2 (δ_C 51.9), and H_3-3 to the C-4 carbolyl (δ_C 171.1).

The 4-amino-3-hydroxy-2-methylpentanoic acid fragment (fragment **III**) was clearly indicated by the H,H COSY experiment. The amide proton (δ_H 6.45) exhibited correlation to the methine proton at δ_H 4.05 (H-5) which was in turn correlated to the other methine proton at δ_H 3.66 (H-7) and the methyl protons at δ_H 1.18 (H_3-6). H-7 was further coupled to the methine proton at δ_H 3.86 (H-8) which in turn showed correlation to the methyl protons at δ_H 1.11 (H_3-9). In $CDCl_3$ solution, the oxygenated methine proton signal at H-7 appeared as a broad signal and was simplified to a doublet of doublets in D_2O exchangeable experiment (Figure 51) with $^3J_{H-5,H-7}$= 2.6 Hz and $^3J_{H-7,H-8}$= 8.9 Hz, suggesting the hydroxyl substituted on this position. The HMBC correlations between H_3-6 and H_3-9 to oxygenated carbon at δ_C 77.4 (C-7) and additional HMBC correlation of H_3-9 to the imide carbonyl at δ_C 175.4 (C-10) completed the assignment of fragment **III**. The occurrence of this unusual amino acid with different stereochemistry was previously reported in only two natural compounds including a middle portion of the nudibranch neurotoxin tripeptide, janolusimide (Sodano and Spinella, 1986) and the antitumor antibiotic bleomycin A_2 (Giordano et al., 2000 and references cited therein). The structures of naturally occurring 4-amino-3-hydroxy-2-methylpentanoic acid are shown in Figure 24.

The presence of 5-isopropyl-4-methoxy-Δ^3-pyrrolin-2-one portion (fragment **IV**) was proven by HMBC correlations between the methine proton at δ_H 4.51 (H-14) to the imide carbonyl at C-11 (δ_C 170.8) and the olefinic carbons at

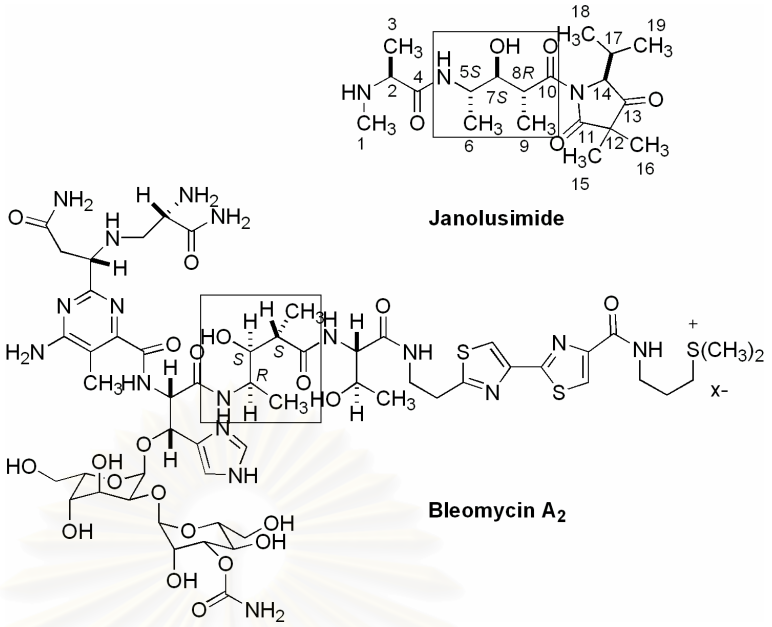

Figure 24. The structures of 4-amino-3-hydroxy-2-methylpentanoic acid-containing natural products.

δ_C 94.6 (C-12) and δ_C 179.6 (C-13). The methoxyl substituted on C-13 was deduced from the HMBC cross-peak of the methoxyl protons at δ_H 3.82 (H_3-18) to the olefinic at C-13 (Table 5). This methoxy substitution was responsible for a pair of unusual carbon chemical shifts at C-12 and C-13, a common feature of the 4-methoxy-Δ^3-pyrrolin-2-one heterocycles (Paik et al., 1994; Royles, 1995; Milligan, Márquez, Williamson, Davies-Coleman et al., 2000). The isopropyl side chain was placed at C-14 (δ_C 64.4) on the basis of H-H COSY correlations of both H_3-16 (δ_H 0.74) and H_3-17 (δ_H 1.07) to H-15 (δ_H 2.60) which was in turn coupled to H-14.

The connection of fragments **I** and **II** resulted from the HMBC correlation observed from the *N*-methyl protons at H_3-1 to C-1' of the fatty acid residue (Table 5). Further connection to fragment **III** was suggested by the interpretation of the NOESY spectrum whereas HMBC correlations were virtually absent. The NOESY correlation observed between H-2 and NH led to furnish the linearity connection of fragments **I**, **II**, and **III**. Finally, fragment **IV** was unambiguously placed as a terminal residue at C-10. Therefore, the gross structure of the first malyngamide possessing a tripeptide skeleton in its amine-derived portion was completed as malyngamide X.

Table 5. ^{1}H and ^{13}C NMR spectral data of malyngamide X [**SHO27**] recorded in $CDCl_3$

atom no.	$^{1}H^{a}$ δ_H (mult., *J* in Hz)	$^{13}C^{b}$ δ_C	H,H COSY[c]	HMBC[c] $^{n}J_{CH}$ *n* = 2,3)	NOESY[a]
1	2.93 (3H, s)	30.7		C-1', C-2	H_3-3, H_2-2', H_2-3', H-8
2	5.20 (1H, q, 7.0)	51.9	H_3-3	C-1, C-4	NH
3	1.32 (3H, d, 7.3)	13.9	H-2	C-2, C-4	H_3-1
4	-	171.1			
5	4.05 (1H, m)	46.7	NH, H_3-6, H-7		H_3-9
6	1.18 (3H, d, 6.7)	18.3	H-5	C-5, C-7	NH, H-7
7	3.66 (1H, m)[d]	77.4	H-5, H-8, OH	C-5	H_3-6, $_3$H-9
8	3.86 (1H, dq, 8.9, 6.7)	42.4	H-7, H_3-9		H_3-1
9	1.11 (3H, d, 6.7)	14.3	H-8	C-7, C-8, C-10	H-5, H-7
10	-	175.4			
11	-	170.8			
12	5.05 (1H, s)	94.6		C-11, C-14	H_3-18
13	-	179.6			
14	4.51 (1H, d, 2.8)	64.5	H-15	C-11, C-12, C-13, C-16	H_3-16, H_3-17, H_3-18
15	2.60 (1H, m)	29.1	H-14, H_3-16, H_3-17	C-16	
16	0.74 (3H, d, 7.0)	15.5	H-15	C-14, C-15, C-17	H-14, H_3-18
17	1.07 (3H, d, 7.3)	18.9	H-15	C-14, C-15, C-16	H-14, H_3-18
18	3.82 (3H, s)	58.6		C-13	H-12, H_3-16, H_3-17
NH	6.45 (1H, d, 8.9)	-	H-5		H-2, H_3-6
OH	3.49 (1H, br d, 7.6)	-	H-7		
1'	-	173.2			
2'	2.38 (2H, m)	33.9	H_2-3'		H_3-1
3'	2.34 (2H, m)	28.2	H_2-2', H-4'		H-5'
4'	5.50 (1H, dt, 15.3, 5.8)	127.1	H_2-3', H-5'	C-3'	H_2-6'
5'	5.45 (1H, dt, 15.3, 6.4)	130.9	H-4', H_6-6'	C-3'	H_2-3'
6'	2.16 (2H, dd, 5.8, 5.8)	36.5	H-5', H-7'	C-4' , C-5', C-7', C-8'	H-4'
7'	3.12 (1H, quin, 5.8)	80.8	H_2-6', H_2-8'		
8'	1.40 (2H, m)	33.5	H-7'		
9'	1.20-1.30 (2H)	25.4			
10'	1.20-1.30 (2H)	29.4			
11'	1.20-1.30 (2H)	29.9			
12'	1.20-1.30 (2H)	31.9			
13'	1.20-1.30 (2H)	22.8	H_3-14'		
14'	0.85 (3H, t, 7.2)	14.3	H_2-13'	C-12', C-13'	
15'	3.30 (3H, s)	56.5		C-7'	

[a] Recorded at 500 MHz. [b] Recorded at 75 MHz. [c] Recorded at 300 MHz. [d] After D_2O addition, the signal simplified to a doublet of doublets (*J* = 8.9, 2.6 Hz) recorded at 300 MHz.

Stereochemistry. The absolute stereochemistry of compound **SHO27** was determined through a combination of biosynthetic consideration and non-hydrolytic degradation methods comprising NMR applications of the modified Mosher's method and NMR chiral solvation experiments, together with conformational calculations. The current strategy in using non-hydrolytic method for determining absolute stereochemistry of a compound **SHO27** differs from those reported for other malyngamides (or lipopeptides). The details will be discussed later.

1.2. Identification of Hectochlorin [SHOII-28]

Gross structure. Compound **SHOII-28** was obtained as white crystals. HREIMS established a molecular ion M^+ peak at *m/z* 664.1082 (Figure 73) for the molecular formula $C_{27}H_{34}Cl_2N_2O_9S_2$ (calcd. 664.1083), indicating a structure with eleven degrees of unsaturation. The observed isotope peaks at *m/z* 664/666/668, in an approximate intensity of 5:4:1, are consistent with the presence of two chlorine atoms in the molecule. Analysis of the ^{1}H and ^{13}C NMR data (Table 6) indicated a short aliphatic chain, a *gem*-dichloromethyl functionality, three sp^3 methines bound to heteroatoms, two sp^2 methines, one methine in the α-position of a carbonyl, two quaternary sp^3 carbons bound to heteroatoms, and eight downfield resonances in the amide/ester carbonyl or heterocyclic quaternary sp^2 carbon chemical shift range. The two chlorine atoms were suggested to be geminal to each other because the ^{13}C NMR spectrum displayed a signal at δ_C 90.4 for a quaternary carbon (C-7). Further interpretation of 1D NMR data in combination with 2D NMR experiments, including H,H COSY, HMQC, and HMBC defined partial structures **I**–**III** (Figure 25).

The thiazole unit in fragment **I** was assembled from the HMBC correlations from the methine proton δ_H 7.91 (H-20) to three quaternary sp^2 carbons including δ_C 147.3 (C-19), 160.2 (C-18), and 165.0 (C-21). The methyl protons at δ_H 2.07 (H_3-8) showed a HMBC correlation to a *gem*-dichloro methyl unit, thus, connecting this unit as $-C(Cl)_2CH_3$. Further HMBC correlation from H_3-8 to δ_C 49.4 (C-6) of a $-(CH_2)_3-CH(X)-CH(CH_3)-$ residue, obtained by H,H COSY experiment,

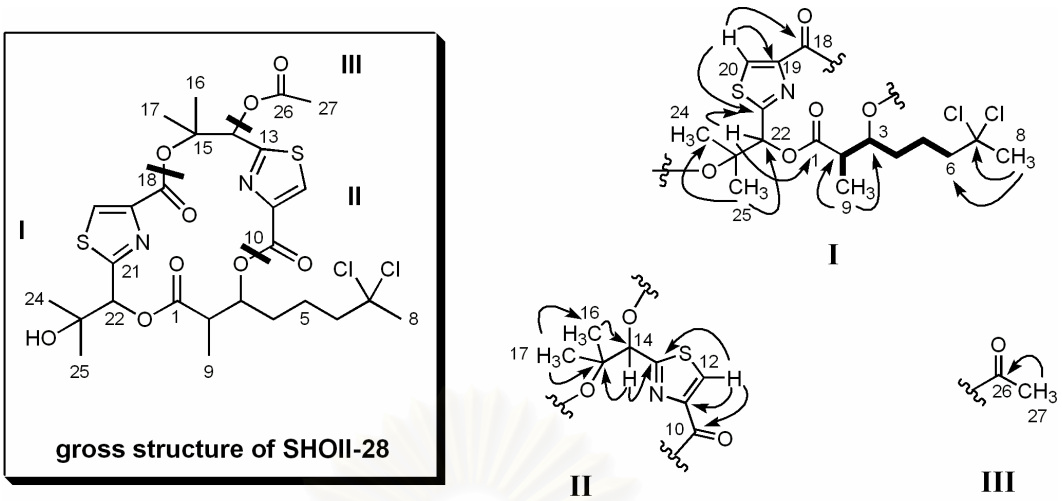

Figure 25. Partial structures of hectochlorin [**SHOII-28**] showing H,H COSY correlations (▬) and important HMBC correlations (→).

and H_3-9 to δ_C 172.8 (C-1) allowed the presence of 7,7-dichloro-3-acyloxy-2-methyl-octanoate (DCAO) containing fragment **I**. Next, the presence of α,*β*-dihydroxyisovalerate (DHIV) in the molecule was established due to the HMBC correlations from both methyl groups of the *gem*-dimethyl unit at δ_H 1.31 (H_3-24) and 1.34 (H_3-25) to the pseudo-α carbon at δ_C 77.9 (C-22) and quaternary carbon at δ_C 71.6(C-23). The methine proton at δ_H 5.61 (H-22) was in turn showed HMBC connectivity to the quaternary carbons at δ_C 165.0 (C-21) and 172.8 (C-1), thus, completing the connectivity in partial structure **I**. Likewise, the complete partial structure **II** was based on the methine proton δ_H 6.78 (H-14) showing HMBC correlations to quaternary carbons at δ_C 82.0 (C-15) of a *gem*-dimethyl unit and δ_C 166.1 (C-13) of a second thiazole unit. Similarly, in fragment **II**, connectivity could be observed from the methine proton δ_H 8.14 (H-12) to three quaternary carbons including δ_C 147.0 (C-11), 160.9 (C-10), and 166.1 (C-13). The acetyl containing fragment **III** was assembled by HMBC correlation of the methyl protons at δ_H 2.16 (H_3-27) to the carbonyl carbon at δ_C 168.5 (C-26). These partial structures **I**, **II** and **III** accounted for ten degrees of unsaturation required by the molecular formula, thus compound **SHOII-28** was a monocyclic in nature.

Chemical shift at δ_H 5.33 and δ_C 75.1 of C-3 in fragment **I** clearly indicated an acyloxy substituted on this position. This was satisfied only by ester

bond with C-10 of fragment **II**. The acetyl containing fragment **III** was, therefore, placed on C-14. This was confirmed with the HMBC correlation between H-14 and the ester carbonyl of C-26. Finally, the cyclic nature of **SHOII-28** was accomplished with the ester bond linkage between C-15 and C-18. The IR spectrum (Figure 72) showed a strong absorption at 1745 and 1712 cm^{-1} confirming the presence of ester moieties in the molecule. The broad band at 3456 cm^{-1} further confirmed the presence of a hydroxyl group at C-23. After gross structure of **SHOII-28** could be established, the compound was identified as a recently reported cyanobacterial metabolite, hectochlorin (Marquez et al., 2002) or its stereomers. All of the above spectral data were also consistent with the previously published data of hectochlorin (Table 6).

Stereochemistry. The absolute stereochemistry of the known compound hectochlorin has been reported to be 2(*R*), 3(*S*), 14(*S*), and 22(*S*) by X-ray analysis referring to anomalous scattering data (Marquez et al., 2002). Hectochlorin showed negative $[\alpha]_D$ of 8.7 (c 1.04, MeOH) similarly to negative $[\alpha]_D$ of 7.5 (c 0.28, MeOH) shown by compound **SHOII-28**. The structural characterization of **SHOII-28** by single-crystal x-ray analysis (Figure 26) further confirmed the gross and stereo structure of this compound as hectochlorin.

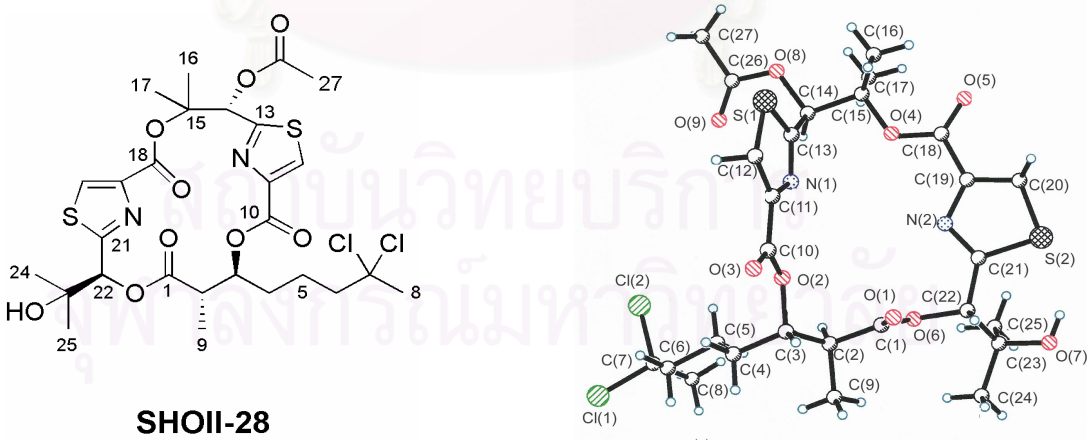

Figure 26. ORTEP plot of hectochlorin [**SHOII-28**]

Hectochlorin was recently isolated from the cyanobacterium, *Lyngbya majuscula* (Oscillariaceae) and acted as a potent stimulator of actin assembly (Marquez et al., 2002). Therefore, the real producer of compound **SHOII-28** might be the cyanobacteria fed on by the sea hares.

Table 6. ^{1}H and ^{13}C NMR spectral data of hectochlorin and **SHOII-28** recorded in $CDCl_3$

	Hectochlorin[a]		**SHOII-28**			
atom no.	^{1}H δ_H(mult., *J*/ Hz)	^{13}C δ_C	$^{1}H^{b}$ δ_H(mult., *J*/ Hz)	^{13}C δ_C	H,H-COSY[b]	HMBC[b, d] ($^{n}J_{CH}$ n = 2,3)
1	-	173.0		172.8		C-1
2	3.16 (m)	42.6	3.15 (1H, m)	42.7	H-3, H_3-9	
3	5.33 (m)	75.1	5.33 (1H, m)	75.1	H-2, H_2-4ab	
4a	1.72 (m)	30.9	1.69 (1H, m)	31.0	H-3, H_2-5	
4b	1.82 (m)		1.78 (1H, m)			
5	1.69 (m)	20.8	1.69 (2H, m)	21.0	H_2-4ab, H_2-6ab	
6a	2.13 (m)	49.3	2.11 (1H, m)	49.4		
6b	2.25 (m)		2.25 (1H, m)		H-5	C-8
7	-	90.4		90.4		
8	2.09 (s)	37.2	2.07 (3H, s)	37.3		C-6, C-7
9	1.28 (d, 7.4)	15.0	1.28 (3H, d, 7.4)	15.2	H-2	C-1, C-2[e], C-3
10	-	161.1		160.9		
11	-	147.0		146.8		
12	8.14 (s)	128.5	8.14 (1H, s)	128.3		C-10, C-11, C-13
13	-	166.2		166.1		
14	6.78 (s)	74.7	6.78 (1H, s)	74.7		C-13, C-15, C-16, C-17, C-26[e]
15	-	81.9		82.0		
16	1.83 (s)	24.4	1.82 (3H, s)	24.6		C-14, C-15, C-17
17	1.60 (s)	21.9	1.59 (3H, s)	22.0		C-14, C-15, C-16
18	-	160.4		160.2		
19	-	147.4		147.3		
20	7.90 (s)	127.7	7.91 (1H, s)	127.6		C-18[e], C-19, C-21
21	-	165.2		165.0		
22	5.64 (s)	77.9	5.61 (1H, s)	77.9		C-1[e], C-21, C-23[e],
23	-	71.6		71.6		
24	1.31 (s)	26.7	1.29 (3H, s)	26.8		C-22[e], C-23, C-25[e]
25	1.34 (s)	25.8	1.35 (3H, s)	26.1		C-22[e], C-23, C-24
26	-	168.7		168.5		
27	2.17 (s)	20.8	2.16 (3H, s)	21.0		C-26

[a] ^{1}H (600 MHz) and ^{13}C (150 MHz) NMR data reported by Marquez (2002). [b] Recorded at 300 MHz. [c] Recorded at 75 MHz [d] If not indicated otherwise, correlations were observed after optimization for $^{n}J_{CH}$ = 8 Hz. [e] Correlations after optimization for $^{n}J_{CH}$ = 4 Hz.

1.3. Structure Elucidation of Deacetylhectochlorin [SHOII-51]

Gross structure. Deacetylhectochlorin [**SHOII-51**] was obtained as a white amorphous solid from reversed-phase HPLC. The close relationships of **SHOII-51** to hectochlorin [**SHOII-28**] became evident by inspecting the ^{1}H, ^{13}C, H,H COSY, HMQC, and HMBC spectra of the compound (Table 7). HREIMS of **SHOII-51** (Figure 87) showed a molecular ion M^{+} peak at *m/z* 622.0984 corresponding to the molecular formula $C_{25}H_{32}Cl_2N_2O_8S_2$ (calcd. 622.0977). The molecular formula of **SHOII-51** corresponded to ten degrees of unsaturation and differed from hectochlorin by 42 amu. In contrast to hectochlorin, **SHOII-51** lacked the signals of an acetyl group which established **SHOII-51** as deacetylhectochlorin. Further interpretation of 1D NMR data in combination with 2D NMR experiments defined partial structures **I**–**III** (Figure 27).

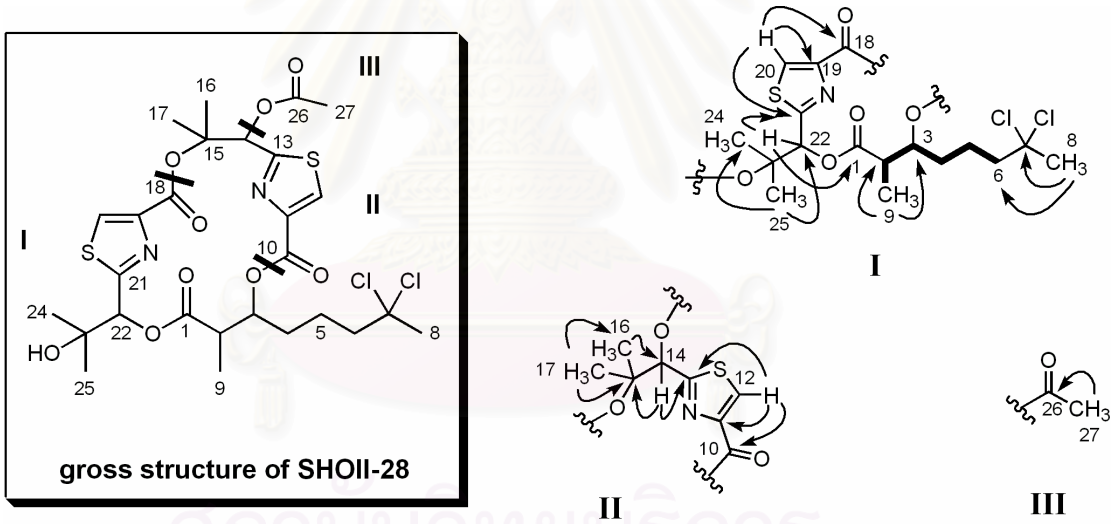

Figure 27. Partial structures of deacetylhectochlorin [**SHOII-51**] showing H,H COSY correlations (▬) and important HMBC correlations (→).

The ^{1}H and ^{13}C NMR spectra of **SHOII-51** were nearly identical to those of hectochlorin, which contained two units of 2-alkylthiazole-4-carboxylic acid (C-10 to C-13 and C-18 to C-21) and a 7,7-dichloro-3-acyloxy-2-methyl-octanoate (DCAO) fragment (C-1 to C-9). The 2-alkylthiazole-4-carboxylic acid units containing fragments **I** and **II** were indicated by two singlets of the methine proton

signals at δ_H 8.25 (H-12) and 8.15 (H-20) in the ^{1}H NMR spectrum as well as eight sp^2 carbon signals at δ_C 159.2 (C-10), 142.9 (C-11), 129.0 (C-12), 177.5 (C-13) and 158.6 (C-18), 146.4 (C-19), 128.6 (C-20), 167.6 (C-21) in the ^{13}C NMR spectrum (Table 7). The NMR data further assigned the presence of the DCAO fragment containing fragment **I** as follow. Analysis of the H,H COSY spectrum and additional HMBC correlations of the methyl protons at δ_H 2.10 (H_3-8) to the *gem*-dichloromethyl carbon at δ_C 90.2 (C-7) and the methylene carbon at δ_C 49.5 (C-6) clearly established the aliphatic chain (C-2 to C-9). The carbonyl signal at δ_C 174.0 was assigned to C-1 of the DCAO fragment by HMBC correlation observed from the methyl protons at δ_H 1.28 (H_3-9). The first α,β-dihydroxyisovalerate (DHIV, C-21 to C-25) containing fragment **I** was observed due to the HMBC correlations from the *gem*-dimethyl protons at δ_H 1.23 (H_3-24) and 1.44 (H_3-25) to the pseudo-α carbon at δ_C 78.9 (C-22) and the quaternary carbon at δ_C 71.7 (C-23). The downfield signals of C-22 (δ_H 5.38 and δ_C 78.9) and C-23 (δ_C 71.7) were satisfied with an ester bond linkage and a tertiary alcohol functionality as observed in a DHIV unit of hectochlorin, respectively. Finally, fragment **I** was assembled since H-22 of the DHIV unit showed HMBC correlations to C-1 and C-21 of the DCAO and the first thiazole (C-18 to C-21) residues, respectively. Similarly, the second DHIV unit (C-13 to C-17) containing fragment **III** was confirmed as a part of **SHOII-51** structure on the basis of HMBC correlations from the *gem*-dimethyl protons at δ_H 1.85 (H_3-16) and 1.57 (H_3-17) to the pseudo-α carbon at δ_C 73.8 (C-14) and the quaternary carbon at δ_C 85.7 (C-15). The methine proton signal of H-14 in **SHOII-51** (δ_H 5.55) is shifted upfield by about 1 ppm compared with hectochlorin (δ_H 6.78), consistent with a hydroxyl group at C-14 in **SHOII-51** rather than an acetoxy group as in hecthochlorin.

Chemical shifts at δ_H 5.22 and δ_C 76.9 of C-3 in the DCAO unit further indicated an acyloxy substituted on this position. This was satisfied with the ester bond linkage between C-3 and C-10 of the second thiazole unit (C-10 to C-13) of fragment **II**. Likewise, the downfield signal at δ_C 85.7 of C-15 (fragment **III**) was consequently satisfied with the ester bond linkage to the carbonyl carbon C-18 of the first thiazole unit (fragment **I**). The IR spectrum of **SHOII-51** showed strong absorptions at 1739 and 1717 cm^{-1} confirming the presence of the ester moieties and a

strong broad band at 3391 cm^{-1} further supporting the hydroxyl groups in the molecule (Figure 86). Finally, the cyclic nature of **SHOII-51** was furnished by ring closer of C-13 and C-14. This cyclic structure could complete ten degrees of unsaturation required by the molecular formula of **SHOII-51**. Therefore, **SHOII-51** was established as a new deacetylhectochlorin.

Stereochemistry. To determine the absolute stereochemistry in **SHOII-51**, the acetyl group of hectochlorin was removed by hydrazine hydrolysis of hectochlorin in MeOH at 0 ^{o}C for 2 h (Figure 28). The ^{1}H spectrum and the specific rotation of the hydrolysis product were identical to those of **SHOII-51** (Figure 29). The absolute stereochemistry of **SHOII-51** was then suggested by comparing the CD spectra of the natural and the transformed **SHOII-51**, which displayed similar positive cotton effect at 228 nm and two negatives at 209 (210) and 257 (258) nm. On the basis of this information, the absolute configuration of **SHOII-51** was concluded to be the same as that of hectochlorin. Moreover, since the compound could be derived from hectochlorin, this also supported the gross structure of **SHOII-51** as the new deacetylhectochlorin.

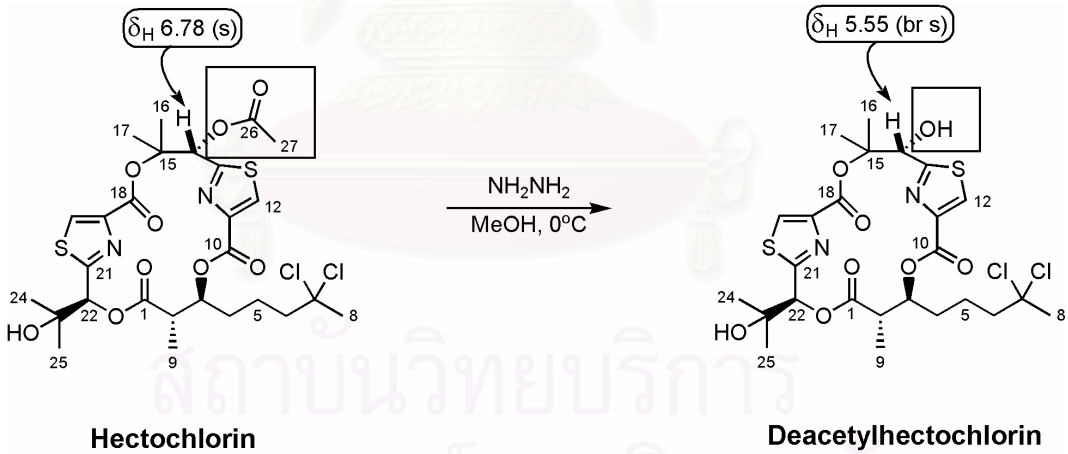

Figure 28. Hydrazine hydrolysis of hectochlorin and key ^{1}H NMR signals.

Table 7. ^{1}H and ^{13}C NMR spectral data of hectochlorin [**SHOII-28**] and deacetylhectochlorin [**SHOII-51**] recorded in $CDCl_3$

atom no.	SHOII-28		SHOII-51			
	$^{1}H^{a}$	$^{13}C^{b}$	$^{1}H^{a}$	$^{13}C^{b}$	H,H COSY^{a}	HMBC$^{a, c}$
	δ_H (mult., J in Hz)	δ_C	δ_H (mult., J in Hz)	δ_C		($^{n}J_{CH}$, n = 2, 3)
1	-	172.8	-	174.0		
2	3.15 (1H, m)	42.7	3.77 (1H, m)	42.3	H-3, H_3-9	
3	5.33 (1H, m)	75.1	5.22 (1H, m)	76.9	H-2, H_2-4ab	
4a	1.69 (1H, m)	31.0	1.76 (1H, m)	30.5	H-3, H_2-5	
4b	1.78 (1H, m)		2.02 (1H, m)			
5	1.69 (2H, m)	21.0	1.76 (2H, m)	20.6	H_2-4ab, H_2-6	
6a	2.11 (1H, m)	49.4	2.19 (1H, m)	49.5	H_2-5	
6b	2.25 (1H, m)		-	-		
7	-	90.4	-	90.2		
8	2.07 (3H, s)	37.3	2.10 (3H, s)	37.3		C-6^{d}, C-7
9	1.28 (3H, d, 7.4)	15.2	1.28 (3H, d, 6.8)	15.2	H-2	C-1, C-2^{d}, C-3
10	-	160.9	-	159.2		
11	-	146.8	-	142.9		
12	8.14 (1H, s)	128.3	8.25 (1H, s)	129.0		C-11, C-13
13	-	166.1	-	177.5		
14	6.78 (1H, s)	74.7	5.55 (1H, brs)	73.8		
15	-	82.0	-	85.7		
16	1.82 (3H, s)	24.6	1.85 (3H, s)	24.3		C-14, C-15, C-17
17	1.59 (3H, s)	22.0	1.57 (3H, s)	20.1		C-14, C-15, C-16
18	-	160.2	-	158.6		
19	-	147.3	-	146.4		
20	7.91 (1H, s)	127.6	8.15 (1H, s)	128.6		C-18^{d}, C-C-21
21	-	165.0	-	167.6		
22	5.61 (1H, s)	77.9	5.38 (1H, s)	78.9		C-1^{d}, C-21, C-23^{d}, C-24^{d}, C-25^{d}
23	-	71.6	-	71.7		
24	1.29 (3H, s)	26.8	1.23 (3H, s)	26.7		C-22^{d}, C-23, C-25^{d}
25	1.35 (3H, s)	26.1	1.44 (3H, s)	26.4		C-22^{d}, C-23, C-24
26	-	168.5	-	-		
27	2.16 (3H, s)	21.0	-	-		

^{a}Recorded at 300 MHz. ^{b}Recorded at 75 MHz. ^{c}If not indicated otherwise, correlations were observed after optimization for $^{n}J_{CH}$ = 8 Hz. ^{d}Correlations after optimization for $^{n}J_{CH}$ = 4 Hz.

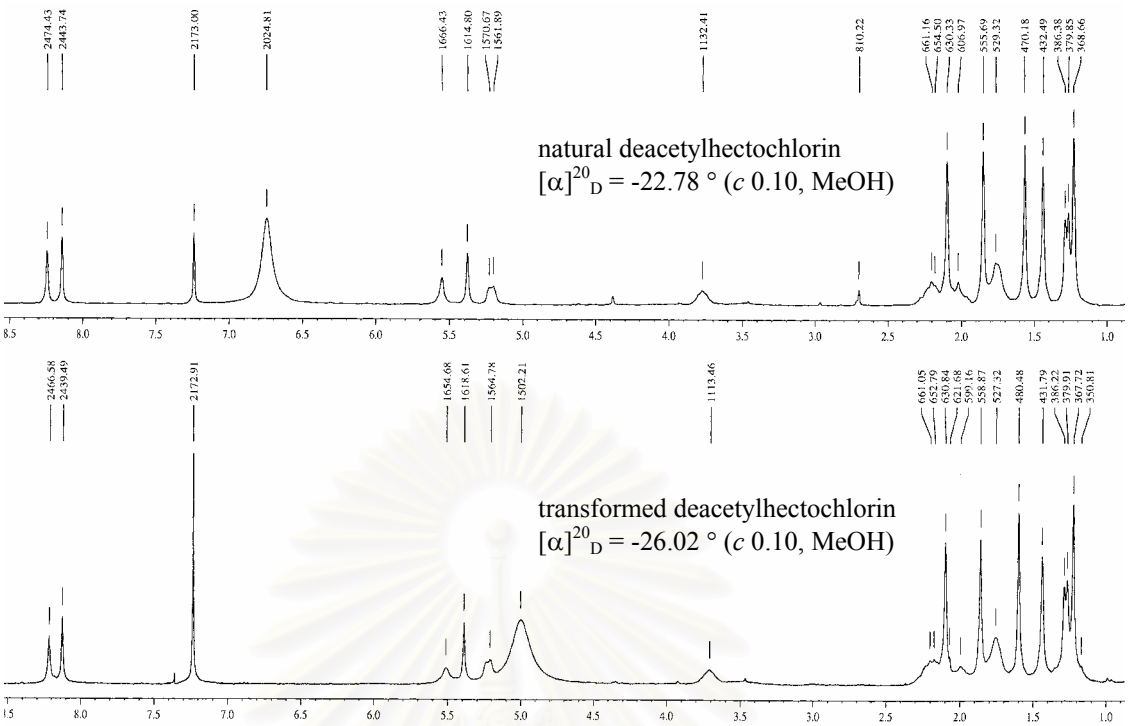

Figure 29. ^{1}H NMR spectra ($CDCl_3$, 300 MHz) of natural and transformed deacetylhectochlorin.

Both hectochlorin and deacetylhectochlorin were directly detected by Si gel TLC from a fraction prior to purification with reversed-phase HPLC with R_f values of 0.50 and 0.38 (solvent system: EtOAc-hexane = 3:1), respectively. This evidence ruled out the possibility that deacetylhectochlorin was an artifact from acid hydrolysis of hectochlorin during the HPLC purification process using a mixture of CH_3CN/MeOH/1% TFA in water (2:1:1) as the eluting solvent. The co-occurrence of hectochlorin and deacetylhectochlorin in the extract from *B. leachii* suggested that deacetylhectochlorin could be a metabolism product formed from hectochlorin as a result of the ester bond cleavage occurring in the acidic digestive gland of the mollusc. This eventual metabolism was earlier implied in the biogenesis of dolabellin found in the sea hare, *Dolabella auricularia* (Luesch, Yoshida, Moore, and Paul, 2002).

1.4. Structure Elucidation of s*yn*-3-Isopropyl-6-(4-methoxy-benzyl)-4-methyl-morpholine-2,5-dione [SHOII-76]

Gross structure. Compound **SHOII-76** was obtained as a white solid in trace amount (0.5 mg, 0.007% yield of the crude extract). Further interpretation of 1D NMR data in combination with 2D NMR experiments, including H,H COSY, HMQC, HMBC, and NOESY (Table 8) defined **SHOII-76** as a morpholine-2,5-dione containing natural compound (Figure 30).

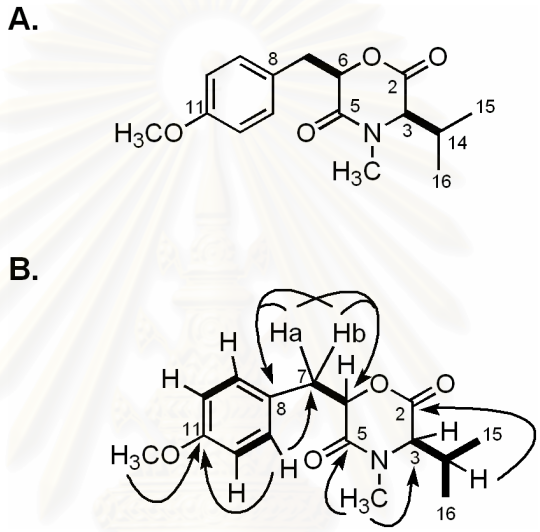

Figure 30. (A) Structure of s*yn*-3-isopropyl-6-(4-methoxy-benzyl)-4-methyl-morpholine-2,5-dione [**SHO-II 76**] showing (B) H,H COSY correlations (▬) and important HMBC correlations (→).

SHOII-76 has the molecular formula $C_{16}H_{21}NO_4$ (M.W. 291.1471) accounting for seven degrees of unsaturation, as determined by ESITOFMS (m/z 314.1679 $[M + Na]^+$; 292.1653 $[M + H]^+$, calcd for $C_{16}H_{22}NO_4$, 292.1549) (Figure 98). The ^{1}H NMR spectrum (Figure 99) of **SHOII-76** exhibited a 1,4-disubstituted aromatic ring, in which proton signals were observed at δ_H 7.18 (H-9/ H-13, 2H, d, J = 8.4 Hz) and 6.84 (H-10/ H-12, 2H, d, J = 8.4 Hz). The $^3J_{H,H}$ couplings of H-6 (δ_H 5.00, dd, J = 8.4, 4.0 Hz) to both methylene protons H_2-7ab (H_{7a} δ_H 3.17, dd, J = 14.4, 8.0 Hz and H_{7b} δ_H 3.33, dd, J = 14.4, 4.0 Hz) suggested a series of ABX coupling signals as a $-CH(X)-CH_2-$ residue. The H,H COSY experiment revealed the presence of an additional partial structure, $-CH(X)-CH(CH_3)_2$ of the *N*-methylvaline

unit (C-3 and C-14 to C-16, Table 8). The presence of *N*-methylvaline in the molecule was established from the HMBC correlations of the *N*-methyl protons (δ_H 3.00) to the methine carbon at δ_C 66.3 (C-3) and that of methine proton at δ_H 1.99 (H-14) to the ester carbonyl carbon at δ_C 164.2 (C-2). The HMBC correlation observed for the *N*-methyl protons and the carbonyl carbon at δ_C 164.7 (C-5), thus, suggested the amide functionality in the molecule. The IR spectrum (Figure 98) showing two strong absorption bands at 1744 and 1651 cm^{-1} further confirmed the presence of ester and amide functionalities in the molecule. The methoxyl substituted at C-11 was indicated from HMBC correlations of δ_H 3.78 (11-OCH_3), δ_H 7.18 (H-9/H-13), and δ_H 6.84 (H-10/H-12) to the oxygenated quaternary carbon at δ_C 158.9 (C-11). The substitution at C-8 was the remaining -CH(X)-CH2- residue since the methylene protons at δ 3.17 (H-7a) and 3.33 (H-7b) showed HMBC correlations to the aromatic carbons at δ 127.6 (C-8) and 130.8 (C-9/C-13). The downfield chemical shifts of H-6 at δ 5.00 and C-6 at δ 79.9 were satisfied by an ester bond linkage between C-6 and C-2 of the *N*-methylvaline fragment. Although the HMBC correlations of H-6 and H-7ab to C-5 were virtually absent, the morpholine nucleus of **SHOII-76** was assembled with the ring closure between the amide carbonyl (C-5) and the methine carbon (C-6). With this ring closure, the seven degrees of unsaturation required by the molecular formula of **SHOII-76** were finally satisfied.

Stereochemistry. The relative stereochemistry of **SHOII-76** was revealed by analyses of *J* values from the ^{1}H NMR spectrum and the 2D NOESY experiment (Figure 106 and Table 8). H-3 was coupled to H-14 with $^3J_{3\text{-}14}$ = 5.4 Hz, and H-6 was coupled to H-7ab with $^3J_{6\text{-}7a}$ = 8.4 and $^3J_{6\text{-}7b}$ = 4.0 Hz. Accordingly, the dihedral angles of H^3–C–C–H^{14}, H^6–C–C–H^{7a}, and H^6–C–C–H^{7b} were approximately 60°, 180°, and 60°, respectively. Interestingly, only H-7a displayed NOESY correlations to H-14 and H_3-15. The data implied that the methoxyl benzyl and the isopropyl substituents were in the pseudo-axial orientation and H-6 and H-3 were in the pseudo-equatorial orientation. Therefore, **SHOII-76** was established as *syn*-3-isopropyl-6-(4-methoxy-benzyl)-4-methyl-morpholine-2,5-dione.

Table 8. ^{1}H and ^{13}C NMR spectral data of *syn*-3-isopropyl-6-(4-methoxy-benzyl)-4-methyl-morpholine-2,5-dione [**SHOII-76**] recorded in $CDCl_3$

atom no.	$^{1}H^{a}$ δ_H(mult., *J* in Hz)	$^{13}C^{b}$ δ_C	H,H COSY	HMBC^{c} ($^{n}J_{CH}$ $n = 3$)	NOESY
2		164.2			
3	3.82 (1H, d, 5.4)	66.3	H-14	C-2, C-14, C-15, C-16	$-NCH_3$, H_3-15, H_3-16
5		164.7			
6	5.00 (1H, dd, 4.0, 8.0)	79.9	H_2-7ab		H-9/ H-13
7a	3.17 (1H, dd, 8.0, 14.4)	38.9	H-6	C-6, C-8, C-9/ C-13	H-9/ H-13, H-14, H_3-15
7b	3.33 (1H, dd, 4.0, 14.4)				H-9/ H-13
8		127.6			
9/ 13	7.18 (1H, d, 8.4)	130.8	H-10/ H-12	C-7, C-9/ C-13, C-11	H-6, H_2-7ab
10/ 12	6.84 (1H, d, 8.4)	114.1	H-9/ H-13	C-8, C-11, C-10/ C-12	$-OCH_3$
11		158.9			
14	1.99 (1H, m)	29.7	H-3, H_3-15, H_3-16	C-2, C-3, C-15, C-16	H-7a, $-NCH_3$
15	0.82 (3H, d, 6.6)	17.6	H-14	C-3, C-14, C-16	H-7a, $-NCH_3$
16	1.09 (3H, d, 6.6)	19.8	H-14	C-3, C-14, C-15	$-NCH_3$
$-NCH_3$	3.00 (3H, s)	34.2		C-3, C-5	H-3, H-14, H_3-15, H_3-16
$-OCH_3$	3.78 (3H, s)	55.3		C-11	H-10/ H-12

[a]Recorded at 600 MHz and [b]Recorded at 150 MHz with a 5-mm inverse probe. [c]Correlations after optimization for $^{n}J_{CH}$ = 8 Hz.

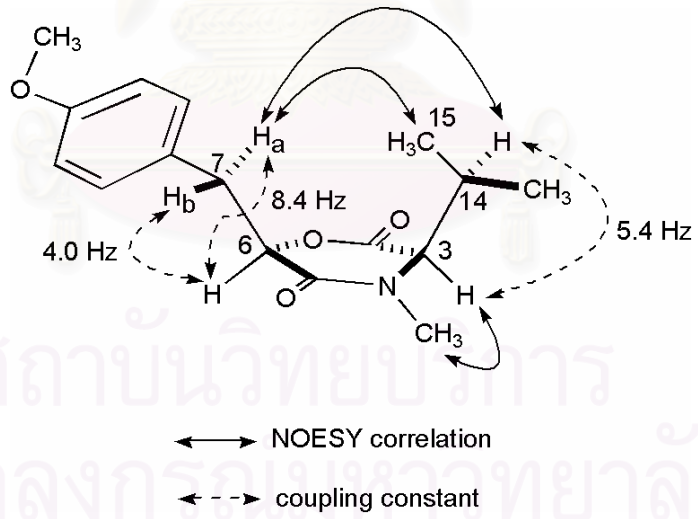

Figure 31. Selected NOESY correlations and the *J* values observed in *syn*-3-isopropyl-6-(4-methoxy-benzyl)-4-methyl-morpholine-2,5-dione [**SHOII-76**].

SHOII-76 is the second example of morpholine-2,5-dione containing natural products after the discovery of ergosecalinine in the fungus *Claviceps*

purpurea in 1959 (Cordell et al., 1989). The structure of ergosecalinine is shown in Figure 32. From a biogenetic point of view, **SHOII-76** could be derived by condensation of 2-hydroxy-3-(4-methoxy-phenyl)-propionate, a product of the shikimate pathway, and a modified amino acid, *N*-methylvaline, which is often found as an amino acid component in cyanobacterial metabolites (Harrigan, Yoshida et al., 1998; Burja et al., 2001; Horgen et al., 2002; Luesch, Yoshida, Moore, and Paul, 2002). Unfortunately, the absolute configuration assignment and biological testing of this new compound were not done due to its limited amount.

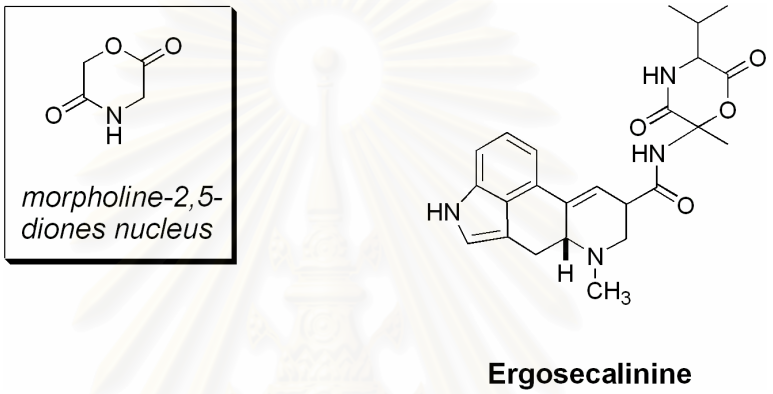

Figure 32. The structure of ergosecaline, the first example of morpholine 2,5-diones containing natural product.

2. Non-hydrolytic Degradation Method for Absolute Configurational Assignment: Application to Malyngamide X

The new lipopeptide, malyngamide X [**SHO27**] is unable to be crystallized, and its conformationally flexible system has been obstacles to the stereochemical assignment by spectral analysis alone. The six stereogenic centers of **SHO27** located in both the amine-derived portion (C-2, C-5, C-7, C-8, and C-14) and in the fatty acid side chain (C-7'). In general, to determine absolute configuration of fatty acid and amino acid substructures of the lipopeptides, the compounds have to be hydrolyze to give free fatty acids and free amino acids prior to analysis with chromatographic and/or $[\alpha]_D$ value measurements, then comparing the results with authentic standards (Kan et al., 2000, Milligan, Márquez, Williamson, and Davies-Coleman et al., 2000; Appleton et al., 2002). However, the limited amount together

with the failure in re-isolation of **SHO27** from the second collection of the molluscs, ruled out this common method for determining absolute stereochemistry of the compound.

Attention was therefore focused on the application of non-hydrolytic degradation methods comprising of the NMR chiral solvating agent (Parker, 1992; Wenzel and Wilcox, 2003), the modified Mosher's method (Ohtani et al., 1991), the NMR-based methods of interproton spin-spin coupling constants ($^3J_{H,H}$) and partly NOEs (Heatcock, Pirrung, and Sohn, 1979; Paik et al., 1994; Williamson et al., 2002), and the analysis of molecular models in conjunction with NOEs data (Ubutaka et al., 1993; Luesch et al., 2001; Williams, Yoshida, Quon et al., 2003) together with biogenetic considerations for the absolute configurational assignments of **SHO27**. The six stereogenic centers in **SHO27** can be categorized into two groups: isolated stereogenic centers (C-7', C-2 and C-14) and adjacent stereogenic centers (C-5, C-7 and C-8). NMR chiral solvating agent (CSA) and NOE-based method were mainly applied in combination with molecular mechanics calculations, and biogenic consideration for the former stereogenic centers. For the latter stereogenic centers, application of modified Mosher's method, $^3J_{H,H}$ and partly NOEs were employed. The strategy for determining absolute stereochemistry of **SHO27** as 2(*S*), 5(*S*), 7(*S*), 8(*R*), 14(*S*), and 7'(*S*)-configurations is shown in Figure 33.

2.1. Determination of Absolute Configuration at C-7'

The absolute stereochemistry at C-7' of 7'-methoxytetradec-4'(*E*)-enoic acid containing malyngamides has been previously reported to be exclusively (*S*)-configuration mainly by comparing the $[\alpha]_D$ values of the fatty acids obtained by hydrolysis with those of the co-isolated free fatty acids, or with that of the precedent literatures (Kan et al., 2000, Milligan, Márquez, Williamson, and Davies-Coleman, 2000; Appleton et al., 2002). To obtain quantitative amount of the fatty acid hydrolysate for $[\alpha]_D$ measurement, generally, about 10 mg of malyngamide is required. In some cases, biogenetic considerations have been useful to determine the C-7' configuration in malyngamides (Wu, Milligan and Gerwick, 1997; Mesquiche et al., 1999; Gallimore and Scheuer, 2000). With trace amount of **SHO27** available and lacked of co-isolated free fatty acid, the absolute configuration at C-7' in **SHO27** was

presumed to be 7'(*S*) on the biogenetic fashion consistent with other malyngamides. Thus, the fatty acid portion was identified as lyngbic acid, primarily found in cyanobacterium, *Lyngbya majuscula* (Cardellina et al., 1978; Ainslie et al., 1985).

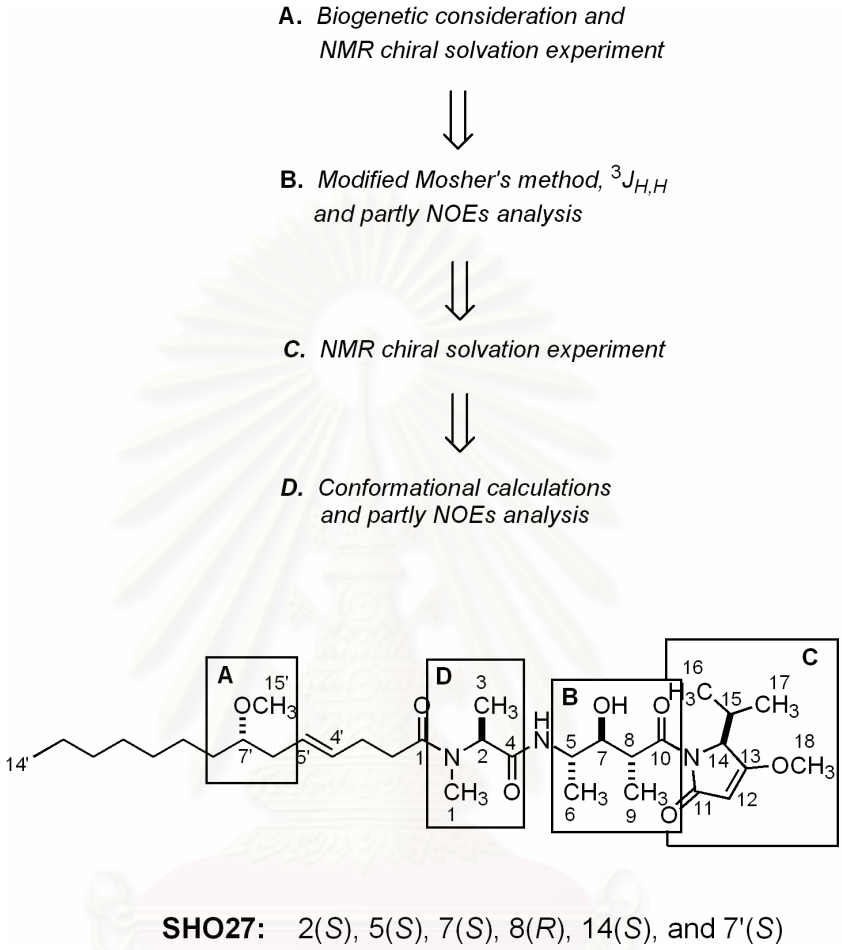

Figure 33. The sequence of non-hydrolytic degradation methods for determining absolute stereochemistry of malyngamide X [**SHO27**].

NMR chiral solvation experiments were then used as an alternative method for determining the absolute configuration at C-7 within 7-methoxytetradec-4'(*E*)-enoic acid substructure in **SHO27**. The assignment was based on the non-equivalence shifts of the ^{1}H signals when the compound was solvated with two different enantiomers of NMR chiral solvating agent (CSA). The chemical shift non-equivalence of the solvate complexes is defined as $\Delta\delta_{RS} = \delta_R - \delta_S$ whereas δ_R is the ^{1}H chemical shift of the compound in (*R*)-TFAE solvate and δ_S is that in (*S*)-TFAE solvate. The chiral methyl homoallyl ether at C-7' of **SHO27** and the chiral allyl ether

at C-23(*S*) of the model compound, the alkaline degradation product of tautomycin [**M1**], have two sites that can bind to two sites of donor-acceptor CSA such as 2,2,2-trifluoro-1-(9-anthrylethanol) or TFAE *via* hydrogen bonding or other dipole-dipole interactions. Accordingly, the solvate complexes between both enantiomers of TFAE with 7'(*R*)- and 7'(*S*)-configurations of **SHO27** (n = 1, Figure 34**A**) as well as 23(*R*)- and 23(*S*)-configuration of **M1** (n = 0, Figure 34**A**) were proposed to display the relationship between the ^{1}H NMR non-equivalence shifts (upfield or downfield) and the stereochemistry at C-7' of **SHO27** or C-23 of **M1**. The proposed solvation model is supported by the solvation model between chiral allyl ethers and (*R*)-TFAE (Figure 34**B**) proposed by Pirkle and Boeder (1977).

Pirkle and Boeder proposed that, in the presence of TFAE, the hydrogen bond interactions between the two "Lewis acidic sites" of TFAE (carbinol and carbinyl hydrogens) and the two "Lewis basic sites" in a chiral methyl allyl ether (methoxyl oxygen and π-electrons in a double bond) served to populate chelate-like conformations of the diastereomeric solvates, $R_{\mathrm{TFAE}}R_{\mathrm{ether}}$ and $R_{\mathrm{TFAE}}S_{\mathrm{ether}}$. For steric reasons, a significantly populated rotamer is one in which the methoxyl group is approximately eclipsed with the carbinyl hydrogen of the ether, the smaller of the three remaining substituent upon the chiral center. The enantiomeric purity and absolute configurations of which can be assigned relative to the stereochemically dependent shielding exerted by the anthryl substituent of (*R*)-TFAE to the methoxyl protons upon the chiral center. Thus, giving the methoxyl protons signal of (*S*)-ether appears at higher field region relative to (*R*)-ether.

In order to prove the proposed solvation model depicted in Figure 34**A**, NMR experiment was carried out with alkaline degradation product of tautomycin [**M1**] having known stereochemistry at C-23. Two solutions of **M1** in $CDCl_3$ (each 2 mg, 3.5 μmole) for ^{1}H-NMR experiments (274 °K, 600 MHz) were separately prepared by mixing with 6 mg (21.8 μmole, 6 equiv.) of the chiral acid (*R*)- or (*S*)-TFAE. The ^{1}H NMR spectra were measured at low temperature under dilute concentration of substrate to better stabilized of the major solvated complex (Latypov et al., 2002). The results are shown in Figure 35.

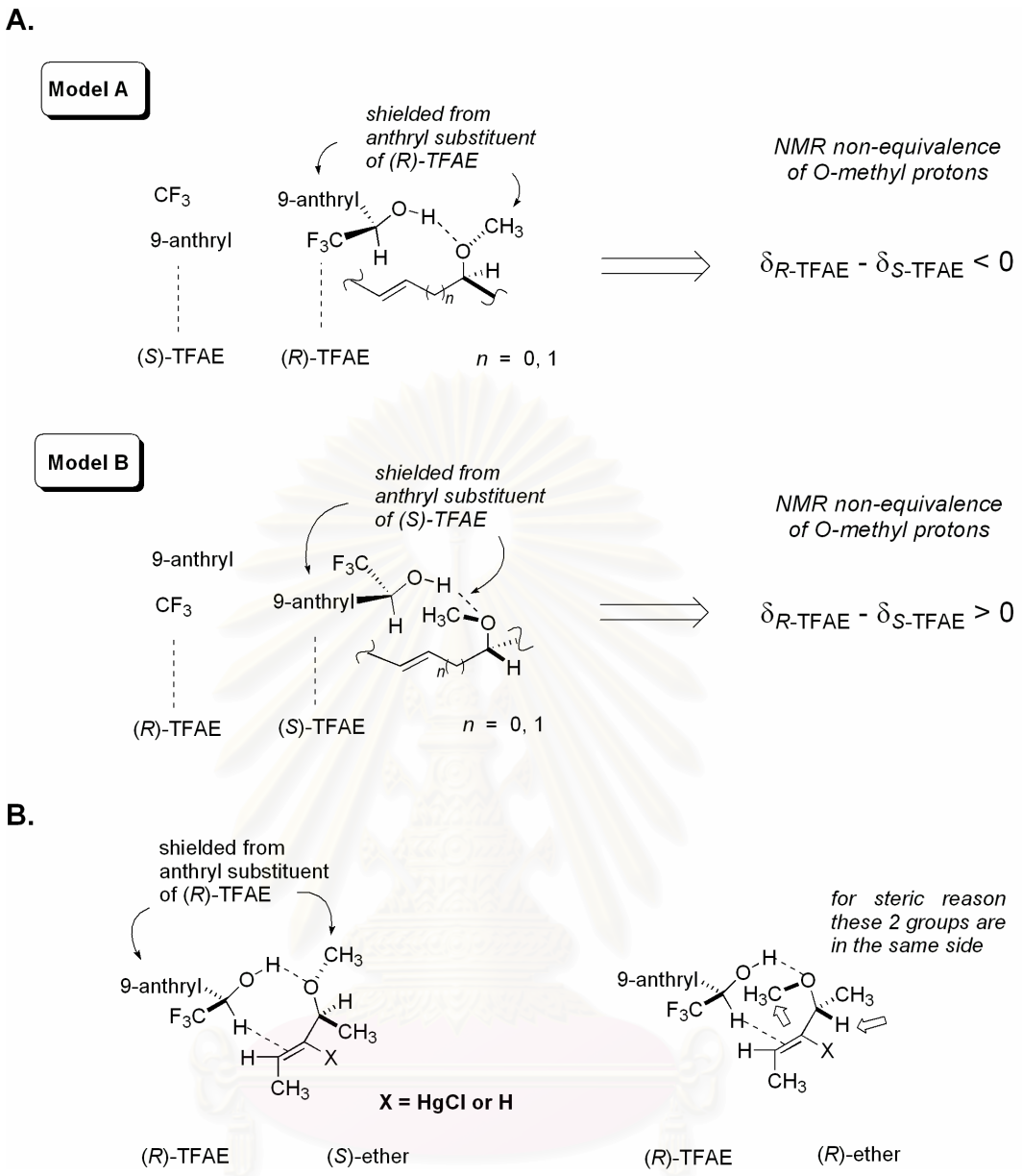

Figure 34. Proposed solvation model between (A) chiral methyl homoallyl ether or chiral allyl ether with both enantiomer of TFAE, and (B) (*R*) and (*S*) chiral allyl ether with (*R*)-TFAE by Pirkle and Boeder (1977).

The absolute configuration at C-23 of **M1** has already been established as (*S*) through semisynthetic, spectroscopic analyses, and molecular mechanic calculations (Ubutaka et al., 1993). Analysis of its known stereochemistry in conjunction with the observed $\Delta\delta_{RS}$ for the 23-OCH_3 protons of **M1** as +0.014 ppm ($\Delta\delta_{RS} > 0$) suggested the major populate chelate-like conformations as if the hydrogen bonding interactions would arise from a carbinol and carbinyl hydrogens of TFAE to

the methoxyl oxygen (23-OCH_3) and the π-electrons (Δ^{21}) of **M1**, respectively. Therefore, the solvate complexes gave the positive $\Delta\delta_{RS}$ of 23(*S*)-OCH_3, due to the stereochemically dependent shielding exerted by the 9-anthryl substituent of (*S*)-TFAE to the methoxyl protons upon the chiral center C-23(*S*) of **M1**. This was in agreement with the model **B** shown in Figures 34 and 35.

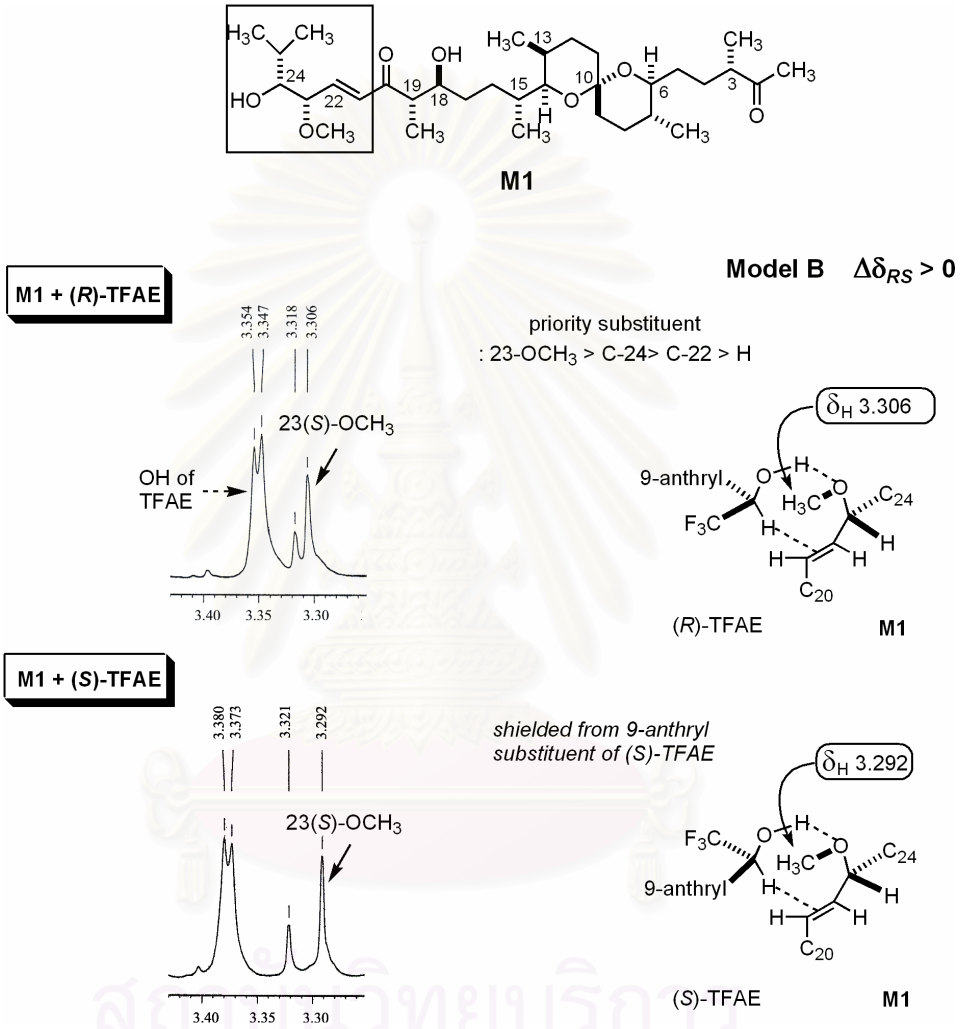

Figure 35. The 500 MHz ^{1}H NMR spectra at 273 °K (3.10 – 3.60 ppm) of the alkaline degradation product of tautomycin [**M1**] having 6 equiv. of (*R*)- and (*S*)-TFAE and the solvation model.

Although the hydroxyl substituted at C-24 would involve the solvate complexes between TFAE and the chiral allyl ether at C-23 of **M1**, the result of 23(*S*)-OCH_3 $\Delta\delta_{RS} > 0$ clearly demonstrated the preferential solvate complexes depicted in Figure 35. This was supported by the experiment of Julian and colleages (2003) in

which the major solvate complexes between TFAE and natural 5-methylfuran-2(5*H*)ones (annonaceous butenolides) were studied.

Since the absolute configuration at the C-23 of **M1** was confirmed through the resulting NMR discrimination and the solvate models in Figure 34, the absolute configuration of C-7' in the structure of **SHO27** could be established with some confidence. The method for assigning the absolute configuration at C-23 of **M1** was applied to establish C-7' stereochemistry of **SHO27** following three principle operations: (i) separate measurements of the ^{1}H NMR spectra of the sample in a mixture with (*R*)- or (*S*)-TFAE; (ii) deduction of the sign of chemical shift non-equivalence for 7'-OCH_3 signal ($\Delta\delta_{RS} = \delta_{R\text{-TFAE}} - \delta_{S\text{-TFAE}}$) and (iii) application to the solvation model in Figure 34 to assign absolute stereochemistry of C-7'. The results are shown in Fig. 36.

The $\Delta\delta_{RS}$ of the 7'-OCH_3 protons observed by the diastereomeric solvation complexes between **SHO27** and TFAE with 5 equiv. of both enantiomers was –0.008 ppm. In the presence of (*R*)-TFAE, the 7'(*S*)-OCH_3 proton signal was shielded by the anthryl substituent on the chiral carbon of (*R*)-TFAE causing the upfield shift of the 7'-OCH_3 protons signal more than in the presence of (*S*)-TFAE. The phenomenon appeared to fit the uniform model **A** in Figure 34 and confirmed the assignment at C-7' of malyngamide X to be (*S*)-configuration.

In order to increase the value of $\Delta\delta_{RS}$ for 7'-OCH_3 protons, effects of concentration (substrate stoichiometry) and temperature were studied. It was clear that at higher concentration of substrate and lower temperature, the $\Delta\delta_{RS}$ increased significantly (Figure 67). Finally, the magnitude of $\Delta\delta_{RS}$ value for the 7'-OCH_3 could be simply enhanced from –0.008 ppm to –0.038 ppm at 20:1 equiv. ratio of TFAE and **SHO27** (274 °K, $CDCl_3$,). The results implied that at higher TFAE concentration, the equilibrium enhanced towards formation of the solvate complexes. In addition, as the temperature is lowered, there will be decrease in the dissociation of the complexes. Non-equivalence in chemical shift will reach a maximum value when diastereomeric complex formation is complete (Wenzel and Wilcox, 2003).

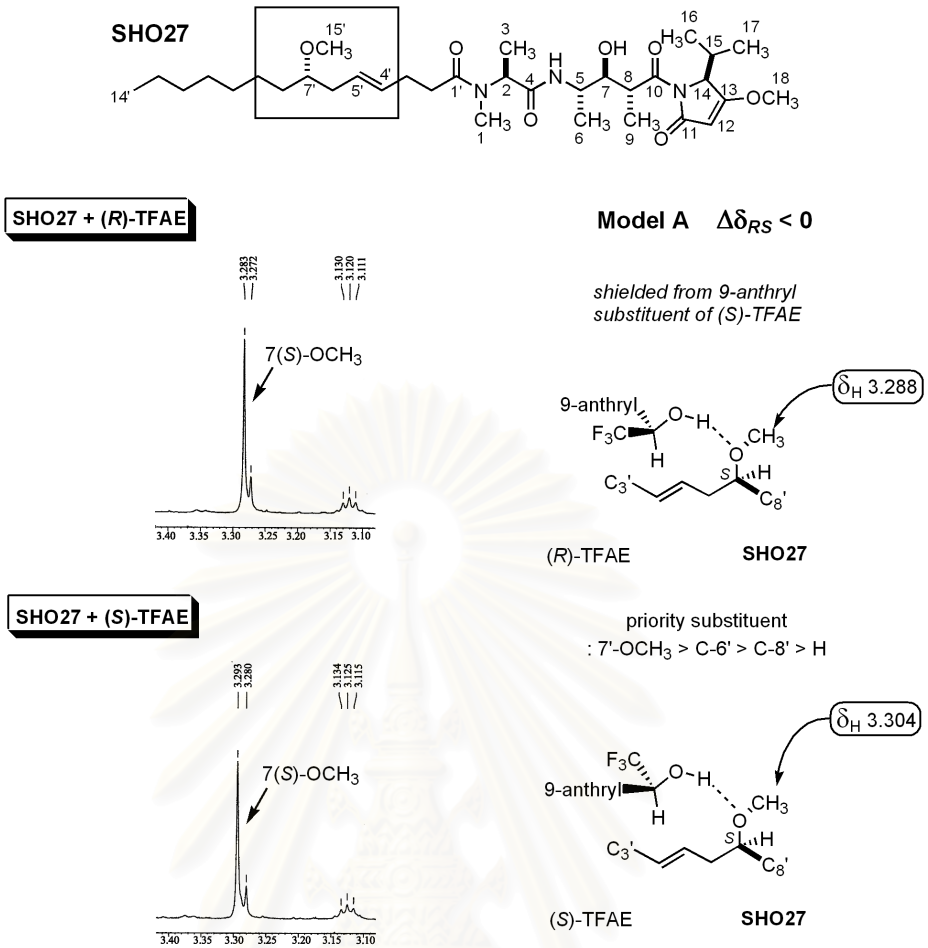

Figure 36. 500 MHz ^{1}H NMR spectra at 273 °K (3.05 - 3.45 ppm) of malyngamide X [**SHO27**] having 5 equiv. of (*R*)- and (*S*)-TFAE and the solvation model.

2.2. Determination of Absolute Configuration at C-5, C-7, and C-8

To establish the absolute configurations at the three adjacent stereogenic centers (C-5, C-7, and C-8) in pentanoic acid moiety of **SHO27**, attempt had been made to use a combination of NMR data obtained from the modified Mosher's method (Ohtani et al., 1991), proton coupling constants, and 2D NOESY data. The work started from C-7 in which the modified Mosher analysis could be performed. 7-O-(*R*)-(+)-MTPA ester [**SHO27a**] and 7-O-(*S*)-(–)-MTPA ester [**SHO27b**] were then prepared from malyngamide X (Figure 37).

The chemical shifts of the proton signals were assigned to each ester from the H,H COSY spectra (Figure 64). However, the overlapping of H-5 and H-14 in δ_H 4.47–4.57 region of **SHO27a** caused ambiguous assignment of the H-5 proton

signal (Figure 60). To overcome this drawback, the relatively upfield shift of H-5 at δ_H 4.49 of **SHO27a** comparing to δ_H 4.50 of **SHO27b** was evaluated with confidence by overlaying the H,H COSY spectrum of **SHO27a** on that of **SHO27b** (Figure 63). Hence, by using the overlaid spectra, the chemical shift differences ($\Delta\delta_{SR} = \delta_{\mathbf{SHO27b}} - \delta_{\mathbf{SHO27a}}$) observed for all proton signals were easily determined and the result is shown in Table 9 and Figure 38. The $\Delta\delta_{SR}$ values (–0.02 for H-8; –0.01 for H_3-9; +0.01 for H-5; +0.08 for H_3-6; +0.15 for NH) revealed the C-7(*S*) for malyngamide X.

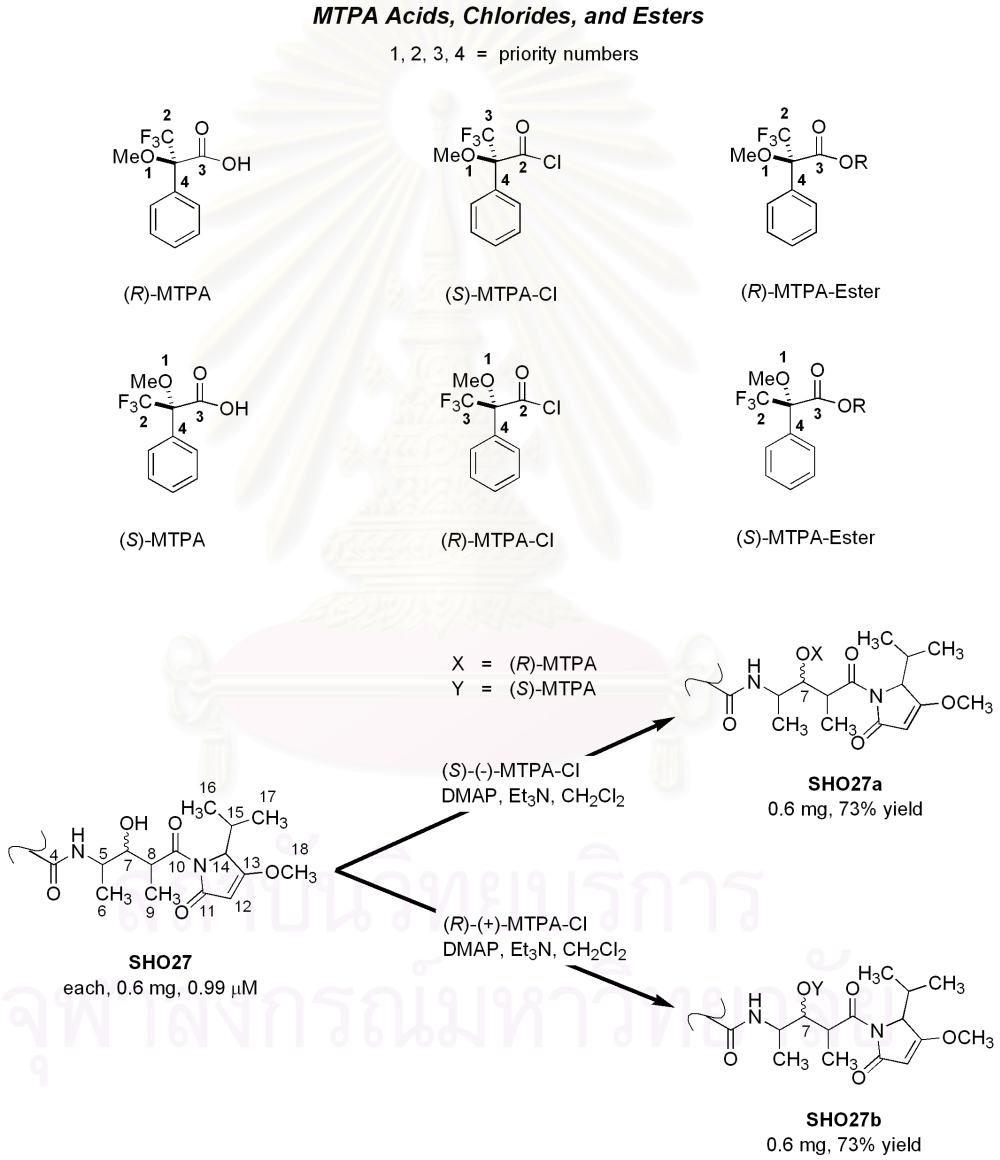

SHO27a 7-*O*-(*R*)-(+)-MTPA ester of malyngamide X
SHO27b 7-*O*-(*S*)-(-)-MTPA ester of malyngamide X

Figure 37. Preparation of MTPA esters, **SHO27a** and **SHO27b**.

Table 9. ^{1}H NMR data ($CDCl_3$, 600 MHz) of malyngamide X [**SHO27**], (*R*)-MTPA ester of malyngamide X [**SHO27a**], (*S*)-MTPA ester of malyngamide X [**SHO27b**] and difference in chemical shift ($\Delta\delta_{SR} = \delta_{\mathbf{SHO27b}} - \delta_{\mathbf{SHO27a}}$)

	$^{1}H^{a}$, δ_H (mult., *J* in Hz)			
atom no.	**SHO27**^{a}	**SHO27b**^{b}	**SHO27a**^{b}	$\Delta\delta_{SR}$
1	2.93 (3H, s)	2.924 (3H, s)	2.895 (3H, s)	0.029
2	5.20 (1H, q, 7.0)	5.20 (1H, q, 7.2)	5.156 (1H, q, 7.2)	0.044
3	1.32 (3H, d, 7.3)	1.371 (3H, d, 7.2)	1.351 (3H, d, 7.2)	0.020
4	-	-	-	-
5	4.05 (1H, m)	4.500 (1H, m)	4.487 (1H, m)	0.013
6	1.18 (3H, d, 6.7)	1.132 (3H, d, 7.0)	1.053 (3H, d, 7.0)	0.079
7	3.66 (1H, m)^{c}	5.630 (1H, dd, 9.6, 1.6)	5.623 (1H, dd, 9.6, 1.6)	0.070
8	3.86 (1H, dq, 8.9, 6.7)	4.195 (1H, m)	4.218 (1H, m)	-0.023
9	1.11 (3H, d, 6.7)	1.193 (3H, d, 7.0)	1.206 (3H, d, 7.0)	-0.013
10	-	-	-	-
11	-	-	-	-
12	5.05 (1H, s)	5.007 (1H, s)	5.043 (1H, s)	-0.036
13	-	-	-	-
14	4.51 (1H, d, 2.8)	4.382 (1H, d, 2.0)	4.477 (1H, d, 2.0)	-0.095
15	2.60 (1H, m)	2.112 (1H, m)	2.456 (1H, m)	-0.344
16	0.74 (3H, d, 7.0)	0.351 (3H, d, 7.0)	0.522 (3H, d, 7.0)	-0.171
17	1.07 (3H, d, 7.3)	0.979 (3H, d, 7.0)	1.081 (3H, d, 7.0)	-0.102
18	3.82 (3H, s)	3.800 (3H, s)	3.826 (3H, s)	-0.026
NH	6.45 (1H, d, 8.9)	6.187 (1H, d, 9.6)	6.039 (1H, d, 9.6)	0.148
1'	-	-	-	-
2'	2.38 (2H, m)	2.389 (2H, m)	2.345 (2H, m)	0.001
3'	2.34 (2H, m)	2.368 (2H, m)	2.309 (2H, m)	-0.002
4'	5.50 (1H, dt, 15.3, 5.8)	5.532 (1H, m)	5.517 (1H, m)	0
5'	5.45 (1H, dt, 15.3, 6.4)	5.464 (1H, m)	5.450 (1H, m)	0
6'	2.16 (2H, dd, 5.8, 5.8)	2.188 (2H, dd, 5.6, 5.6)	2.187 (2H, dd, 5.6, 5.6)	0
7'	3.12 (1H, quin, 5.8)	3.146 (1H, m)	3.148 (1H, m)	0
8'	1.40 (2H, m)	1.427 (2H, m)	1.430 (2H, m)	0
9'	1.20-1.30 (2H)	1.250-1.330 (2H)	1.250-1.330 (2H)	0
10'	1.20-1.30 (2H)	1.250-1.330 (2H)	1.250-1.330 (2H)	0
11'	1.20-1.30 (2H)	1.250-1.330 (2H)	1.250-1.330 (2H)	0
12'	1.20-1.30 (2H)	1.250-1.330 (2H)	1.250-1.330 (2H)	0
13'	1.20-1.30 (2H)	1.250-1.330 (2H)	1.250-1.330 (2H)	0
14'	0.85 (3H, t, 7.2)	0.875 (3H, t, 6.4)	0.877 (3H, t, 6.4)	0
15'	3.30 (3H, s)	3.403 (3H, s)	3.501 (3H, s)	-0.098

^{a} Recorded at 500 MHz. ^{b} Recorded at 600 MHz. ^{c} After D_2O addition, the signal simplified to a doublet of doublet (*J* = 8.9, 2.6 Hz) recorded at 300 MHz. Digital error = 0.0003 pp,. Technical error = ± 0.001 ppm.

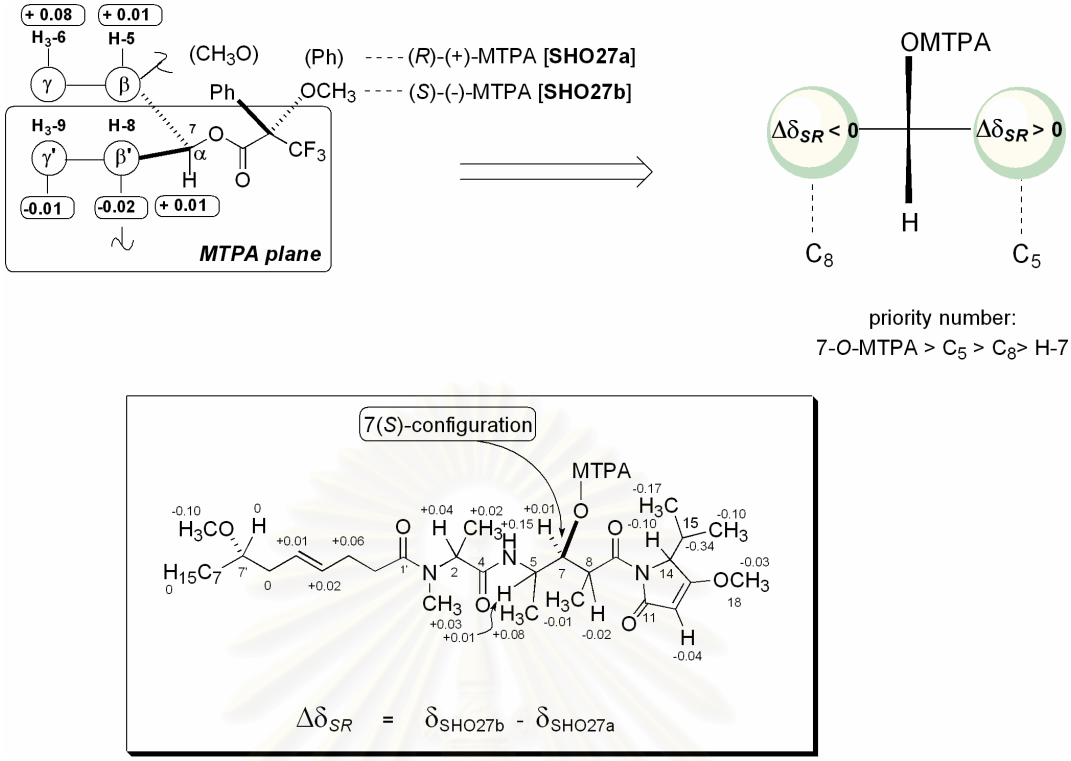

Figure 38. $\Delta\delta_{SR}$ ($\delta_{\mathbf{SHO27b}} - \delta_{\mathbf{SHO27a}}$) values for the MTPA esters of malyngamide X ($CDCl_3$, 600 MHz) and the absolute configurational assignment at C-7(*S*).

After establishing the absolute configuration for C-7(*S*), the absolute stereochemistry for C-5 and C-8 was assigned with NMR-based method comprising of interproton spin-spin coupling constants ($^3J_{H,H}$) and partly NOEs. As shown in Figure 39, the proton chemical shifts and the $^3J_{H,H}$ values of the pentanoic acid portion of malyngamide X are similar to those of jalonusimide (Sodano and Spinella, 1986) and bleomycin A2 (Pardo and Bock, 1983). Matsumori and colleages (1999) reported that acyclic systems would exist in a series of staggered rotamers and its stereochemistry can be deduced by the magnitude of their coupling constants in combination with NOE data. Accordingly, all possible absolute stereochemistry at C-5 and C-8 with $^3J_{H,H}$ values with suspect to the experimental ^{1}H NMR data of **SHO27** were depicted as shown in Figure 39. The 8.9 Hz coupling between H-7 and H-8 in the ^{1}H NMR spectrum suggested that the H-7 and H-8 were anti-relationship. This was consistent with $^3J_{H,H}$ values observed for other methyl anti-β-hydroxy-α-methylalkanoates (Heatcock, Pirrung, and Sohn, 1979; Sodano and Spinella, 1986; Paik et al., 1994). The *s*-trans conformation of the C-7 and C-8 was demonstrated by NOESY correlations between H_3-9 to H-5, in other word, the acyl substituent on C-7

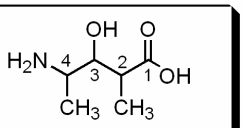

4-amino-3-hydroxy-2-methylpentanoic acid

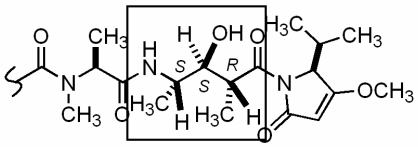

amine-derived portion of Malyngamide X

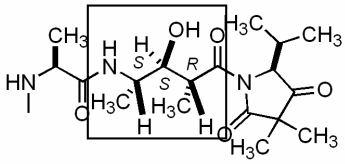

Janolusimide

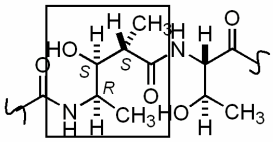

partial structure of Bleomycin A_2

	^{1}H, δ_H (mult., *J* in Hz) 4-amino-3-hydroxy-2-methylpentanoic acid unit		
atom no.[a]	Malyngamide X[b]	Janolusimide[c]	Bleomycin A_2[d]
H-2	3.86 (dq, 8.9, 6.7)	3.95 (dq, 9.4, 6.7)	3.59 (dq, 9.5, 7.0)
H-3	3.66 (dd, 8.9, 2.6)[e]	3.77 (dd, 9.4, 2.6)	3.90 (dd, 9.5, 3.0)
H-4	4.05 (m)	4.15 (m)	3.53 (dq, 3.0, 7.0)
2-CH_3	6.45 (d, 8.9)	7.62 (d, 8.6)	-
4-CH_3	1.11 (d, 6.7)	1.18 (d, 6.7)	1.26 (d, 7.0)
NH	1.18 (d, 6.7)	1.28 (d, 6.9)	1.29 (d, 7.0)

[a]Numbering are follow the 4-amino-3-hydroxy-2-methylpntanoic acid systeml [b]$CDCl_3$, 500 MHz NMR spectrometer. [c] $CDCl_3$, 500 MHz NMR spectrometer (Sodano and Spinella, 1986). [d] D_2O, 500 MHz NMR spectrometer (Pardo and Bock, 1983). [e] D_2O plus $CDCl_3$, 300 MHz NMR spectrometer.

Figure 39. The ^{1}H and $^3J_{H,H}$ values in the 4(*S*)-amino-3(*S*)-hydroxy-2(*R*)-methylpentanoic acid containing **SHO27**, janolusimide, and bleomycin A_2.

(C-10) and alkyl substituent on C-8 (C-5) were anti-relationship (Figure 40**A** and **B**). As the absolute stereochemistry of C-7 was already established as (*S*) by the modified Mosher's method, the absolute stereochemistry at C-8 was unambiguously assigned to (*R*)-configuration.

In addition, the $^3J_{H,H}$ value of 2.6 Hz between H-5 and H-7 revealed that the rotamers **A1** and **A2** having 5(*S*), 7(*S*), 8(*R*), and **B1** and **B2** having 5(*R*), 7(*S*), 8(*R*) could be possible for **SHO27**. Further considerations on the NOESY correlations between H_3-9/H-5 and H_3-6/H-7, and no NOESY correlation between H-7/NH, led to the conclusion that only the rotamer **A1** met all of these observations. Therefore, the stereochemistry assignment in the pentanoic acid moiety of malyngamide X was confidentially completed as 5(*S*),7(*S*), 8(*R*). The ^{1}H and $^3J_{H,H}$ values observed from the 4-amino-3-hydroxy-2-methylpentanoic acid containing **SHO27** are similar to that of the tripeptide janulusimide (Figure 39, Sodano and Spinella, 1986).

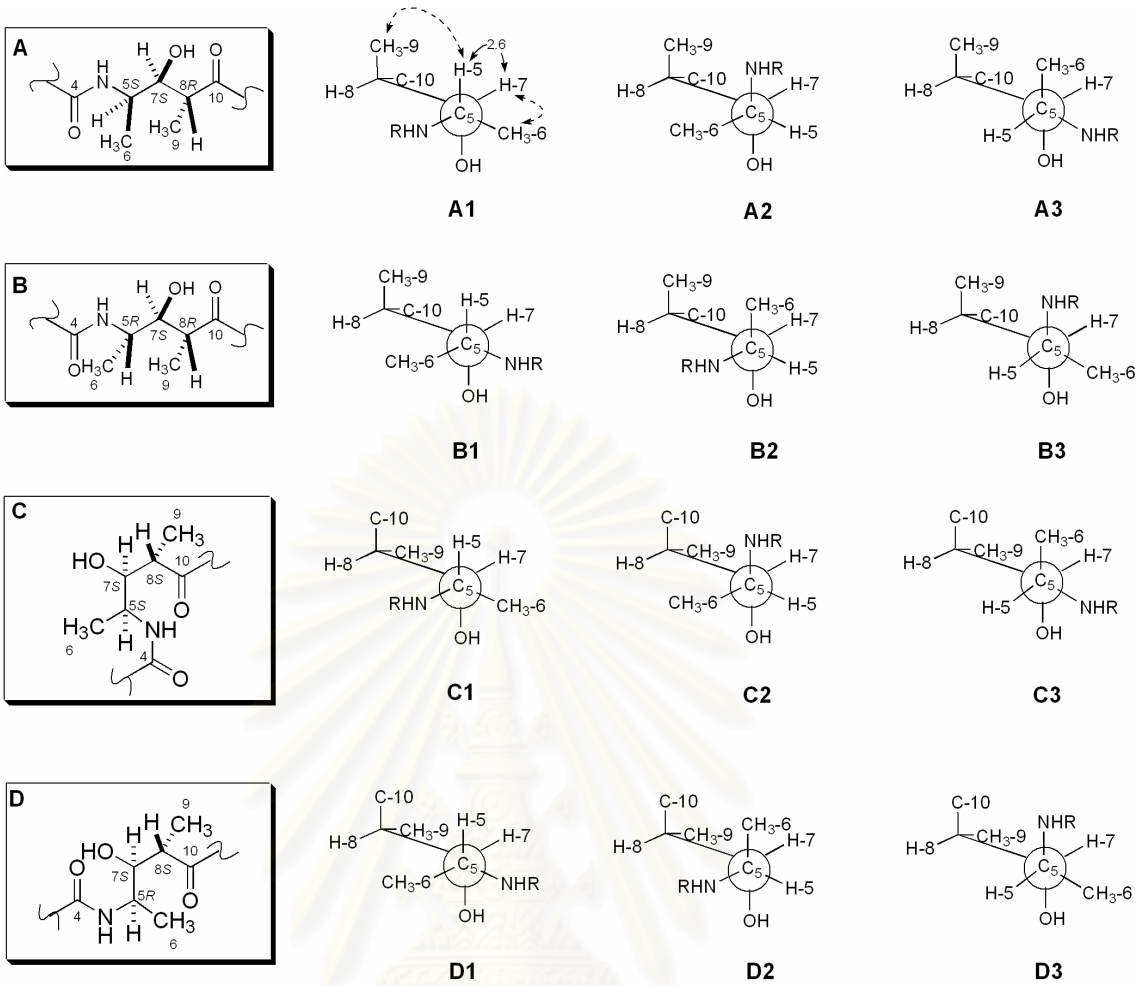

Figure 40. Possible rotamers of the four diastereotopic orientations (**A**) 5(*S*), 7(*S*), 8(*R*); (**B**) 5(*R*), 7(S), 8(*R*); (**C**) 5(*S*), 7(*S*), 8(*S*); and (**D**) 5(*R*), 7(S), 8(*S*) of malyngamide X [**SHO27**] with dihedral angles between H^7–C–C–H^8 approximately 180°, NOESY correlations (⟷), $^3J_{H,H}$ value (⟷).

2.3. Determination of Absolute Configuration at C-14

Next attempt was made at NMR chiral solvation experiments employing 2,2,2-trifluoro-1-(9-anthryl)ethanol (TFAE or Pirkle's alcohol) as a chiral solvating agent (CSA) for determining the absolute stereochemistry at C-14 in the terminal *N*-acylpyrrolinone moiety of **SHO27**. Recently, the enantiomers of TFAE have been noteworthily used to distinguish absolute stereochemistry of natural 5-methylfuran-2(5*H*)ones in butenolide moiety of annonaceous acetogenins (Latypov et

al., 2002; Juliana et al., 2003). Similarly, if the interaction between 4-methoxy-Δ^3-pyrrolin-2-one heterocycle in **SHO27** and TFAE leading to chemical shift non-equivalence is well understood, the absolute configuration at C-14 of **SHO27** can be established.

To clarify the application of TFAE for assigning the absolute configuration at C-14 within the terminal *N*-acylpyrrolinone ring of **SHO27**, the enantiomers of 5-isopropyl-4-methoxy-Δ^3-pyrrolin-2-one derivatives were synthesized and used as model compounds, including compounds **M2**–**M4** with 5(*S*)-configuration and compounds **M5**–**M7** with 5(*R*)-configuration. Samples with a single enantiomer of the model compounds (0.01 M in total) were separately prepared and added in the NMR tubes with 10 equiv. of (*R*)- or (*S*)-TFAE, followed by 400 μL of $CDCl_3$. The homogenous mixtures were gently shaken for a few minutes (usually 5 to 10 min), and the ^{1}H NMR spectra were then recorded at 274 °K. As shown in Figure 41**A**, the chemical shift non-equivalence of H-5 of the model compounds is defined as $\Delta\delta_{RS} = \delta_R - \delta_S$ whereas δ_R is the chemical shift of H-5 in (*R*)-TFAE solvate and δ_S is that in (*S*)-TFAE solvate. The chemical shifts of H-5(*S*) protons with (*R*)-TFAE solvates generally appeared at higher field than with (*S*)-TFAE solvates (entries **1**–**3**, $\Delta\delta_{RS} < 0$) and vice versa for those of H-5(*R*) at lower field (entries **4**–**6**, $\Delta\delta_{RS} > 0$). Analysis from the sense of chemical shift non-equivalences to the configuration of the substrates, the solvation model between TFAE and 4-methoxy-Δ^3-pyrrolin-2-one was then proposed (Figure 41**A**).

Apparently, the first hydrogen bonding occurred between the carbinol hydrogen of TFAE and the vinylogous ester carbonyl at C-2 of the substrate, making the substrate and TFAE come close to form a preferentially chelate-like solvation complex. The observed ^{1}H NMR non-equivalence shifts, thus, suggested the major solvation as if a secondary hydrogen bond would arise from the carbinyl hydrogen of TFAE and the methoxyl oxygen of the substrate. The solvation complex showed NMR non-equivalence shift due to the stereochemically dependant shielding exerted by the 9-anthryl group of TFAE. In this regard, the 9-anthryl group of (*R*)-TFAE has a pronounce shielding effect on H-5(*S*), whereas less (or no) effect on the H-5(*R*). The observed results in Figure 41**A** are all in accord with this proposed solvation

model, and confirm compounds **M2**–**M4** with H-5 $\Delta\delta_{RS} < 0$ having (*S*)-configuration, whereas compounds **M5** to **M7** with H-5 $\Delta\delta_{RS} > 0$ having (*R*)-configuration.

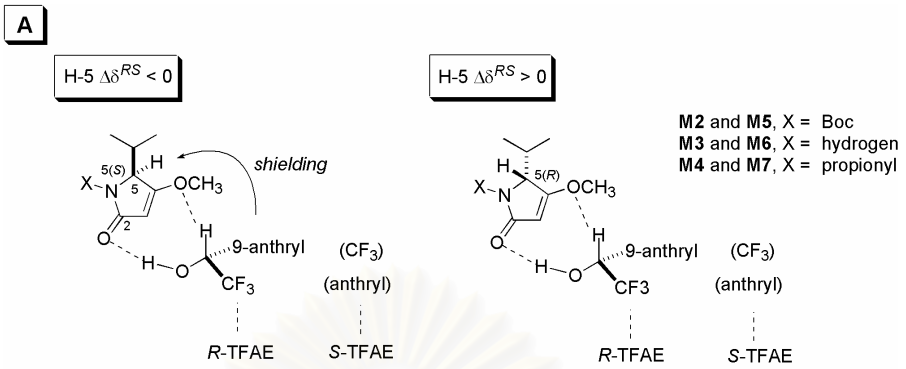

Entry	Substrate	H–5 $\Delta\delta^{RS}$	Absolute config. at C-5 (ee)[a]
1	**M2**	-0.014	*S* (>90)
2	**M3**	-0.092	*S* (>90)
3	**M4**	-0.042	*S* (>80)
4	**M5**	+0.001	*R* (>90)
5	**M6**	+0.084	*R* (>80)
6	**M7**	+0.030	*R* (>80)

[a] Calculated from the areas under methoxyl resonances in the presence of (*R*)-TFAE

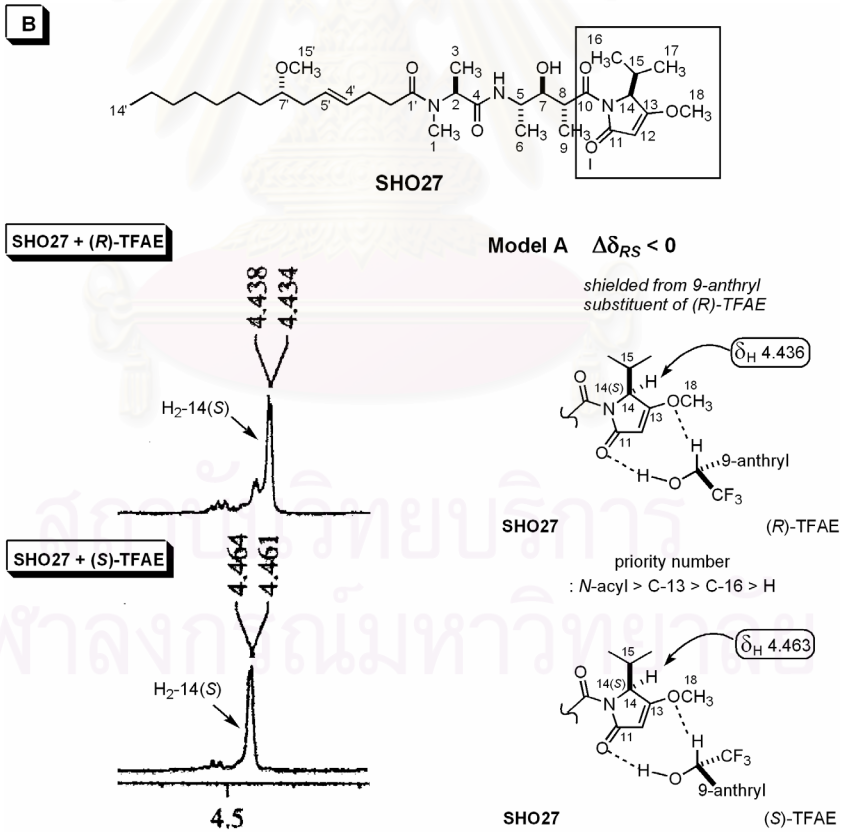

Figure 41. (A) Experimental $\Delta\delta_{RS} = \delta_R - \delta_S$ values observed for H-5 of compounds **M2**–**M7** ($CDCl_3$, 274° K, 600 MHz) and the proposed solvation model. (B) ^{1}H NMR spectra between 4.40 and 4.60 ppm of malyngamide X [**SHO27**] having 5 equiv. of (*R*)- and (*S*)-TFAE (274 K, $CDCl_3$, 600 MHz).

The NMR chiral solvation experiments of **SHO27** were then prepared by separate mixing of **SHO27** (3 mg, 0.01 M in total) with 5 equiv. of (*R*)- or (*S*)-TFAE in the NMR tubes, and dissolving in 400 μL $CDCl_3$ (Figure 66). The ^{1}H-NMR spectrum of the mixture was recorded at 274 °K. The chemical shifts of the proton signals were assigned to each solvate from the H,H COSY data. The solvate between **SHO27** and (*R*)-TFAE gave the H-14 proton signal at δ_H 4.436 while in the solvate with (*S*)-TFAE at δ_H 4.463, corresponding to chemical shift non-equivalence H-14 $\Delta\delta_{RS} = -0.027$ (Figure 41**B**). The high-field sense of H-14 in the (*R*)-TFAE solvate relative to the (*S*)-TFAE solvate is in good agreement with the uniform model of H-5 $\Delta\delta_{RS} < 0$ shown in Figure 41**A**. Therefore, the absolute stereochemistry at C-14 was assigned to be (*S*)-configuration. The presence of basic sites (e.g. hydroxyl) did not interfere with the major solvation of the reagent with the pyrrolinone moiety as has been discussed for those of annonaceous acetogenins (Jullian et al., 2003).

2.4. Determination of Absolute Configuration at C-2

After five of the six stereogenic centers in the molecule of malyngamide X were well established as 5(*S*), 7(*S*), 8(*R*); 14(*S*), and 7'(*S*), an integrated use of NOESY data and molecular mechanics study was employed in determining the absolute configuration at C-2 (Ubutaka et al., 1993; Luesch et al., 2001; Williams, Yoshida, Quon et al., 2003). To find the 3D chemical structure of the epimer that is in agreement with the experimental data (NOEs distance, $^3J_{H,H}$ values), the lowest energy conformations of the models with C-2(*R*) and C-2(*S*) epimers (each, 3,000 structures searched) were obtained from the MacroModel molecular modeling program using the Monte Carlo conformational searching. After energy minimization of each epimer running on the MMFF94S force field in $CDCl_3$ solution, the lowest energy structures of the 2(*R*)- and 2(*S*)-epimer (Figure 42**A** and 42**B**, respectively) were then analyzed to determine a single structure that did not break any NOE interactions and coupling constant data shown in Table 5. The distance obtained by the NOESY experiment has been generally semi-quantitatively classified into strong (< 2.5 Å), medium (2.5–3.5 Å), and weak (3.5–5.0 Å) NOE interaction (Luesch et al., 2001). The observed medium interessidual NOESY cross peak between H_3-1 and H-8 in the NOESY spectrum of **SHO27** indicated that the *N*-methylalanine fragment

should be close to the pentanoic acid fragment. However, this was satisfied only by the 2(*S*)-epimer of which the calculated NOE distance between H_3-1 and H-8 was 2.937 Å (Figure 42**B**). Therefore, the stereostructure of malyngamide X was finally assigned as 2(*S*),5(*S*),7(*S*),8(*R*),14(*S*), and 7'(*S*)-configurations. Analysis from the stereochemical structure shown in Figure 42**B**, the dihedral angle close to 0° of H–N–C–H^5 where NH almost eclipsed H-5 fitted with the large coupling constant (8.9 Hz) between NH and H-5 in the ^{1}H NMR spectrum of **SHO27**. Furthermore, the fact that NH proton could not be exchanged with D_2O (Figure 51) indicated its participation in hydrogen bonding with the C-1' carbonyl. The stereochemical solution of the *trans* geometry for the NH–C4 and NCH_3–C1' amides as resulted from the NOESY correlations (Table 5) between the amide proton NH/H-2 and H_3-1/H_2-2' were in good agreement with these lowest energy structures.

Malyngamide X possesses a novel carbon skeleton in its amine-derived portion compared to other malyngamides, specifically the tripeptide of *N*-Me-L-alanine, 4(*S*)-amino-3(*S*)-hydroxy-2(*R*)-methylpentanoic acid, and 5(*S*)-isopropyl-4-methoxy-Δ^3-pyrrolin-2-one. Overall, the biosynthesis of the malyngamides appears to be of mixed polyketide/amino acid origin, whereas the 7(*S*)-methoxylated fatty acids serves as a substrate for extension by a variety of amino acids (McPhail and Gerwick, 2003; Nogle and Gerwick, 2003). In this regard, we propose the biosynthesis of malyngamide X as depicted in Figure 43**A**. The 7(*S*)-methoxytetradec-4(*E*)-enoic acid or lyngbic acid [**a**] is first condensed with L-alanine. Further extension is through coupling with 4(*S*)-amino-3(*S*)-hydroxy-2(*R*)-methylpentanoic acid [**b**] derived by condensation of L-alanine and methyl malonyl CoA (from propionate; Sodano and Spinella, 1986) and with 5(*S*)-isopropyl-4-methoxy-Δ^3-pyrrolin-2-one [**c**] formed by Claisen-type condensation of L-valine and malonyl CoA (from acetate). Final modifications by *O*-methylation and *N*-methylation afford malyngamide X. Malyngamide X represents the first product of a biosynthetic pathway in which L-alanine is the first extension unit of the fatty acyl chain, whereas in most malyngamides this unit is derived from glycine (or in some cases, *β*-alanine; Figure 43**B**). The presence of an amide connectivity between *N*-methylalanine and pentanoic acid fragment without modification of the carbonyl functionality to chloromethylene, methoxy, or hydroxy group as found in other malyngamides suggests a different pathway for the construction of malyngamide X.

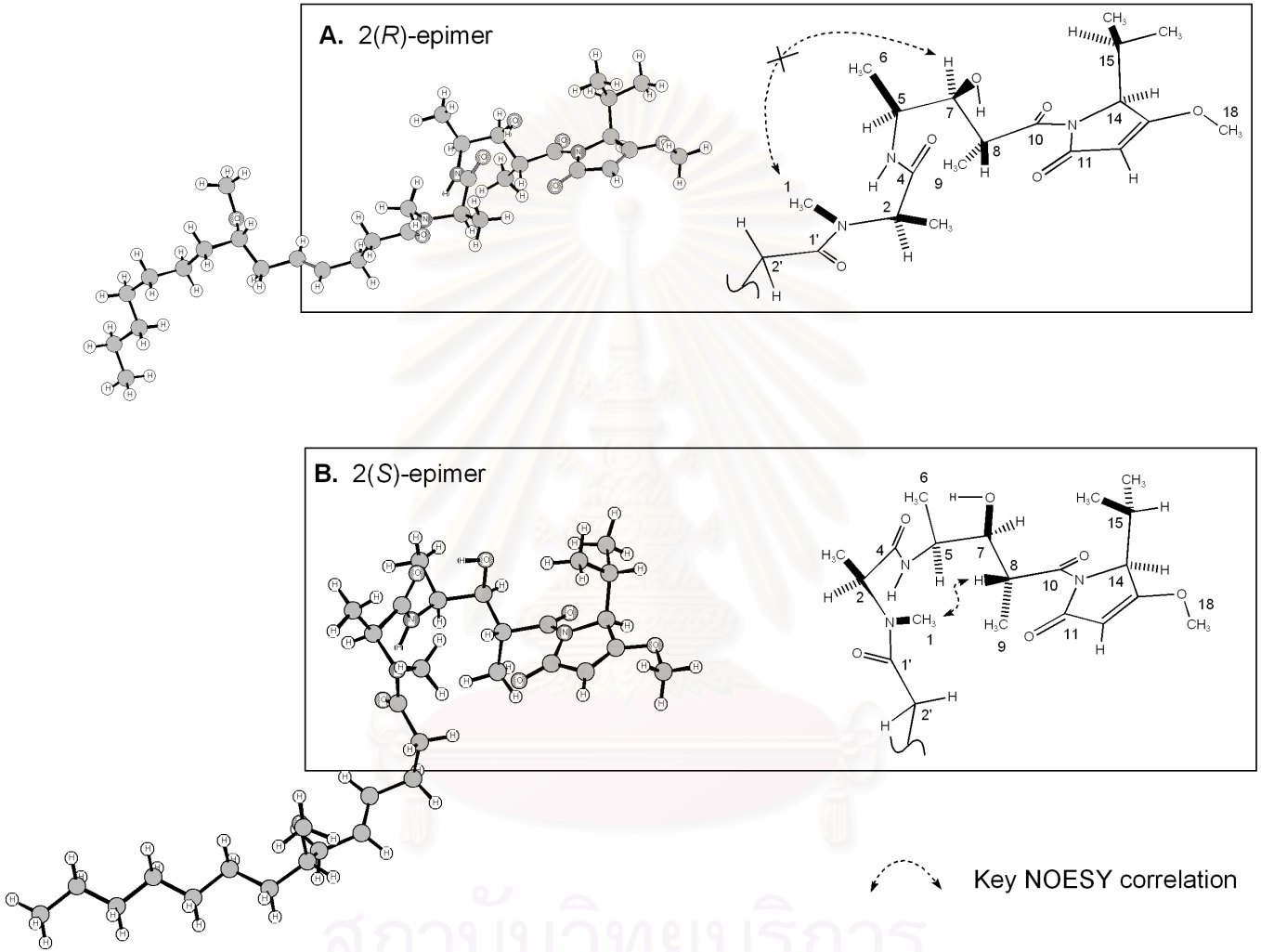

Figure 42. Stereoview of the lowest-energy conformations for malyngamide X [**SHO27**] with two possible absolute configurations at C-2, (A) 2(*R*) and (B) 2(*S*)-epimer, obtained by the Monte Carlo conformational search on MacroModel molecular modeling and key NOESY correlation which defined the 2(*S*)-configuration to be corrected for malyngamide X.

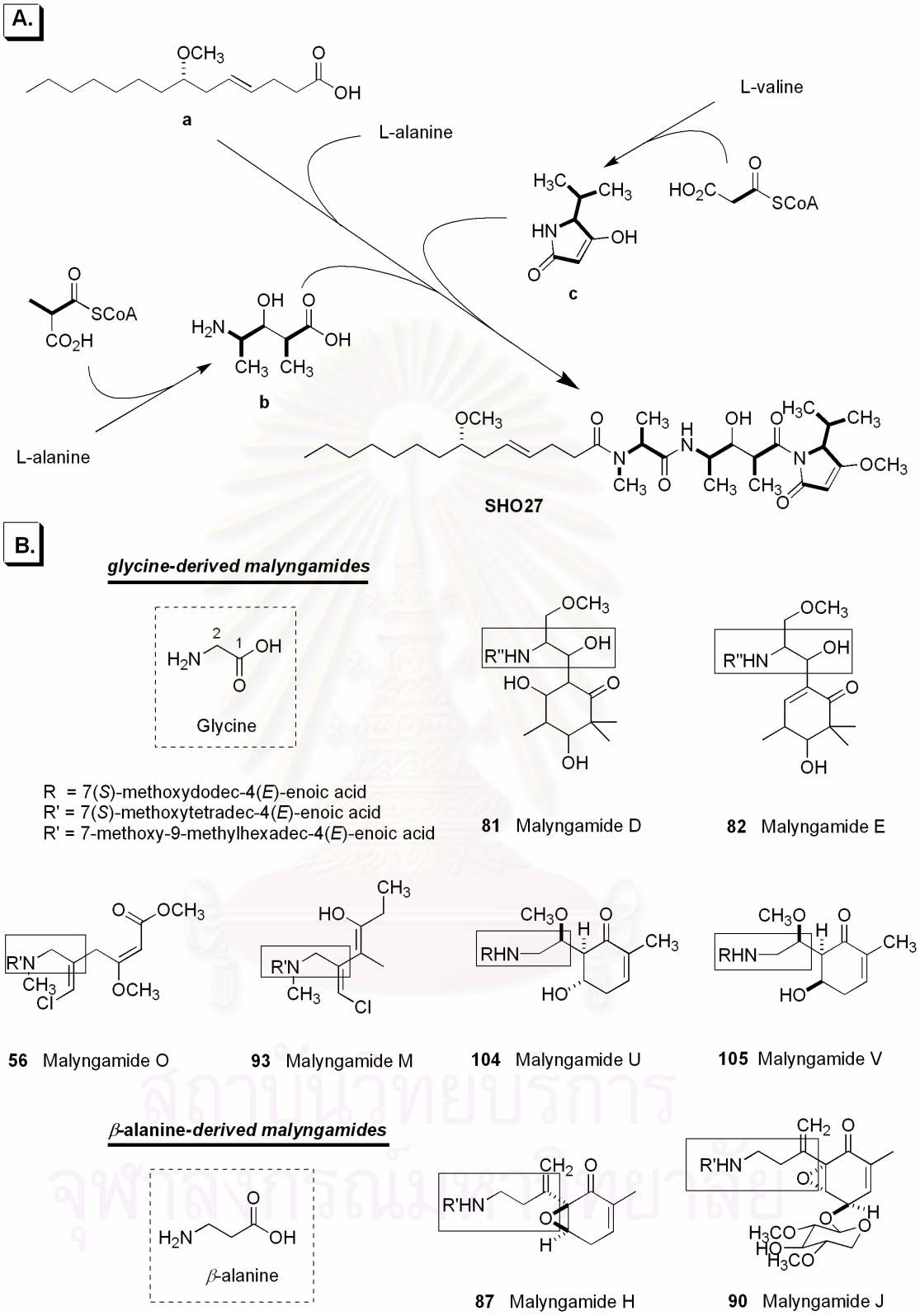

Figure 43. (A) The proposed biosynthesis of malyngamide X [**SHO27**]. (B) Selected glycine- or *β*-alanine derived malyngamides.

3. Biological Activity of the Isolated Compounds

Malyngamide X [**SHO27**] showed several biological activities including moderate cytotoxicity against oral human epidermoid carcinoma of nasopharynx (KB), human small cell lung cancer (NCI-H187), and breast cancer (BC) cell lines with ED_{50}'s of 8.20, 4.12 and 7.03 μM, respectively. Malyngamide X also exhibited antitubercular activity against *Mycobacterium tuberculosis* H37Ra strain with MIC's of 80 μM, and antimalarial activity against *Plasmodium falciparum* (K1, multidrug resistant strain) with ED_{50}'s of 5.44 μM.

Hectochlorin [**SHOII-28**] and the new deacetylhectochlorin [**SHOII-51**] were subjected to cytotoxic testing against oral human epidermoid carcinoma of nasopharynx (KB), human small cell lung cancer (NCI-H187), and breast cancer (BC) cell lines. The new hectochlorin derivative **SHOII-51** showed potent cytotoxicity against KB and NCI-H187 with ED_{50}'s of 0.31 and 0.32 μM while **SHOII-28** display ED_{50}'s of 0.86 and 1.20 μM, respectively. In addition, **SHOII-51** showed moderate cytotoxic activity against the BC cancer cell line with ED_{50} of 1.03 μM. Both compounds were inactive to *in vitro* antimalarial and antituberculous assays.

4. Preparation of Model Compounds for the NMR Chiral Solvation Experiments

4.1. Alkaline degradation product of tautomycin

Absolute configuration of tautomycin [**140**], a protein phosphatase inhibitors from a culture broth of *Streptomyces spiroverticillatus*, was established to be 3(*S*), 6(*S*), 7(*R*), 10(*R*), 13(*S*), 14(*S*), 15(*R*), 18(*S*), 19(*R*), 22(*R*), 24(*R*), and 3'(*R*) through chemical transformation, spectroscopic analyses, and conformational calculations (Ubutaka et al, 1993). The alkaline degradation product **M1** was prepared according to the method of Sugiyama and colleagues (1996) as shown in Scheme 7.

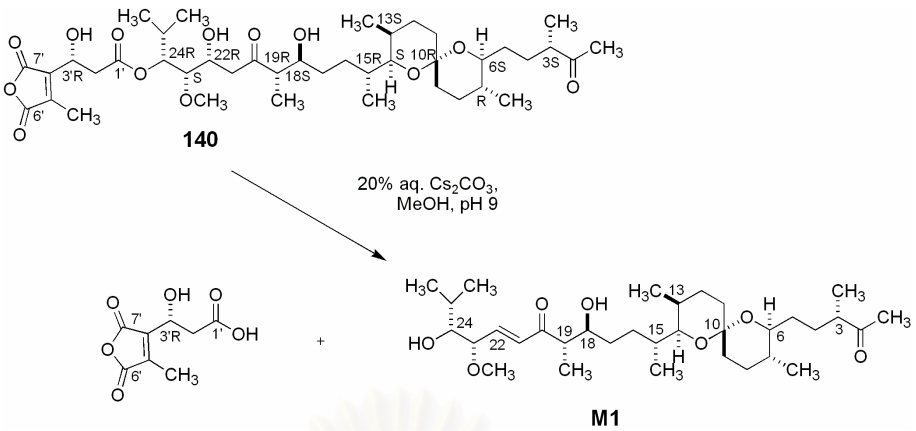

Scheme 7. Preparation of the alkali degradation product of tautomycin.

Alkali hydrolysis of malenic anhydride moiety at pH 9 of **140** with 20% Cs_2CO_3 in MeOH gave the diacid **141** having the lowest energy conformation in which the oxygen atom of OH at the C-22 situated near to the ester carbon of the C-1' (Sugiyama et al., 1996). This could render migration of the ester group at C-24 hydroxyl group to C-22, resulting in β-elimination and formation of alkaline degradation product **M1** (Scheme 8).

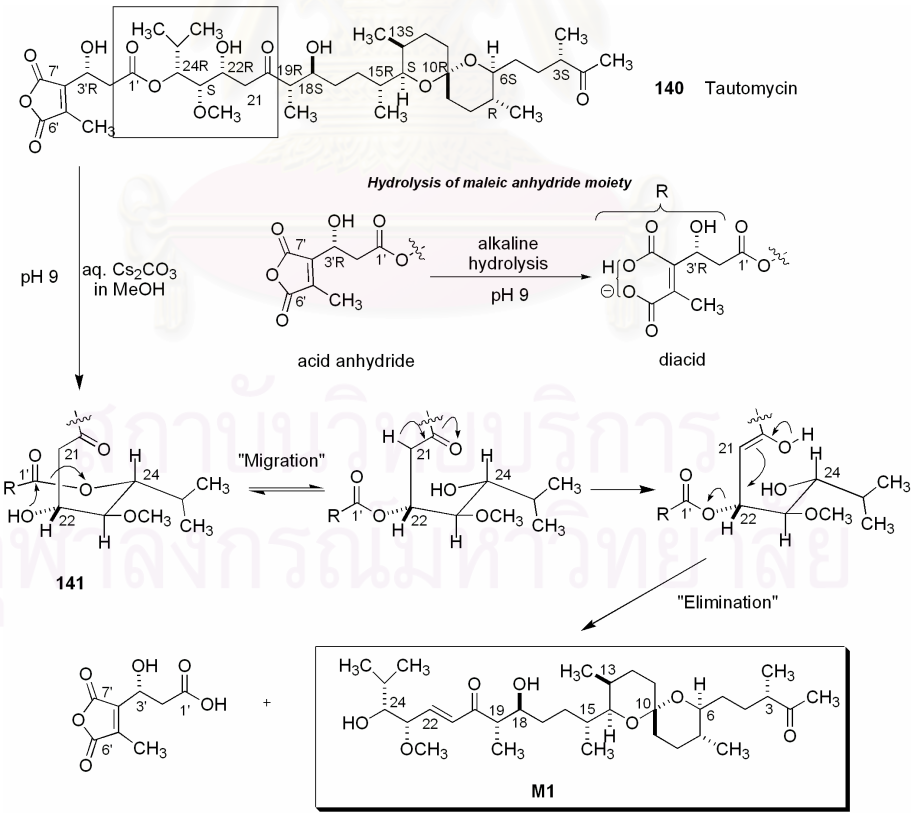

Scheme 8. Proposed *trans*-esterification and elimination mechanism on alkali degradation of tautomycin by Sugiyama and colleagues (1996).

4.2. The enantiomers of 5-isopropyl-4-methoxy-Δ^3-pyrrolin-2-ones

There are several synthetic routes leading to *N*-acyl-4-methoxy-Δ^3-pyrrolin-2-ones, or in other words, the 4-*O*-methylethers of *N*-acylated tetramic acids (tetramic acid = pyrrolidine-2,4-dione). Those methods have been discussed involving both racemic and enantioselective syntheses (for review see: Royles, 1995). We employed the enantioselective synthesis utilizing chiral amino acids to introduce asymmetry into the desired analogues **M2**–**M7** (Scheme 9). The first step is to construct the key cyclized heterocycle 4-hydroxy-Δ^3-pyrrolin-2-one derivative **143** or **144**, having known absolute stereochemistry at C-5. This chiral center can be controlled by using optically pure *N*-Boc-L-valine or *N*-Boc-D-valine as a starting material which will be further incorporated with C_2-derived molecule (i.e. Meldrum's acid). After *O*-methylation of the enolic function at C-4 of the cyclized product **143** affords *N*-Boc-4-methoxy-Δ^3-pyrrolin-2-one **M2** or **M5** (step **II**). In step **III**, the Boc group is removed under the usual condition yielding **M3** or **M6**. For the final step **IV**, *N*-propionylation of **M3** or **M6** further yields **M4** or **M7**, respectively.

4.2.1. Step I: formation of *N*-Boc-5(*S*)-isopropyl-4-hydroxy-Δ^3-pyrrolin-2-one [143]

The key cyclized heterocycle, *N*-Boc-5(*S*)-isopropyl-4-hydroxy-Δ^3-pyrrolin-2-one [**143**] derived from thermal rearrangement of the Meldrum's derivative **142** is an important step to construct the model analogues **M2**–**M4**. Two general methods for the preparation of **142** are (i) condensation of *N*-Boc-L-valine and Meldrum's acid with a condensing agent such as isopropenyl chloroformate (IPCF) or 2-chloro-1,3-dimethyl-2-imidazolinium hexafluorophosphate (CIP) together with a base (Akaji et al., 1999; Courcambeck et al., 2001; Kim, Oh and Han, 2001) or (ii) reaction of Meldrum's acid with an acid chloride of *N*-protected amino acid and a base (Oikawa, Sugano and Yonemitsu, 1978; Oikawa et al., 1985). The former procedure which involved the use of IPCF (method A, Scheme 10) or CIP (method B, Scheme 10) was selected.

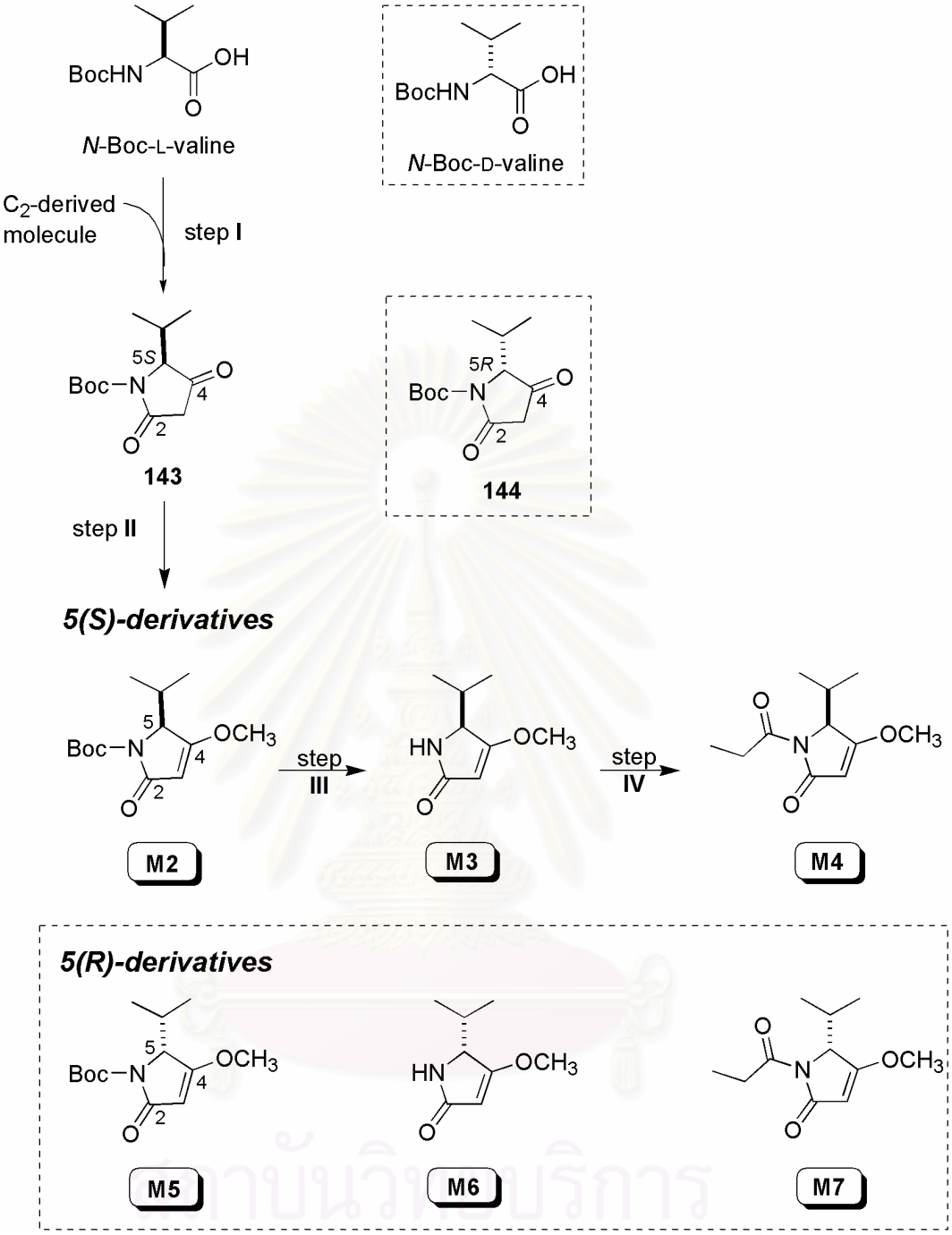

Scheme 9. Preparation of of 5(*S*)-isopropyl-4-methoxy-Δ^3-pyrrolin-2-one derivatives **M2** to **M4** and its enantiomers **M5** to **M7** *via* (step **I**) 4-hydroxy-Δ^3-pyrrolin-2-one formation, (step **II**) *O*-methylation, (step **III**) deprotection, and (step **IV**) *N*-propionylation.

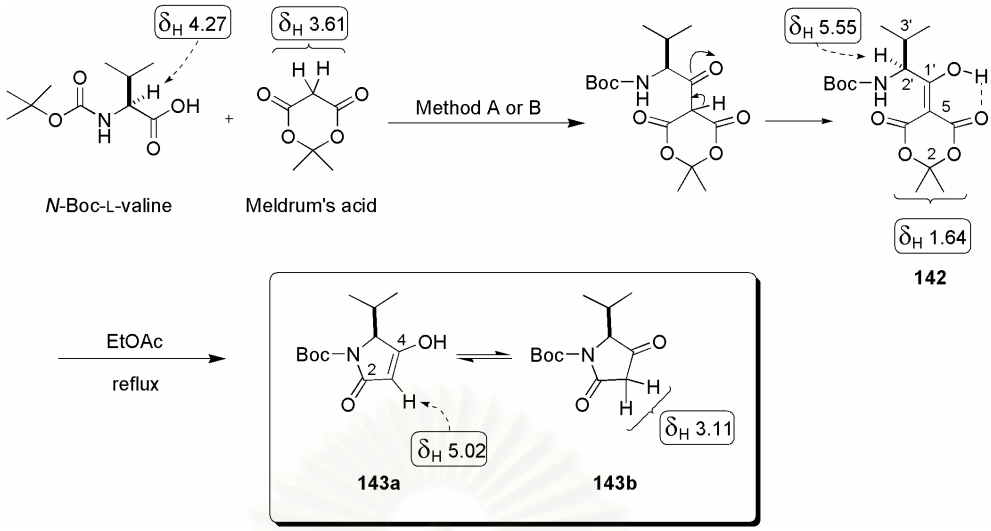

Scheme 10. Preparation of *N*-Boc-5(*S*)-isopropyl-4-hydroxy-Δ^3-pyrrolin-2-one [**143**] employing IPCF (method A) or CIP (method B) as a condensing agent, and key ^{1}H signals.

Method A. The acylation of Meldrum's acid with *N*-protected chiral amino acid was achieved using isopropenyl chloroformate (IPCF) as a condensing agent. The reaction conditions were very stringent; any change in the procedure leading to a lower yield (Jouin and Castro, 1987). This method did not lead to 100% diastereoselectivity when applied to a chiral N-Boc-benzyl amino acid as claimed by Courcambeck and colleagues (2001).

Method B. The acylation employed 2-chloro-1,3-dimethyl-2-imidazolinium hexafluorophosphate (CIP) as a condensing agent. This method has been reported to yield 4-hydroxy-Δ^3-pyrrolin-2-one without epimerization (Akaji et al, 1999).

Both condensing agents gave similar yield of the Meldrum's derivative **142** when observed on Si gel TLC (R_f 0.5, solvent system: MeOH-EtOAc-Acetic acid = 3:95:2). Compound **142** is unstable to nucleophile such as H_2O, resulting in the formation of undesired side products (i.e. *β*-ketocompound). In my case, an additional spot was observed after the usual aqueous extraction. The use of two equivalent of DMAP without aqueous workup was then employed. This afforded the corresponding DMAP salt **142** which has been proved to be superior in its stability (Raillard et al., 2002). The downfield signal at δ_H 5.55 (H-2'), a *gem*-dimethyl protons at δ_H 1.64 (6H, H_3-2), and the absence of a methylene proton signal at δ_H 3.61

of Meldrum's acid in the ^{1}H NMR spectrum (Figure 110) of the crude product supported the presence of Meldrum's derivative **142**. Although the crude product derived from method A gave better results as the side product were carbon dioxide and acetone, IPCF was not commercially available. Therefore CIP was used in these experiments. The proposed C-C bond formation mechanism between Meldrum's acid and *N*-Boc-L-valine utilizing IPCF or CIP as a condensing agent are shown as method A and B in Scheme 11, respectively.

The DMAP salt adduct **142** was heated in refluxing dry EtOAc to afford *N*-Boc-5(*S*)-isopropyl-4-hydroxy-Δ^3-pyrrolin-2-one [**143**], whereas no side product was observed after checking with Si gel TLC on several solvent systems. The ^{1}H NMR spectrum of the corresponding crude **143** showed the presence of the enolic tautomer **143a** (enol form, H-3 δ_H 5.02) and **143b** (keto form, H_2-3 δ_H 3.11) in 1:2 ratio by integration of the H-5 methine proton signals (Figure 111). No purification was done at this step. The proposed intramolecular cyclization derived from thermal rearrangement of Meldrum's derivative **142** is shown in Scheme 12.

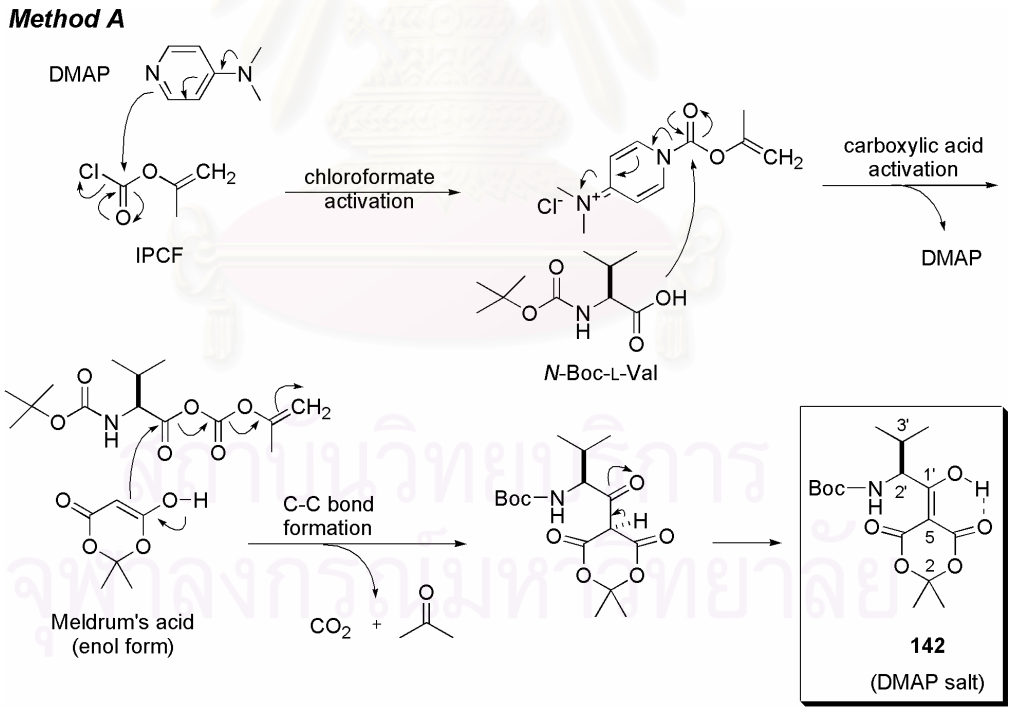

Scheme 11. Proposed acylation mechanism of Meldrum's acid utilizing (Method A) isopropenyl chloroformate, IPCF or (Method B) 2-chloro-1,3-dimethyl-2-imidazolinium hexafluorophosphate, CIP as a condensing agent.

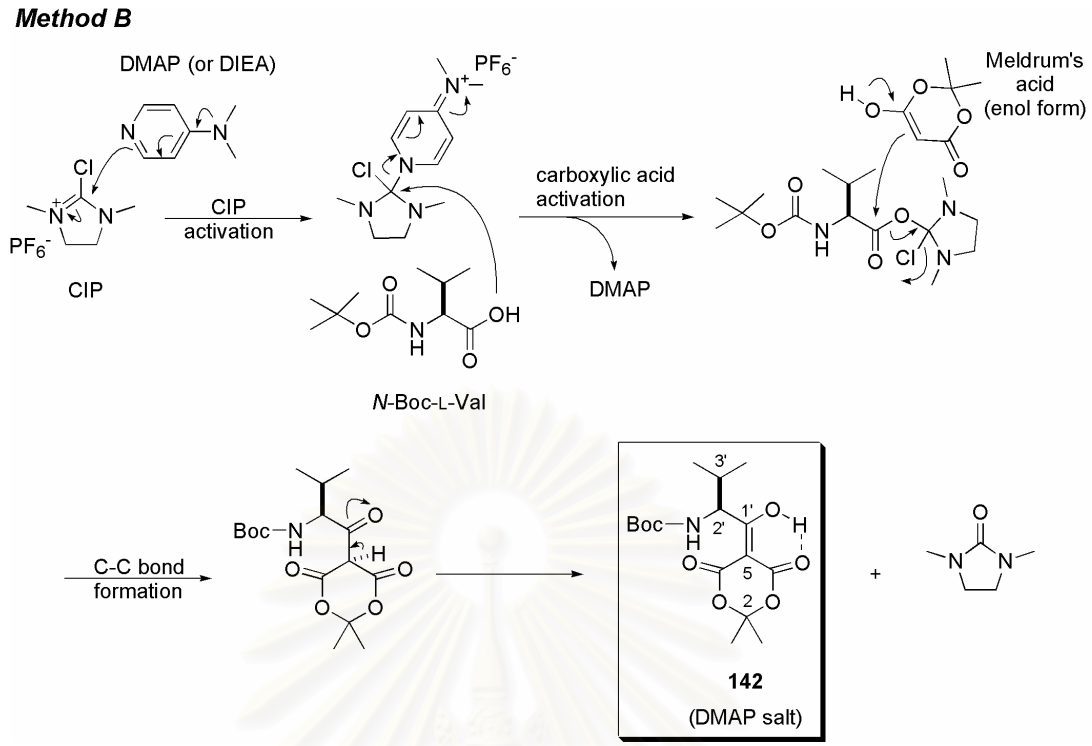

Scheme 11. (*Continued*)

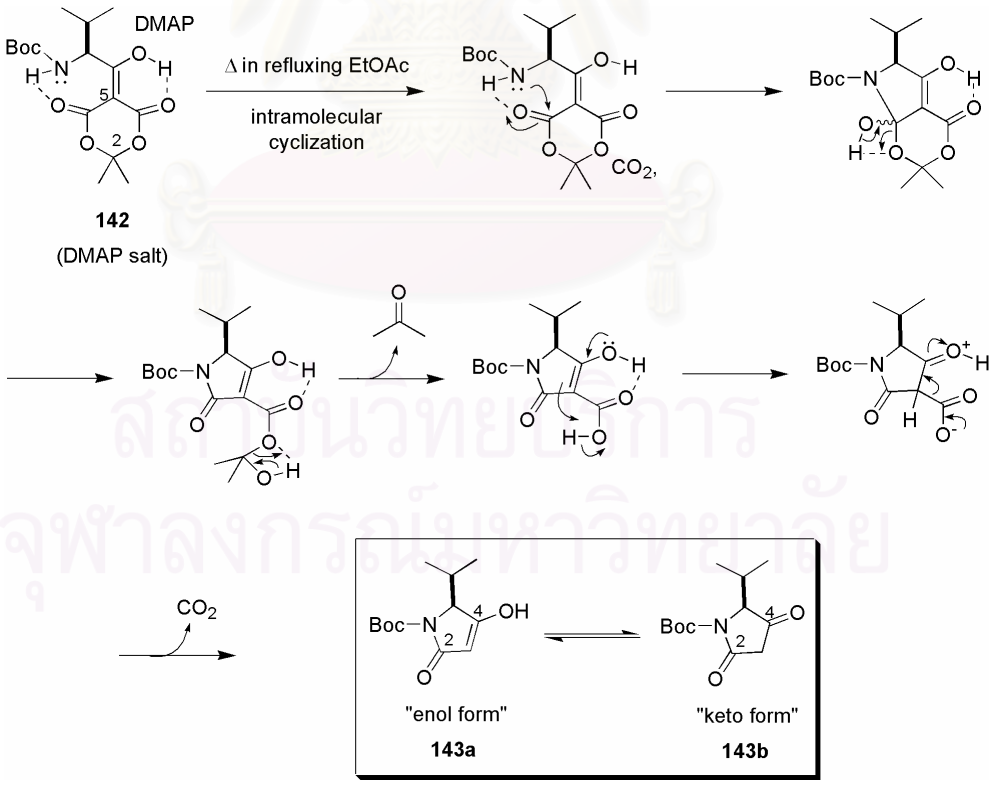

Scheme 12. Proposed intramolecular cyclization mechanism of Meldrum's derivative [**142**] in refluxing EtOAc.

4.2.2. Step II: *O*-methylation

O-Methylation of the crude product **143** was conducted under Mitsunobu condition at room temperature to give *N*-Boc-5(*S*)-isopropyl-4-methoxy-Δ^3-pyrrolin-2-one [**M2**] in 45% overall yield (Scheme 13**A**). In this step, the epimerization can occur due to the activation of an *N*-acyl amino acid as claimed by Akaji and colleagues (1999). The ^{1}H NMR spectrum of **M2** (Figure 113) showed the methoxyl protons signal at δ_H 3.81 (H_3-9), confirming **M2** as the desired product. The proposed reaction mechanism of **M2** is shown in Scheme 13**B**.

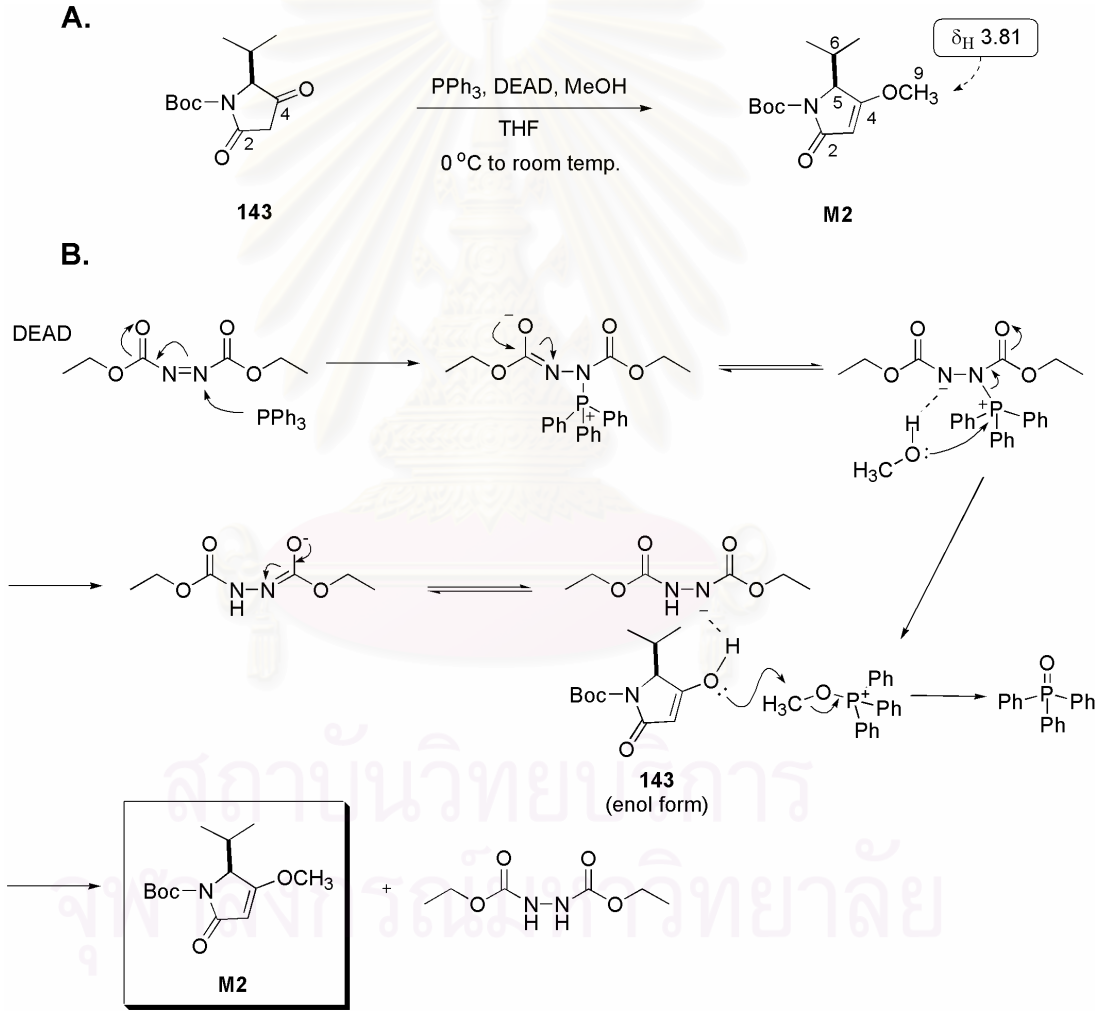

Scheme 13. (A) *O*-methylation *via* Mitsunobu reaction, and (B) the proposed *O*-methylation mechanism of *N*-Boc-5(*S*)-isopropyl-4-hydroxy-Δ^3-pyrrolin-2-one [**143**].

4.2.3. Step III: deprotection

Boc group was removed by treating CH_2Cl_2 solution of **M2** with 50% TFA in MeOH at 0 °C. The desired product, 5(*S*)-isopropyl-4-methoxy-Δ^3-pyrrolin-2-one [**M3**] was obtained in an excellent yield (Scheme 14). Compound **M3** could be crystallized in a mixture of EtOAc–hexane, 1:1. The ^{1}H NMR spectrum of **M3** (Figure 115) showed the absence of *tert*-butyl signal at δ_H 1.54 (9H) of **M2**, thus, confirming **M3** as 5(*S*)-isopropyl-4-methoxyl-Δ^3-pyrrolin-2-one.

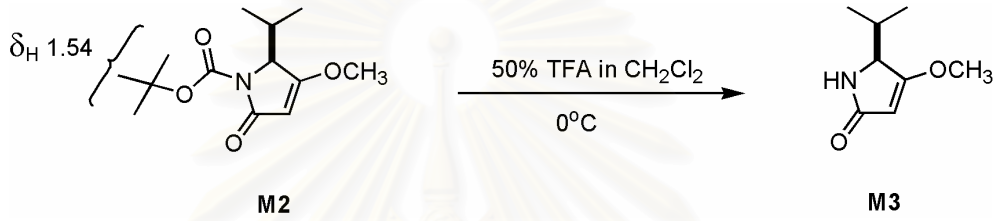

Scheme 14. Deprotection reaction of 5(*S*)-isopropyl-4-methoxy-Δ^3-pyrrolin-2-one [**M3**].

4.2.4. Step IV: *N*-propionylation

To construct the *N*-acylamide structure **M4**, activation of amide and/or acyl donor is generally required, since the nitrogen atom of amide is less basic than the amines due to amide resonance. The method of Yamada, Setsuko, and Matsuda (2002) utilizing amide-MeMgBr-acyl chloride was, thus, employed in this experiment. The reaction of **M3** and propionyl chloride in the presence of MeMgBr gave the *N*-propionyl product **M4** in 90% yield (Scheme 15). The ^{1}H NMR spectrum of **M4** (Figure 117) showed the signals at δ_H 1.15 (t, 7.2, H_3-3') and δ_H 2.94 (q, 7.2, H_2-2'), confirming **M4** as 5(*S*)-isopropyl-4-methoxyl-1-propionyl-Δ^3-pyrrolin-2-one.

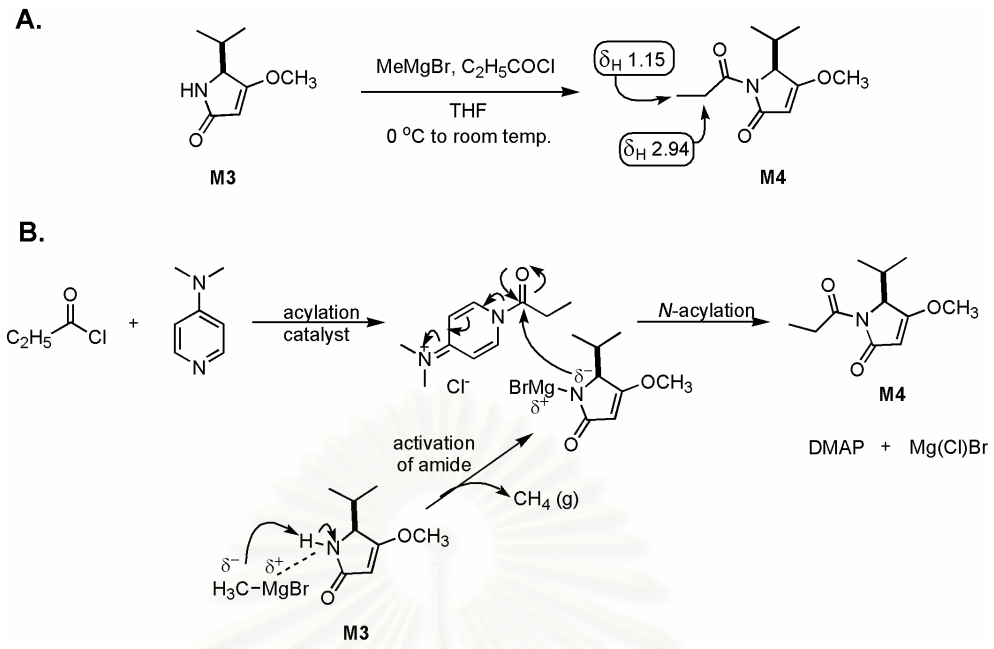

Scheme 15. (A) *N*-propionyl reaction, and (B) the proposed reaction mechanism.

4.2.5. Spectroscopic data of model analogues M2–M7

A series of 5(*R*)-configuration analogues (**M5**–**M7**) were prepared in the same manner described for 5(*S*)-analogues **M2**–**M4**. All the physicochemical and spectroscopic data of these analogues are shown in Table 10.

Table 10. Physicochemical properties and spectroscopic data of model compounds **M2**–**M7**

Compound	% yield (ee)[a]	$[\alpha]_D^{20}$ (c, in CH_2Cl_2)	R_f[b]	Formula	m/z (ESITOF MS)	δ_H ($CDCl_3$, 400 MHz,)
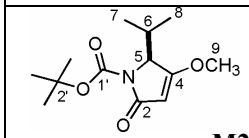 **M2**	44.78[c] (> 90)	+83.5 ° (c 0.20)	0.8	$C_{13}H_{21}NO_4$	278.1373 $[M + Na]^+$, calcd for $C_{13}H_{21}NO_4Na$, 278.1368	0.80 (d, 7.2, H_3-7), 1.09 (d, 7.2, H_3-8), 1.54 (9H, s, 2'-(*tert*)Bu), 2.42 (m, H-6), 3.81 (s, H_3-9), 4.37 (d, 2.4, H-5), 5.06 (s, H-3)
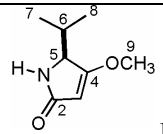 **M3**	100 (> 90)	+5.6 ° (c 1.00)	0.2	$C_8H_{13}NO_2$	156.1016 $[M + H]^+$, calcd for $C_8H_{14}NO_2$, 156.1024	0.80 (d, 6.8, H_3-7), 1.00 (d, 6.8, H_3-8), 2.08 (m, H-6), 3.79 (s, H_3-9), 3.98 (dd, 1.2, 2.8, H-5), 5.03 (d, 1.2, H-3), 5.40 (br s, NH)
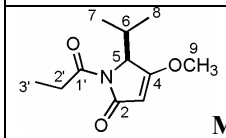 **M4**	91 (> 80)	+75.3 ° (c 0.60)	0.8	$C_{11}H_{17}NO_3$	234.1108 $[M + Na]^+$, calcd for $C_{11}H_{17}NO_3Na$, 234.1106	0.74 (d, 7.2 Hz, H_3-7), 1.11 (d, 7.2, H_3-8), 1.15 (t, 7.2, H_3-3'), 2.55 (m, H-6), 2.94 (q, 7.2, H_2-2'), 3.83 (s, H_3-9), 4.37 (d, 2.4, H-5), 5.06 (s, H-3)
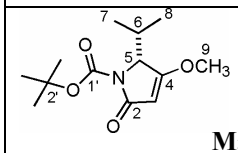 **M5**	10[c] (>90)	−77.0 ° (c 0.20)	0.8	$C_{13}H_{21}NO_4$	278.51 $[M + Na]^+$, calcd for $C_{13}H_{21}NO_4Na$, 278.14	0.80 (d, 7.2, H_3-7), 1.09 (d, 7.2, H_3-8), 1.54 (9H, s, 2'-(*tert*)Bu), 2.42 (m, H-6), 3.81 (s, H_3-9), 4.37 (d, 2.4, H-5), 5.06 (s, H-3).
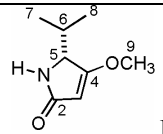 **M6**	107 (> 90)	−6.5 ° (c 1.00)	0.2	$C_8H_{13}NO_2$	156.44 $[M + H]^+$, calcd for $C_8H_{14}NO_2$, 156.09	0.80 (d, 6.8, H_3-7), 1.00 (d, 6.8, H_3-8), 2.08 (m, H-6), 3.79 (s, H_3-9), 3.98 (dd, 1.2, 2.8, H-5), 5.03 (d, 1.2, H-3), 5.40 (br s, NH)
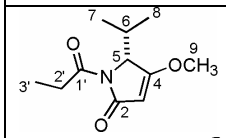 **M7**	67 (> 80)	−60.9° (c 0.60)	0.8	$C_{11}H_{17}NO_3$	234.51 $[M + Na]^+$, calcd for $C_{11}H_{17}NO_3Na$, 234.11	0.74 (d, 7.2 Hz, H_3-7), 1.11 (d, 7.2, H_3-8), 1.15 (t, 7.2, H_3-3'), 2.55 (m, H-6), 2.94 (q, 7.2, H_2-2'), 3.83 (s, H_3-9), 4.37 (d, 2.4, H-5), 5.06 (s, H-3)

[a] ee, calculated from the areas under methoxyl resonances in the presence of (*R*)-TFAE. [b] Si gel TLC, solvent synstem: EtOAc-hexane = 3:1. [c] % over all yield.

CHAPTER V

CONCLUSION

Bioassay-guided fractionation of the crude EtOAc extract from the first collection of the Thai sea hare, *Bursatella leachii*, collected from the Gulf of Thailand in October 2000, yielded the first tripeptide-containing malyngamide, malyngamide X (**SHO27**, 0.71**%** yield of the crude extract). Investigation of the crude EtOAc extract from the second collection of the mollusc in July 2002 resulted in the isolation of a potent stimulator of actin assembly, hectochlorin (**SHOII-28**, 0.25**%** yield of the crude extract) and its new derivative, deacetylhectochlorin (**SHOII-51**, 0.09 % yield of the crude extract). In addition, a new structurally unrelated molecule, *syn*-3-isopropyl-6-(4-methoxy-benzyl)-4-methyl-morpholine-2,5-dione (**SHOII-76**, 0.007% yield of the crude extract), was co-isolated.

The gross structure of malyngamide X [**SHO27**], established by extensive analyses of 1D, 2D NMR and MS data, is a lipopeptide derived from 7-methoxytetradec-4(*E*)-enoic acid and a tripeptide constructed from *N*-methyl alanine, 4-amino-3-hydroxy-2-methylpentanoic acid, and 5-isopropyl-4-methoxy-Δ^3-pyrrolin-2-one. Compound **SHO27** has 6 stereogenic centers in the molecule including 5 stereogenic centers in the amine-derived portion (C-2, C-5, C-7, C-8, and C-14) and one stereogenic center in the fatty acid side chain (C-7'). The stereo structure of the compound was established as 2(*S*), 5(*S*), 7(*S*), 8(*R*), 14(*S*), and 7'(*S*)-configurations, employing non-hydrolytic degradation method in conjunction with biogenetic considerations of the malyngamide-type natural products. The non-hydrolytic degradation method comprised the NMR-based methods of interproton spin-spin coupling constants ($^3J_{H,H}$), 2D NOESY experiment, NMR chiral solvating agent utilizing 2,2,2-trifluoro-1-(9-anthryl)ethanol (TFAE or Pirkle's alcohol), and NMR chiral derivatizing agent (MTPA) of the modified Mosher's method; together with analysis of molecular models.

Information on the gross structure of hectochlorin (**SHOII-28**) was obtained by extensive analyses of 1D and 2D NMR data and confirmed by comparison with previously published data. The absolute stereochemistry of hectochlorin was already established as 2(*R*), 3(*S*), 14(*S*), and 22(*S*) by X-ray analysis referring to anomalous scattering data. This was also consistent with the single crystal X-ray crystallography of **SHOII-28**.

The ^{1}H and ^{13}C NMR spectra of the new compound, deacetylhectochlorin, were nearly identical to those of hectochlorin, which contains two units of 2-alkylthiazole-4-carboxylic acid, two units of α,β-dihydroxyisovalerate (DHIV), and a 7,7-dichloro-3-acyloxy-2-methyl-octanoate (DCAO) fragment. In contrast to hectochlorin, **SHOII-51** lacked the signals of an acetyl group which established **SHOII-51** as deacetylhectochlorin, a new hectochlorin derivative. The absolute stereochemistry of **SHOII-51** was then studied by comparing the CD spectrum of **SHOII-51** to that of deacetylhectochlorin obtained by hydrazine hydrolysis. Both compounds displayed similar positive cotton effect at 228 nm and two negatives at 209 (210) and 257 (258) nm, respectively. On the basis of this information, in conjunction with their identical ^{1}H, ^{13}C NMR spectra and specific rotation $[\alpha]^{20}_{D}$ values, the stereo structure of **SHOII-51** was confidently established as 2(*R*), 3(*S*), 14(*S*), and 22(*S*), the same as that of **SHOII-28**.

The second morpholine-2,5-dione containing natural compound, *syn*-3-isopropyl-6-(4-methoxy-benzyl)-4-methyl-morpholine-2,5-dione [**SHOII-76**] was obtained in trace amount. Its gross structure was mainly elucidated by extensive analyses of 1D, 2D NMR and MS data. Substituents on C-3 and C-6 of **SHOII-76** lie on the same side of the plane as implied by analyses of $^{3}J_{H,H}$ values and partly 2D NOESY data, thus, the 3,6 stereochemistry was *syn*. Unfortunately, the absolute configuration assignment and biological testing of **SHOII-76** were not done due to limited amount of the compound.

Malyngamide X, hectochlorin, and deacetylhectochlorin were subjected to cytotoxic testing against oral human epidermoid carcinoma of nasopharynx (KB), human small cell lung cancer (NCI-H187), and breast cancer (BC) cell lines, antimalarial against *Plasmodium falciparum* (K1, multidrug resistant strain), and antituberculous against *Mycobacterium tuberculosis* H37Ra strain.

Malyngamide X showed several biological activities; thus moderate cytotoxicities (ED_{50}'s of 8.20, 4.12 and 7.03 μM, respectively), antituberculous (MIC's of 50 μg/ml) and antimalarial (ED_{50}'s of 5.44 μM) activities. Hectochlorin showed strong cytotoxicity against KB and NCI-H187 with ED_{50}'s of 0.86 and 1.20 μM, while deacetylhectochlorin exhibited more potent cytotoxicity with ED_{50}'s of 0.31 and 0.32 μM, respectively. In addition, deacetylhectochlorin exhibited strong cytotoxicity against BC cancer cell line with ED_{50}'s of 1.03 μM. Both compounds were inactive in *in vitro* antimalarial and antituberculous assays.

Application of non-hydrolytic degradation method was established as an exemplary study for assigning absolute stereochemistry of the natural compound having conformationally flexible system similar to malyngamide X. The achievement in applying the NMR chiral solvation experiments for absolute stereochemistry determination at some chiral carbons of malyngamide X and several synthetic analogues including alkaline degradation product of tautomycin [**M1**] and enantiomers of Δ^3-pyrrolin-2-one derivatives [**M2** to **M7**] encourage the use of the current strategy to other natural compounds as well. However, the application of NMR chiral solvating agent for absolute configurational assignment is limited to the stereogenic center of which its solvate complexes with TFAE are well understood, such as the compounds having stereogenic centers identical to the proposed solvation model of this study.

The one known (**SHOII-28**) and three new (**SHO27**, **SHOII-51** and **SHOII-76**) metabolites from two collections of the Thai sea hare *B. leachii* described here have provided an insight into the potentially interesting chemistry of the unexplored Thai sea hares. More works should also be focused on the bioactive constituents of their dietary cyanobacteria as well, since they might be the true origin of the secondary metabolites from the sea hares.

REFERENCES

ภาษาไทย

สุชาติ อุปถัมภ์, มาลียา เครือตาชู, เยาวลักษณ์ จิตรามวงศ์, และ ศิริวรรณ จันทเตมีย์. 2538. สังขวิทยา. กรุงเทพฯ: ศักดิโสภาการพิมพ์.

ภาษาอังกฤษ

Ainslie, R. D., Barchi, J. J., Kuniyoshi, M., Moore, R., and Mynderse, J. S. 1985. Structure of malyngamide C. J. Org. Chem. 50: 2859–2862.

Akaji, K., Hayashi, Y., Kiso, Y., and Kuriyama, N. 1999. Convergent synthesis of dolastatin 15 by solid phase coupling of an *N*-methylamino acid. J. Org. Chem. 64: 405–411.

Amnuoypol, S., Suwanborirux, K., Pummangura, S., Kubo, A., Tanaka, C., Saito, N. 2004. Chemistry of renieramycins. Part 5. Structure elucidation of renieramycin type derivatives O, Q, R, and S from Thai marine sponge *Xestospongia* species pretreated with potassium cyanide. J. Nat. Prod. 67(6): 1023–1028.

Appleton, D. R., Babcock, R. C., and Copp, B. R. 2001. Novel tryptophan-derived dipeptides and bioactive metabolites from the sea hare *Aplysia dactylomela*. Tetrahedron 57: 10181–10189.

Appleton, D. R., Sewell, M. A., Berridge, M. V., and Copp, B. R. 2002. A new biologically active malyngamide S from a New Zealand collection of the sea hare *Bursatella leachii*. J. Nat. Prod. 65(4): 630–631.

Burja, A. M., Banaigs, B., Abou-Mansour, E., Burgess, J. G., and Wright, P. C. 2001. Marine cyanobacteria–a prolific source of natural products. Tetrahedron 57: 9347–9377.

Cardellina II, J. H., Dalietos, D., Marner, F.-J., Mynderse, J. S., and Moore, R. E. 1978. (–)-*trans*-7(*S*)-methoxytetradec-4(*E*)-enoic acid and related amides from the marine cyanophyte *Lyngbya majuscula*. Phytochemistry 17: 2091–2095.

Cardellina II, J. H., Marner, F.-J., and Moore, R. E. 1979. Seaweed dermatitis: structure of lyngbyatoxin A. Sciences 204: 193–195.

Carballeira, N. M., and Pagán, M. 2001. New methoxylated fatty acids from the Caribbean sponge *Callyspongia fallax*. J. Nat. Prod. 64: 620–623.

Cetusic, J. R. P., Green III, F. R., Graupner, P. R., and Oliver, M. P. 2002. Total synthesis of hectochlorin. Organic Lett. 4: 1307–1310.

Cimino, G., Ciavatta, M. L., Fontana, A., and Gavagnin, M. 2001. Metabolites of marine opistobranchs: chemistry and biological activity. In Corrado T. Bioactive Compounds from Natural Sources. London: Taylor & Francis, pp. 577–638.

Coleman–Davies, M., and et al. 2003. Isolation of homodolastatin 16, a new cyclic depsipeptide from a Kenyan comllection of *Lyngbya majuscula*. J. Nat. Prod. 66, 712–715.

Collins, L., and Franzblau, S. G. 1997. Microplate Alarmar Blue assay versus BACTEC 460 system for high-through put screening of compounds against Mycobacterium tuberculosis and *Mycobacterium avium*. Antimicrob. Agents Chemother. 41: 1004–1009.

Cordell, G. A., Shamma, M., Saxton, J. E., Smith, G. F. 1989. Dictionary of Alkaloids. London: Chapman and Hall, p. 404.

Courcambeck, J., Bihel, F., Michelis, C., Quelever, G., and Kraus, J. L. 2001. Design of potential new HIV protease inhibitors: enantioconvergent synthesis of new pyrrolidin-3-ol, and pyrrolidin-3-one peptide conjugates. J. Chem. Soc. Perkin Trans. 1,1421–1430.

Dale, J. A., and Mosher, H. S. 1968. Nuclear magnetic resonance nonequivalence of diastereomeric esters of α-substituted phenylacetic acids for the determination of stereochemical purity. J. Am. Chem. Soc. 90: 2543–2549.

Davies-Coleman, M. T. and et al. 2003. Isolation of homodolastatin 16, a new cyclic depsipeptide from a Kenyan collection of *Lyngbya majuscula*. J. Nat. Prod. 66: 712–715.

Dembitsky, V. M., and Srebnik, M. 2002. Natural halogenated fatty acids, their analogues and derivatives. Prog. Lipid Res. 41: 315–367.

Desjardins, R. E., Canfield, C. J., Haynes, J. D., Chulay, J. D. 1979. Quantitative assessment of antimarial activity in vitro by a semiautomated microdilution technique. Antimicrob. Agents and Chemother. 16: 710–718.

Eliel, E. L., Wilen, S. H., and Mander, L. N. 1994. Determination of enantiomer and diastereomer composition. In Stereochemistry of Organic Compounds, pp. 124–296. Toronto: John Wieley & Sons.

Fedorov, S. N, Radchenko, O. S., Shubina, L. K., Kalinaovsky, A. I., Gerasimenko, A. V., Popov, D. Y., and Stanik, V. A. 2001. Aplydactone, a new sesquiterpenoid with an unprecedented carbon skeleton from the sea hare *Aplysia dactylomela*, and its cargill-like rearrangement. J. Am. Chem. Soc. 123: 504–505.

Fedorov, S. N., Shubina, L. K., Kalinovsky, A. I., Lyakhova, E. G., and Stonik, V. A. 2000. Structure and absolute configuration of a new rearranged chamigrne-type sesquiterpenoid from the sea hare *Aplysia* sp. Tetrahedron Lett. 41: 1979–1982.

Ferreiro M. J., Latypov, S. V., Quiñoá, E., and Riguera, R. 2000. Assignment of the absolute configuration of α–chiral caroxylic acid by 1H NMR septroscopy. J. Org. Chem. 65: 2658–2666.

Fujii, K., Shimoya, T., Ikai, Y., Oka, H., and Harada, K.-I. 1998. Further application of advanced Marfey's method for determination of absolute configuration of primary amino compound. Tetrahedron Lett. 39: 2579–2582.

Fujii, K. F., Yahashi, Y., Nakano, T., Imanishi, S., Baldia, S. F., and Harada, K.-I. 2002. Simultaneous detection and determination of the absolute configuration of thiazole-conataing amino acids in a pepetide. Tetrahedron 58: 6873–6879.

Fuller, R. W., Cardellina, J. H., Kato, Y., Brinen, L. S., Clardy, J., Snader, K. M., Boyd, M. R. 1992. A pentahalogenated monoterpene from the red alga *Portieria hornemannii* produces a novel cytotoxicity profile against a diverse panel of human tumor cell lines. J. Med. Chem. 35: 3007–3011.

Gallimore, W. A., Galario, D. L., Lacy, C., Zhu, Y., and Scheuer, P. J. 2000. Two complex proline esters from the sea hare *Stylocheilus longicauda*. J. Nat. Prod. 63: 1022–1026.

Gallimore, W. A. and Scheuer, P. J. 2000. Malyngamides O and P from the sea hare *Stylocheilus longicauda*. J. Nat. Prod. 63: 1422–1424.

Gerwick, W. H., Reyes, S. and Alvarado, B. 1987. Two malyngamides from the Caribbean cyanobacterium *Lyngbya majuscula*. Phytochemistry 26(6): 1701–1704.

Giordano, A., Monica, C. D., Landi, F., Spinella, A., and Sodano, G. 2000. Stereochemistry and total synthesis of janolusimide, a tripeptide marine toxin. Tetrahedron Lett. 41: 3979–3982.

Hannak, D., and Bayer, E. 1979. Malyngamide A, a novel chlorinated metabolite of the marine canophyte *Lyngbya majuscula*. J. Am. Soc. 101: 240–242.

Harrigan, G. G., Luesch, H., Yoshida, W. Y., Moore, R. E., Nagle, D. G., and Paul, V. J. 1999. Symaplostatin 2: a dolastatin 13 analogue from the marine cyanobacterium *Symploca hydnoides*. J. Nat. Prod. 62: 655–658.

Harrigan, G. G., Luesch, H., Yoshida, W. Y., Moore, R. E., Nagle, D. G., Paul, V. J., Mooberry, S. L., Corbett, T. H., and Valeriote, F. A. 1998a. Symplostatin 1: a dolastatin 10 analogue from the marine cyanobacterium *Symploca hydnoides*. J. Nat. Prod. 61: 1075–1077.

Harrigan, G. G., Yoshida, W. Y., Moore, R. E., Nagle, D. G., Park, P. U., Biggs, J., Paul, V. J., Mooberry, S. L., Corbett, T. H., Valeriote, F. A. 1998b. Isolation, structure determination, and biological activity of dolastatin 12 and Lyngbyastatin 1 from *Lyngbya majuscula*/*Schizothrix calccola* cytanobacterial assemblages. J. Nat. Prod. 61: 1221–1225.

Hayashi, M., Kim, Y. P., Hiraoka, H., Natori, M., Takamatsu, S., Kawakubo, T., Masuma, R., Komiyama, K., Omura, S. 1995. Macrosphelide, a novel inhibitor of cell-cell adhesion molecule. Taxonomy, fermentation, isolation and biological activities. J. Antibiot 48: 1435–1439.

Heathcock, C. H., Pirrung, M. C., and Sohn, J. E. 1979. Acyclic steroselection. 4. Assignment of stereostructure to β-hydroxycarbonyl compounds by carbon-13 nuclear magnetic resonance. J. Org. Chem. 44: 4294–4299.

Horgen, F. D., Kazmierski, E. B., Westenburg, H. E., Yoshida, W. Y., and Scheuer, P. J. 2002. Malevamide D: isolation and structure determination of an isodolastatin H analogue from the marine cyanobacterium *Symploca hydnoides*. J. Nat. Prod. 65: 487–491.

Hoffmann, M. A., Blessing, J. A., Lentz, S. S. 2003. A phase II trial of dolastatin 10 in recurrent platinum-sensitive ovarian carcinoma: a gynecologic oncology group study. Gynecologic Oncol. 89, 95–98.

Jaruchoktaweechai, C., Suwanborirux, K., Tanasupawatt, S., Kittakoop, P., and Menasveta, P. 2000. New macrolactins from a marine *Bacillus* sp. Sc026. J. Nat. Prod. 63(7): 984–986.

Jensen, K. R. 1998a. Anatomy of some opisthobranch molluscs from Phuket, Thailand, with a list of Opisthobranchia recorded from Thai waters. In J. Hylleberg (ed.), Proceeding of the Eighth Workshop of the Tropical Marine Mollusc Programe (TMMP), pp. 243–262. Phuket: Phuket Marine Biological Center Special Publication.

Jensen, K. R. 1998b. Collection, preservation and identification of Opisthobranch molluscs. In J. Hylleberg (ed.), Proceeding of the Ninth Workshop of the Tropical Marine Mollusc Programe (TMMP), pp. 345–352. Phuket: Phuket Marine Biological Center Special Publication.

Jordan, M. A., Walker, D., Arruda, M., Barlozzari, T., and Panda, D. 1998. Suppression of microtubule dynamics by binding of cemadotin to tubulin: possible mechanism for its antitumor action. Biochemistry 37(50): 17571–17578.

Jouin, P., and Castro, B. 1987. Stereospecific synthesis of N-protected statine and its analogues via chiral tetramic acid. J. Chem. Perkin. Trans. I: 1177–1182.

Jullian, J.–C., Franck, X., Latypov, S., Hocquemiler, R., and Figadère, B. 2003. NMR determination of absolute configuration of α-acyloxy ketones. Tetrahedron Asymmetry. 14: 963–966.

Kan, Y., Fujita, T., Nagai, H., Sakamoto, B., and Hokama, Y. 1998. Malyngamide M and N from the Hawaiian red alga *Gracilaria coronopifolia*. J. Nat. Prod. 61: 152–155.

Kan, Y., Sakamoto, B., Fujita, T., and Nagai, H. 2000. New malyngamides from the Hawaiian cyanobacterium *Lyngbya majuscula*. J. Nat. Prod. 63: 1599–1602.

Kano, K., and Hasegawa, H. 2001. Interactions with charged cyclodextrins and chiral recognition. J. Incl. Phenom. Macrocyclic. Chem. 41: 41–47.

Kano, H., Hasegawa, H., Miyamura, M. 2001. Chiral recognition of dipeptide methyl esters by an anionic *β*-cyclodextrin. Chirality 13: 474–482.

Katae, T., Takashima, H., Kano, K. 1999. Chiral recognitin of phenylacetic acid derivatives by aminated cyclodextrins. J. Incl Phenom Macrocyclic Chem. 33: 345–359.

Kerbrat, P., Dieras, V., Pavlidis, N., Ravaud, A., Wanders, J., and Fumoleau, P. 2003. Phase II study of LU 103793 (dolastatin analogue) in patients with metastatic breast cancer. European Journal of Cancer 39, 317–320.

Kigoshi, H., and et al. 2001. Auriculol, a cytotoxic oxygenated squalene from the Japanese sea hare *Dolabella auricularia*: isolation, stereostructure, and synthesis. Tetrahedron Lett. 42: 7461–7464.

Kigoshi, H., and et al. 2002. Cytotoxicity and actin-depolymerizing activity of aplyronine A, a potent antitumor macrolide of marine origin, and its analogues. Tetrahedron 58: 1075–1102.

Kigoshi, H., Suenaga, K., Takagi, M., Akao, A., Kanematsu, K., Kamei, N., Okugawa, Y., Yamada, K. 1996. Aplyronine A, a potent antitumor substance of marine origin, aplyronines B and C, and artificial analogues: total synthesis and structure–cytotoxicity relationships. J. Org. Chem. 61: 5326–5351.

Kim, Y.–A., Oh, S–M., and Han, S.–Y. 2001. Stereoselective synthesis of *trans*-(2*R*,3*S*)- and *cis*-(2*R*,3*R*)-disubstitued pyrrolidines. Bull. Korean Chem. Soc. 22: 327–329.

Latypov, S., Franck, X., Jullian, J.–C., Hocquemiller, R., Figadère, B. 2002. NMR determination of absolute configuration of butenolides of Annonaceous type. Chem. Eur. J. 8: 5662–5666.

Luesch, H., Moore, R. E., Paul, V. J., Mooberry, S. L., and Corbett, T. H. 2001. Isolation of dolastatin 10 from the marine cyanobacterium *Symploc*a species VP642 and total stereochemistry and biological evaluation of Its analogue symplostatin 1. J. Nat. Prod. 64: 907–910.

Luesch, H., Yoshida, W. Y., Moore, R. E. and Paul, V. J. 1999. Lyngbyastatin 2 and norlyngbyastatin 2, analogues of dolastatin G and nordolastatin G from the marine cyanoacterium *Lyngbya majuscula*. J. Nat. Prod. 62: 1702–1706.

Luesch, H., Yoshida, W. Y., Moore, R. E. and Paul, V. J. 2000. Isolation and structure of the cytotoxin lyngbyabellin B and absolute configuration of lyngbyapeptin A from the marine cyanobacterium *Lyngbya majuscula*. J. Nat. Prod. 63: 1437–1439.

Luesch, H., Yoshida, W. Y., Moore, R. E. and Paul, V. J. 2002. Structurally diverse new alkaloids from Palauan collections of the apratoxin-producing marine cyanobacterium *Lyngbya* sp. Tetrahedron 58: 7959–7966.

Luesch, H., Yoshida, W. Y., Moore, R. E., Paul, V. J., and Mooberry, S. L. 2000. Isolation, structure determination, and biological activity of lyngbyabellin A from the marine cyanobacterium *Lyngbya majuscula*. J. Nat. Prod. 63: 611–615.

Luesch, H., Yoshida, W. Y., Moore, R. E., Paul, V. J., Mooberry, S. L., and Corbett, T. H. 2002. Symplostatin 3, a new dolastatin 10 analogue from the marine cyanobacterium *Symploca* sp. VP452. J. Nat. Prod. 65: 16–20.

Mander, L. N. 1994. Determination of enantiomer and diastereomer composition. In E. L. Eliel, S. H. Wilen, L. N. Mander (eds.), Stereochemistry of Organic Compounds, pp. 124–296. Toronto: John Wieley & Sons.

Marquez, B. and et al. 2002. Structure and absolute stereochemistry of hectochlorin, a potent stimulator of actin assembly. J. Nat. Prod. 65: 866–871.

Matsumori, N., Kaneno, D., Murata, M., Nakamura, H., and Tachibana, K. 1999. Stereochemical determination of acyclic structures based on carbon-proton spin coupling constants. A method of configuration analysis for natural products. J. Org. Chem. 64: 866–876.

McMillan, J. B., Ernst-Russell, M. A., Ropp, J. S., and Molinski, T. F. 2002. Lobocyclamides A–C, lipopeptides from a bryptic cyanobacterial mat containing *Lyngbya confervoides*. J. Org. Chem. 67: 8210–8215.

McPhail, K. L., Davies-Coleman, M. T., Copley, R. C. B., and Eggleston, D. S. 1999. New halogenated sesquiterpenes from south African specimens of the circumtropical sea hare *Aplysia dactylomela*. J. Nat. Prod. 62: 1618–1623.

McPhail, K. L., and Gerwick, W. H. 2003. Three new malyngamides from a Papua New Guinea collection of the marine cyanobacterium *Lyngbya majuscula*. J. Nat. Prod. 66: 132–135.

Mesguiche, V., Valls, R., Piovetti, L., and Peiffer, G. 1999. Characterization and synthesis of (–)-7-methoxydodec-4(*E*)-enoic acid, a novel fatty acid isolated from *Lyngbya majuscula*. Tetrahedron Lett. 40: 7473–7476.

Milligan, K. E., Márquez, B., Williamson, R. T., Devies-Coleman, M., and Gerwick, W. H. 2000. Two new malyngamides from a Madagascan *Lyngbya majuscula*. J. Nat. Prod. 63: 965–968.

Milligan, K. E., Marquez, B. L., Williamson, T. and Gerwick, W. H. 2000. Lyngbyabellin B, a toxic and antifungal secondary metabolite from the marine cyanobacterium *Lyngbya majuscula*. J. Nat. Prod. 63: 1440–1443.

Morris, D. G. 2001. Prochirality, enantiotopic and diastereotopic groups and faces: Use of NMR spectroscopy in stereochemistry. In Stereochemistry, pp. 139–160. Cambridge: The Royal Society of Chemistry.

Mutou, T., Kondo, T., Ojika, M., and Yamada, K. 1996. Isolation and stereostructueres of dolastatin G and nordolastatin G, cytotoxic 35-membered cyclodepsipeptides from the Japanese sea hare *Dolabella auricularia*. J. Org. Chem. 61: 6340–6345.

Mynderse, J. S. and Moore, R. E. 1978. Malyngamide D and E, two trans-7-methoxy-9-metylhexadec-4-enamides from a deep water variety of the marine cyanophyte *Lyngbya majuscula*. J. Org. Chem. 43(22): 4359–4363.

National Cancer Institute PDQ Clinical Trials Database. (n.d.). Available from: http://cancernet.nci.nih.gov/trialsrch.shtml [2005, January 10]

Neri, P., and Tringali, C. 2001. Applications of modern NMR techniques in the structural elucidation of bioactive natural products. In C. Tringali (ed.), Bioactive Compounds from Natural Sources, pp. 129–158. London: Taylor & Francis.

Nogle, L. M., and Gerwick, W. H. 2002. Isolation of four new cyclic depsipeptides, antanapeptins A–D, and dolastatin 16 from a Madagascan collection of *Lyngbya majuscula*. J. Nat. Prod. 65: 21–24.

Nogle, L. M., and Gerwick, W. H. 2003. Diverse secondary metabolites from a Puerto Rican collection of *Lyngbya majuscula*. J. Nat. Prod. 66: 217–220.

Nogle, L. M., Williamson, R. T., Gerwick, W. H. 2001. Somamides A and B, two new depsipeptide analogues of dolastatin 13 from a Fijian cyanobacterial assemblages of *Lyngbya majuscula* and *Schizothrix* species. J. Nat. Prod. 64: 716–719.

Oda, T., Crane, Z. D., Dicus, C. W., Sufi, B., A., and Bates, R. B. 2003. Dolastatin 11 connects two long-pitch strands in F-actin to stabilize microfilaments. J. Mol. Biol. 328: 319–324.

Ohtani, I., Kusumi, T., Kashman, Y., and Kakisawa, H. 1991. High-field FT NMR application of Mosher's method. The absolute configurations of mariene terpenoids. J. Am. Chem. Soc. 113: 4092–4096.

Oikawa, Y., Sugano, K., Yonemitsu, O. 1978. Meldrum's acid in organic synthesis. 2. A general and versatile synthesis of β-keto esters. J. Org. Chem. 43: 2087–2088.

Oikawa, Y., Yoshioka, T., Sugano, K, Yonemitsu, O. 1985. Methyl phenylacetylacetate from phenylacetyl chloride and Meldrum's acid. Org. Synth. 63: 359–361.

Ojika, M., Nagoya, T., and Yamada, K. 1995. Dolabelides A and B, cytotoxic 22-membered macrolides isolated from the sea hare *Dolabella auricularia*. Tetrahedron Lett. 36(41): 7491–7494.

Ojika, M., Nemoto, T., Nakamura, M., and Yamada, K. 1995. Dolastatin E, a new cyclic hexapeptide isolated from the sea hare *Dolabella auricularia*. Tetrahedron Lett. 36: 5057–5058.

Orjala, J., Nagle, D. and Gerwick, W. H. 1995. Malyngamide H, an ichthyotoxic amide possessing a new carbon skeleton from the Caribbean cyanobabterium *Lyngbya majuscula*. J. Nat. Prod. 58: 764–768.

Ortega, M. J., Zubía, E., and Salvá, J. 1997. New polyhalogenated monoterpenes from the sea hare *Aplysia punctata*. J. Nat. Prod. 60: 482–484.

Owens, P. K., Fell, A. F., Coleman, M. W., Berridge, J. C. 2000. Complexation of voriconazole stereoisomers with neutral and anionic dervatized cyclodextrins. J. Incl. Phenom. Macrocyclic. Chem. 38: 133–151.

Pardo, R. M., and Bock, M. G. 1983. (2*S*,3*S*,4*R*)-4-amino-3-hydroxy-2-methylpentanoic acid. Enantioselective synthesis of an amino acid constituent of bleomycin. Tetrahedron Lett. 24: 4805–4808.

Parker, D. 1991. NMR determination of enantiomeric purity. Chem. Rev. 91: 1441–1457.

Paik, S., Carmeli, S., Cullingham, J., Moore, R. E., Patterson, G. M. L., and Tius, M. A. 1994. Mirabimide E, an unusual *N*-acylpyrrolinone from the blue-green alga *Scytonema mirabile*: Structure determination and synthesis. J. Am. Chem. Soc. 116: 8116–8125.

Pawlik, J. R. 1993. Marine invertebrate chemical defenses. Chem. Rev. 93: 1911–1922.

Pechenik, J. A. 1993. The molluscs. In Biology of the Invertebrates 3 rd, Boston: Times Mirror Higeher Education Group, pp. 219-290.

Pennings, S. 1994. Interspecific variation in chemical defenses in the sea hares (Opisthobranchia: Anaspidea). J. Exp. Mar. Biol. Ecol. 180(2): 203–219.

Pettit, G. R., Flahive, E. J., Boyd, M. R., Bai, R., Hamel, E., Pettit, R. K., and Schmidt, J. M. 1998. Antineoplastic agents 360. Synthesis and cancer cell growth inhibitory studies of dolastatin 15 structural modifications. Anti-Cancer Drug Des. 13: 47–66.

Pettit, G. R., Kamano, Y., Brown, P., Gust, D., Inoue, M., and Heral, C. L. 1982. Structure of the cyclic peptide dolastatin 3 from *Dolabella auricularia*. J. Am. Chem. Soc. 104: 905–907.

Pettit, R. G., Kamano, Y., Fujii, Y., Herald, C. L., Inoue, M., Browns, P., Gust, D., Kitanara, K., Schmidt, J. M., Douber, D. L., and Michel, C. 1981. Marine animal biosynthetic constituents for cancer chemotherapy. J. Nat. Prod. 44(4): 482–485.

Pettit, G. R., Kamano, Y., Herald, C. L., Fujii, Y., Kizu, H., Boyd, M. R., Boettner, F. E., Doubek, D. L., Schmidt, J. M., Chapuis, J.-C., and Michel, C. 1993. Isolation of dolastatin 10-15 from the marine mollusc *Dolabella auricularia*. Tetrahedron 49(41): 9151–9170.

Pettit, G. R., Kamano, Y., Herald, C. L., Tuinman, A. A., Bottener, F. E., Kizu, H., Schmidt, J. M., Baczynskyj, L., Tomer, K. B., and Bontems, R. J. 1987. The isolation and structure of a remarkable marine animal antineoplastic constituent: dolastatin 10. J. Am. Chem. Soc. 109: 6883–6885.

Pettit, G. R., Singh, S. B., Hogan, F., Iloyd-Williams, P., Herald, D. L., Burkett, D. D., and Clewlow, P. J. 1989. J. Am. Chem. Soc. 111: 5463–5465.

Pettit, G. R., Srirangam, J. K., Barkoczy, J., Williams, M. D., Boyd, M. R., Hamel, E., Pettit, R. K., Hogan, F., Bai, R., Chapuis, J.-C., McAllister, S. C., and Schmidt, J. M. 1998. Antineoplastic agents 365: Dolastatin 10 SAR probes. Anti-Cancer Drug Des. 13: 243–277.

Pettit, G. R., Xu, J.-P., Hogan, F., and Cerny, R. L. 1998. Isolation and structure of dolastatin 17. Heterocycles 47(1): 491–496.

Pettit, G. R., Xu, J.-P., Doubek, D. L., Chapuis, J.-C., and Schmidt, J. M. 2004. Antineoplastic agents. 510. Isolation and structure of dolastatin 19 from the Gulf of California sea hare *Dolabella auricularia*. J. Nat. Prod. 67(8): 1252–1255.

Pettit, G. R., Xu, J.-P., Hogans, F., Williams, M. D., Doubek, D. L., Schmidt, J. M., Cerny, R. L., and Boyd, M. R. 1997. Isolation and structure of the human cancer cell growth inhibitory cyclodepsipeptide dolastatin 16. J. Nat. Prod. 60: 752–754.

Pettit, G. R., Xu, J.-P., Williams, M. D., Hogan, F., and Schmidt, J. M. 1997. Antineoplastic aents 370. Isolation and structure of dolastatin 18. Bioorg. Med. Chem. Lett. 7(7): 827–832.

Pirkle, W. H., and Beare, S. D. 1969. Optically active solvents in nuclear magnetic resonance spectroscopy. IX. Direct determinations of optical purities and correlations of absolute configurations of α-amino acids. J. Am. Chem. Soc. 91: 5150–5155.

Pirkle, W. H., and Boeder, C. W. 1977. Estimation of allene optical purities by nuclear magnetic resonance. J. Org. Chem. 42: 3697–3700.

Poncet, J., Busquet, M., Roux, F., Pierré, A., Atasii, G., and Jouin, P. 1998. Synthesis and biological activity of chimeric structures derived from the cytotoxic natural compounds dolastatin 10 and dolastatin 15. J. Med. Chem. 41: 1542–1530.

Porto, S., Duran, J., Seco, J. M., Quiñoá, E., and Riguera, R. 2003. "Mix and shake" method for configurational assignment by NMR: application to chiral amines and alcohols. Org. Lett. 5: 2979–2982.

Praud, A., Valls, R., Piovetti, L., and Banaigs, B. 1993. Malyngamide G: proposition de structure pour un nouvel amide chloré d'une algue bleu-verte epiphyte de Cystoseira crinita. Tetrahedron Lett. 34: 5437–5440.

Prince, J., Nolen, T. G., and Coelho, L. 1998. Defensive ink pigment prcessing and secretion in *Aplysia californica*: concentration and storage of phycoerythrobilin in the ink gland. J. Exp. Biol. 201: 1595–1613.

Raillard, S. P., Chen, W., Sullivan, E., Bajjalieh, W., Bhandari, A., and Baer, T. A. 2002. Preparation and improved stability of *N*-Boc-α-amino-5-acyl Meldrum's acids, a versatile class of building blocks for combinatorial chemistry. J. Comb. Chem. 4: 470–474.

Royles, B. J. 1995. Naturally occurring tetramic acids: structures, isolation, and synthesis. Chem. Rev. 95: 1981–2001.

Satitpatipan, V., and Suwanborirux, K. 2004. New nitrogenous germacranes from a Thai marine sponge, *Axinyssa* n. sp. J. Nat. Prod. 67: 503–505.

Sea Slug Forum Database. (n.d.). Available from: http://www.seaslugforum.net/[2005, January 10]

Seco, J. M., Quiñoá, E., and Riguera, R. 1999a. 9–anthrylmethoxyacetic acid esterification shifts-correlation with the absolute stereochemistry of secondary alcohols. Tetrahedron 55: 569–584.

Seco, J. M., Quiñá, E., and Riguera, R. 1999b. Boc–phenylglycine: the reagent of choice for the assignment of the absolute configuration of α–chiral primary amines by ^{1}H NMR spcetroscopy. J. Org. Chem. 64: 4669–4675.

Seco, J. M., Quiñoá, E., and Riguera, R. 2001. A practical guide for the assignment of the absolute configuration of alcohols, amines and carboxylic acids by NMR. Tetrahedron: Asymmetry 12: 2915–2925.

Seenaga, K., Nagoya, T., Shibata, T., Kigoshi, H., and Yamada, K. 1997. Dolabelides C and D, cytotoxic macrolides isolated from the sea hare *Dolabella auricularia*. J. Nat. Prod. 60: 155–157.

Skehan, P., Storeng, R., Scudiero, D., Monks, A., McMahon, J., Vistica, D., Warren, J. T., Bokesch, H., Kenney, S., and Boyed, M. R. 1990. New colorimetric cytotoxicity assay for anticancer-drug screening. J. Natl. Cancer Inst. 82: 1107–1112.

Sodano, G., and Spinella, A. 1986. Janolusimide, a lipophilic tripeptide toxin from the nudibranch mollusc *Janolus cristatus*. Tetrahedron Lett. 27: 2505–2508.

Sone, H., Kigoshi, H., and Yamada, K. 1996. Aurisides A and B, cytotoxic macrolide glycosides from the Japanese sea hare *Dolabella auricularia*. J. Org. Chem. 61: 8956–8960.

Sone, H., Kigoshi, H., and Yamada, K. 1997. Isolation and stereostructure of dolastatin I, a cytotoxic cyclic hexapeptide from the Japanese sea hare *Dolabella auricularia*. Tetrahedron 53 (24): 8149–8154.

Sone, H., Kondo, T., Kiryu, M., Ishiwata, H., Ojika, M., Yamada, K. 1995. Dolabellin, a cytotoxic bisthiazole metabolite from the sea hare *Dolabella auricularia*: structural determination and synthesis. J. Org. Chem. 60: 4774–4781.

Sone, H., Nemoto, T., Ishiwata, H., Ojika, M., and Yamada, K. 1993. Isolation, structure, and synthesis of dolastatin D, a cytotoxic cyclic depsipeptide from the sea hare *Dolabella auricularia*. Tetrahedron Lett. 34(52): 8449–8452.

Sone, H., Nemoto, T., Ojika, M., and Yamada, K. 1993. Isolation, structure, and synthesis of dolastatin C, a new depsipeptide from the sea hare *Dolabella auricularia*. Tetrahedron Lett. 34(52): 8445–8448.

Sone, H., Shibata, T., Fujita, T., Ojika, M., and Yamada, K. 1996. Dolastatin H and Isodolastatin H, potent cytotoxic peptides from the sea hare *Dolabella auricularia*: isolation, stereostructures, and synthesis. J. Am. Chem. Soc. 118: 1874–1880.

Spinella, A., Zubía, E., MartÎnez, E., Ortea, J., and Cimio, G. 1997. Structure and stereochemistry of aplyolides A–E, lactonized dihydroxy fatty acids from the skin of the marine mollusk *Aplysia depilans*. J. Org. Chem. 62: 5471–5475.

Stallard, M. O. and Faulkner, D. J. 1974. Chemical constituents of the digestive gland of the sea hare *Aplysia californica*–I. Importance of diet. Comp. Biochem. Physiol. 47B: 25–35.

Stipanovic, R., McCormick, J. P., Schlemper, E. O., Hamper, B. C., Shinmyozu, T., and Pirkle, W. H. 1986. Corroboration of techniques for assigning absolute configuration: lacinilene C methyl ether as an exemplary study. J. Org. Chem. 51: 2500–2504.

Suenaga, K., Mutou, T., Shibata, T., Itoh, T., Fujita, T., Takada, N., Hayamizu, K., Takagi, M., Irifune, T., Kigoshi, H., and Yamada, K. 2004. Auriride, a cytotoxic depsipeptide from the sea hare *Dolabella auricularia*: isolation, structure determination, synthesis, and biological activity. Tetrahedron 60: 8509–8527.

Suenaga, K., Shibata, T., Takada, N., Kigoshi, H., and Yamada, K. 1998. Aurilol, a cytotoxic bromotriterpenes isolated from the sea hare *Dolabella auricularia*. J. Nat. Prod. 61: 515–518.

Suwanborirux, K., Charupant, K., Amnuoypol, S., Pummangura, S., Kubo, A., Saito, N. 2002. Ecteinascidins 770 and 786 from the Thai tunicate *Ecteinascidia thurstoni*. J. Nat. Prod. 65(6): 935–937.

Swennen, C.; Moolenbeek, R. G.; Ruttanadakul, N.; Hobbleink, H.; Dekker, H.; Hajisamae, S., Eds. 2001. The Molluscs of the Southern Gulf of Thailand, p. 140. Bangkok: Biodiversity Research and Training Program.

Takahashi, H., N., Iwashima, M., and Iguchi, K. 1999. Determination of absolute configurations of β– or γ–methyl substituted secondary alcohols by NMR spectroscopy. Tetrahedron Lett. 40: 333–336.

Takahashi, H., Kato, N., Iwashima, M., and Iguchi, K. 1999. Determination of absolute configurations of tertiary alcohols by NMR spectroscopy. Chem. Lett. 1181–1182.

Takeuchi, Y., Itoh, N., and Koizumi, T. 1992. The remarkably high reactivity of α–cyano–α–fluorophenylacetyl chloride (CFPA–Cl) towards hindered nucleophiles in enantiomeric excess determination. J. Chem. Soc. Chem. Commun. 1514–1515.

Takeuchi, Y., Konishi, M., Hori, H., Takahashi, T., Kometani, T., and Kirk, K. L. 1998. Efficient synthesis of a new, highly versatile chiral derivatizing agent, α–cyano–α–fluorophenylacetyl acid (CFTA). Chem. Commun. 365–366.

Tan, L. T., Okino, T., and Gerwick, W. H. 2000. Hermitamides A and B, toxic malyngamide-type natural products from the marine cynanobacterium *Lyngbya majuscula*. J. Nat. Prod. 63: 952–955.

Todd, J. S. and Gerwick, W. H. 1995. Malyngamide I from the tropical marine cyanobacterium *Lyngbya majuscula* and the probable structure revision of stylocheilamide. Tetrahedron Lett. 36(43): 7837–7840.

Trager, W., Jensen, J. B. 1976. Human malaria parasites in continuous culture. Science 193: 673–675.

Ubutaka, M., Cheng, X.-C., Isobe, M., and Isono, K. 993. Absolute configuration of tautomycin, a protein phosphatase inhibitors from a *Streptomycete*. J. Chem. Soc. Perkin Trans. 1, 617–624.

Wan, F. and Erickson, K. L. 1999. Serinol-derived malyngamides from an Australian cyanobacterium. J. Nat. Prod. 62: 1696–1699.

Wenzel, T. J., and Wilcox, J. D. 2003. Chiral reagents for the determination of enantiomeric excess and absolute configuration using NMR spectroscopy. Chirality 15: 256–270.

Wessels, M., Kong, G. M., and Wright, A. D. 2000. New natural product isolation and comparison of the secondary metabolite content of three distinct samples of the sea hare *Aplysia dactylomela* from Tenerife. J. Nat. Prod. 63: 920–928.

Williams, P. G., Luesch, H., Yoshida, W. Y., Moore, R. E. and Paul, V. J. 2003. Continuing studies on the cyanobacterium *Lyngbya* sp.: isolation and structure determination of 15-norlyngbyapeptin A and lyngbyabellin D. J. Nat. Prod. 66: 595–598.

Williams, P. G., Moore, R. E., and Paul, V. J. 2003. Isolation and structure determination of lyngbyastatin 3, a lyngbyastatin 1 homologue from the marine cyanobacterium *lyngbya majuscula*. Determination of the configuration of the 4-amino-2,2-dimethyl-3-oxopentanoic acid unit in majusculamide C, dolastatin 12, lyngbyastatin 1, and lyngbyastatin 3 from cyanobacteria. J. Nat. Prod. 66: 1356–1363.

Williams, P. G., Yoshida, W. Y., Moore, R. E., and Paul, V. J. 2003. Tasipeptins A and B: new cytotoxic depsipeptides from the marine cyanobacterium *Symploca* sp. J. Nat. Prod. 66: 620–624.

Williams, P. G., Yoshida, W. Y., Quon, M. K., Moore, R. E., and Paul, V. J. 2003. The structure of Palau'amide, a potent cytotoxin from a species of the marine cyanobacterium *Lyngbya*. J. Nat. Prod. 66: 1545–1549.

Williamson, R. T., Boulanger, A., Vulpanovici, A., Roberts, M. A., and Gerwick, W. H. 2002. Structure and absolute stereochemistry of phormidolide, a new toxic metabolite from the marine cyanobacterium *Phormidium* sp. J. Org. Chem. 67: 7927–7936.

Wu, M., Milligan, K. E., and Gerwick, W. H. 1997. Three new malyngamides from the marine cyanobacterium *Lyngbya majuscula*. Tetrahedron 53: 15983–15990.

Yabuchi, T., Kusumi, T. 2000. Phenylglycine and methyl ester, a useful tool for absolute configuration determination of various chiral carboxylic acid. J. Org. Chem. 65: 397–404.

Yamada, T., Iritani, M., Doi, M., Minoura, K., Ito, T., and Numata, A. 2001. Absolute stereocstructures of cell-adhesion inhibitors, macrosphelides C, E–G and I, produced by a *Periconia* species separeated from an *Aplysia* sea hare. J. Chem. Soc., Perkin Trans. 1: 3046–3053.

Yamada, T., Ojika, M., Ishigaki, T., and Yoshida, Y. 1993. Aplyronine A, a potent antitumor substance, and the congeners aplyronines B and C isolated from the sea hare *Aplysia kurodai*. J. Am. Chem. Soc. 115: 11020–11021.

Yamada, S., Setsuko, Y., and Matsuda, K. 2002. *N*-acylation of amides with acid anhydrides by way of dual activation using $MgBr_2.OEt_2$. Tetrahedron Lett. 43: 647–651.

Yamazaki, M., Tansho, S., Kisugi, J., Muramoto, K., and Kamiya, H. 1989. Purification and characterization of a cytolytic protein from purple fluid of the sea hare *Dolabella auricularia*. Chem. Pharm. Bull. 37(8): 2179–2182.

สถาบันวิทยบริการ
จุฬาลงกรณ์มหาวิทยาลัย

APPENDIX

สถาบันวิทยบริการ
จุฬาลงกรณ์มหาวิทยาลัย

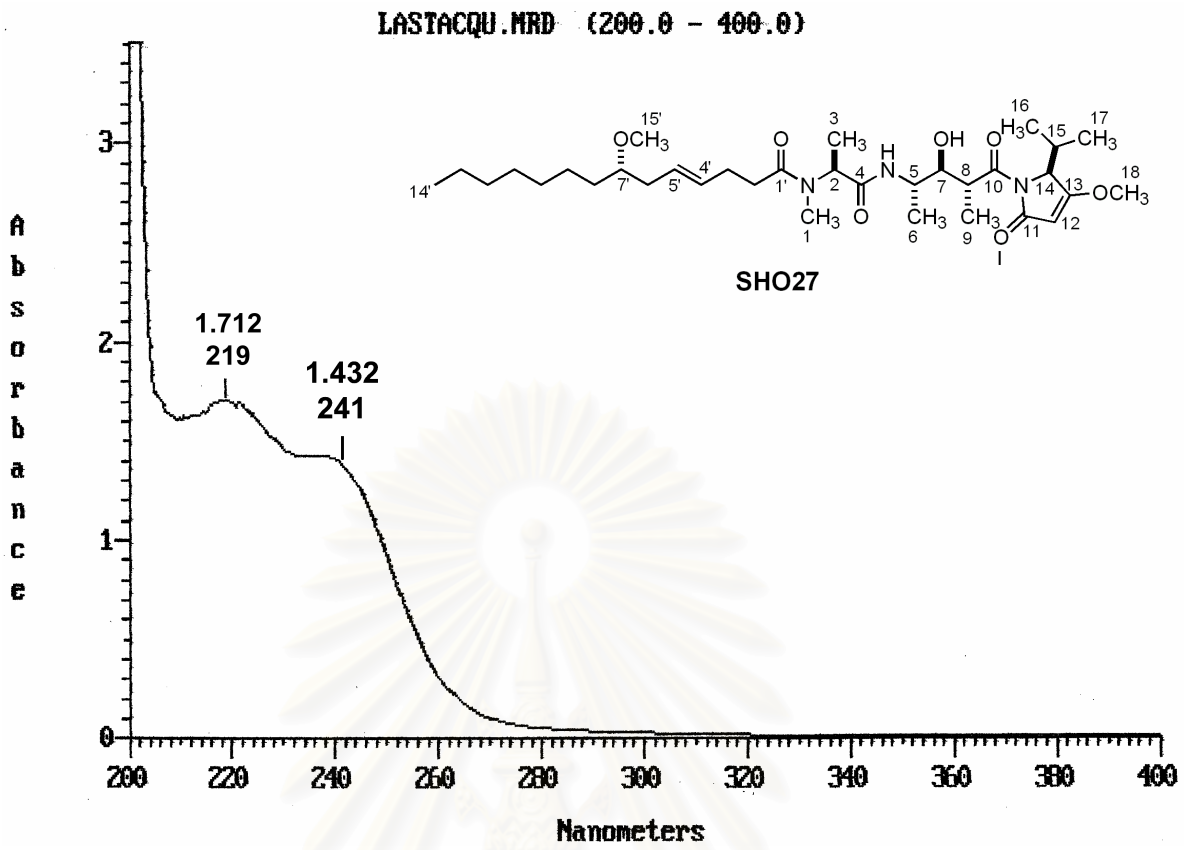

Figure 44 The UV spectrum of malyngamide X [**SHO27**] in methanol.

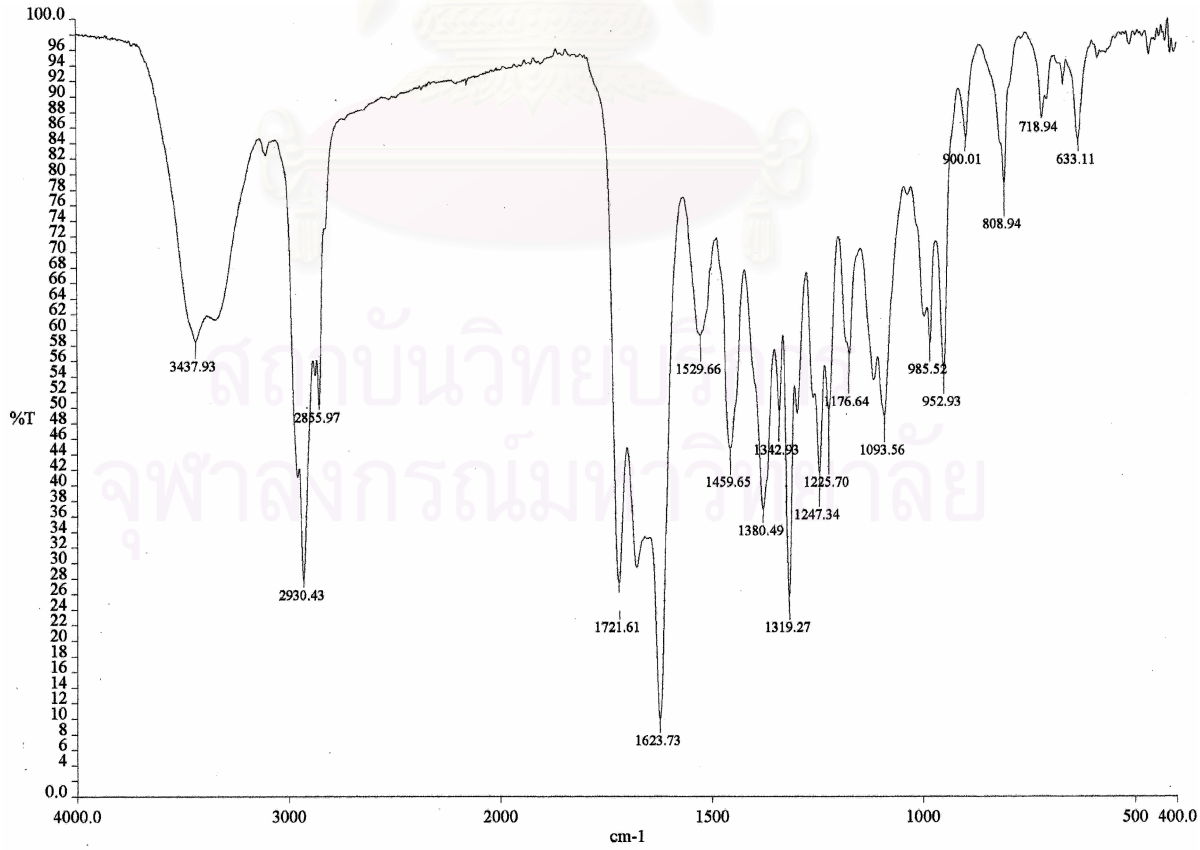

Figure 45. The IR spectrum (Film) of malyngamide X [**SHO27**].

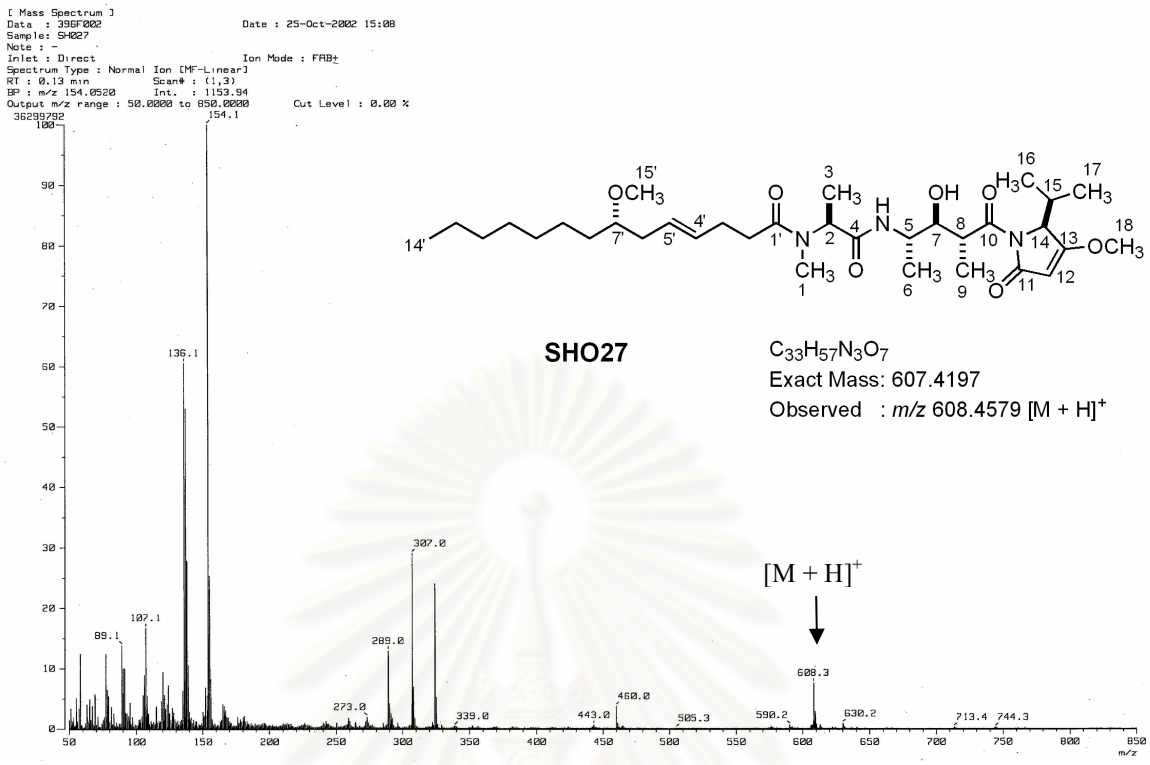

Figure 46. The FAB MS spectrum of malyngamdie X [**SHO27**].

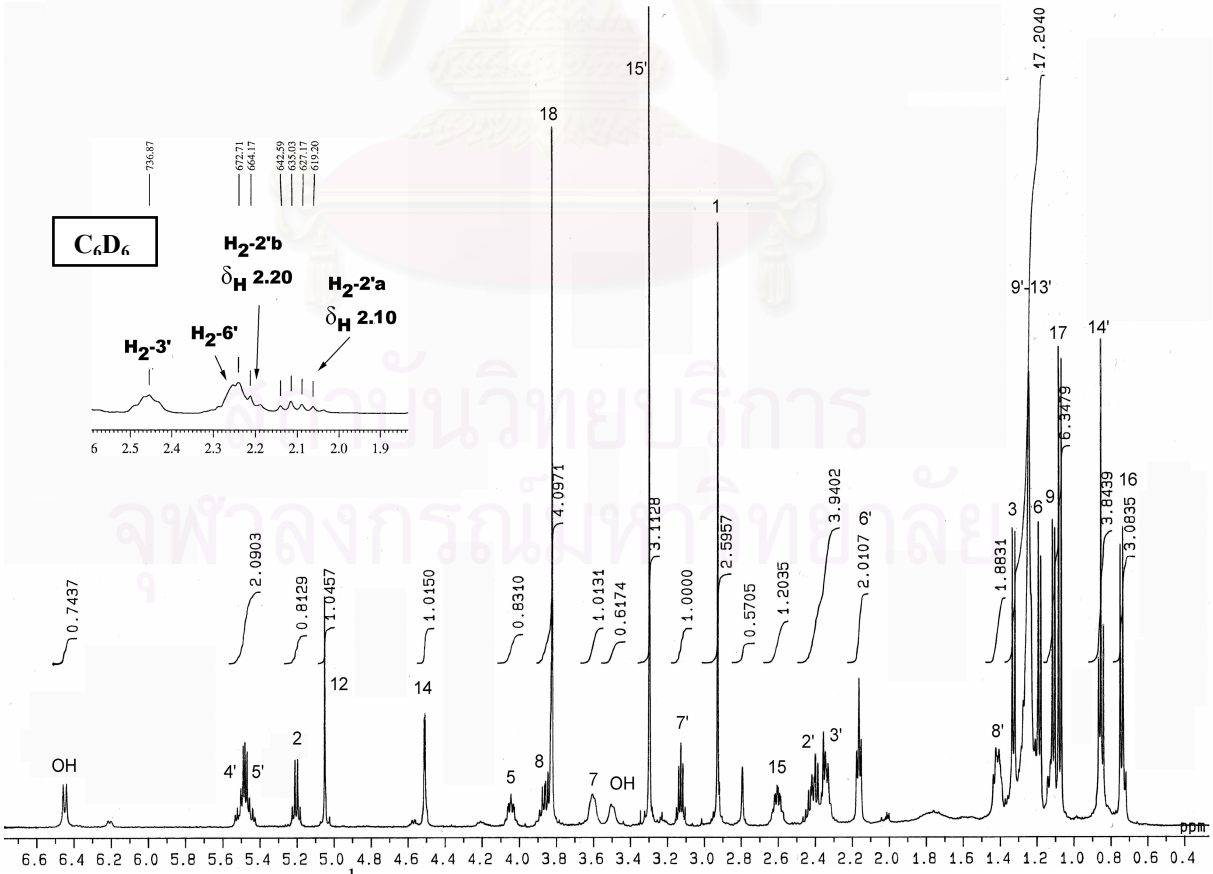

Figure 47. The 500 MHz ^{1}H NMR spectrum of malyngamide X [**SHO27**] in $CDCl_3$ and in C_6D_6 (expanded δ_H 1.9 – 2.6 ppm).

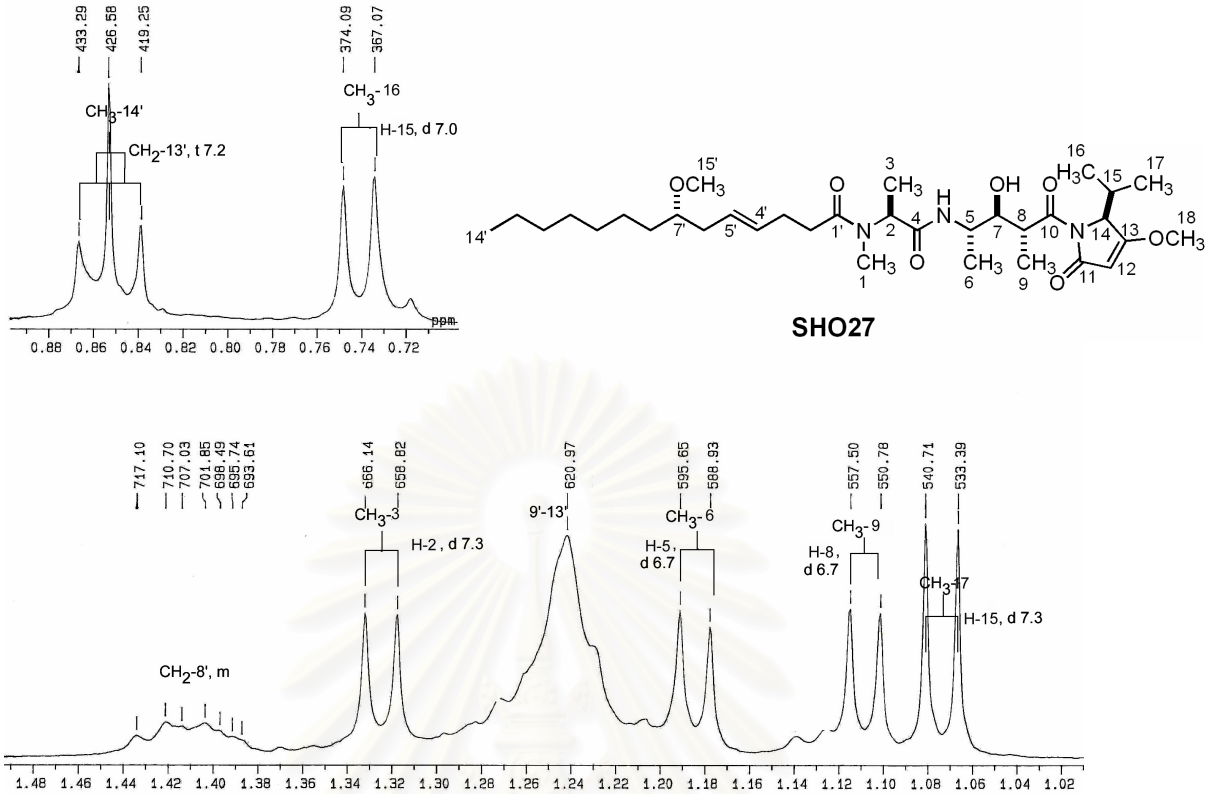

Figure 48. The 500 MHz coupling patterns of malyngamide X [**SHO27**] in $CDCl_3$ (expanded δ_H 0.60–1.50 ppm).

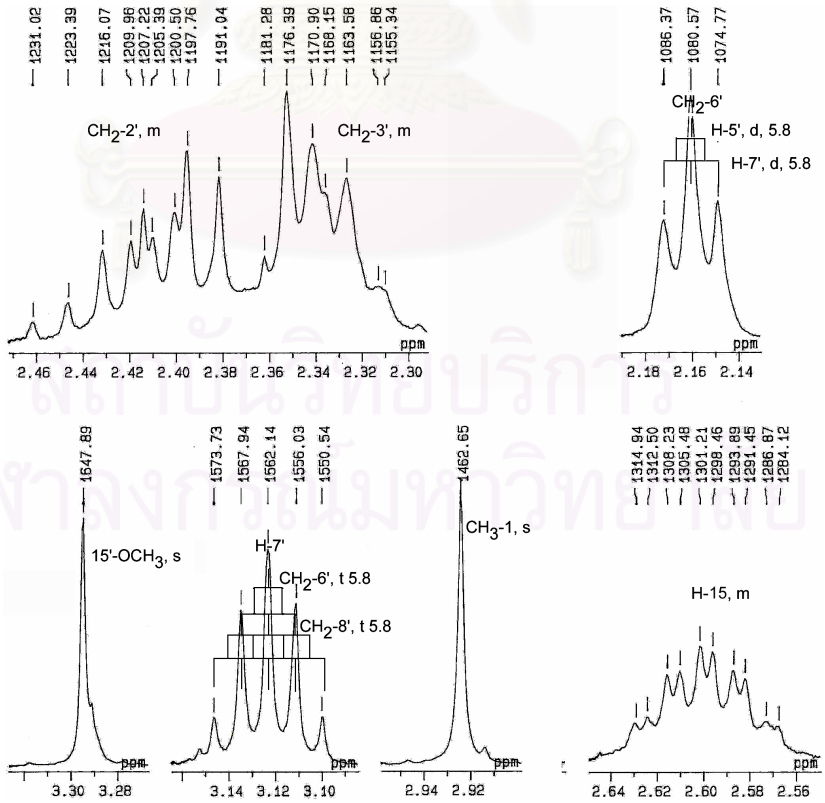

Figure 49. The 500 MHz coupling patterns of malyngamide X [**SHO27**] in $CDCl_3$ (expanded δ_H 2.00–3.50 ppm).

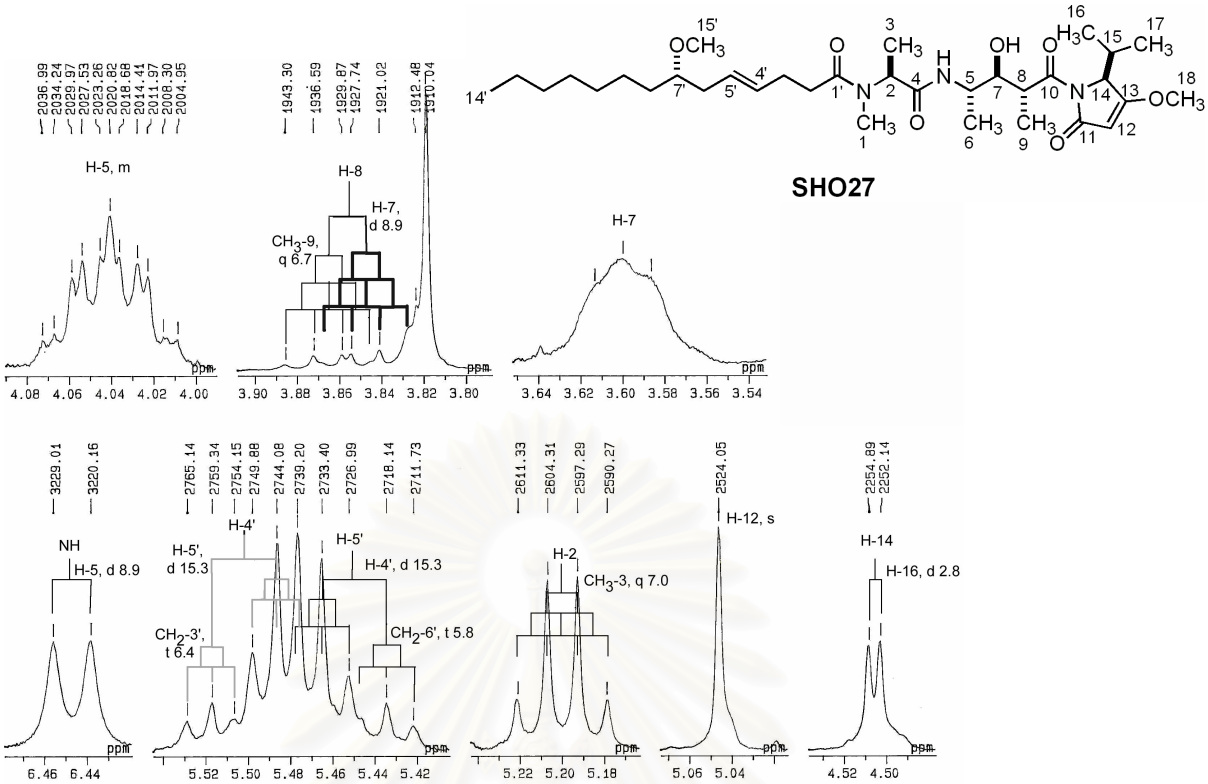

Figure 50. The 500 MHz coupling patterns of malyngamide X [**SHO27**] in $CDCl_3$ (expanded δ_H 3.60–6.50 ppm).

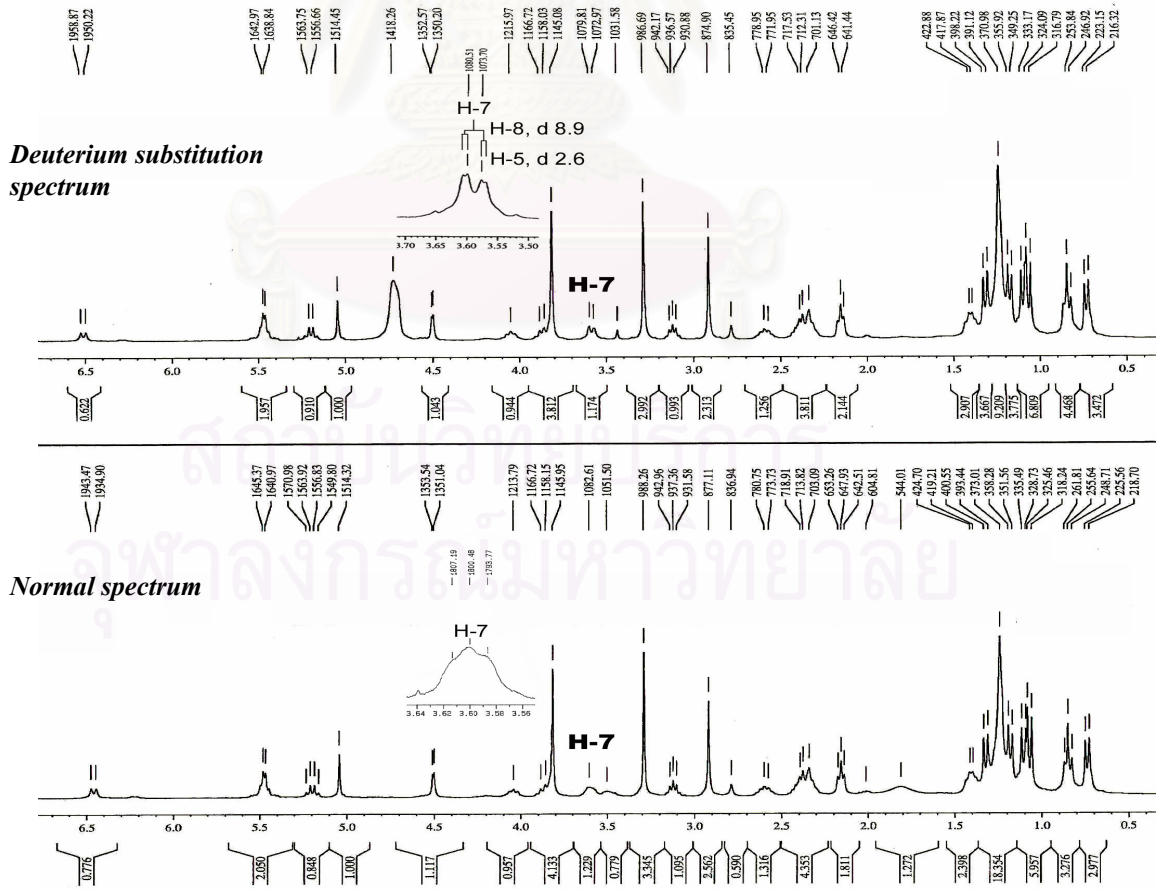

Figure 51. The 300 MHz ^{1}H NMR spectrum of malyngamide X [**SHO27**] in D_2O exchangeable experiment showing $^3J_{H\text{-}7,H\text{-}8}$ = 8.9 Hz and $^3J_{H\text{-}7,H\text{-}5}$ = 2.6 Hz.

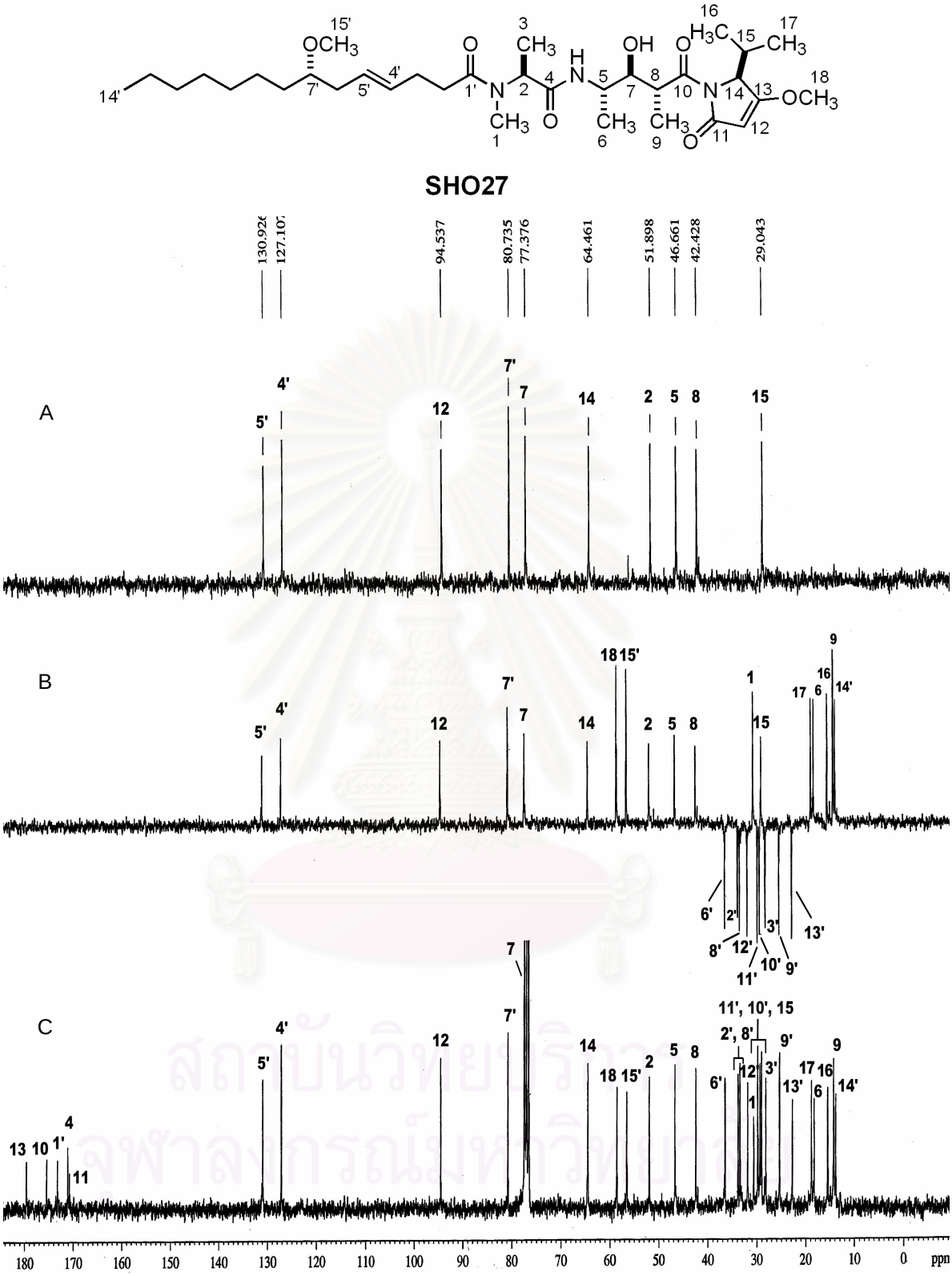

Figure 52. The 75 MHz (A) DEPT-90, (B) DEPT-135, and (C) ^{13}C NMR spectrum of malyngamide X [**SHO27**] in $CDCl_3$.

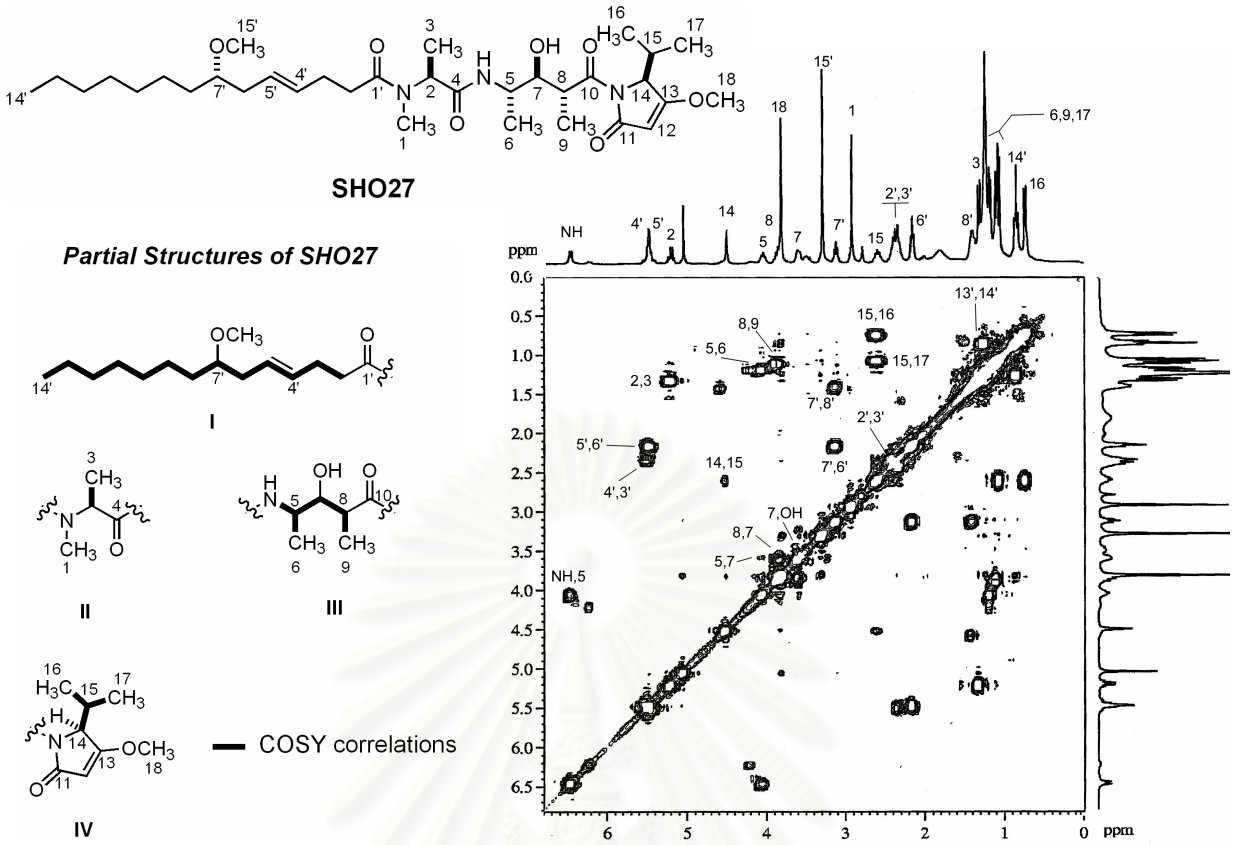

Figure 53. The 300 MHz H, H COSY spectrum of malyngamide X [**SHO27**] in $CDCl_3$.

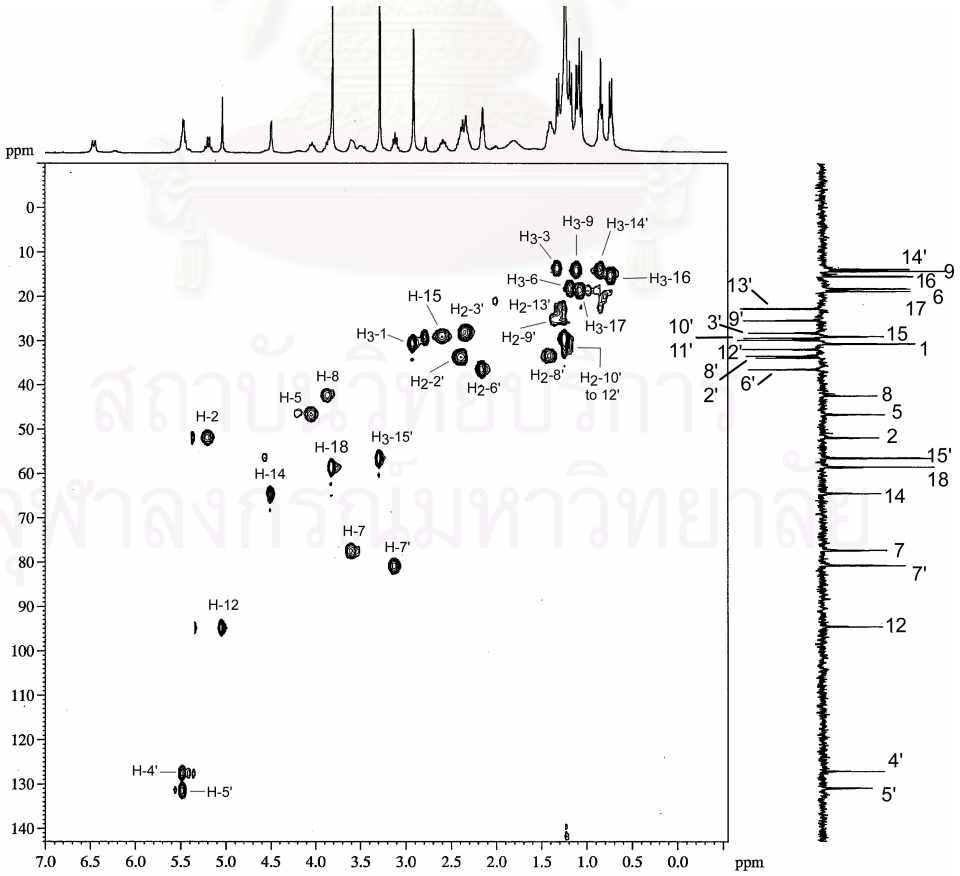

Figure 54. The 300 MHz HMQC spectrum of malyngamide X [**SHO27**] in $CDCl_3$.

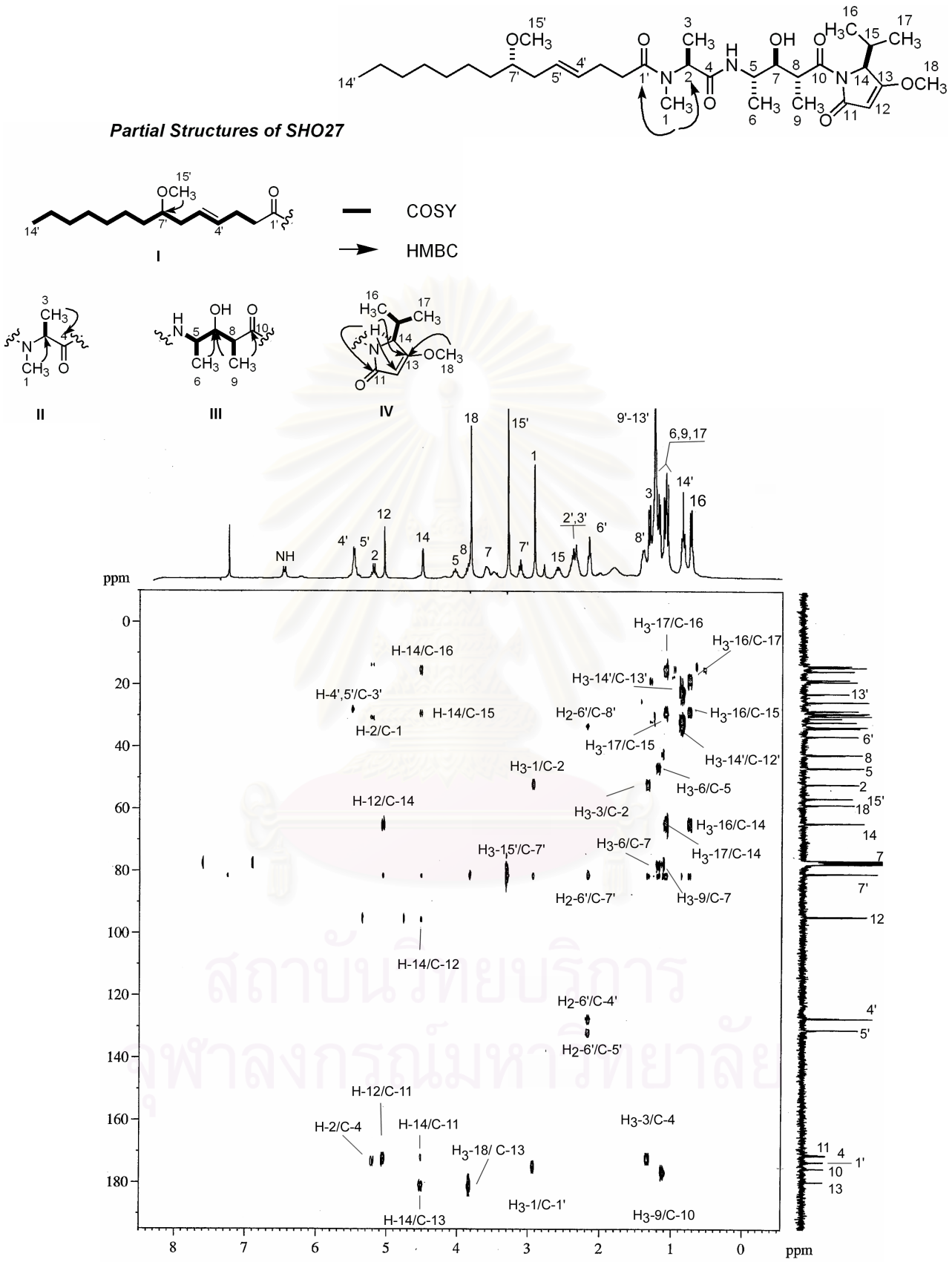

Figure 55. The 300 MHz HMBC spectrum ($^{n}J_{CH}$ = 8 Hz) of malyngamide X [**SHO27**] in $CDCl_3$.

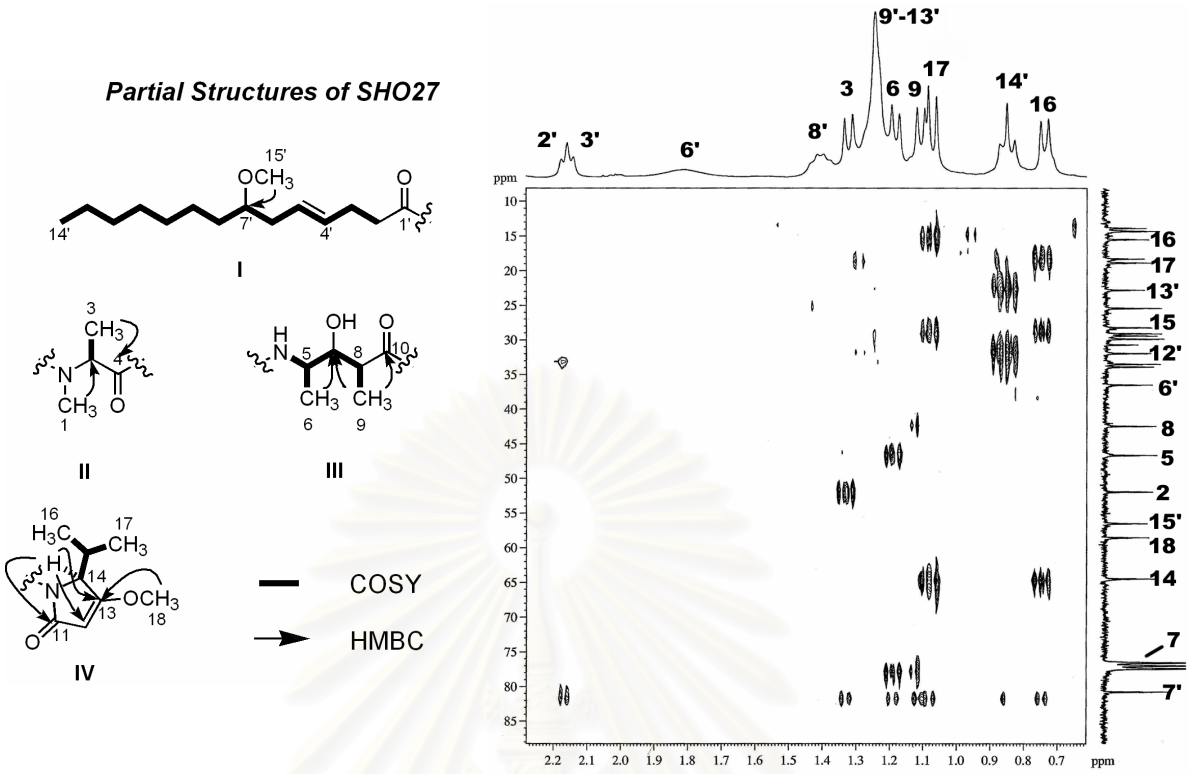

Figure 56. The 300 MHz HMBC spectrum ($^{n}J_{CH}$ = 8 Hz) of malyngamide X [**SHO27**] in $CDCl_3$ (expanded δ_H 3.60–6.50 ppm. and δ_C 15.0–85.0).

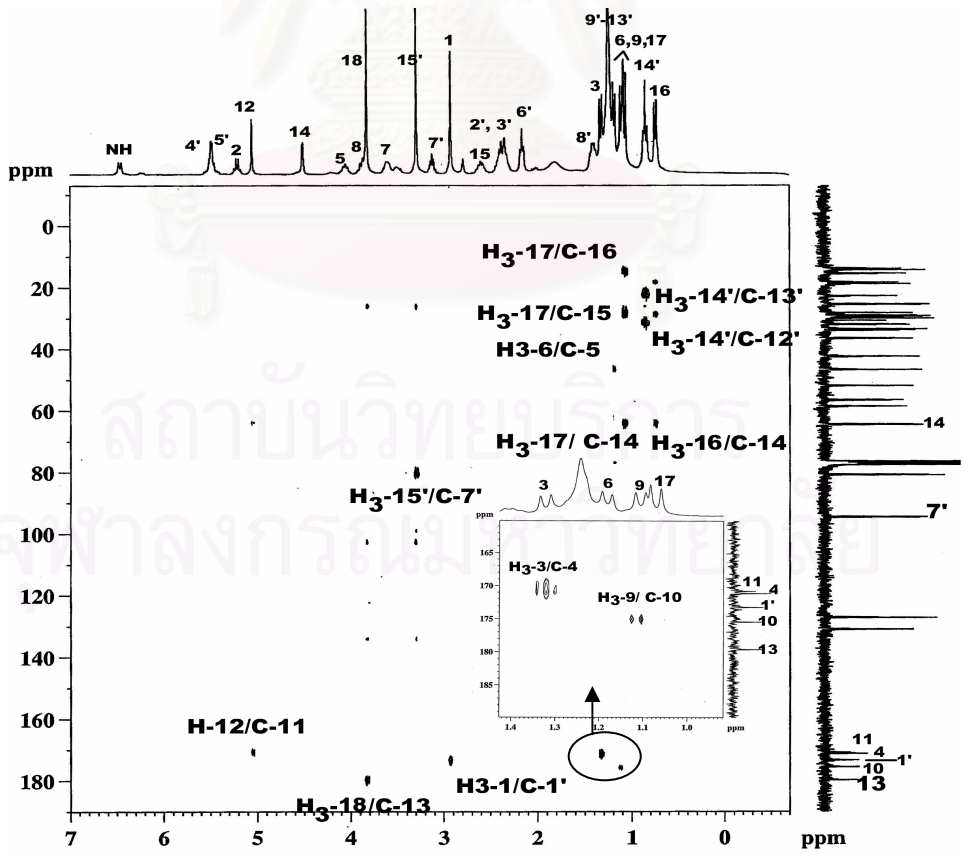

Figure 57. The 300 MHz HMBC spectrum ($^{n}J_{CH}$ = 4 Hz) of malyngamide X [**SHO27**] in $CDCl_3$.

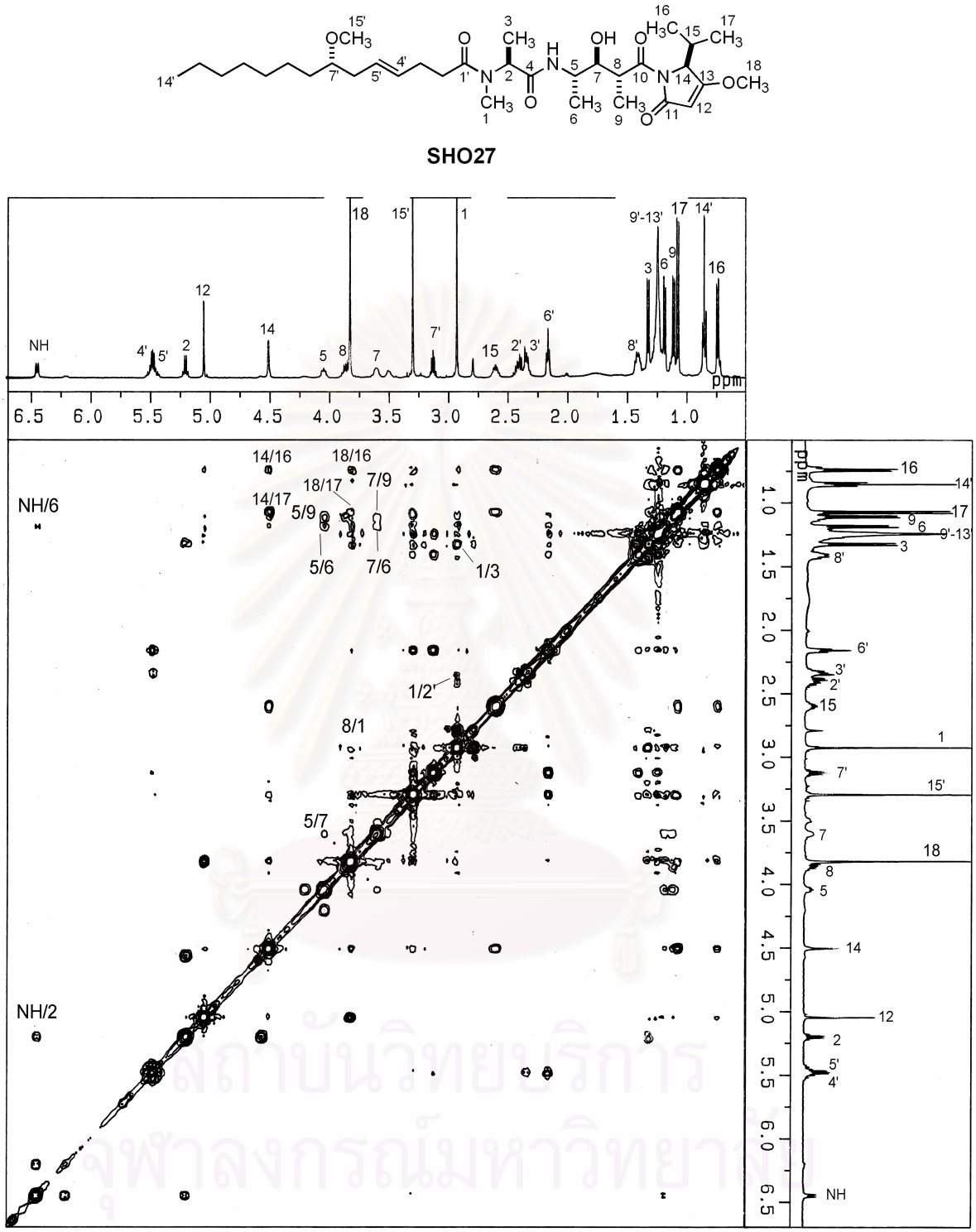

Figure 58. The 500 MHz NOESY spectrum of malyngamide X [**SHO27**] in $CDCl_3$.

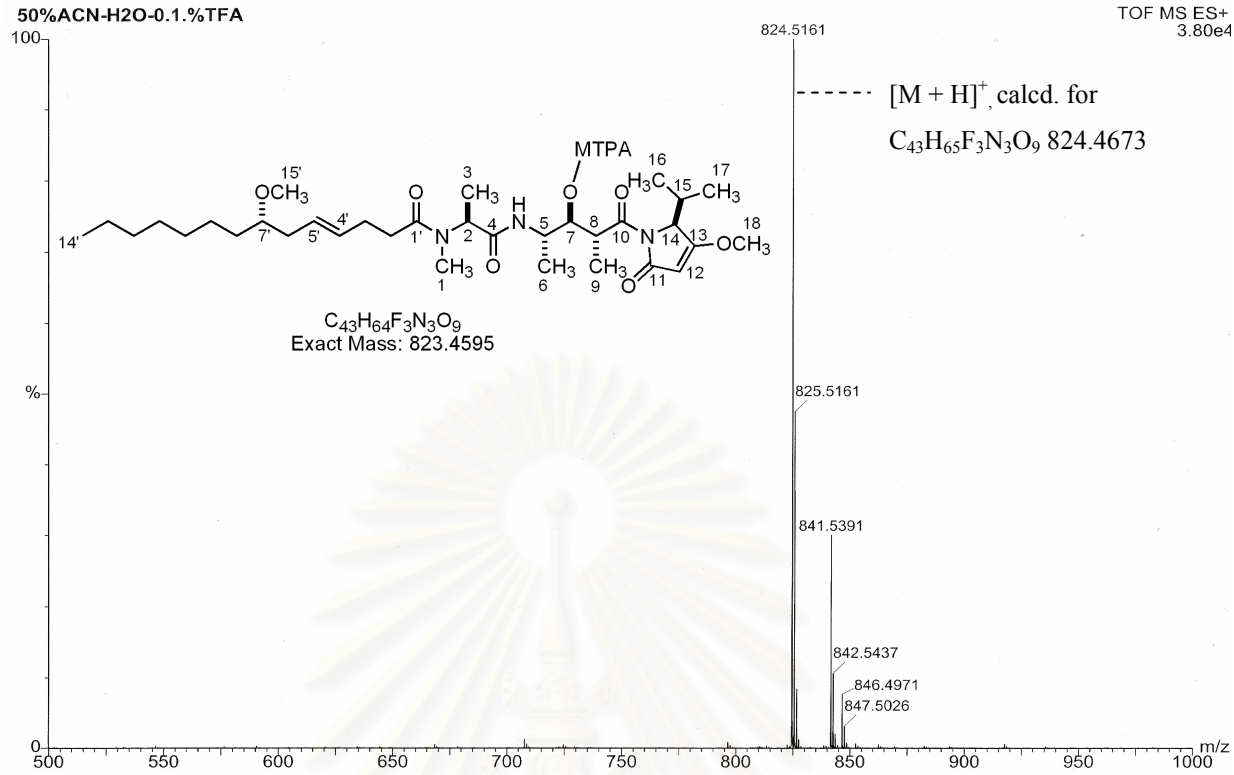

Figure 59. The ESITOF MS spectrum of 7-*O*-(*R*)-(+)-MTPA ester of malyngamide X [**SHO27a**] in $CDCl_3$.

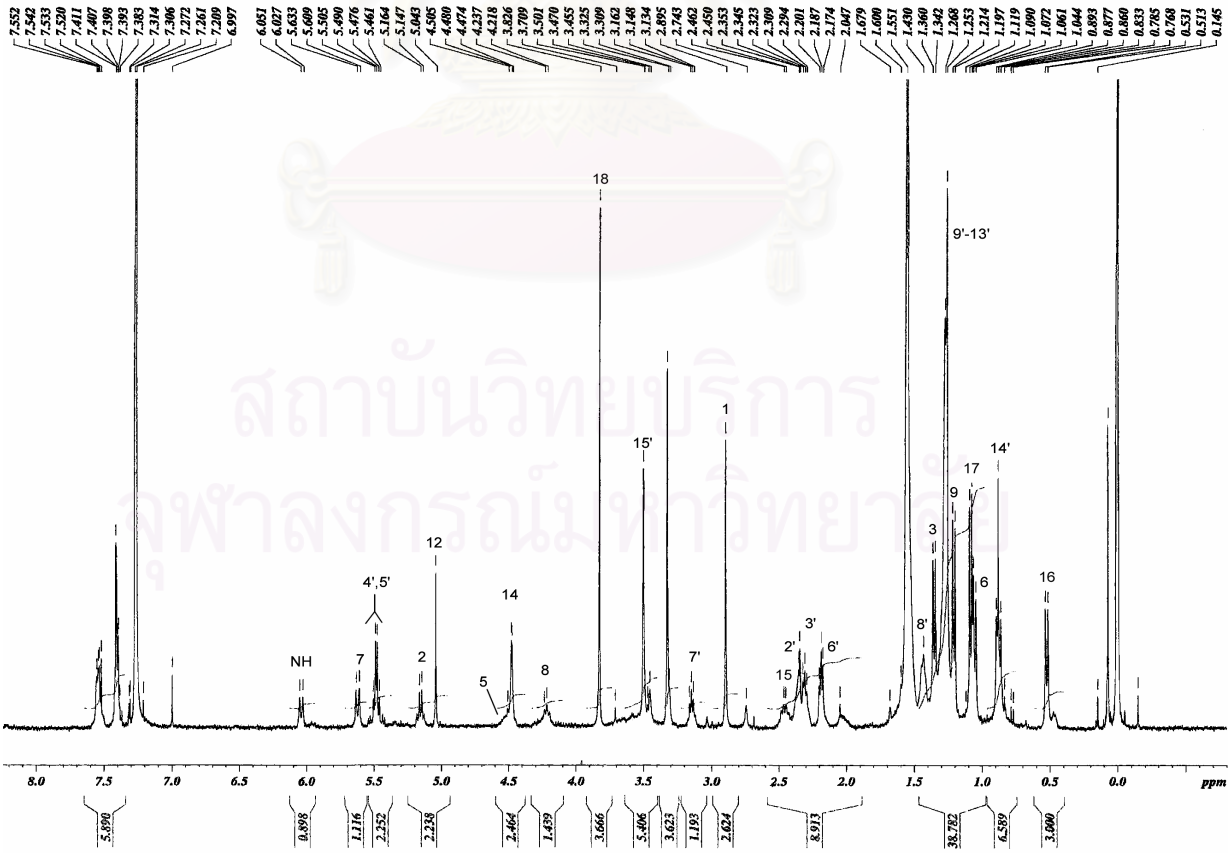

Figure 60. The 600 MHz ^{1}H NMR spectrum of 7-*O*-(*R*)-(+)-MTPA ester of malyngamide X [**SHO27a**] in $CDCl_3$.

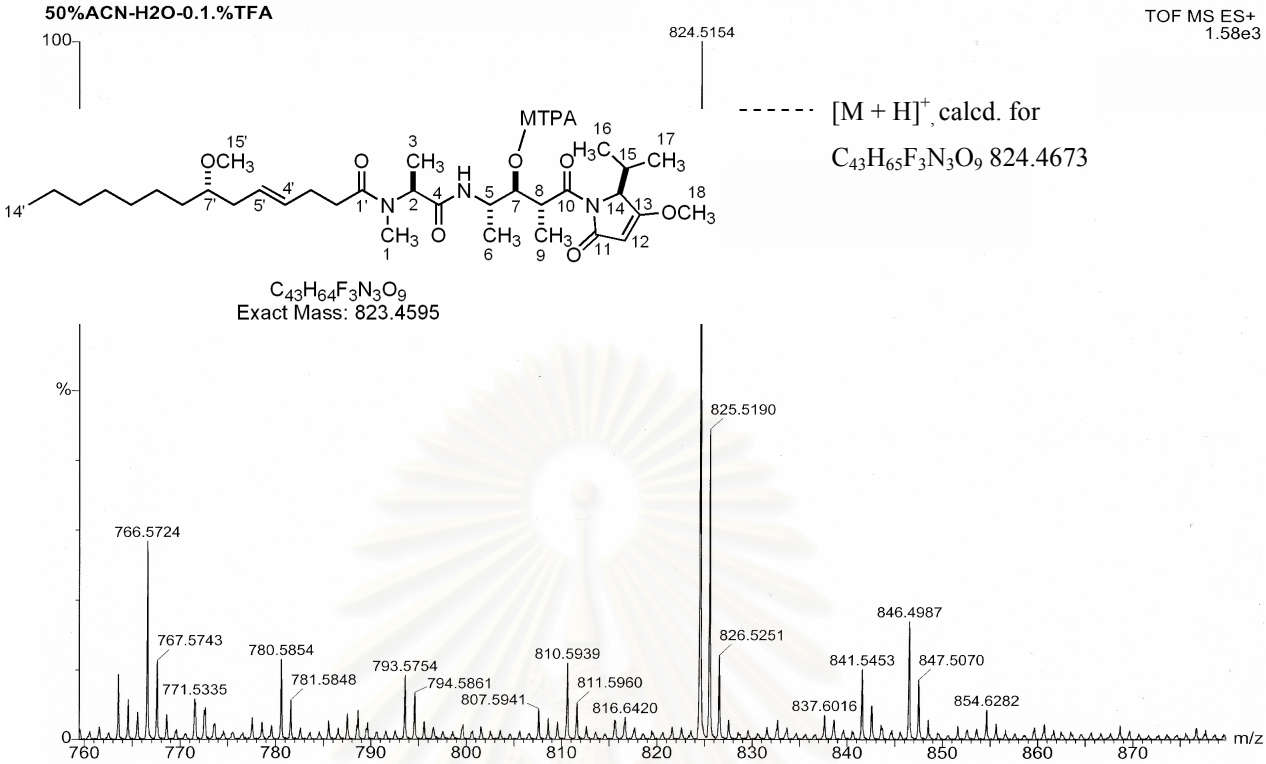

Figure 61. The ESITOF MS spectrum of 7-*O*-(*S*)-(−)-MTPA ester of malyngamide X [**SHO27b**] in $CDCl_3$.

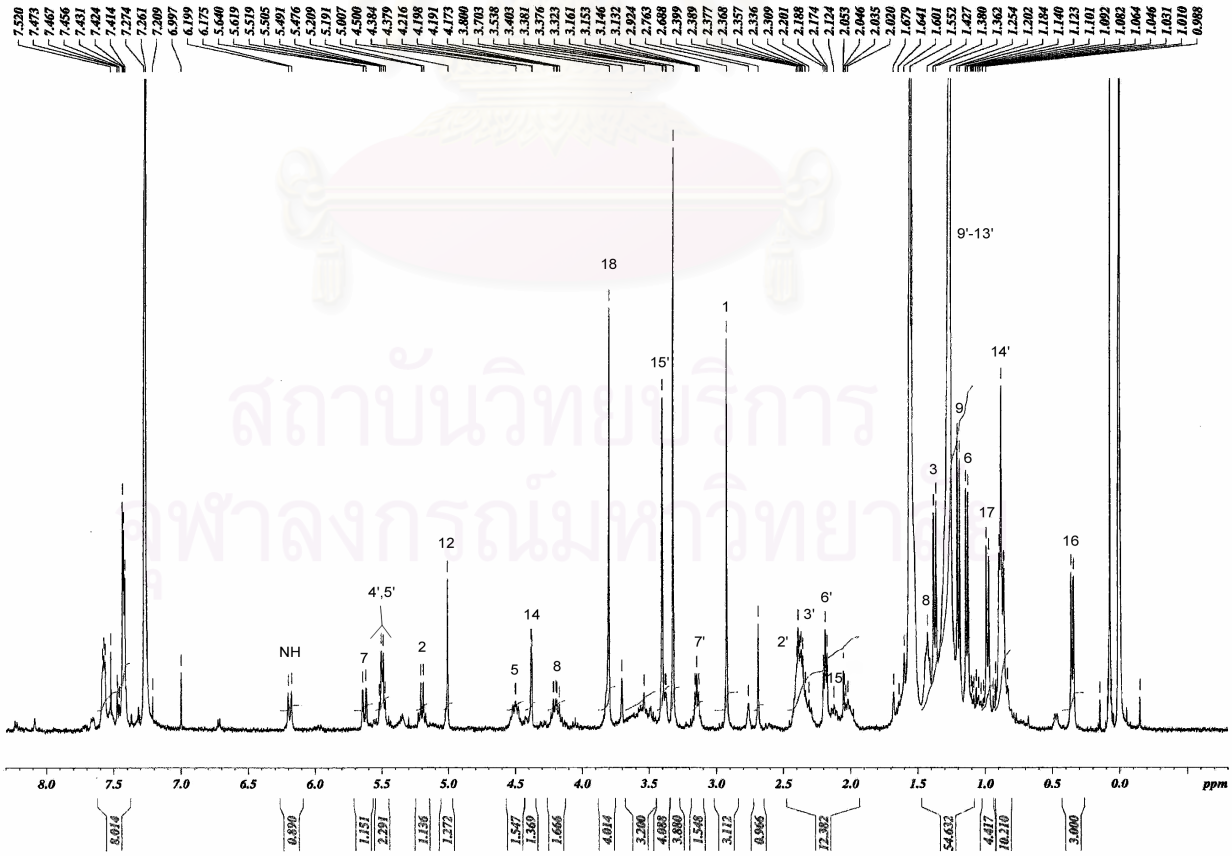

Figure 62. The 600 MHz ^{1}H NMR spectrum of 7-*O*-(*S*)-(−)-MTPA ester of malyngamide X [**SHO27b**] in $CDCl_3$.

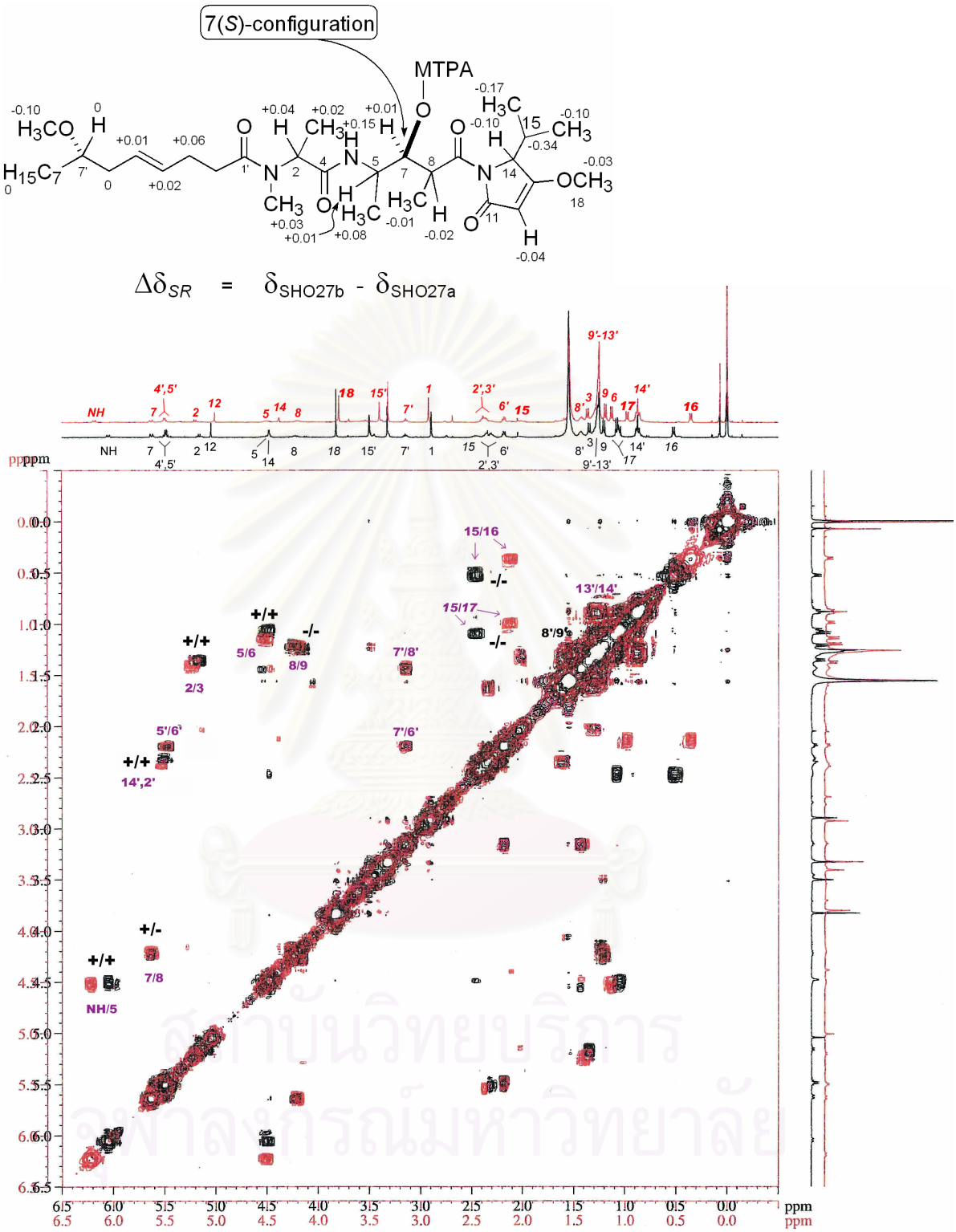

Figure 63. The overlaid H,H COSY spectra of 7-*O*-(*R*)-(+)-MTPA ester **SHO27a** (black) and 7-*O*-(*S*)-(−)-MTPA ester **SHO27b** (red) in $CDCl_3$.

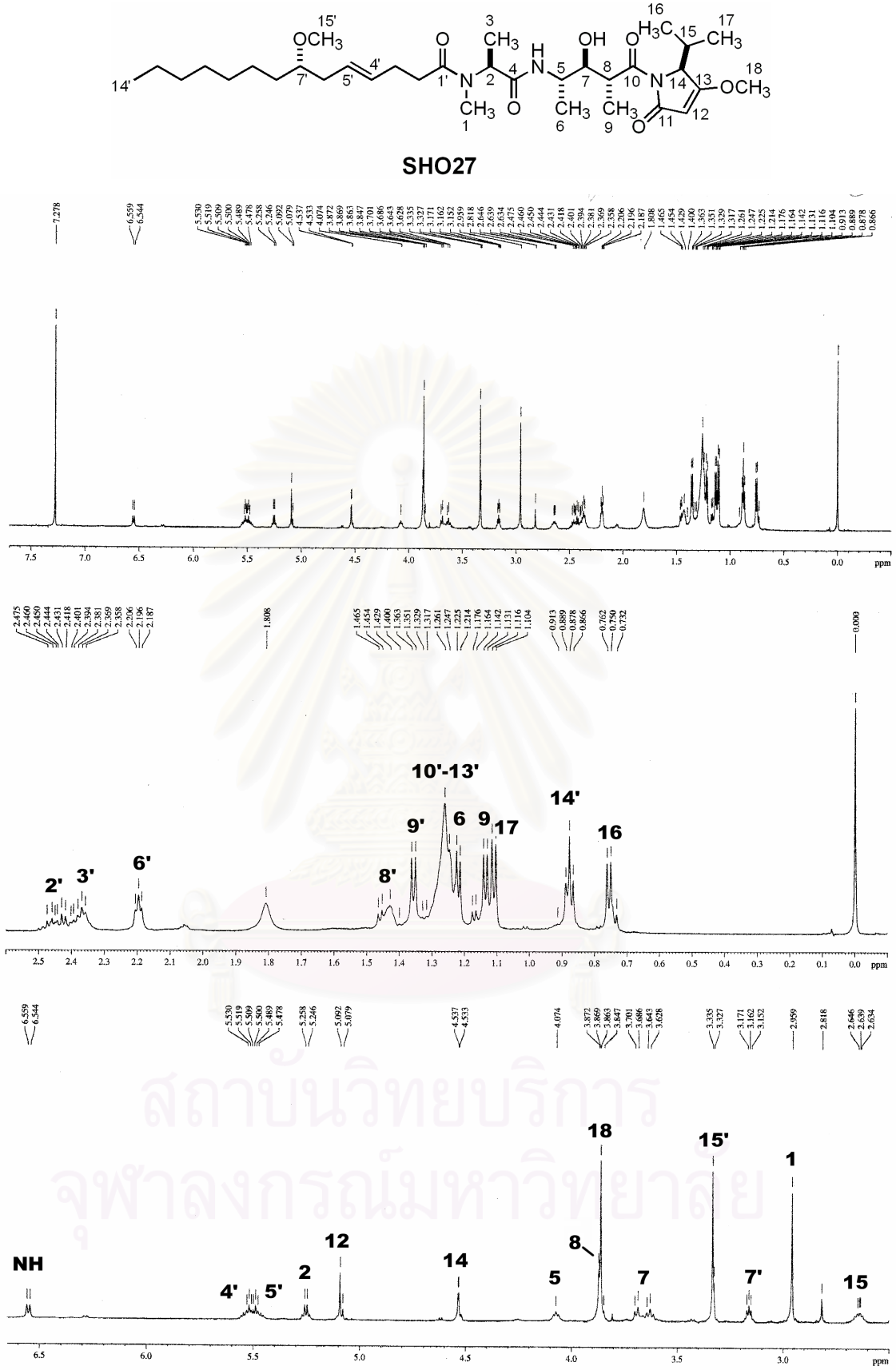

Figure 64. The 600 MHz ^{1}H NMR spectrum of malyngamide X in $CDCl_3$ at 274 °K.

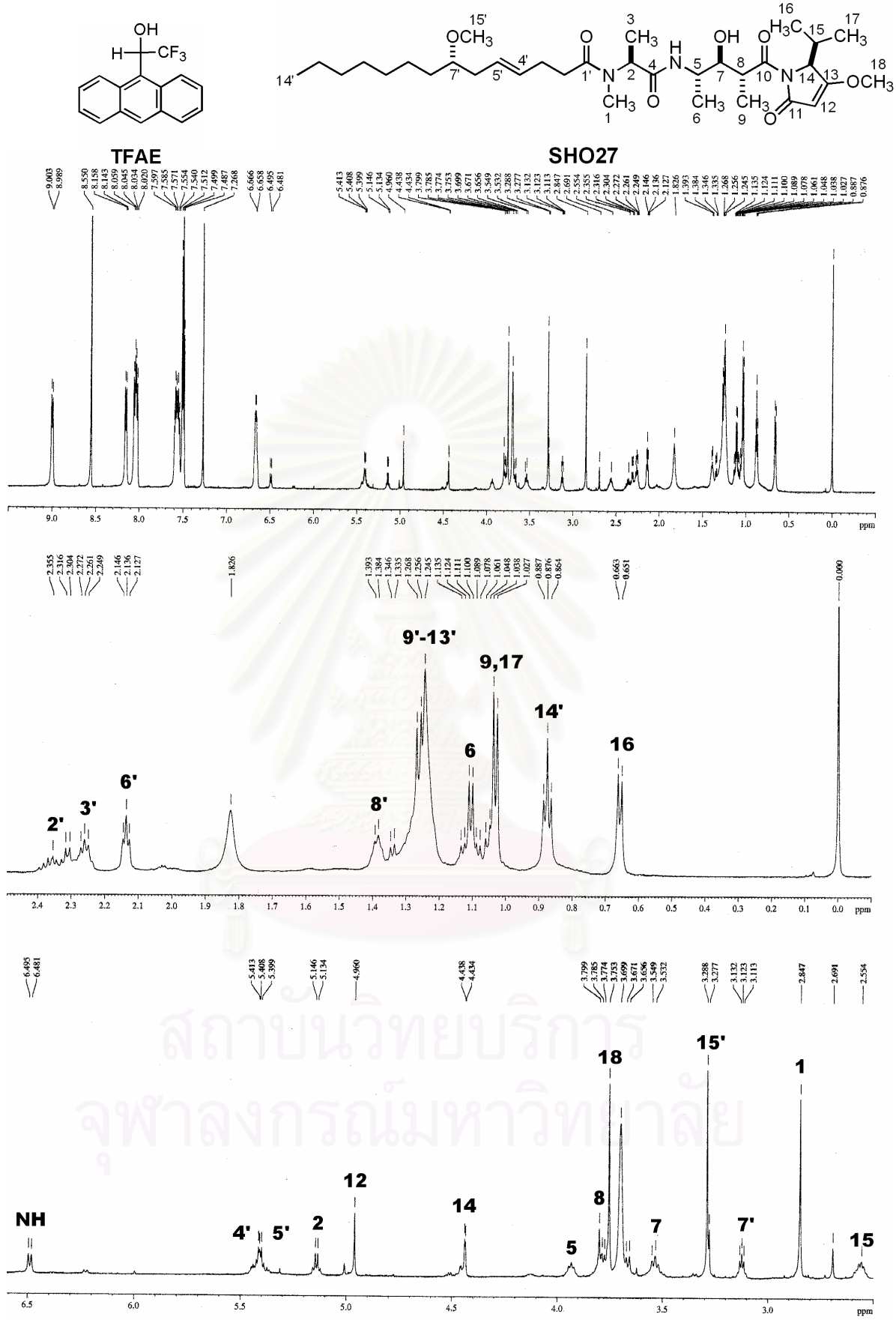

Figure 65. The 600 MHz ^{1}H NMR spectrum of malyngamide X [**SHO27**] plus 5 equiv. of (*R*)-2,2,2-trifuluoro-1-(9-anthryl)-ethanol (*R*-TFAE) in $CDCl_3$ at 274 °K.

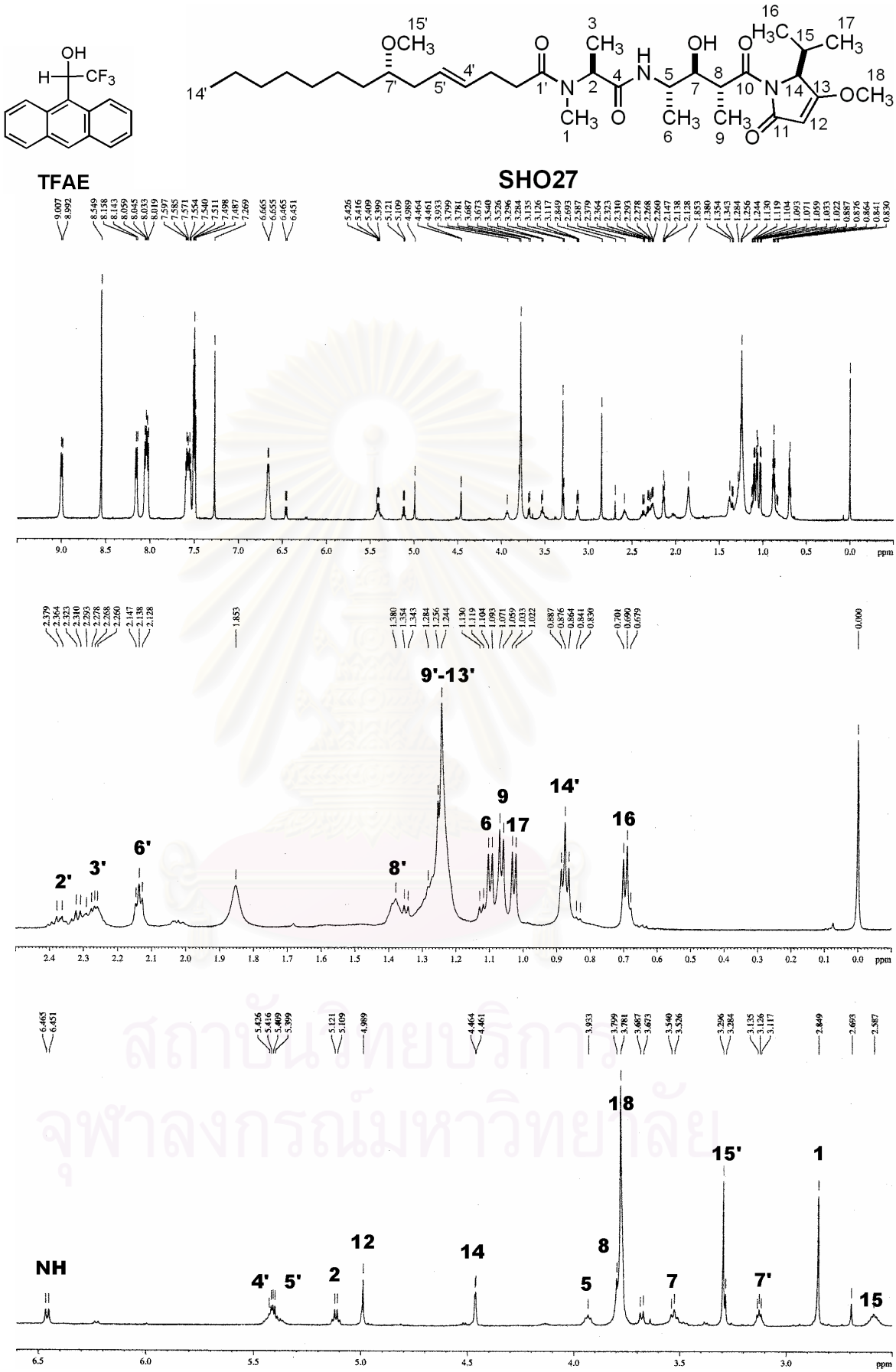

Figure 66. The 600 MHz ^{1}H NMR spectrum of malyngamide X [**SHO27**] plus 5 equiv. of (*S*)-2,2,2-trifuluoro-1-(9-anthryl)-ethanol (*S*-TFAE) in $CDCl_3$ at 274 °K.

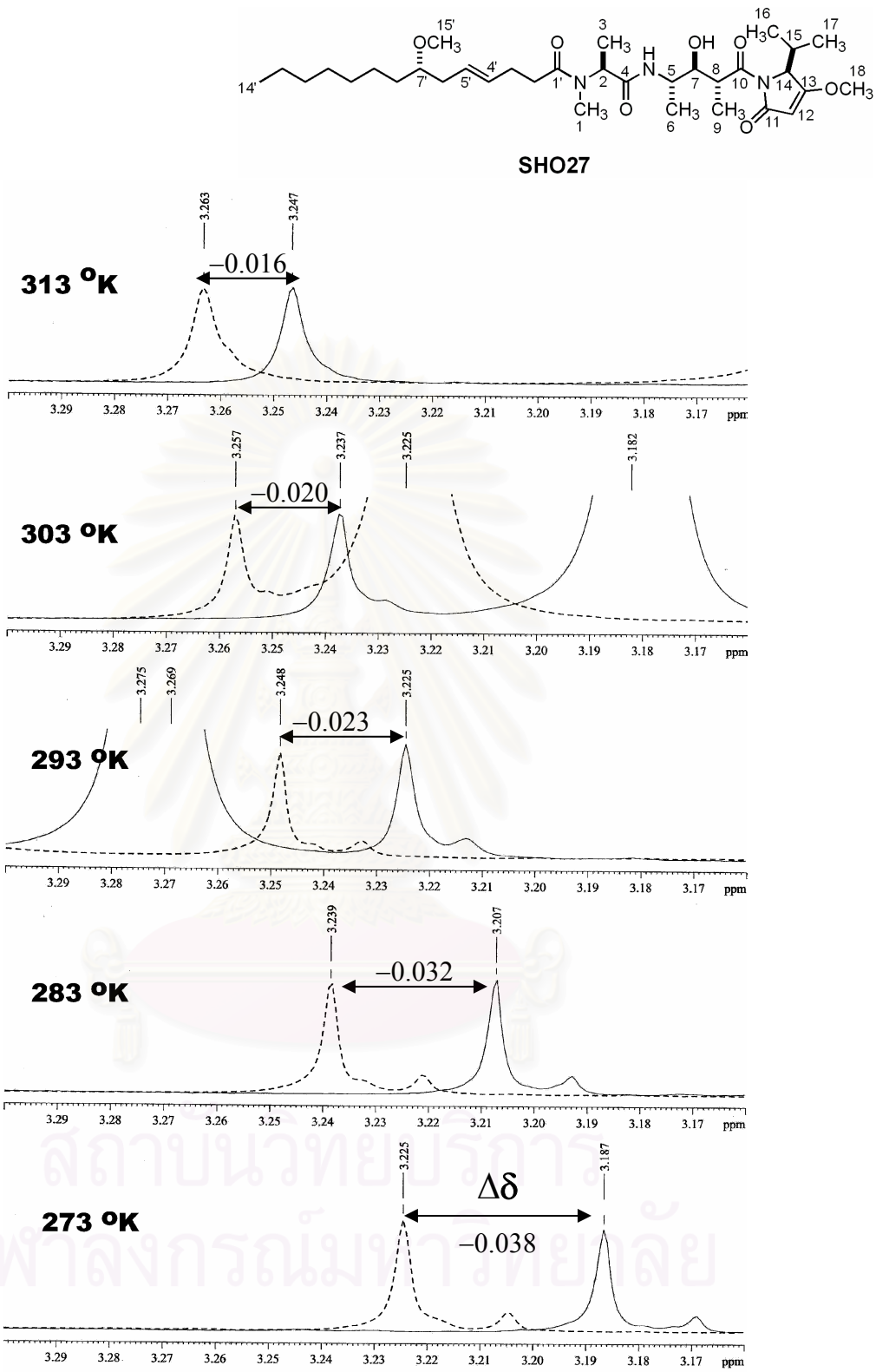

Figure 67. Variation of chemical shift non-equivalence ($\Delta\delta_{RS} = \delta_R - \delta_S$) with temperature for the methoxyl protons at C-7' of malyngamide X [**SHO27**] in the presence of 20 equiv. (*R*)-TFAE (solid line) and (*S*)-TFAE (dashed line) ($CDCl_3$, 600 MHz).

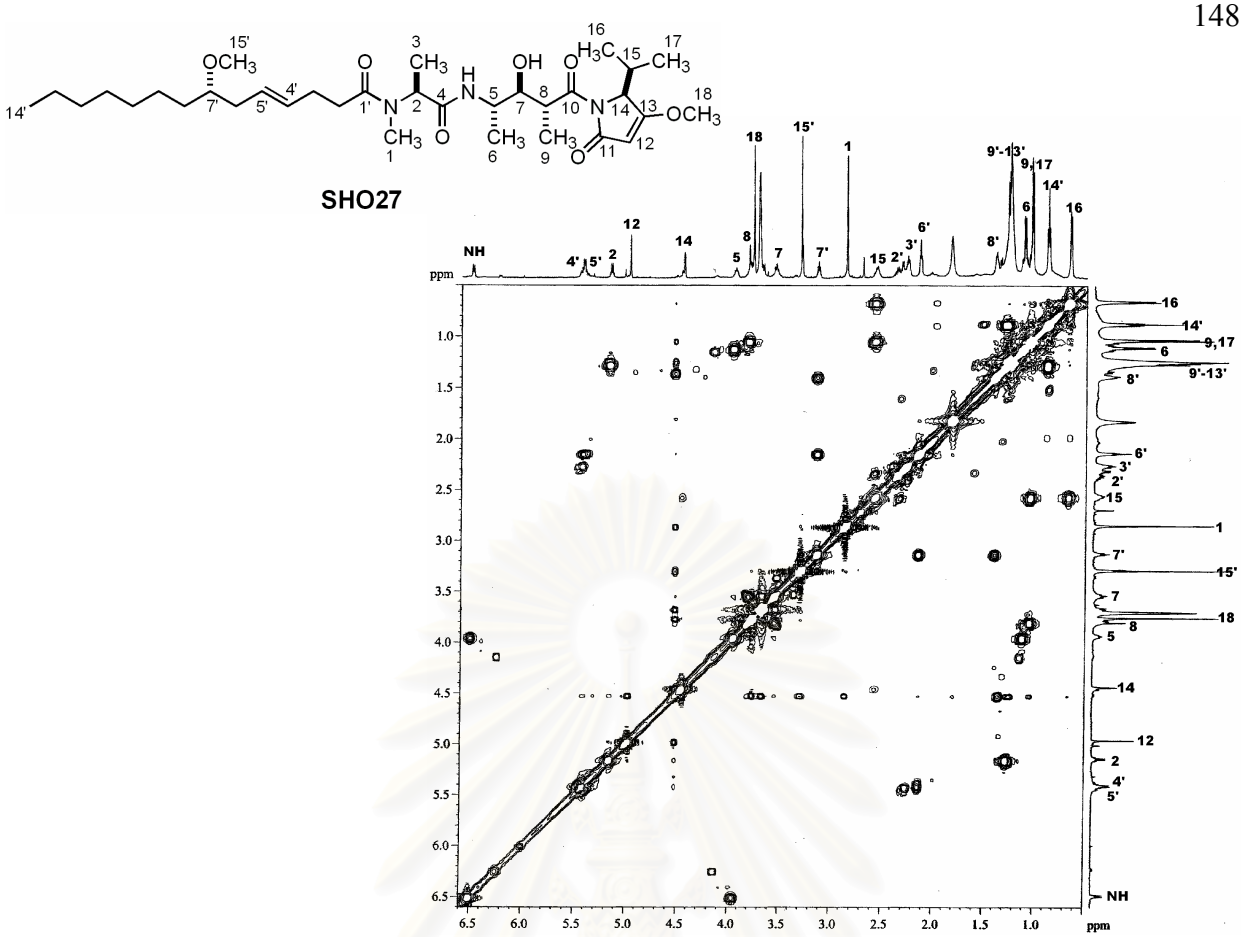

Figure 68. The 600 MHz H, H COSY spectrum of malyngamide X [**SHO27**] plus 5 equiv. (*R*)-TFAE in $CDCl_3$ at 274 °K.

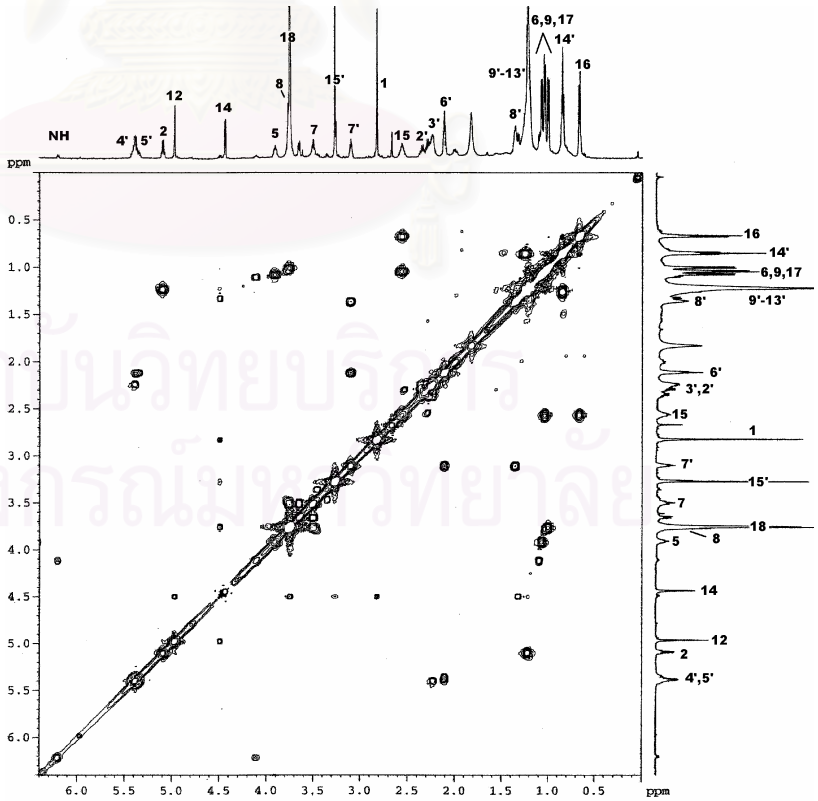

Figure 69. The 600 MHz H, H COSY spectrum of malyngamide X [**SHO27**] plus 5 equiv. (*S*)-TFAE in $CDCl_3$ at 274 °K.

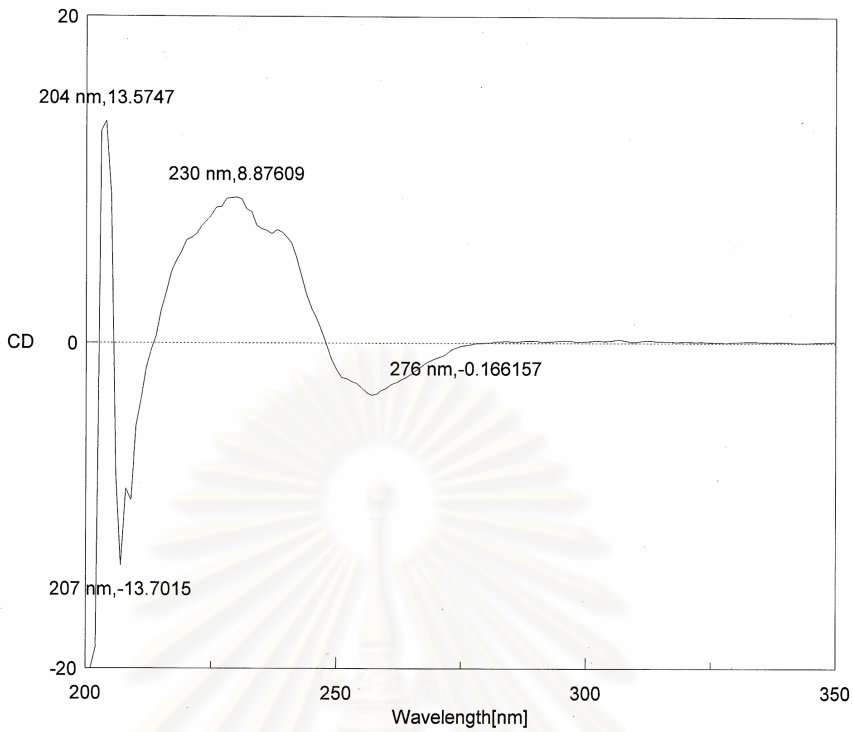

Figure 70. The circular dichroism spectrum of hectochlorin [**SHOII-28**] in methanol.

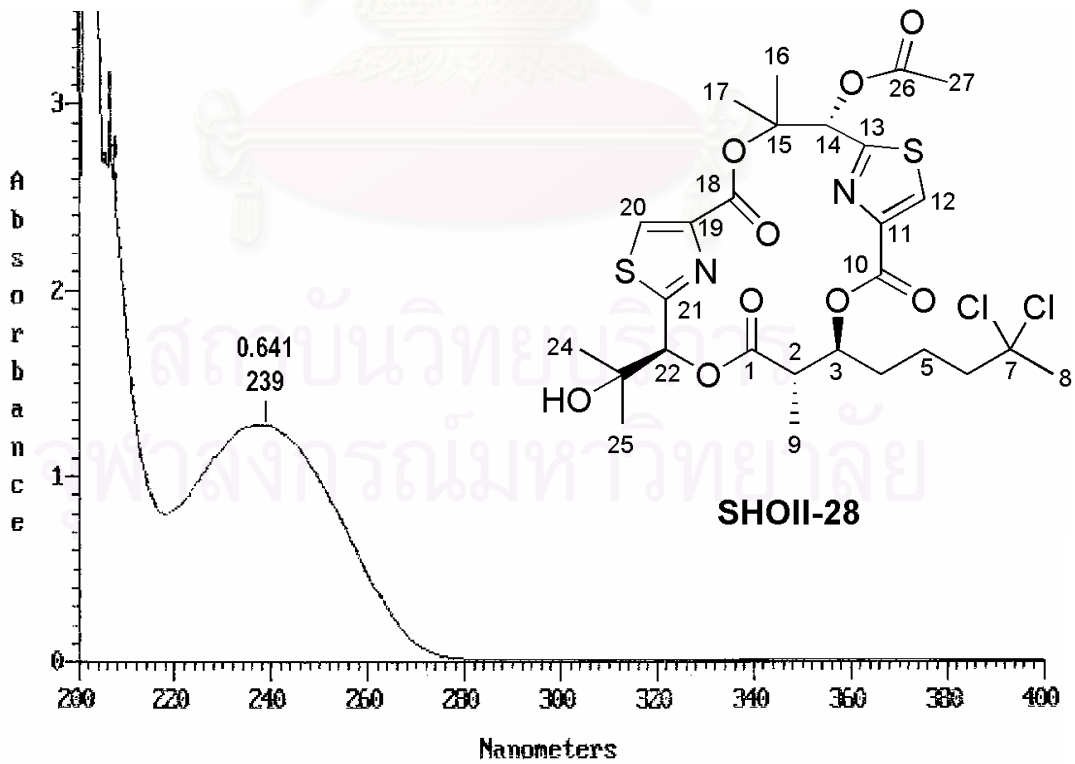

Figure 71. The UV spectrum of hectochlorin [**SHOII-28**] in MeOH.

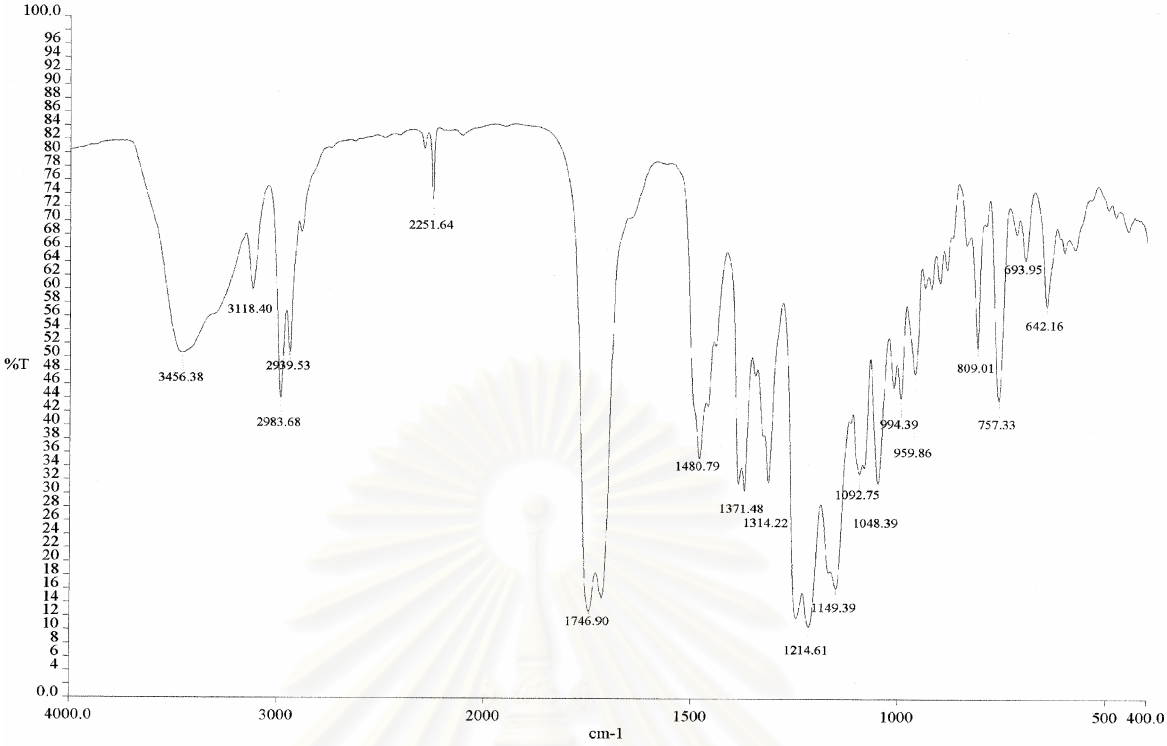

Figure 72. The IR spectrum (Film) of hectochlorin [**SHOII-28**].

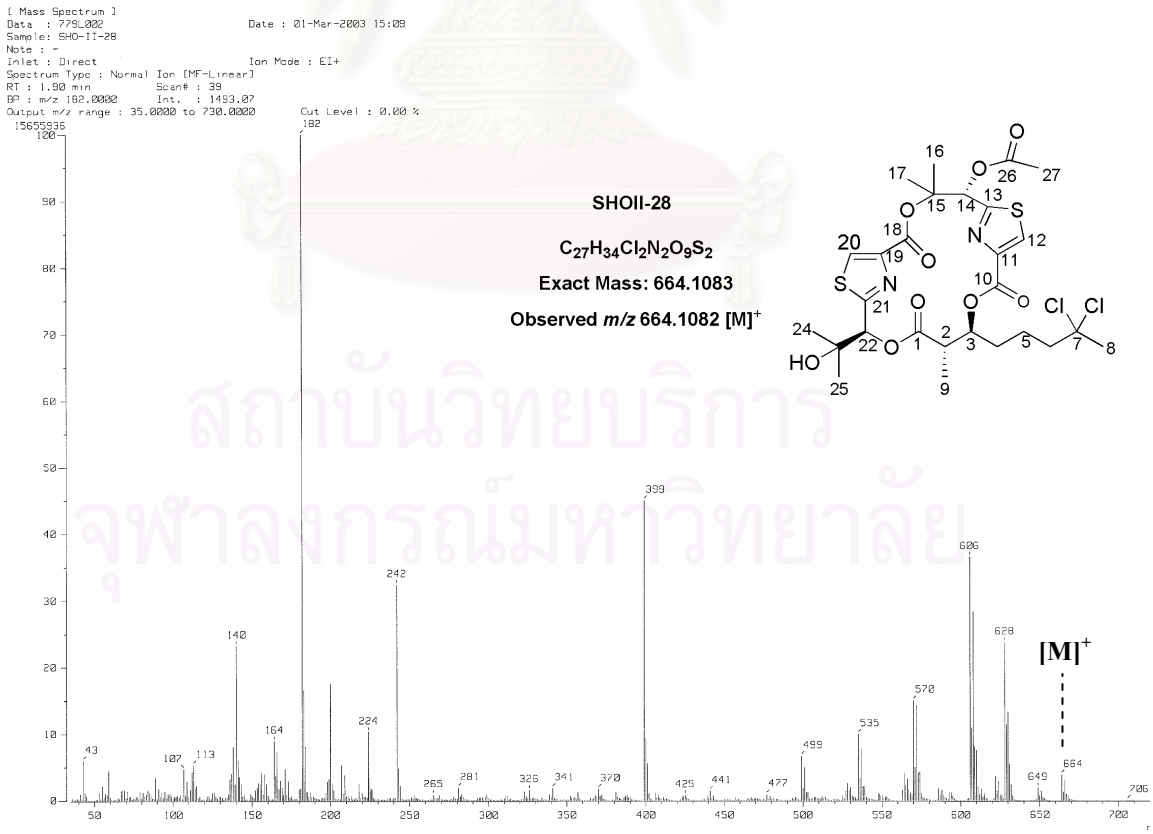

Figure 73. The EIMS mass spectrum of hectochlorin [**SHOII-28**].

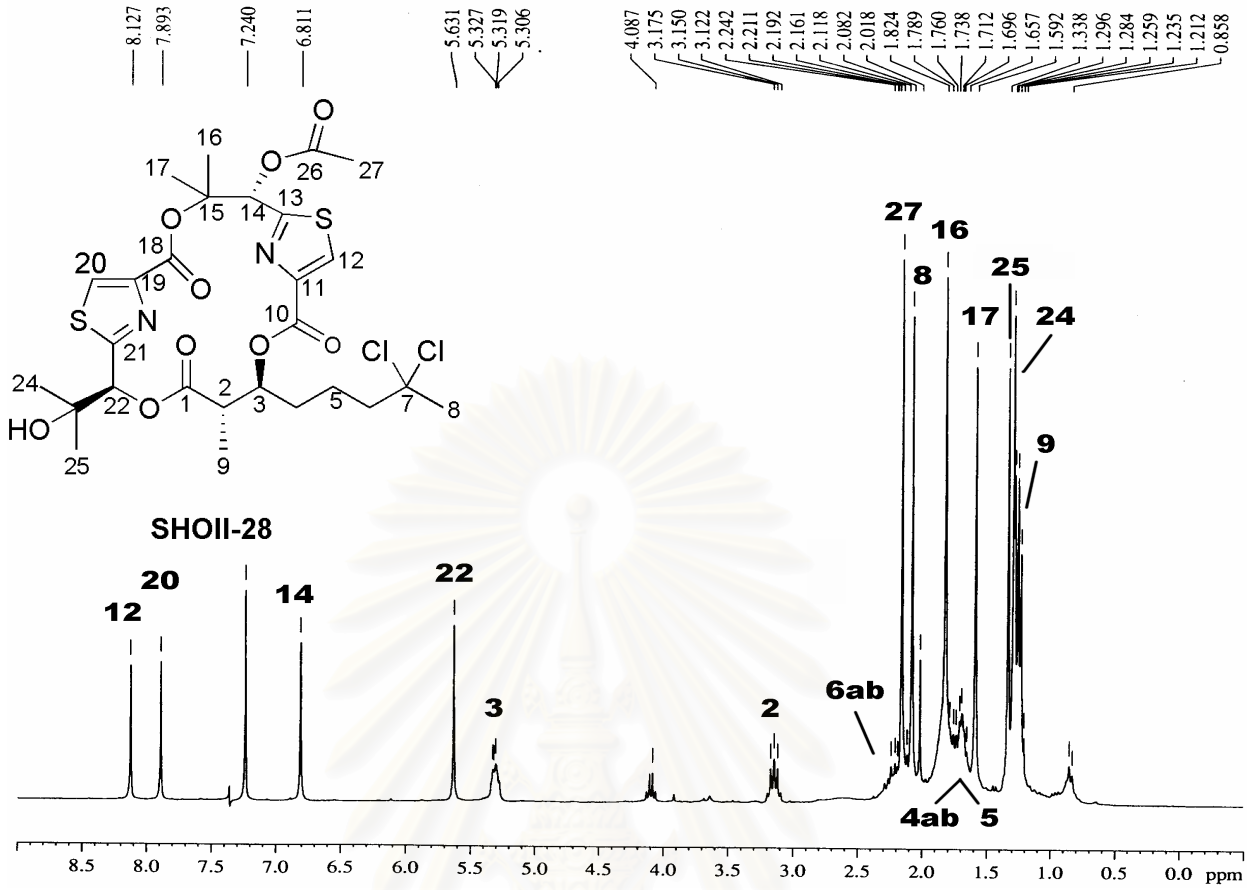

Figure 74. The 300 MHz ^{1}H NMR spectrum of hectochlorin [**SHOII-28**] in $CDCl_3$.

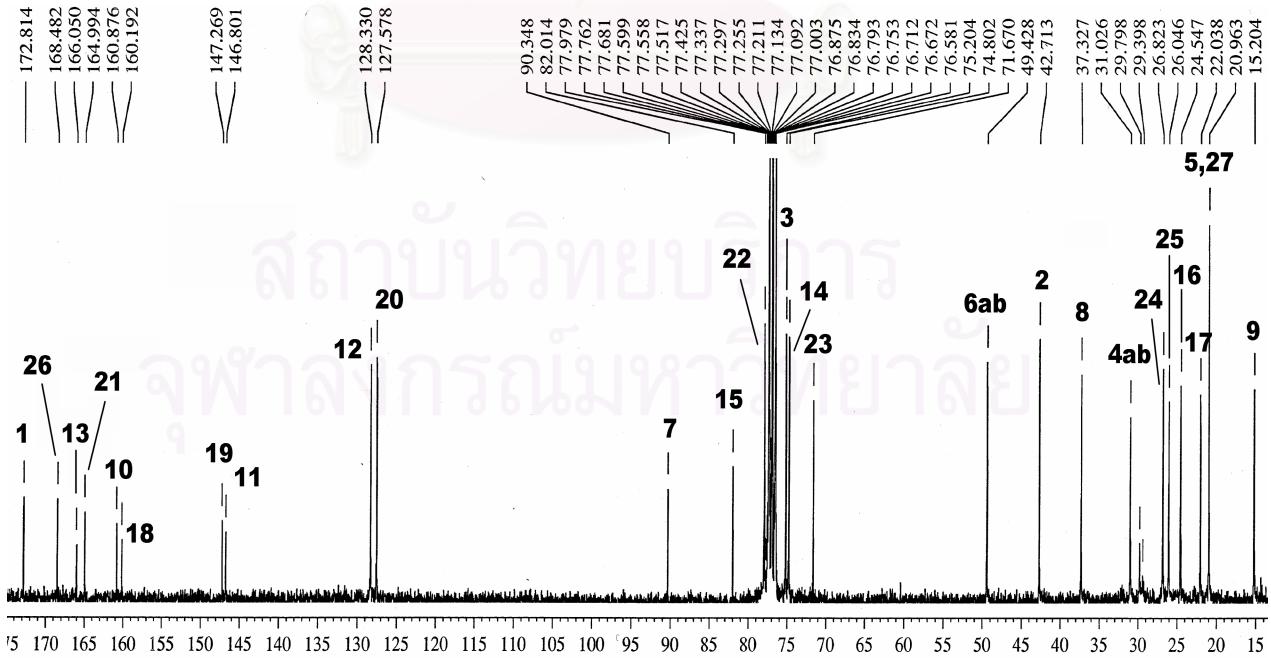

Figure 75. The 75 MHz ^{13}C NMR spectrum of hectochlorin [**SHOII-28**] in $CDCl_3$.

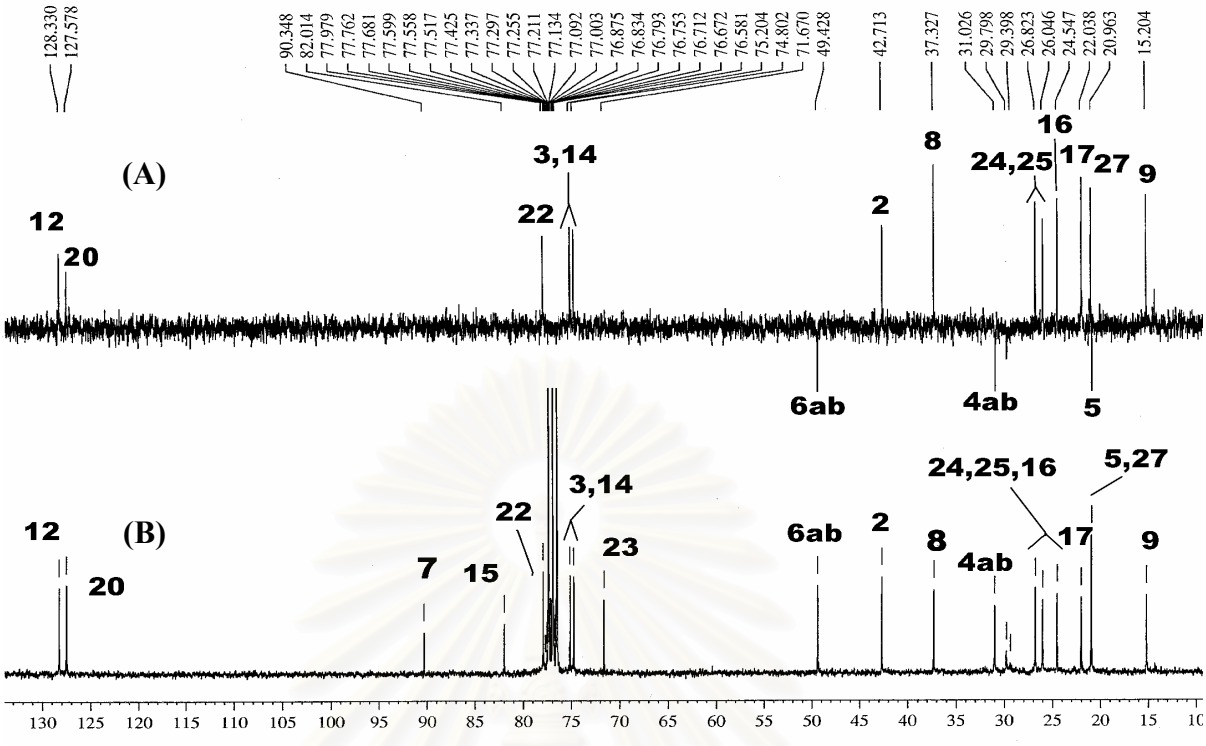

Figure 76. The 75 MHz (A) DEPT-135 and (B) ^{13}C NMR spectrum of hectochlorin [**SHOII-28**] in $CDCl_3$

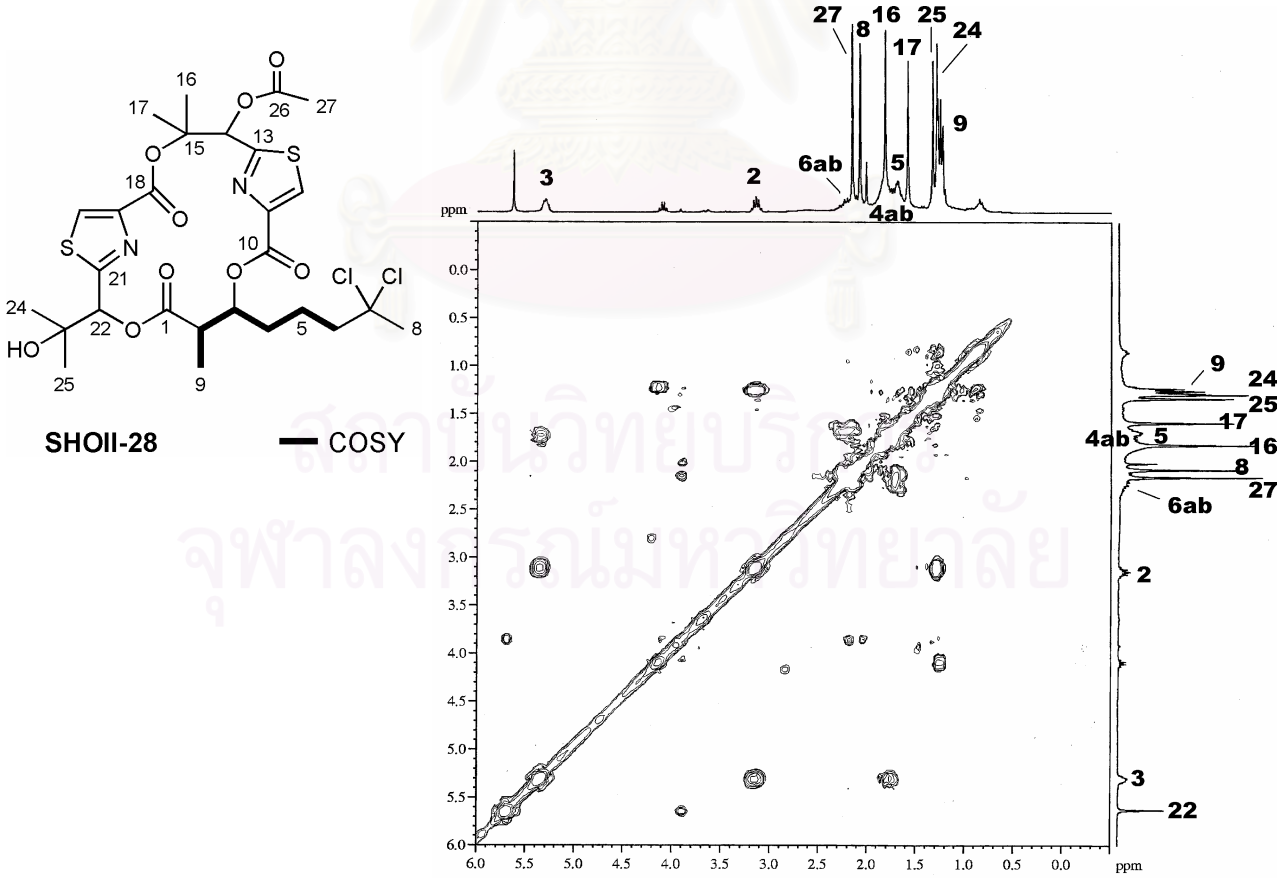

Figure 77. The 300 MHz H,H COSY spectrum of hectochlorin [**SHOII-28**] in $CDCl_3$.

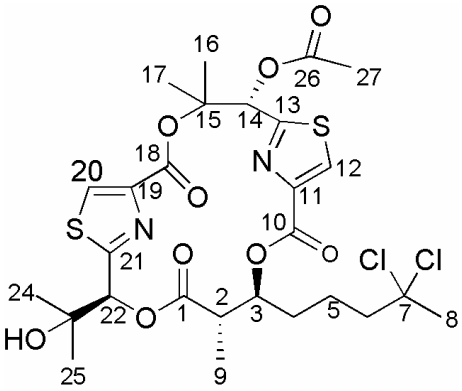

Figure 78. The 300 MHz HMQC spectrum of hectochlorin [**SHOII-28**] in $CDCl_3$.

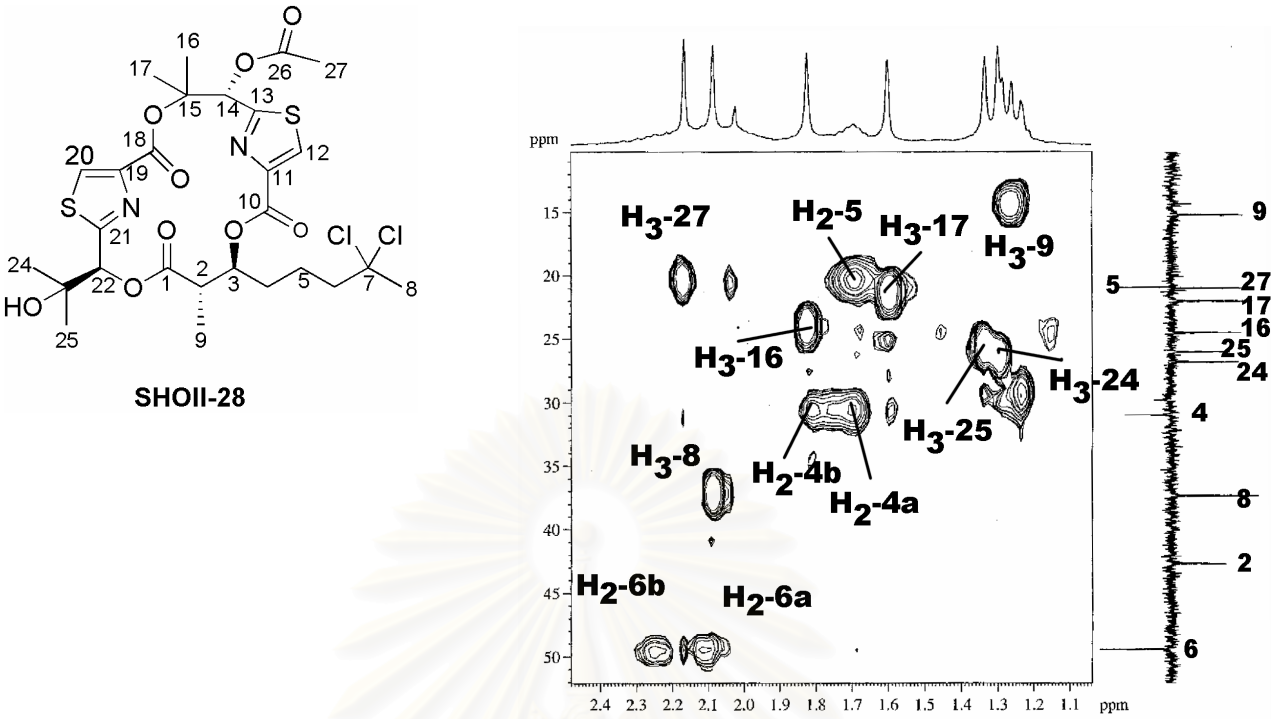

Figure 79. The 300 MHz HMQC spectrum of hectochlorin [**SHOII-28**] in $CDCl_3$ (expanded δ_H 1.0–2.5 ppm and δ_C 10.0–55.0 ppm).

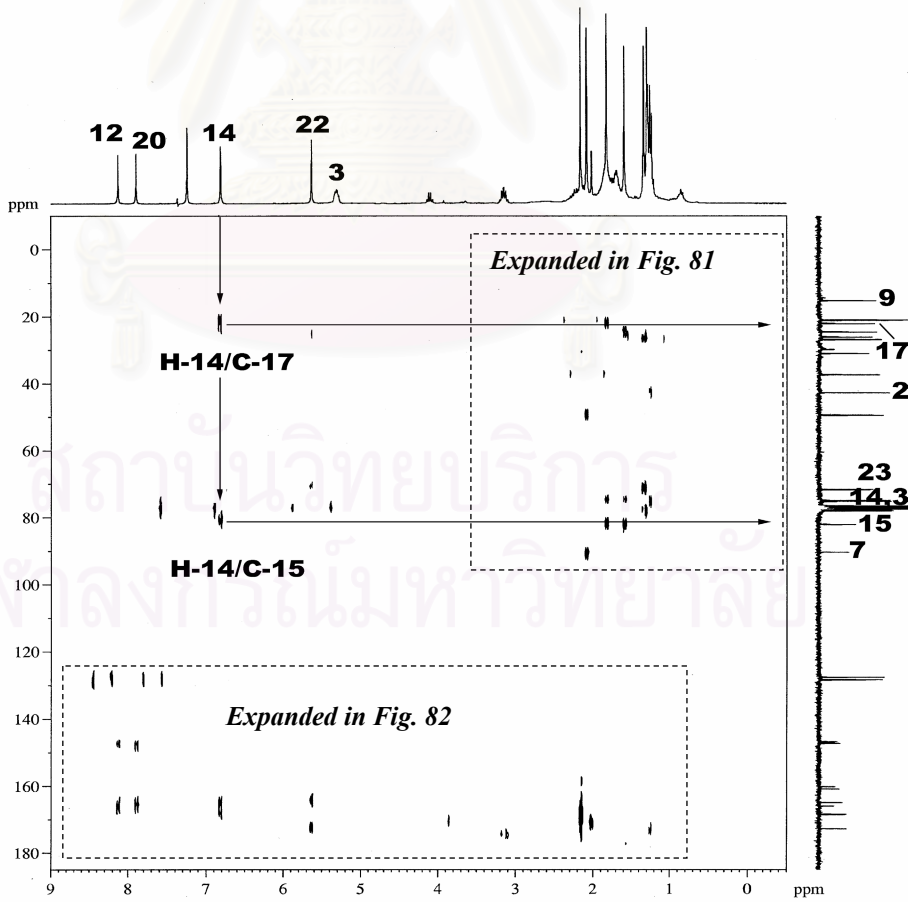

Figure 80. The 300 MHz HMBC spectrum ($^nJ_{CH}$ = 8 Hz) of hectochlorin [**SHOII-28**] in $CDCl_3$.

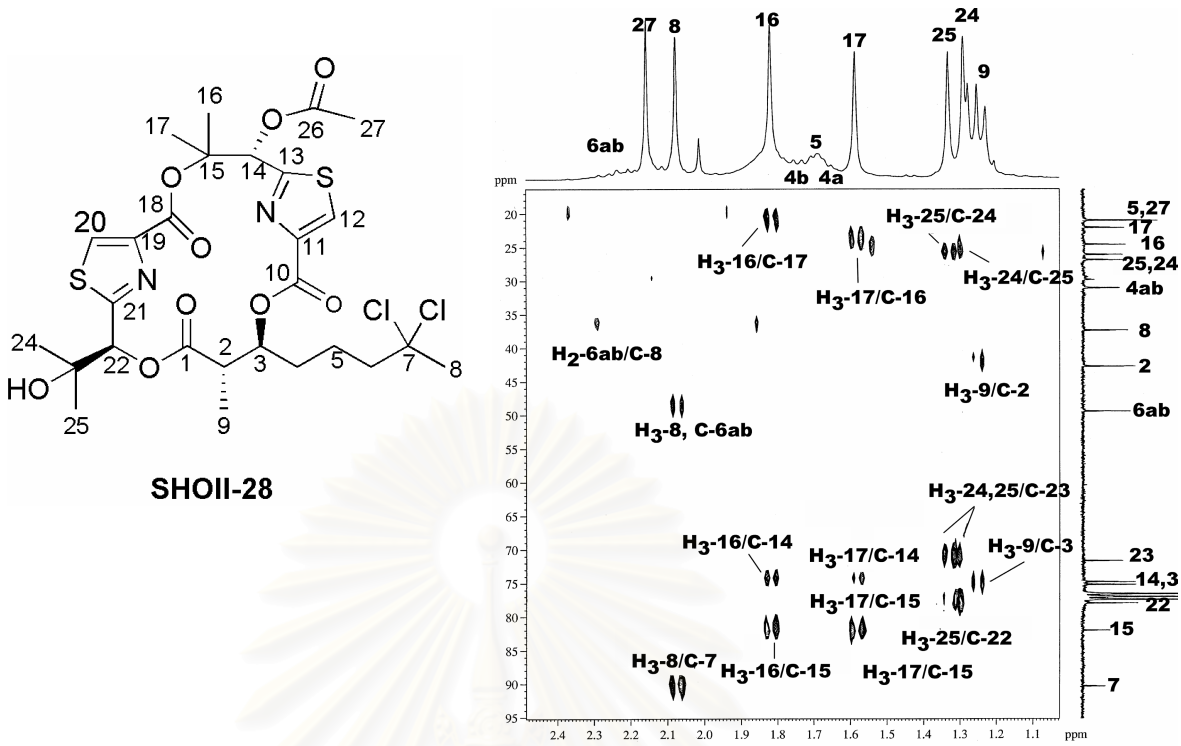

Figure 81. The 300 MHz HMBC spectrum ($^{n}J_{CH}$ = 8 Hz) of hectochlorin [**SHOII-28**] in $CDCl_3$ (expanded δ_H 1.0–2.5 ppm and δ_C 15.0–95.0 ppm).

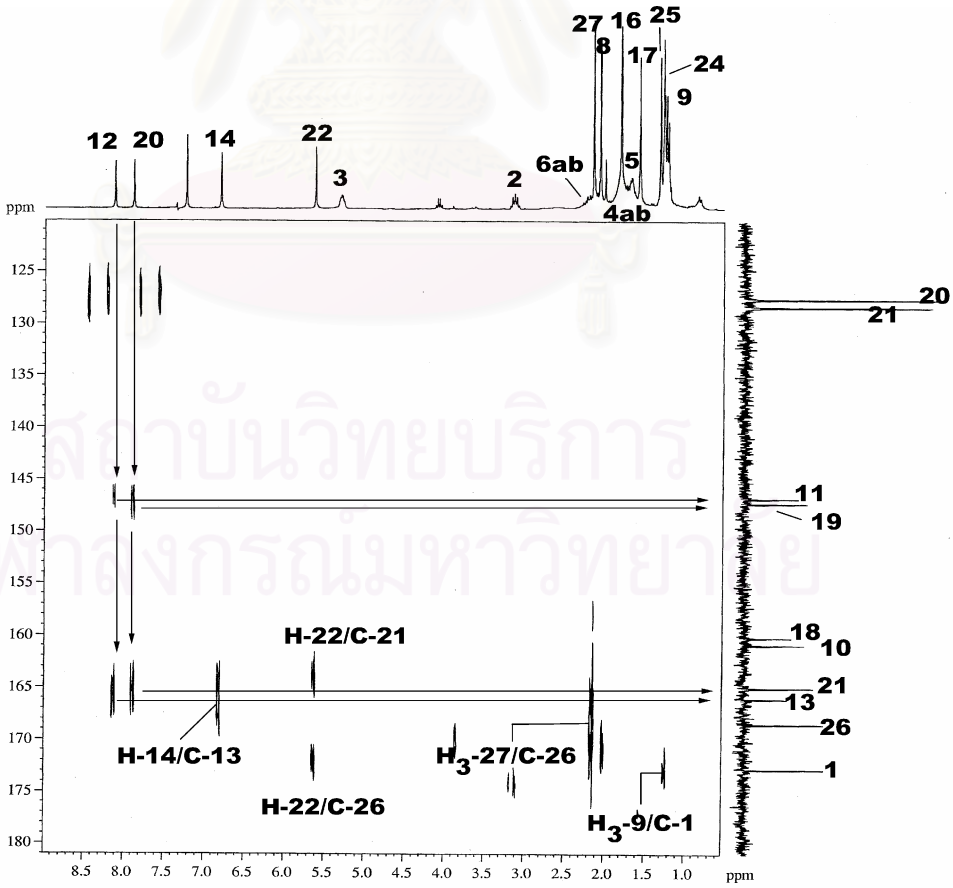

Figure 82. The 300 MHz HMBC spectrum ($^{n}J_{CH}$ = 8 Hz) of hectochlorin [**SHOII-28**] in $CDCl_3$ (expanded δ_H 1.0–9.0 ppm and δ_C 120.0–180.0 ppm).

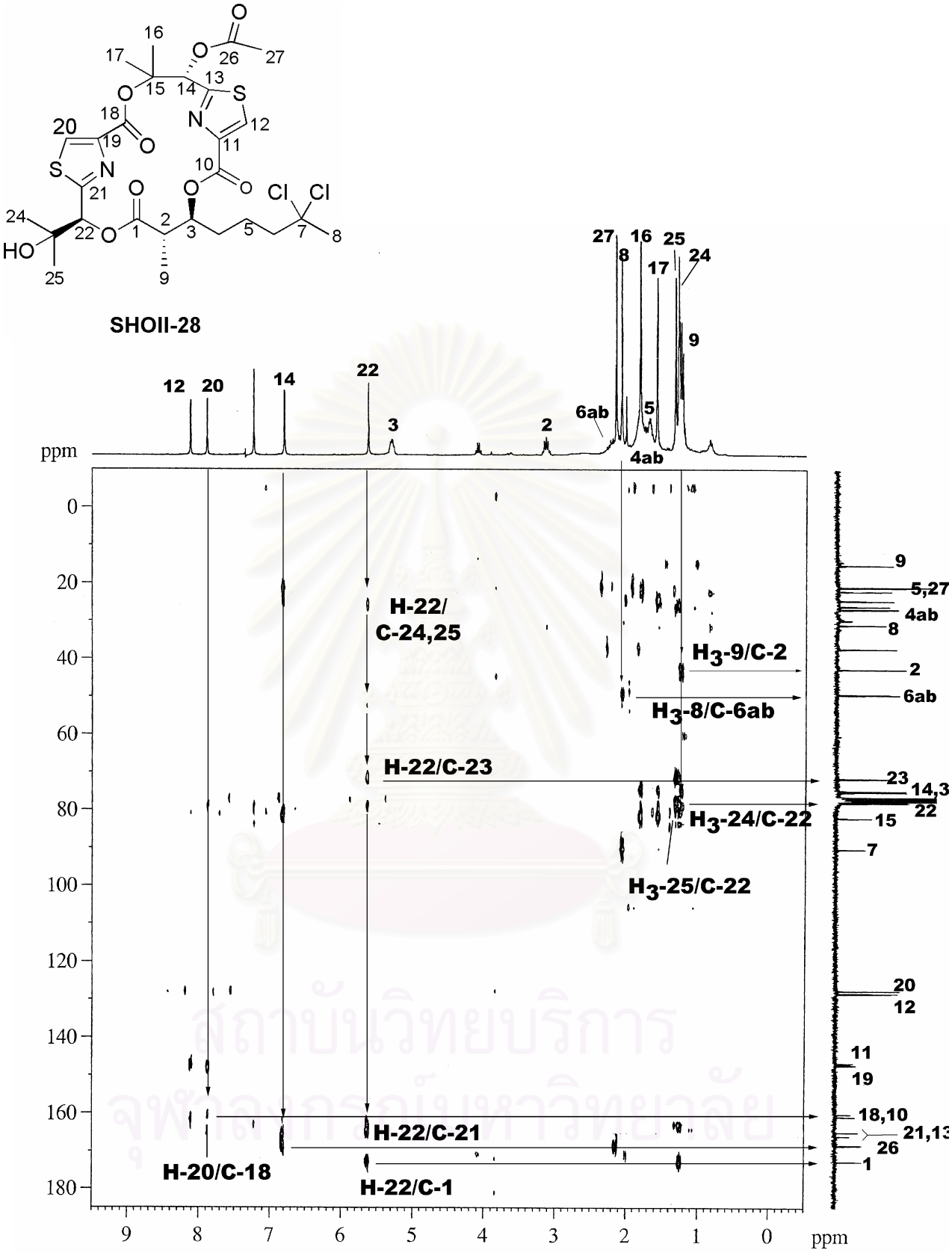

Figure 83. The 300 MHz HMBC spectrum ($^{n}J_{CH}$ = 4 Hz) of hectochlorin [**SHOII-28**] in $CDCl_3$.

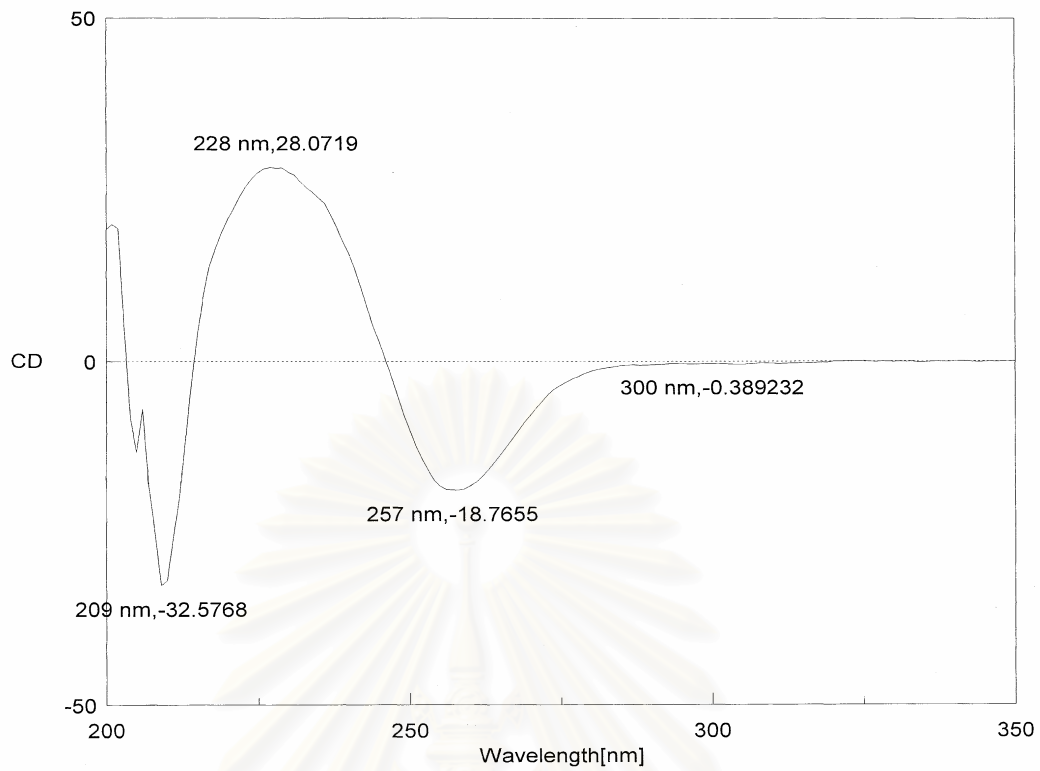

Figure 84. The circular dichroism spectrum of deacetylhectochlorin [**SHOII-51**] in methanol.

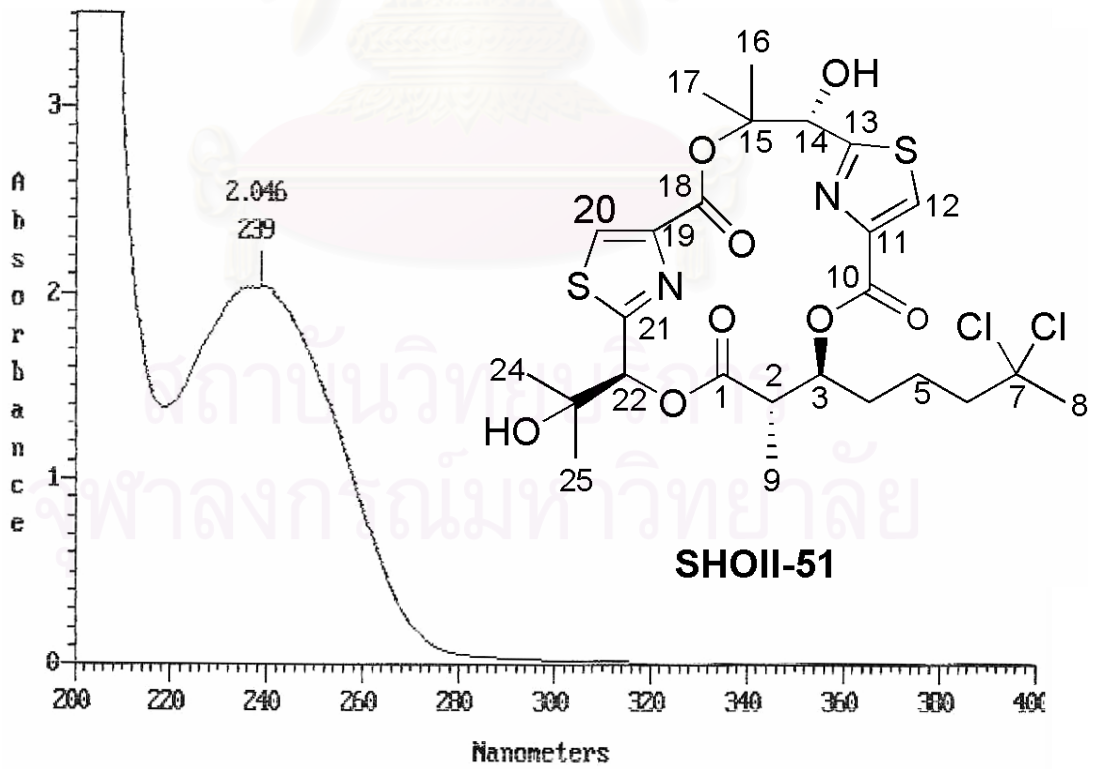

Figure 85. The UV spectrum of deacetylhectochlorin [**SHOII-51**] in MeOH.

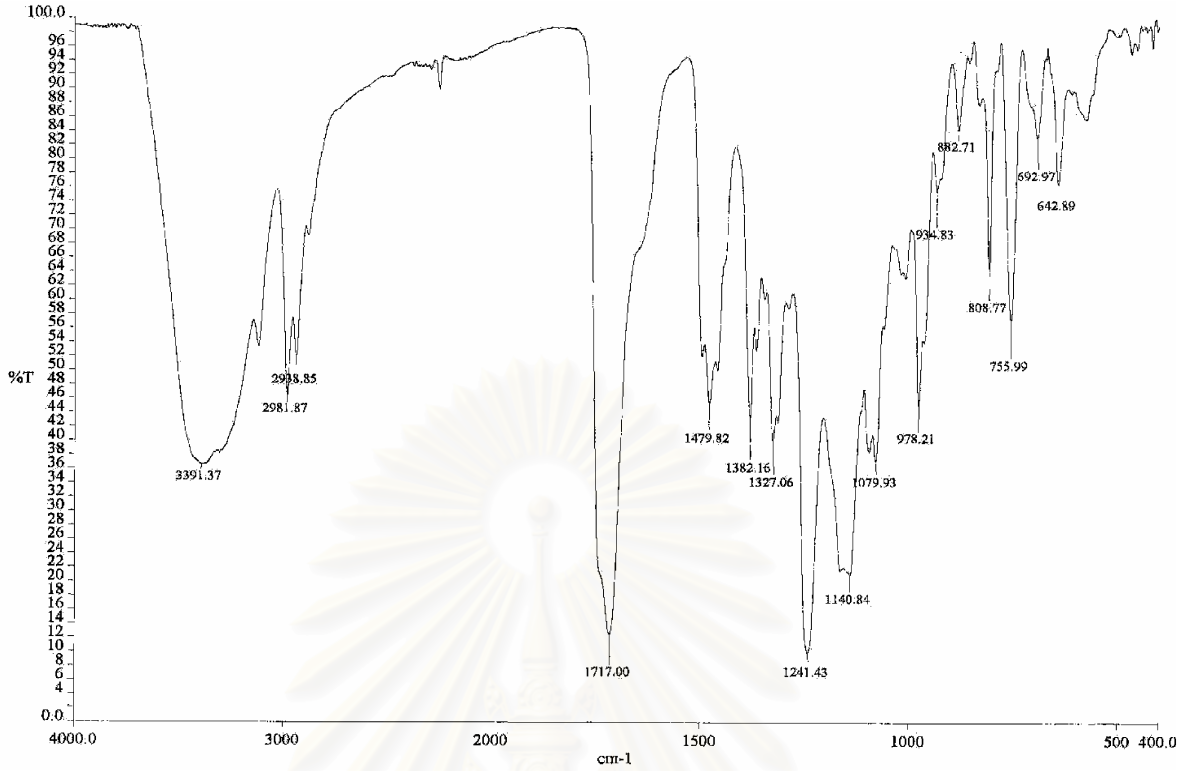

Figure 86. The IR spectrum (Film) of deacetylhectochlorin [**SHOII-51**].

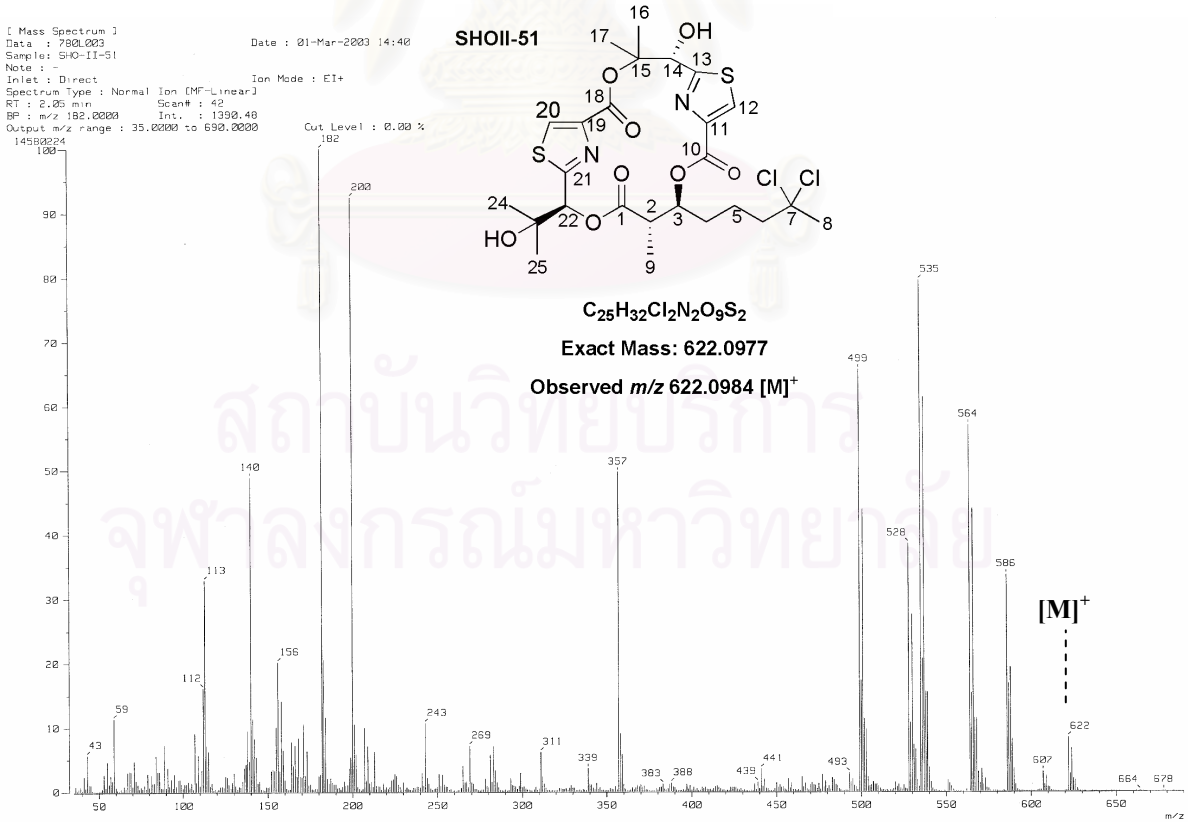

Figure 87. The EIMS mass spectrum of deacetylhectochlorin [**SHOII-51**].

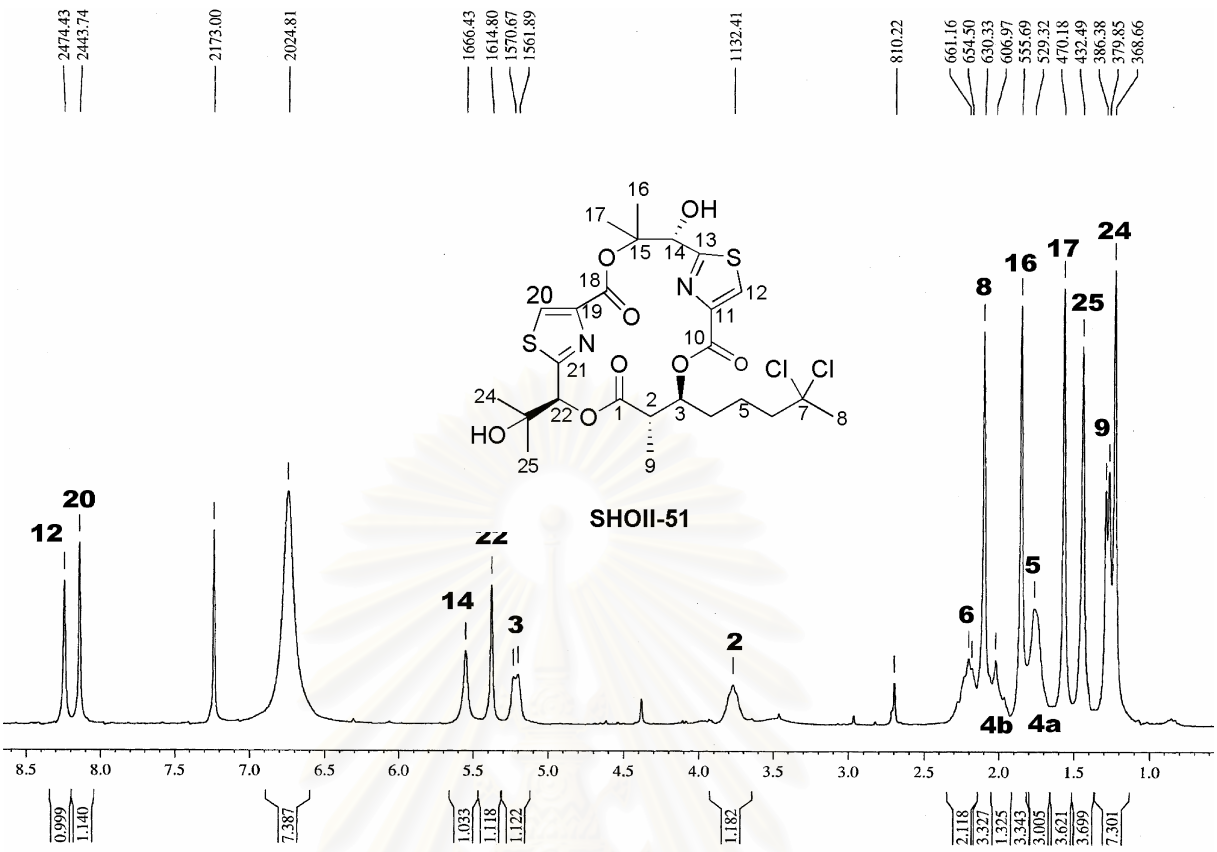

Figure 88. The 300 MHz ^{1}H NMR spectrum of deacetylhectochlorin [**SHOII-51**] in $CDCl_3$.

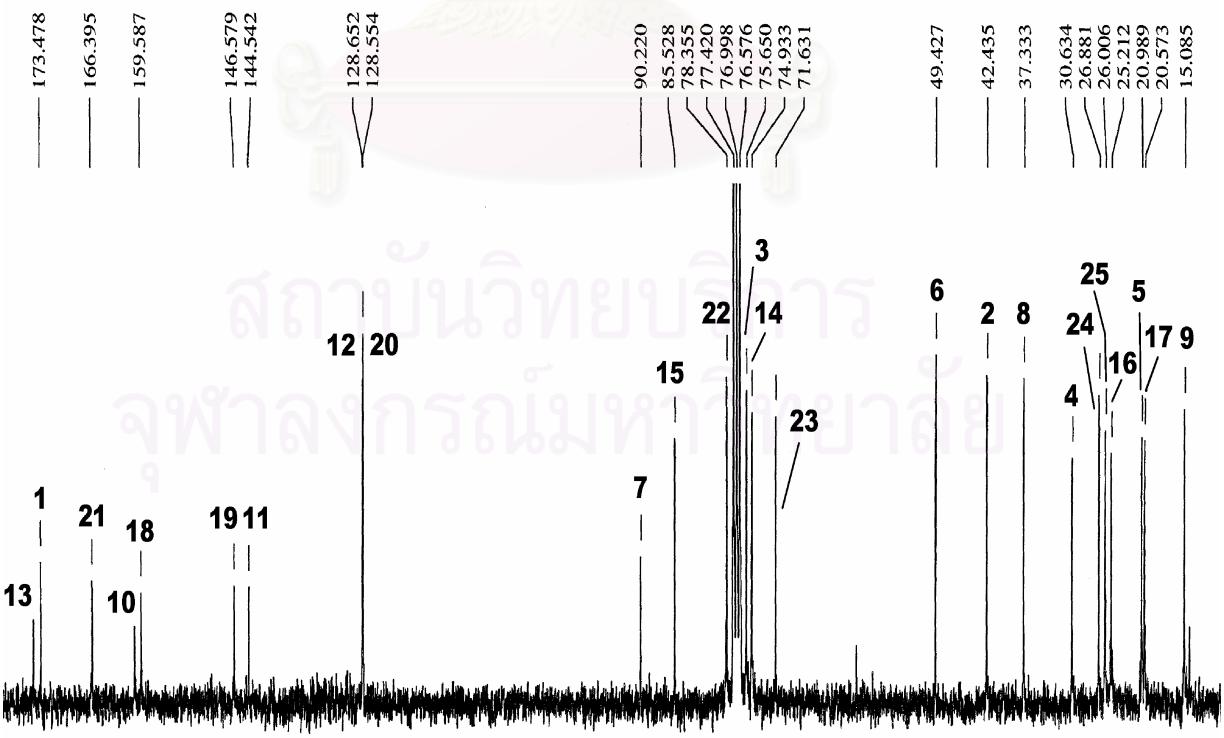

Figure 89. The 75 MHz ^{13}C NMR spectrum of deacetylhectochlorin [**SHOII-51**] in $CDCl_3$.

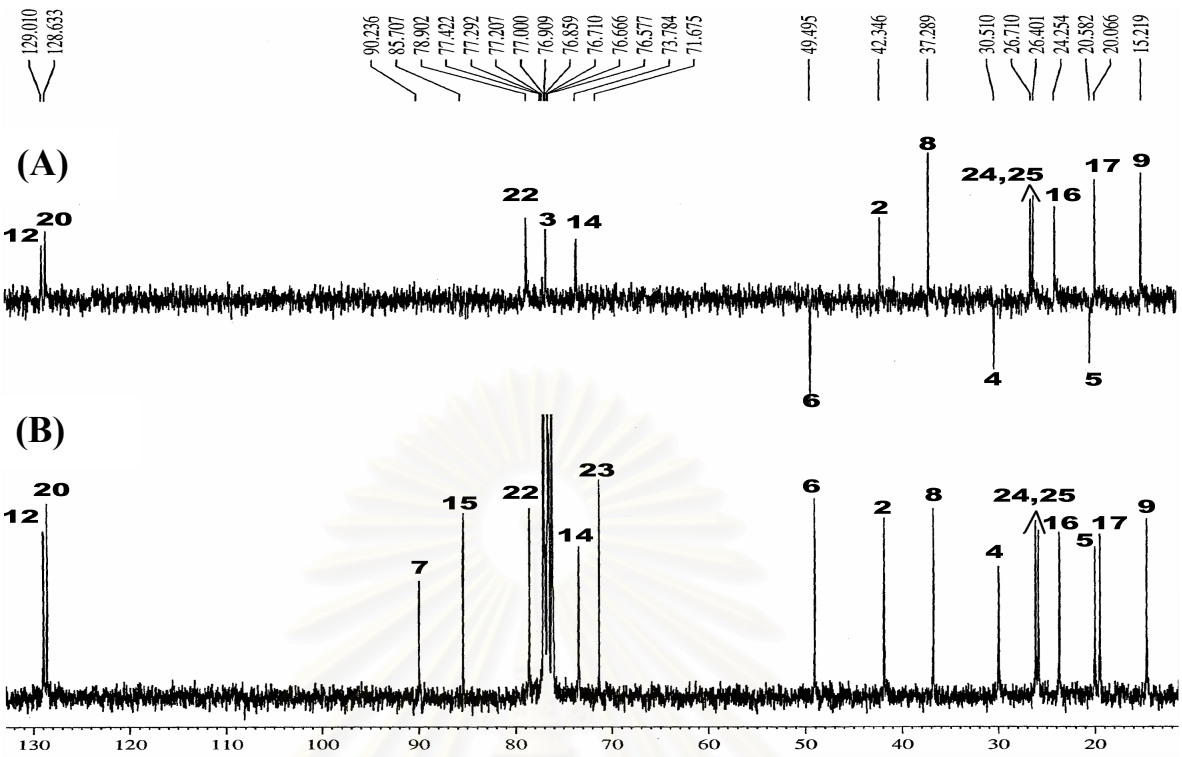

Figure 90. The 75 MHz (A) DEPT-135 and (B) ^{13}C NMR spectrum of deacetylhectochlorin [**SHOII-51**] in $CDCl_3$

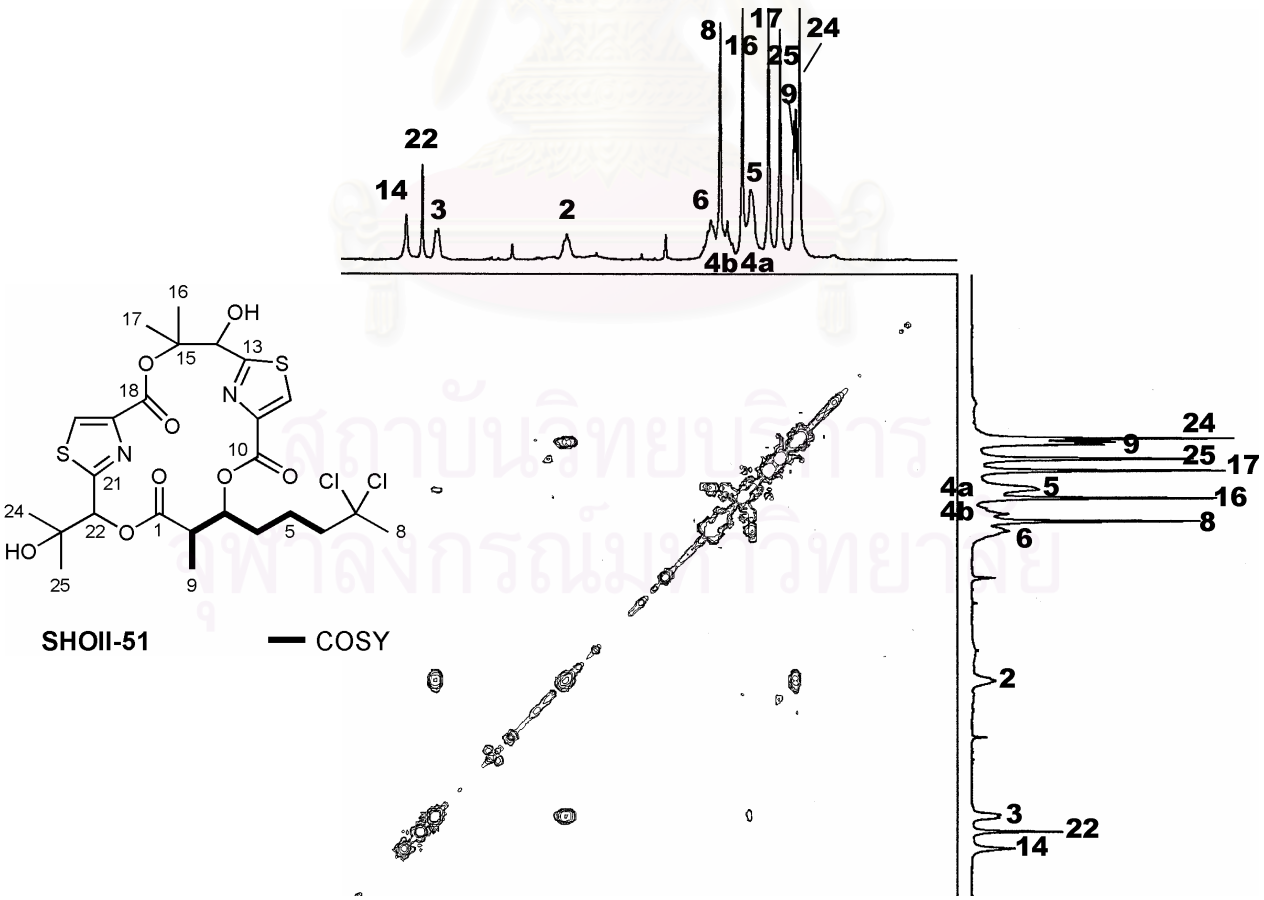

Figure 91. The 300 MHz H,H COSY spectrum of deacetylhectochlorin [**SHOII-51**] in $CDCl_3$.

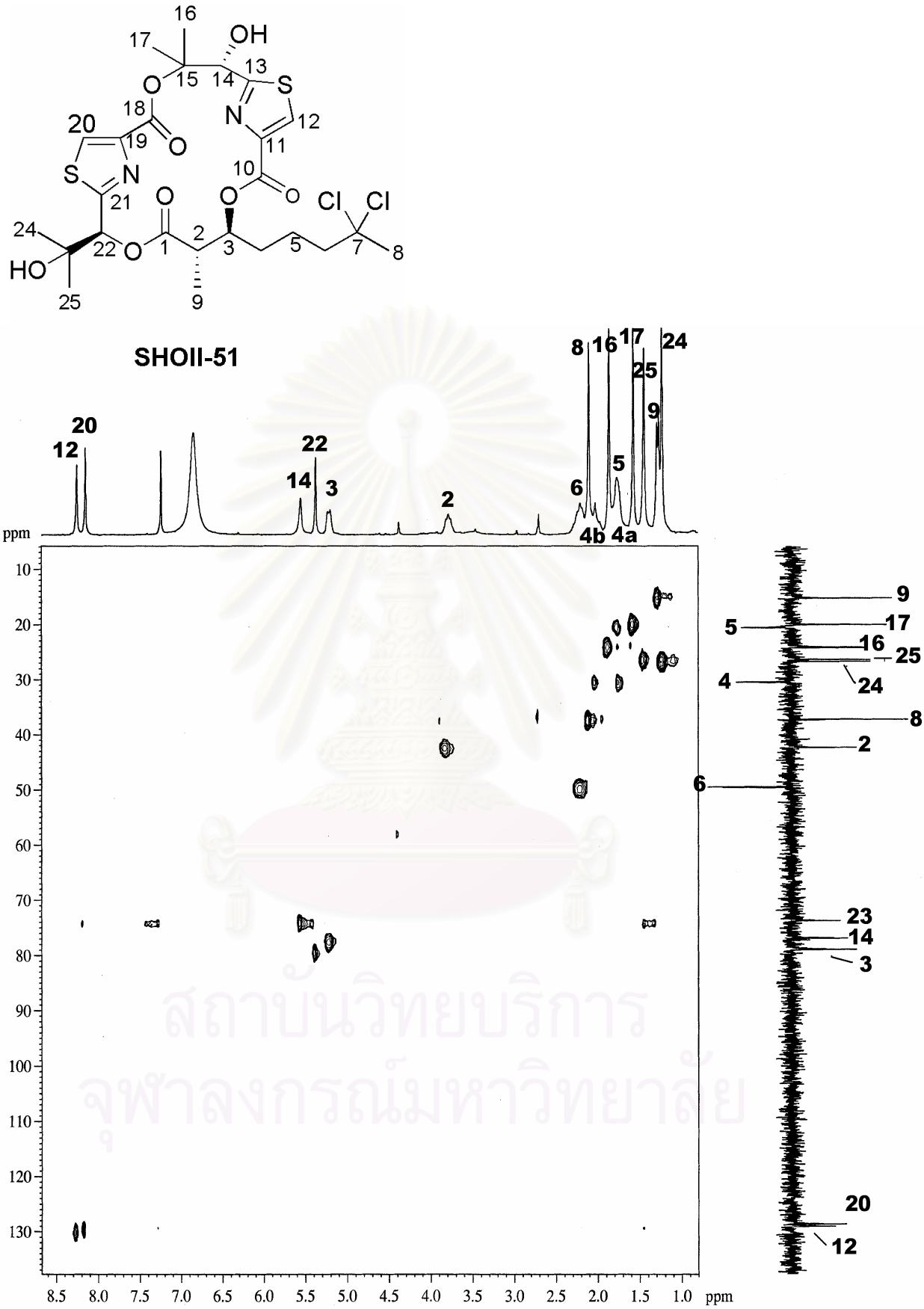

Figure 92. The 300 MHz HMQC spectrum of deacetylhectochlorin [**SHOII-51**] in $CDCl_3$.

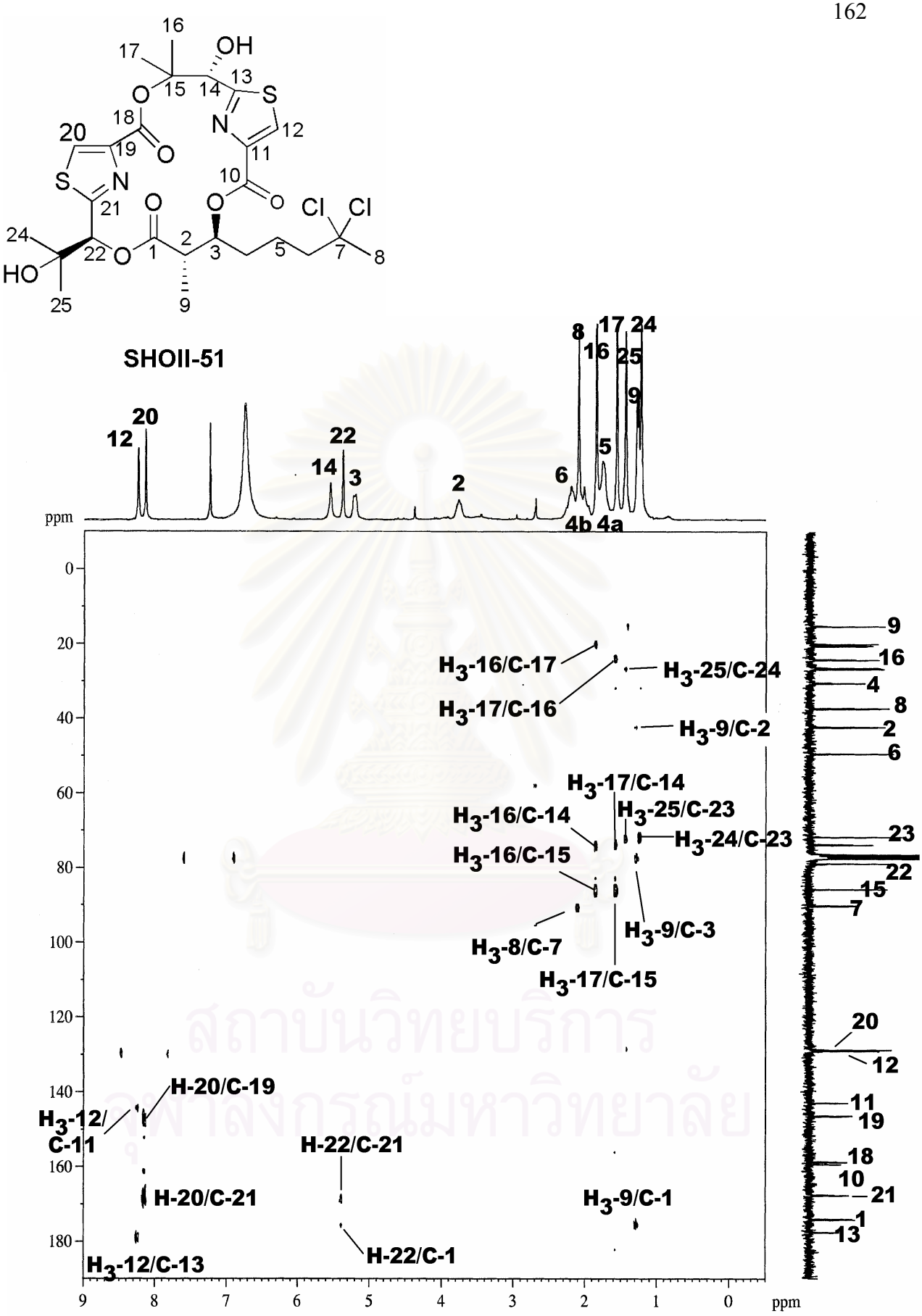

Figure 93. The 300 MHz HMBC spectrum ($^{n}J_{CH}$ = 8 Hz) of deacetylhectochlorin [**SHOII-51**] in $CDCl_3$.

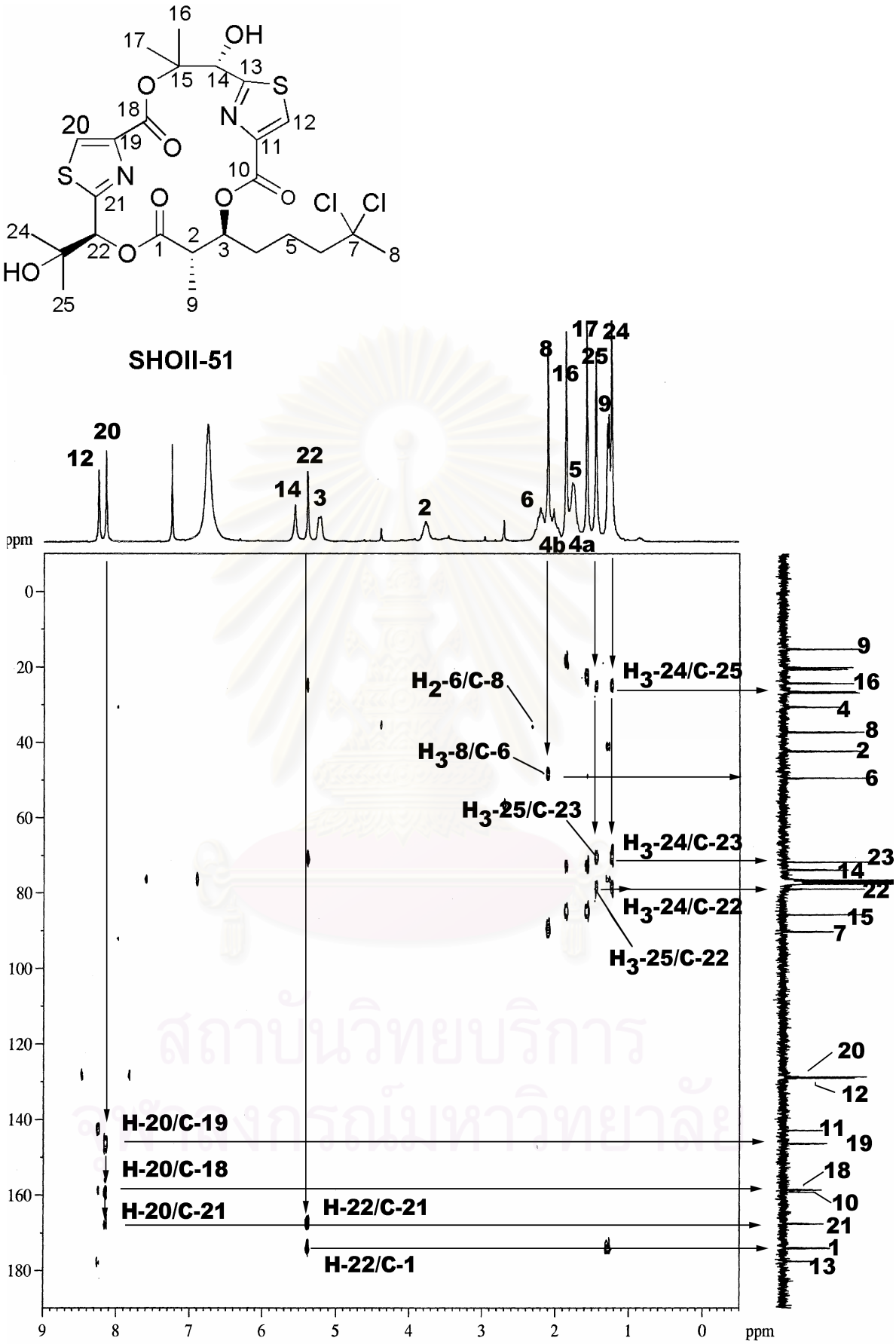

Figure 94. The 300 MHz HMBC spectrum ($^{n}J_{CH}$ = 4 Hz) of deacetylhectochlorin [**SHOII-51**] in $CDCl_3$.

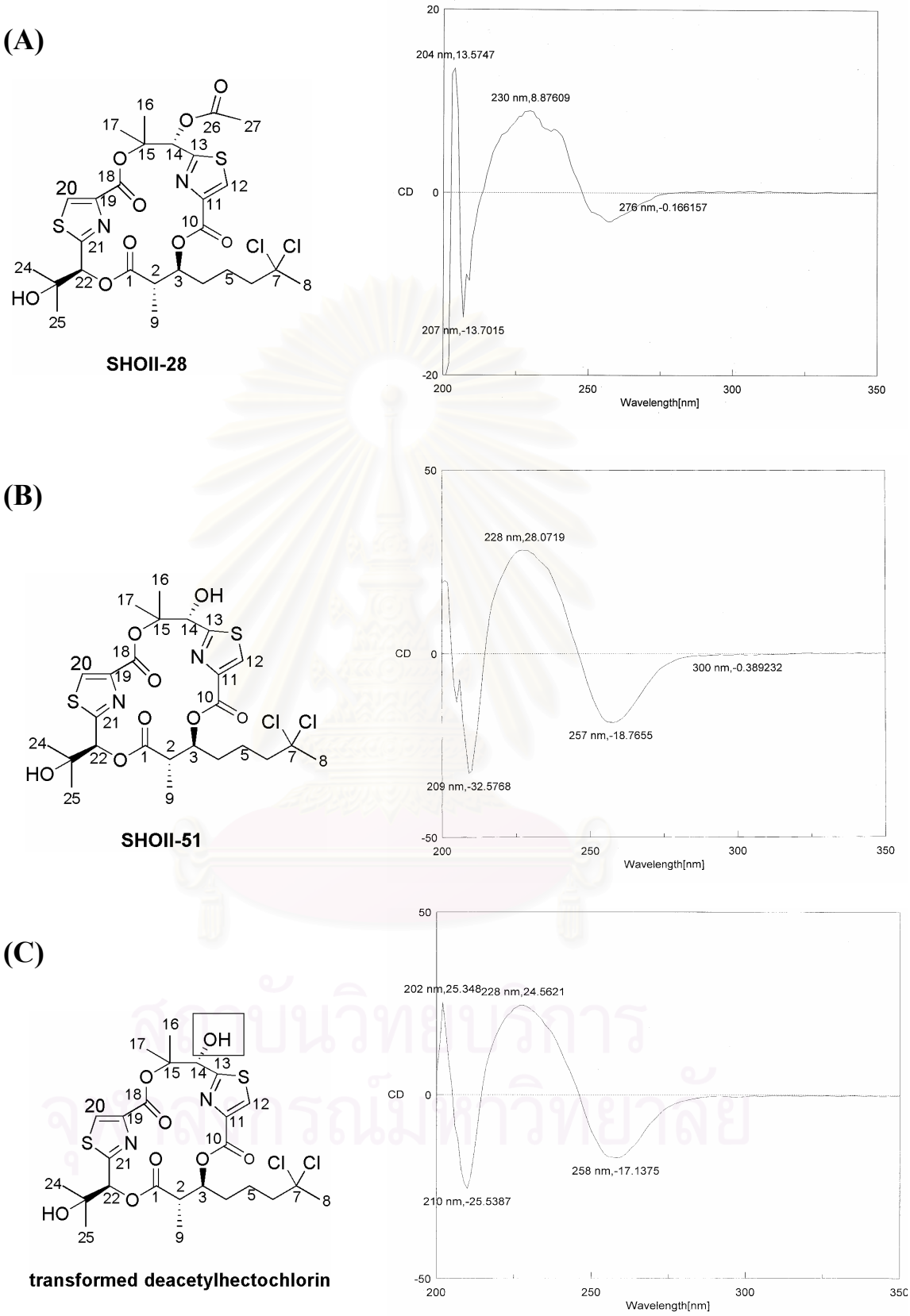

Figure 95. The circular dichroism in MeOH of (A) hectochlorin [**SHOII-28**], (B) natural deacetylhectochlorin [**SHOII-51**] and [C] transformed deacetylhectochlorin obtained by deacetylation of hectochlorin.

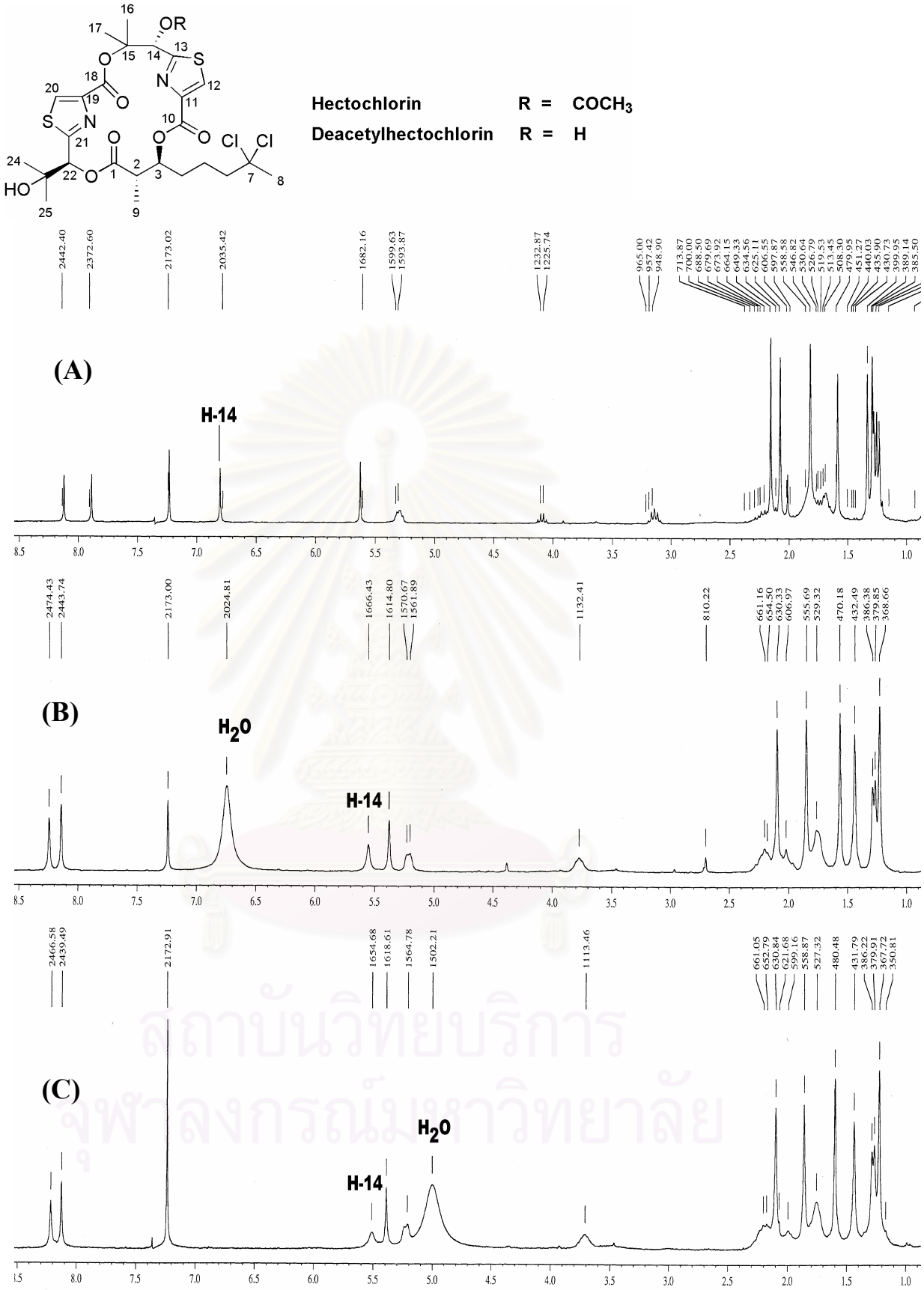

Figure 96. The 300 MHz ^{1}H NMR spectrum in $CDCl_3$ of (A) hectochlorin [**SHOII-28**], (B) natural deacetylhectochlorin [**SHOII-51**], and (C) transformed deacetylhectochlorin obtained by deacetylation of hectochlorin.

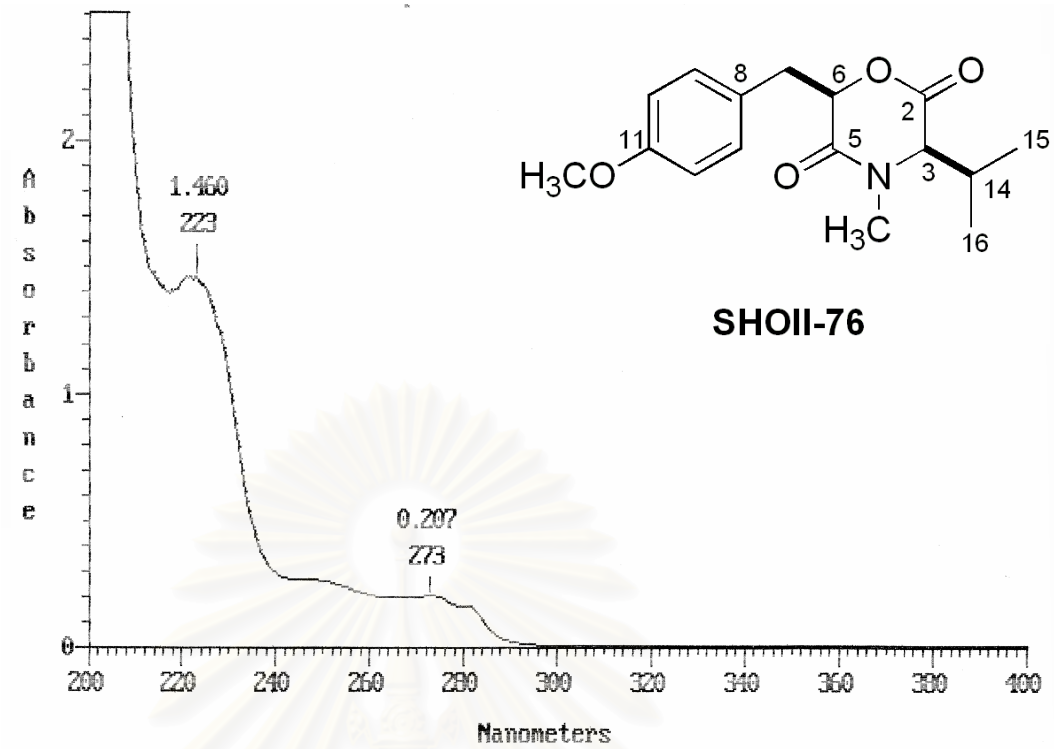

Figure 97. The UV spectrum of *syn*-3-isopropyl-6-(4-methoxy-benzyl)-4-methyl-morpholine-2,5-dione [**SHOII-76**] in MeOH.

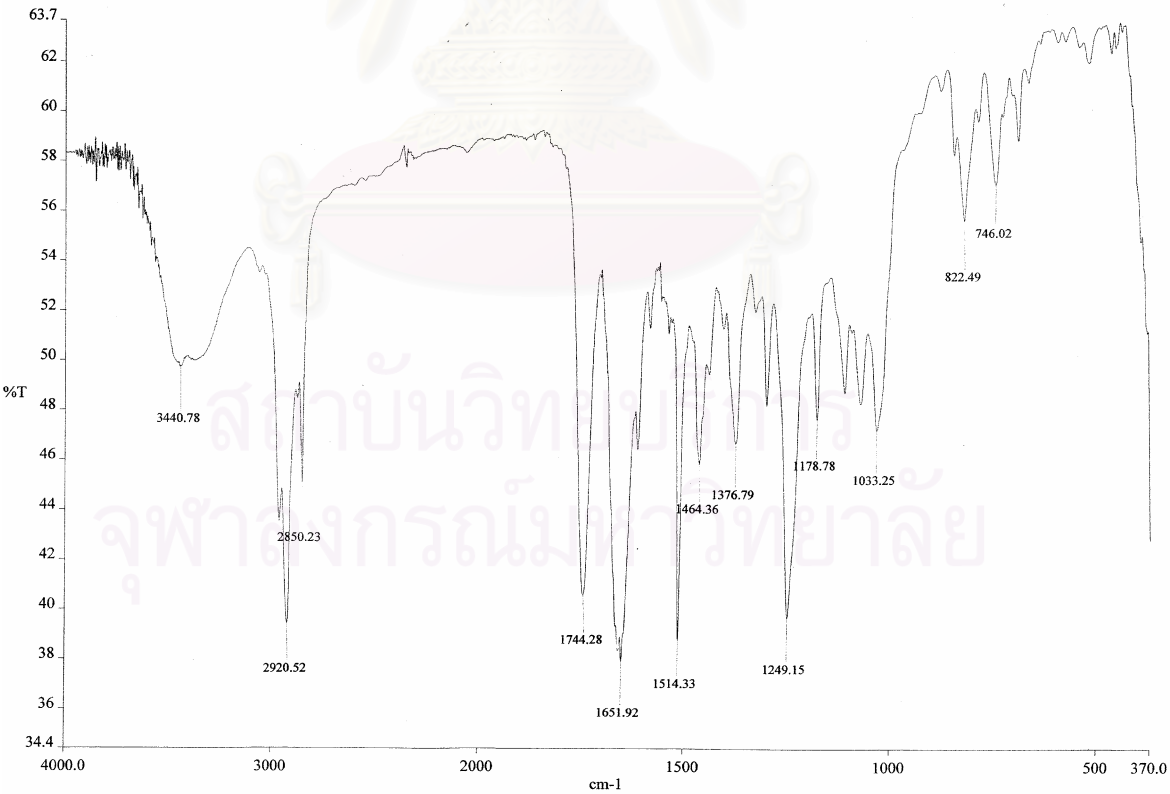

Figure 98. The IR spectrum (Film) of *syn*-3-isopropyl-6-(4-methoxy-benzyl)-4-methyl-morpholine-2,5-dione [**SHOII-76**].

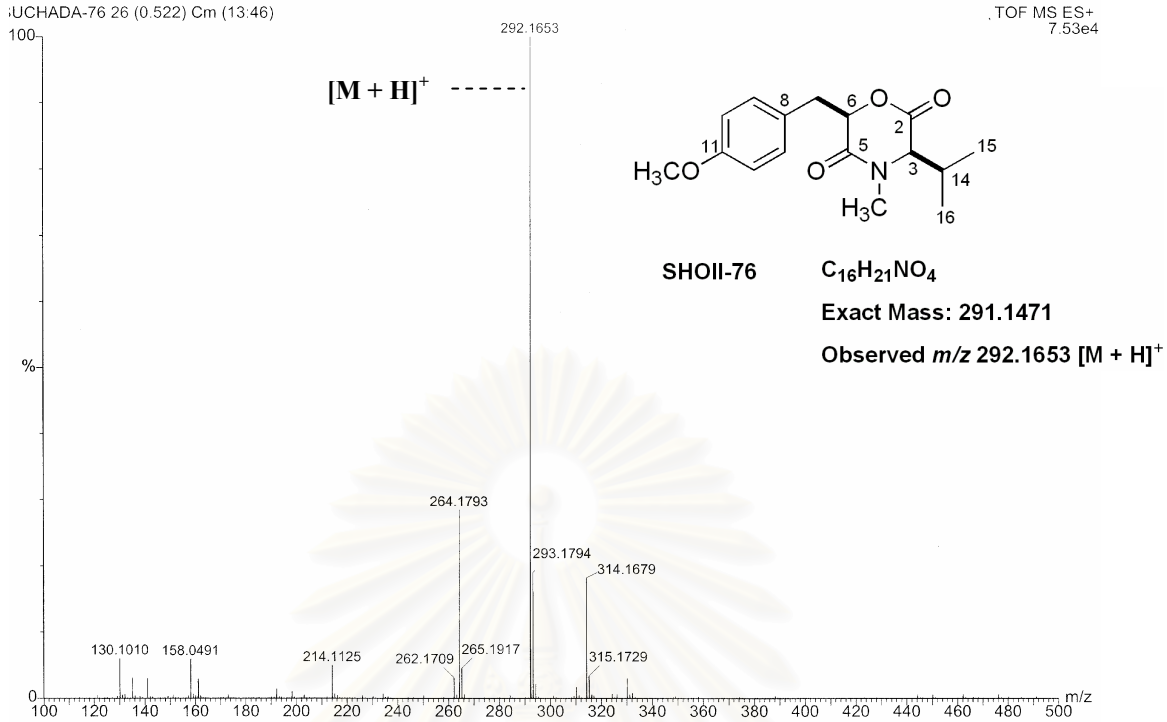

Figure 99. The ESITOF MS mass spectrum of *syn*-3-isopropyl-6-(4-methoxy-benzyl)-4-methyl-morpholine-2,5-dione [**SHOII-76**].

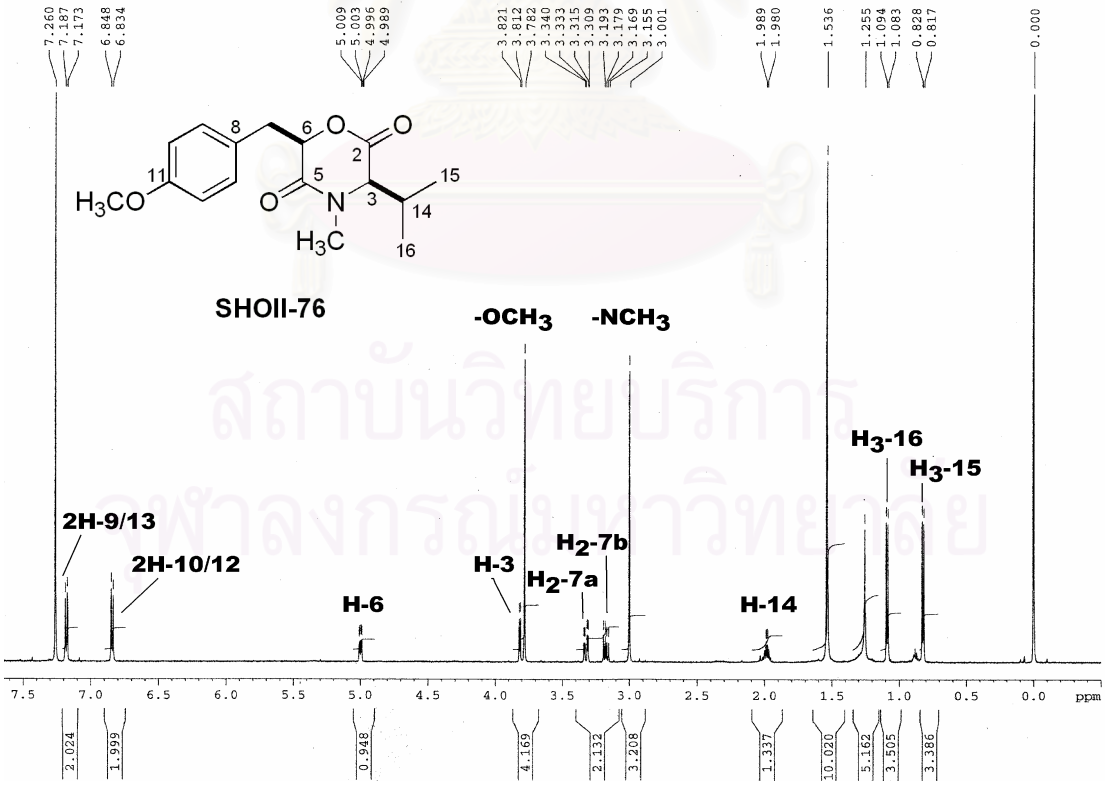

Figure 100. The 600 MHz 1H NMR spectrum of *syn*-3-isopropyl-6-(4-methoxy-benzyl)-4-methyl-morpholine-2,5-dione [**SHOII-76**] in $CDCl_3$.

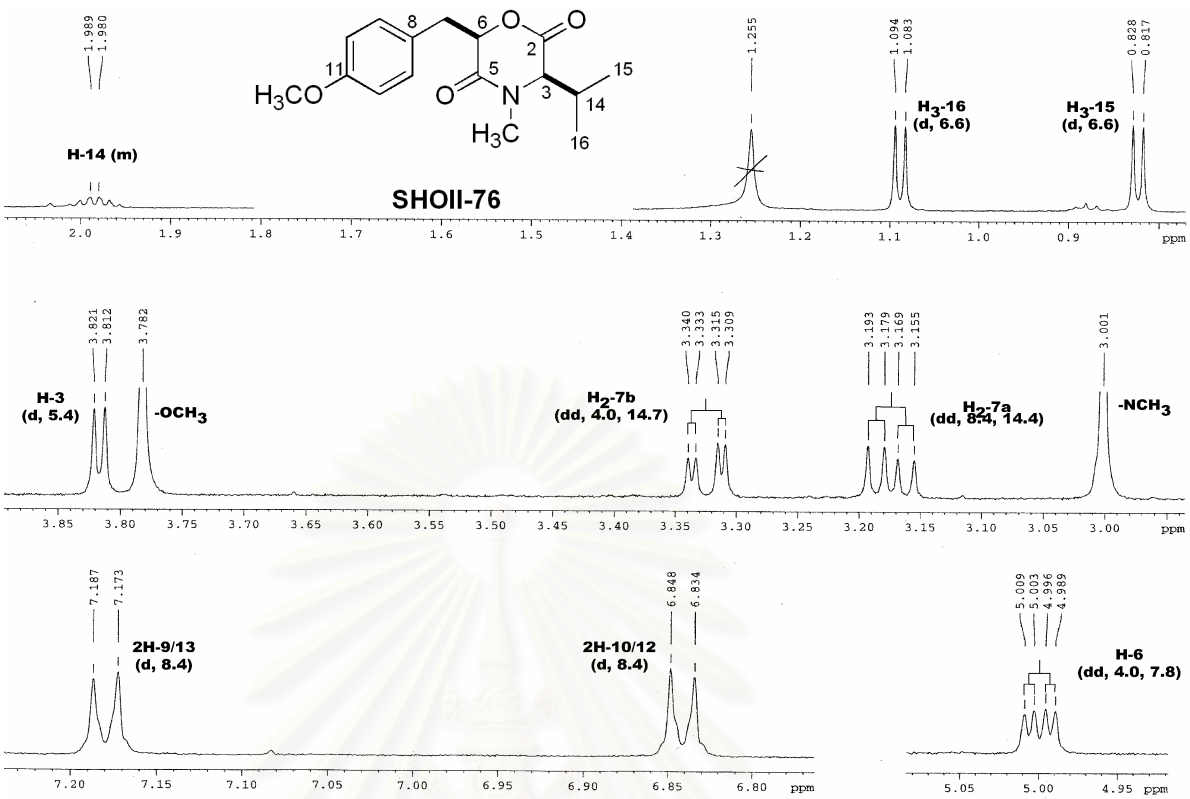

Figure 101. The 600 MHz ^{1}H coupling patterns of *syn*-3-isopropyl-6-(4-methoxy-benzyl)-4-methyl-morpholine-2,5-dione [**SHOII-76**] in $CDCl_3$.

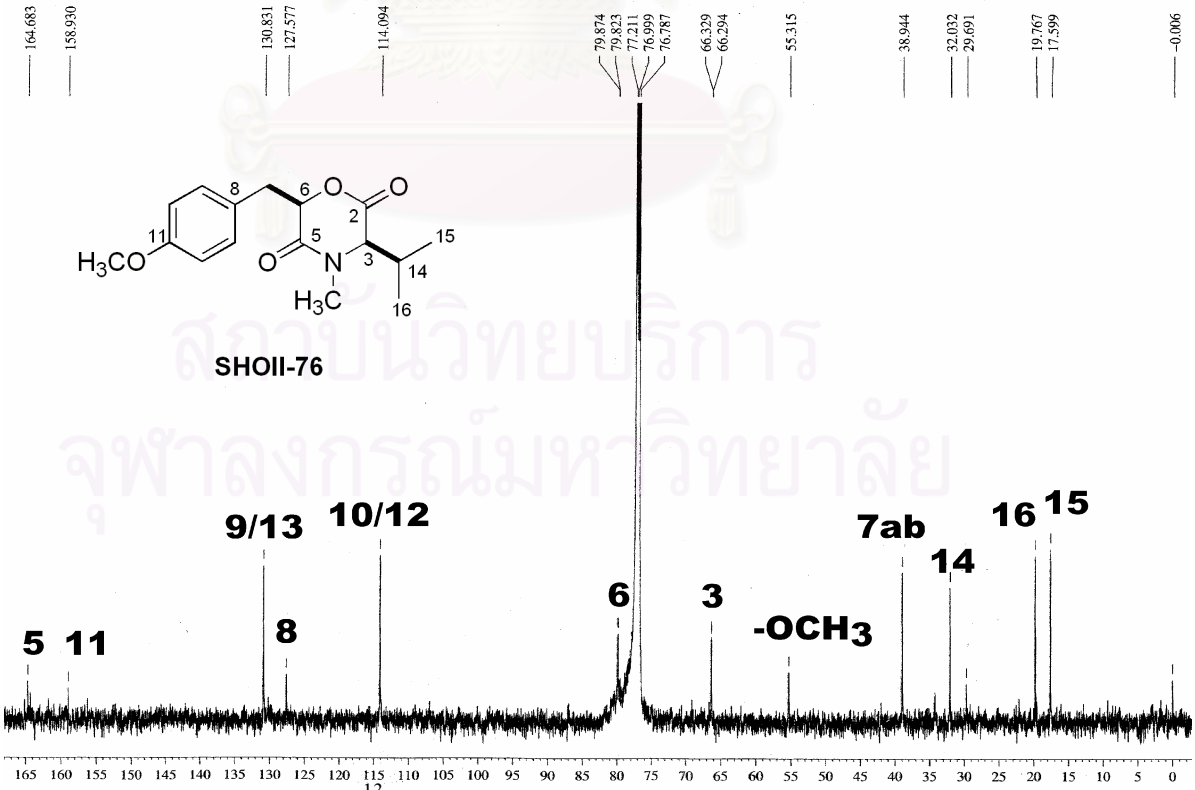

Figure 102. The 150 MHz ^{13}C NMR spectrum of *syn*-3-isopropyl-6-(4-methoxy-benzyl)-4-methyl-morpholine-2,5-dione [**SHOII-76**] in $CDCl_3$.

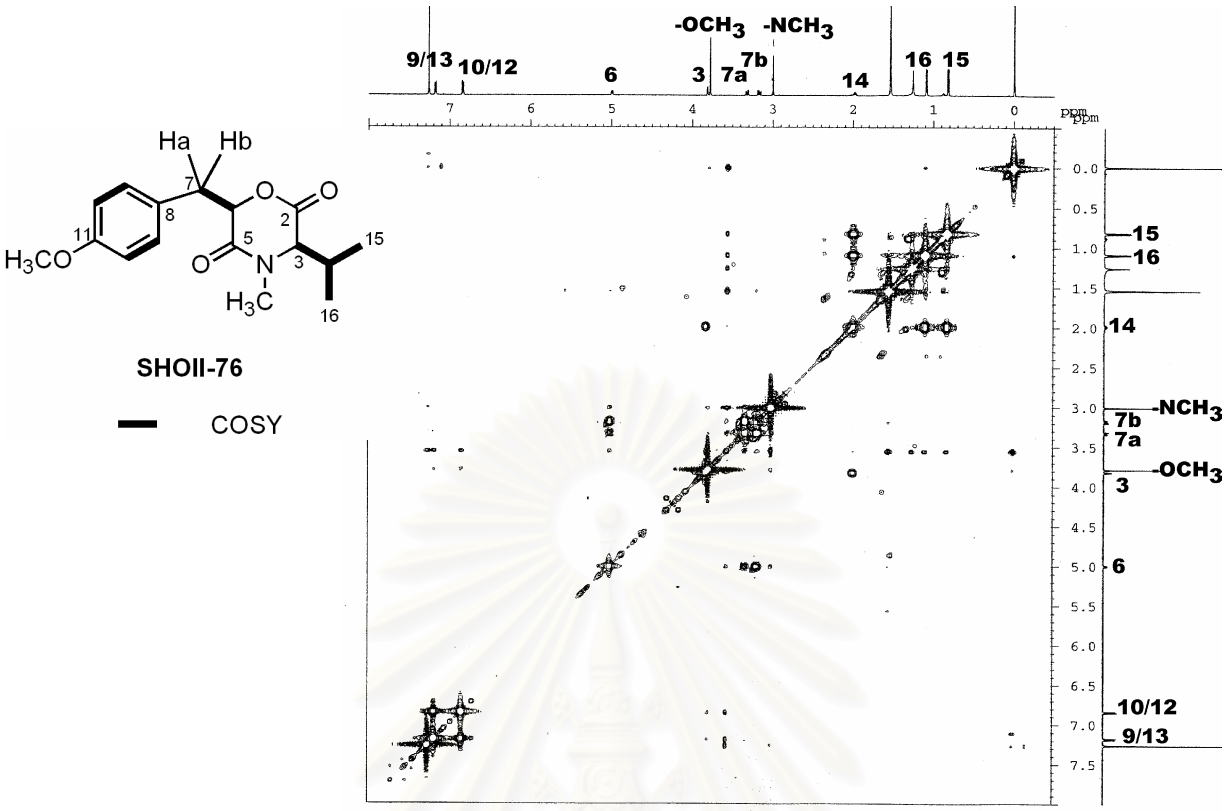

Figure 103. The 600 MHz H,H COSY spectrum of *syn*-3-isopropyl-6-(4-methoxy-benzyl)-4-methyl-morpholine-2,5-dione [**SHOII-76**] in $CDCl_3$.

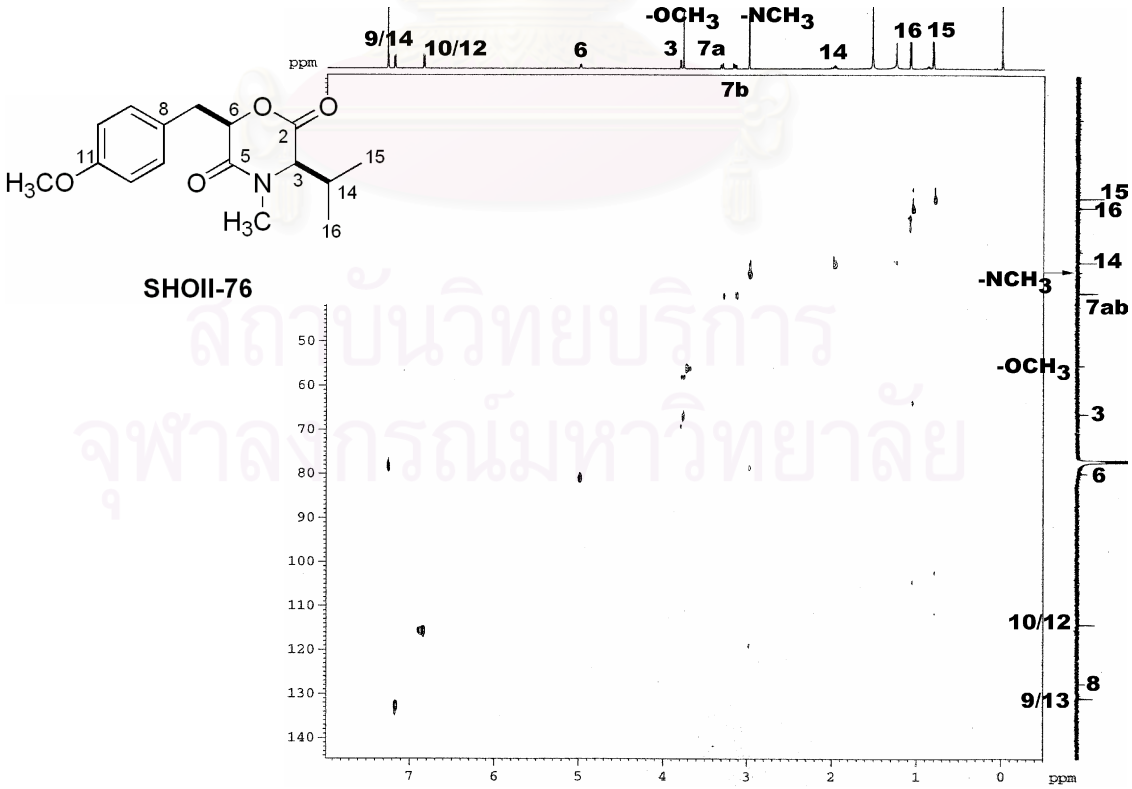

Figure 104. The 600 MHz HMQC spectrum of *syn*-3-isopropyl-6-(4-methoxy-benzyl)-4-methyl-morpholine-2,5-dione [**SHOII-76**] in $CDCl_3$.

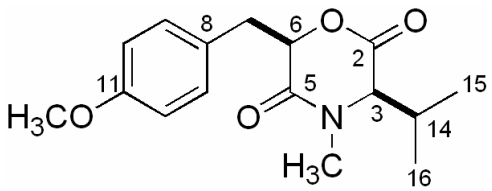

SHOII-76

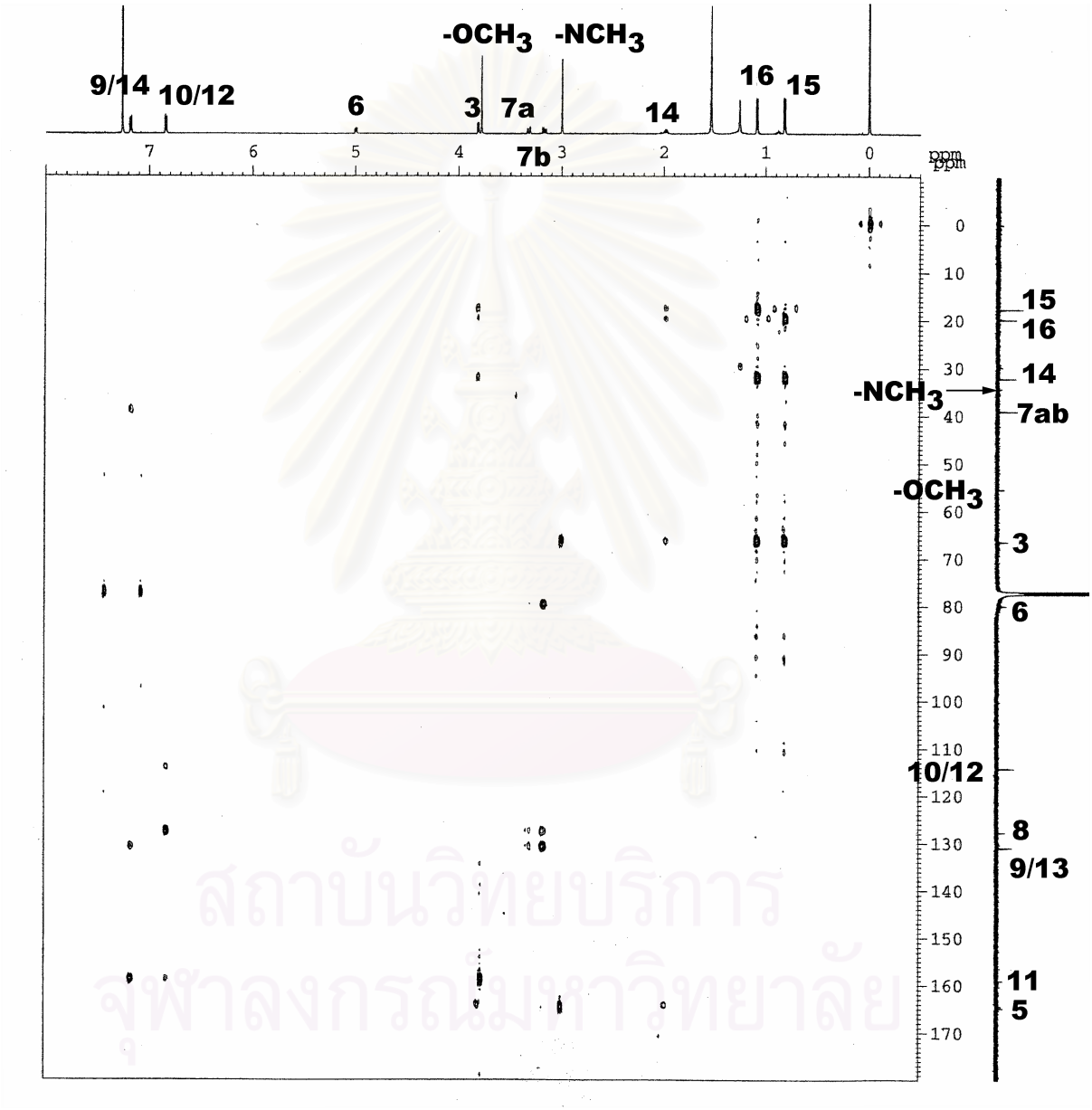

Figure 105. The 600 MHz HMBC spectrum ($^{n}J_{CH}$ = 8 Hz) of *syn*-3-isopropyl-6-(4-methoxy-benzyl)-4-methyl-morpholine-2,5-dione [**SHOII-76**] in $CDCl_3$.

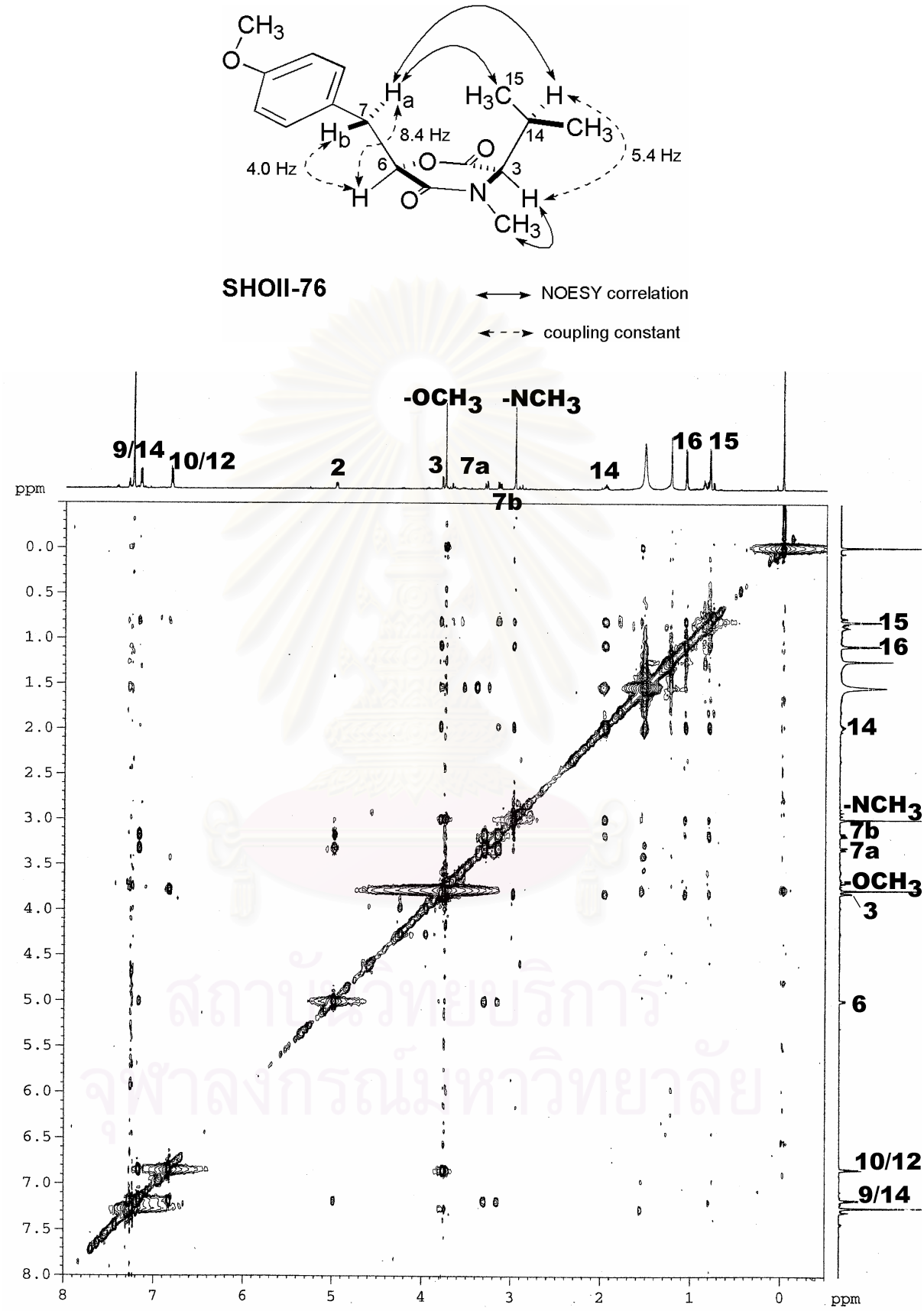

Figure 106. The 600 MHz NOESY spectrum of *syn*-3-isopropyl-6-(4-methoxy-benzyl)-4-methyl-morpholine-2,5-dione [**SHOII-76**] in $CDCl_3$.

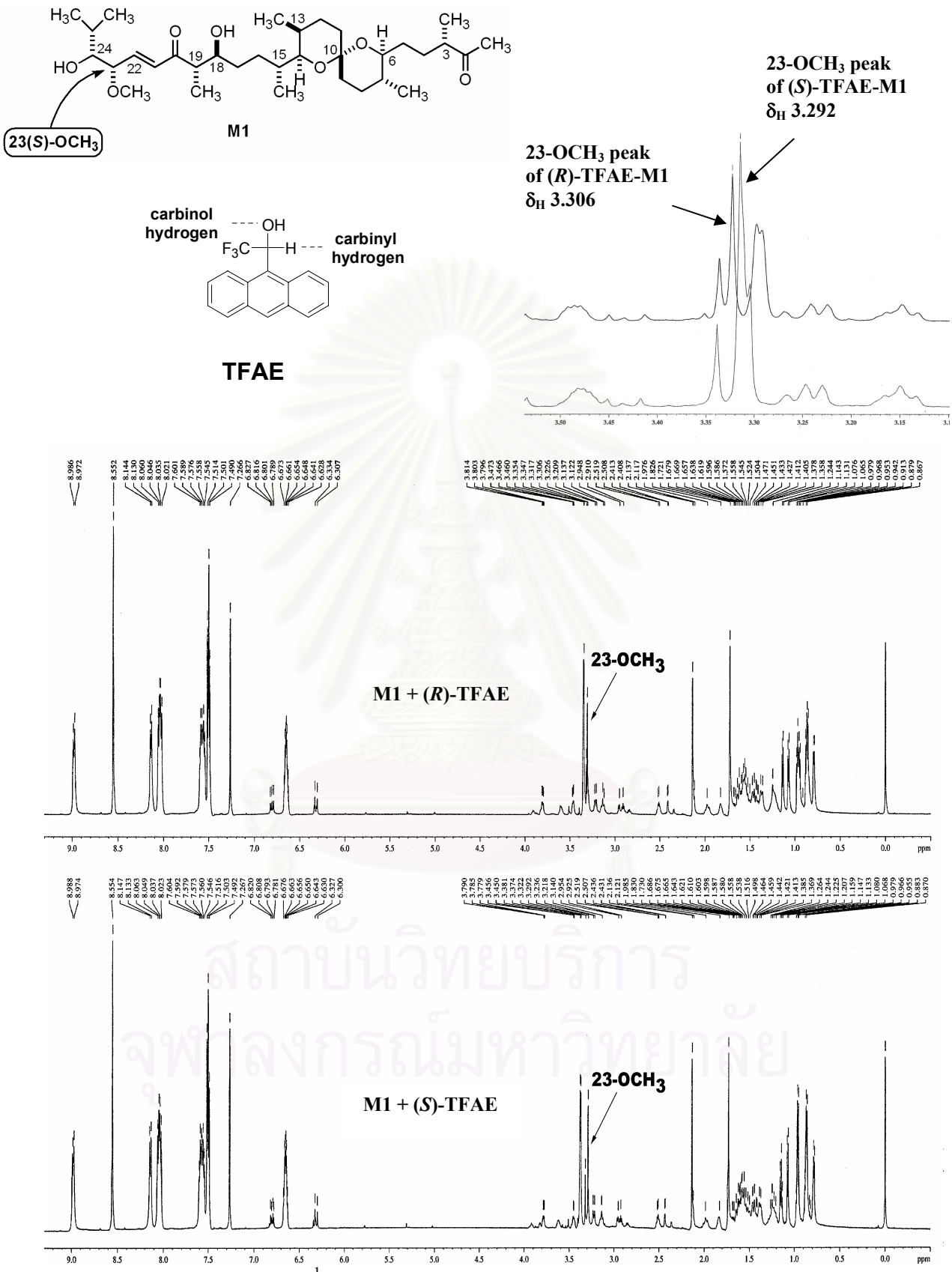

Figure 107. The 600 MHz ^{1}H NMR spectrum of alkaline degradation product of tautomycin **M1** in the presence of (*R*)-TFAE (upper) and (*S*)-TFAE (lower) in $CDCl_3$ at 274 °K.

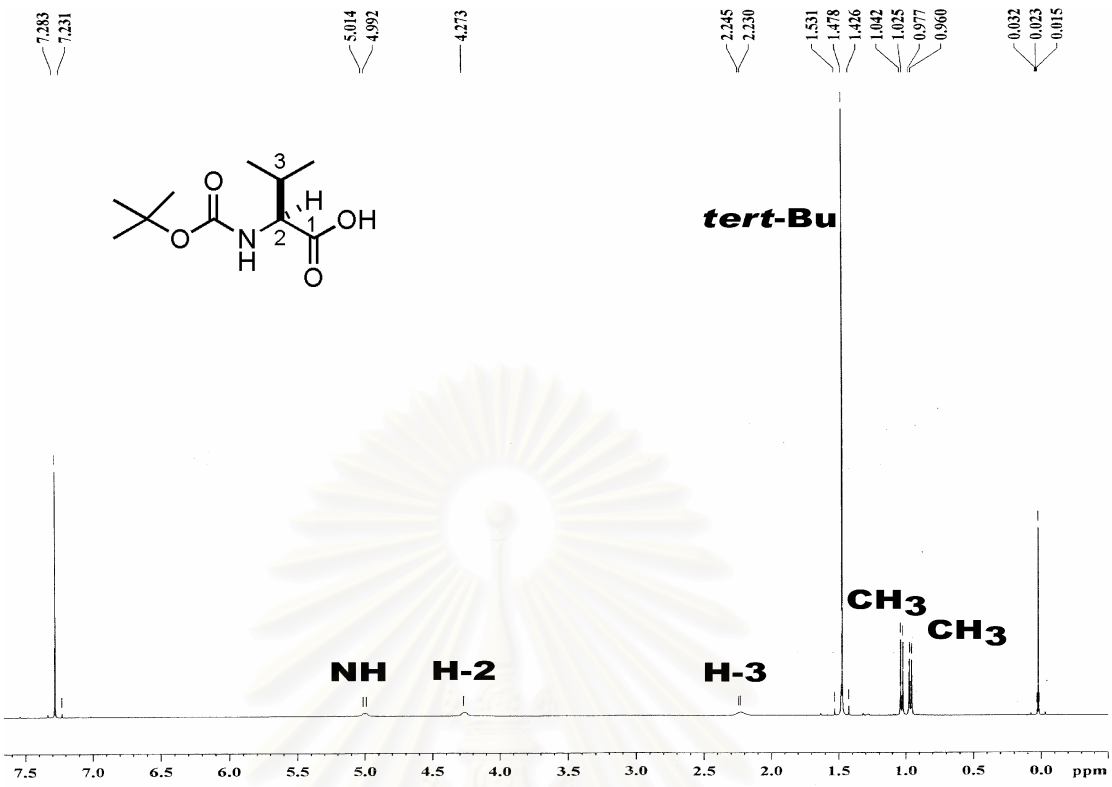

Figure 108. The 400 MHz NMR spectrum of *N*-Boc-L-valine in $CDCl_3$.

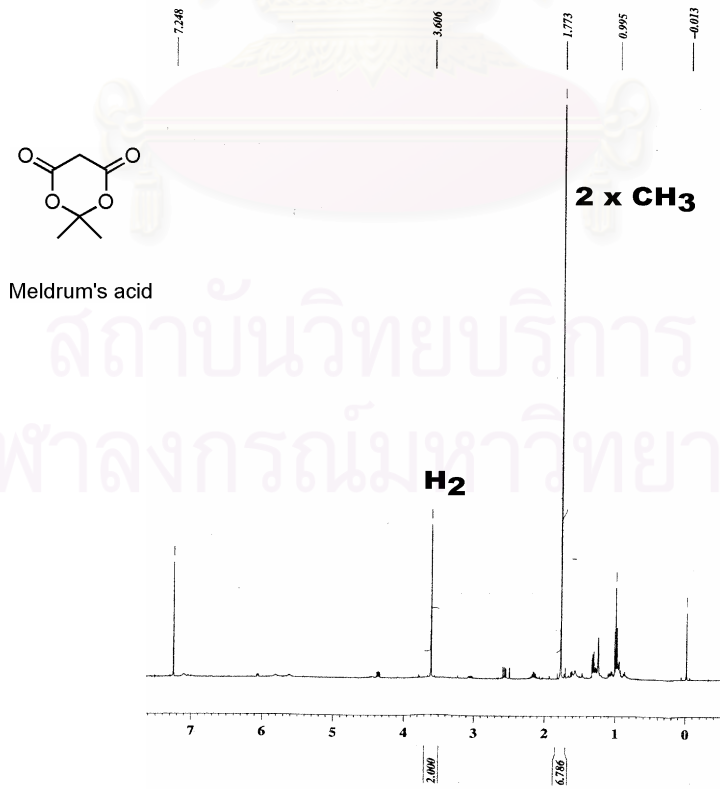

Figure 109. The 400 MHz ^1H NMR spectrum of Meldrum's acid in $CDCl_3$.

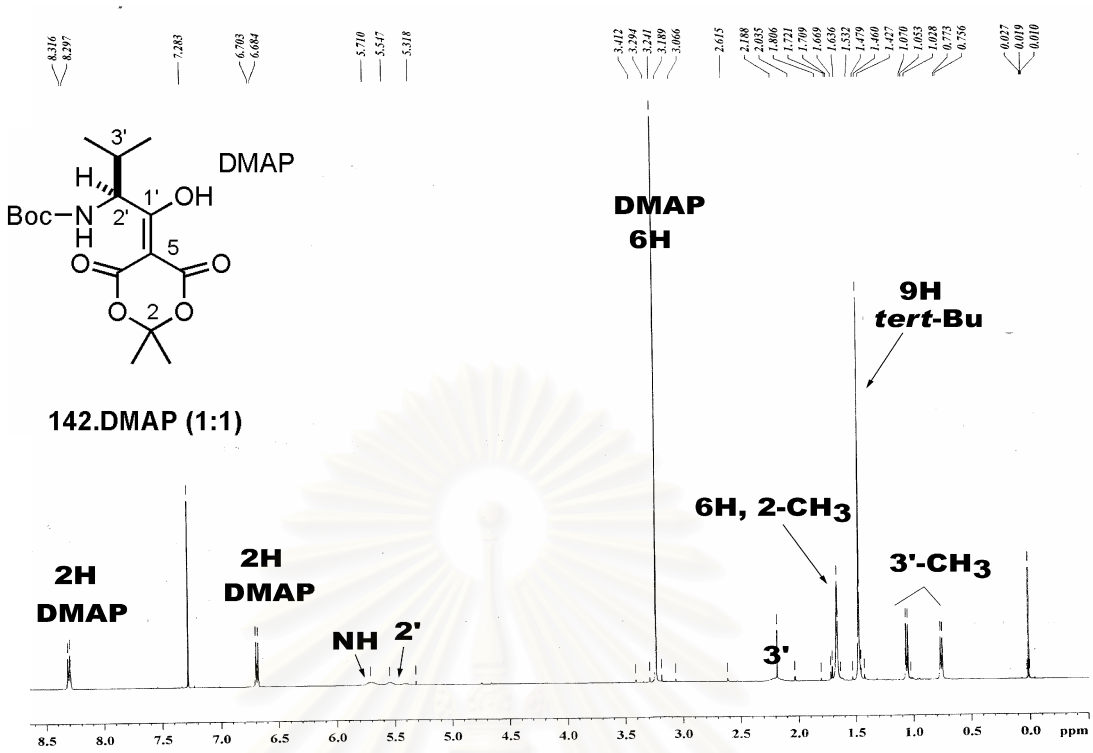

Figure 110. The 400 MHz ^{1}H NMR spectrum of crude product of Meldrum acid's derivative **142** in $CDCl_3$.

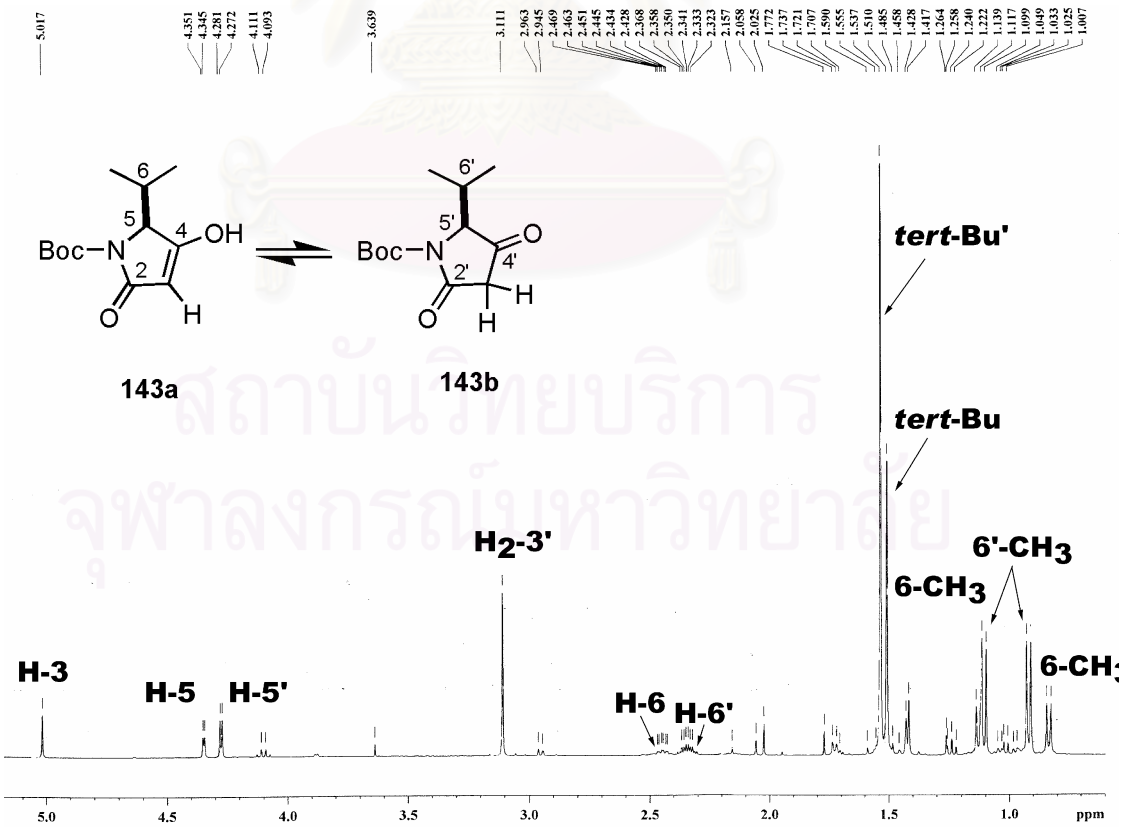

Figure 111. The 400 MHz NMR spectrum of crude product of *N*-Boc-5(*S*)-isopropyl-4-hydroxy-Δ^3-pyrrolin-2-one [**143**] in $CDCl_3$.

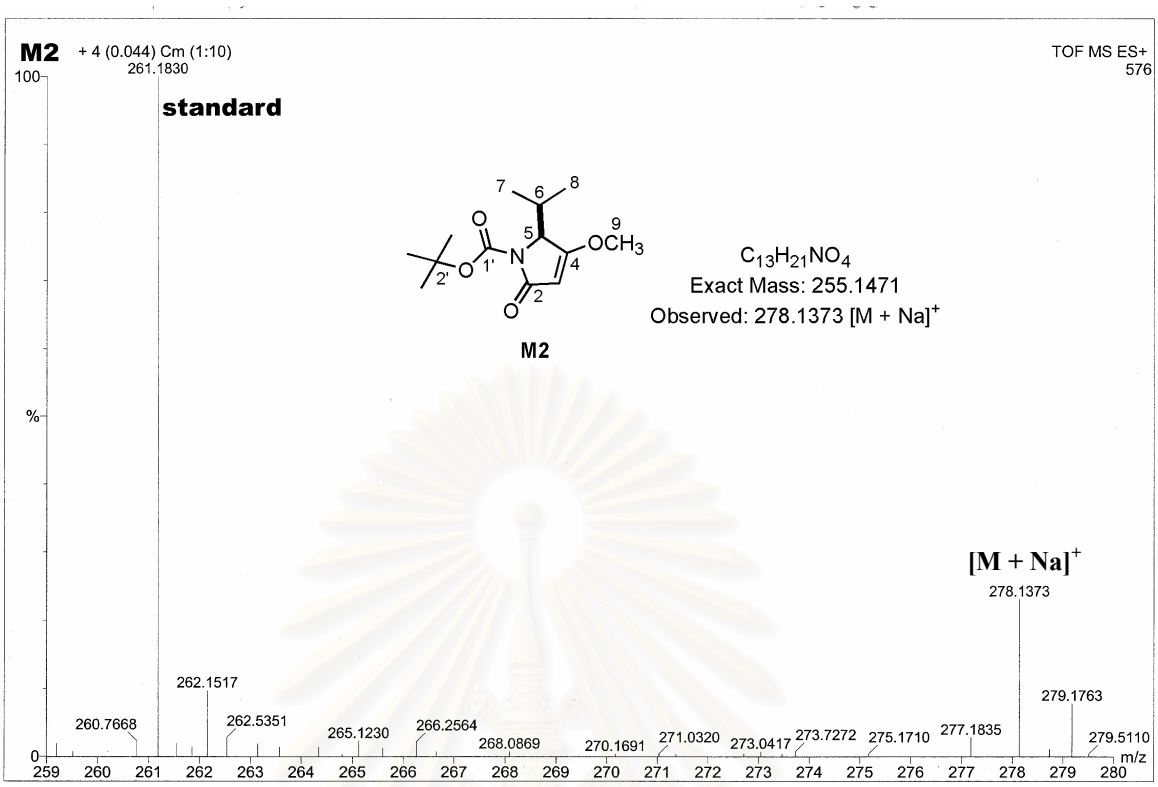

Figure 112. The ESITOF MS spectrum of *N*-Boc-5(*S*)-isopropyl-4-methoxy-Δ^3-pyrrolin-2-one [**M2**] in $CDCl_3$.

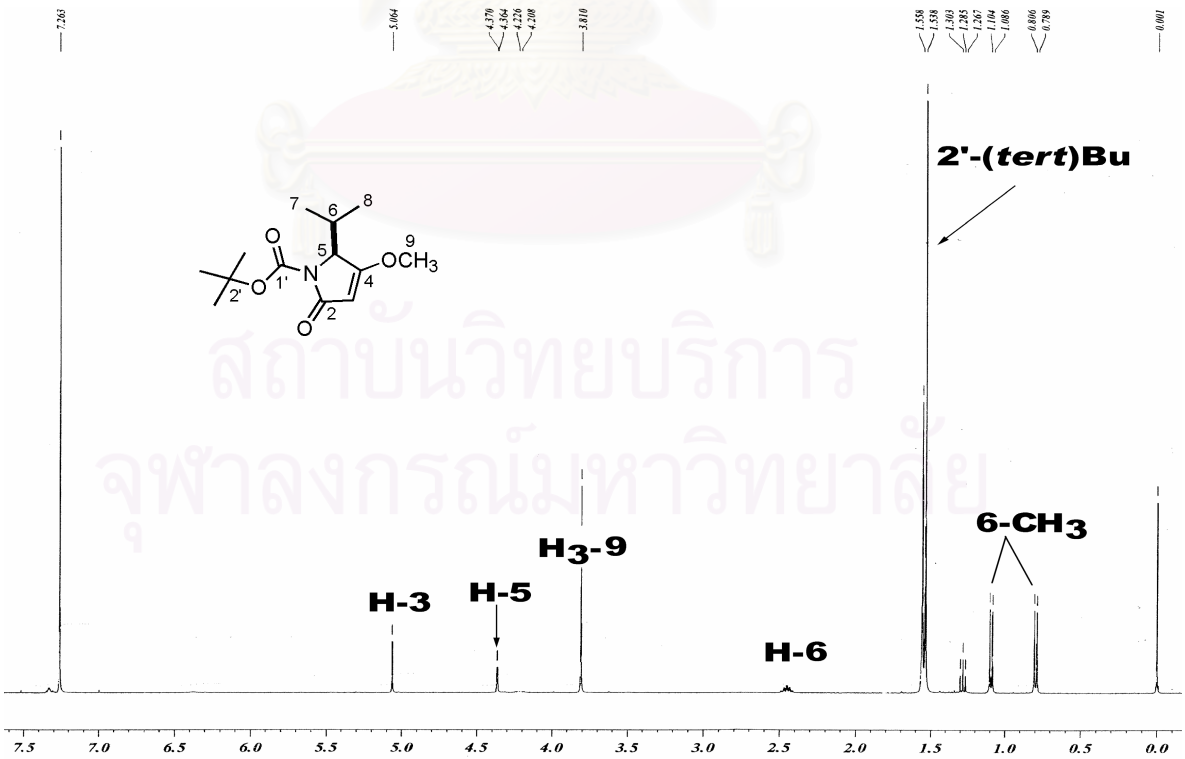

Figure 113. The 400 MHz ^{1}H NMR spectrum of *N*-Boc-5(*S*)-isopropyl-4-methoxy-Δ^3-pyrrolin-2-one [**M2**] in $CDCl_3$.

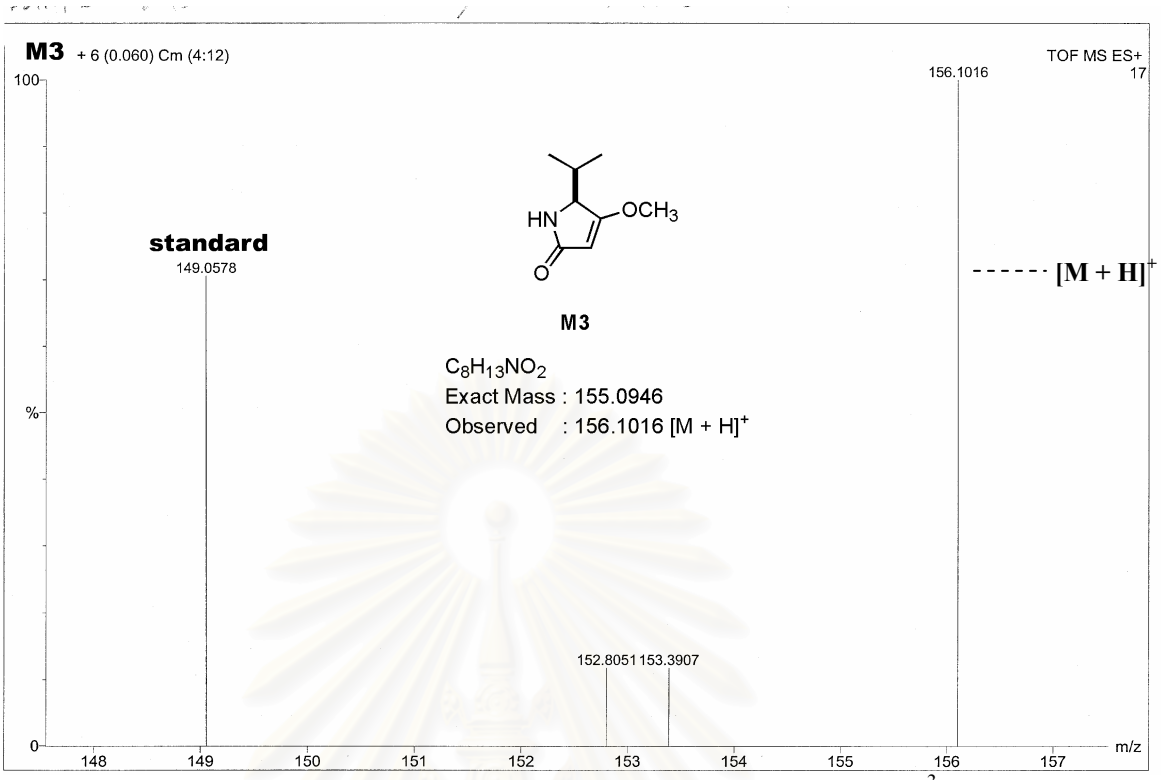

Figure 114. The ESITOF MS spectrum of 5(*S*)-isopropyl-4-methoxy-Δ^3-pyrrolin-2-one [**M3**] in $CDCl_3$.

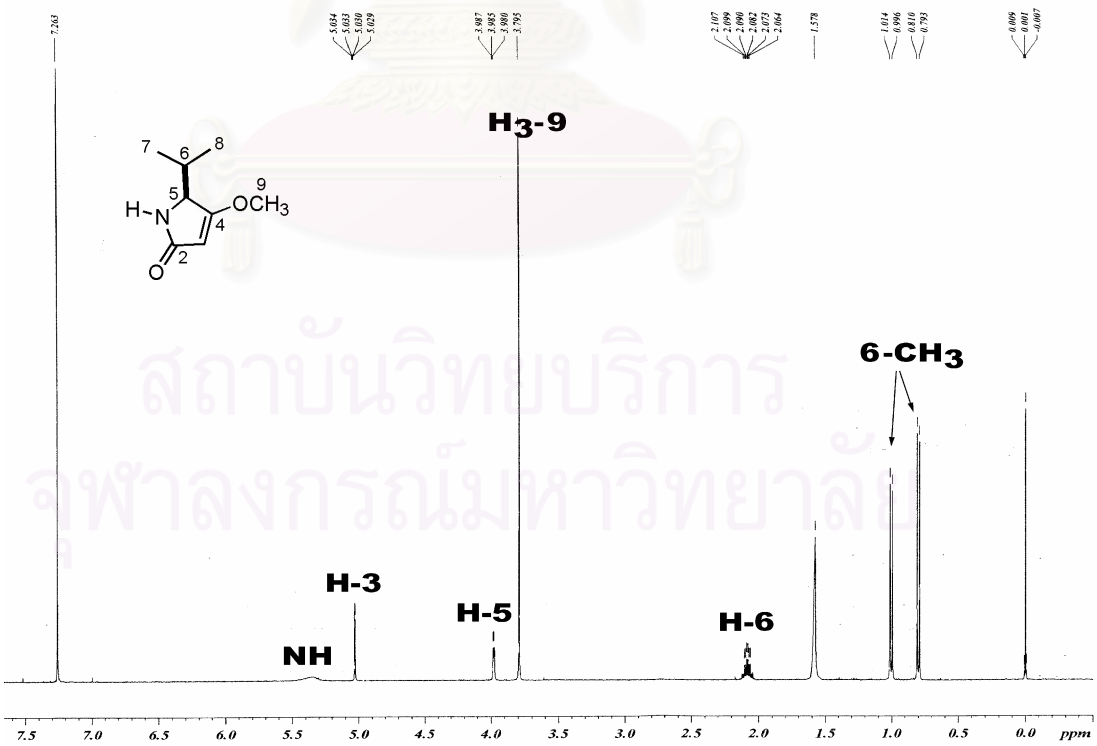

Figure 115. The 400 MHz ^{1}H NMR spectrum of 5(*S*)-isopropyl-4-methoxy-Δ^3-pyrrolin-2-one [**M3**] in $CDCl_3$.

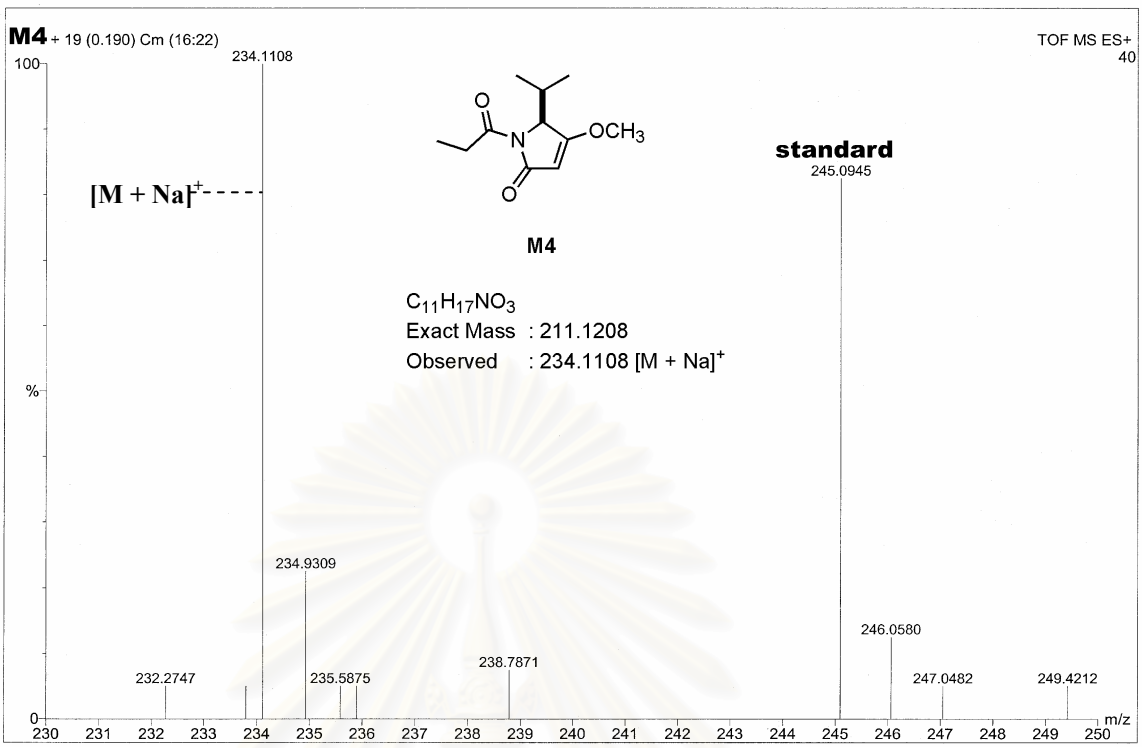

Figure 116. The ESITOF MS spectrum of 5(*S*)-isopropyl-4-methoxy-1-propionyl-Δ^3-pyrrolin-2-one [**M4**] in $CDCl_3$.

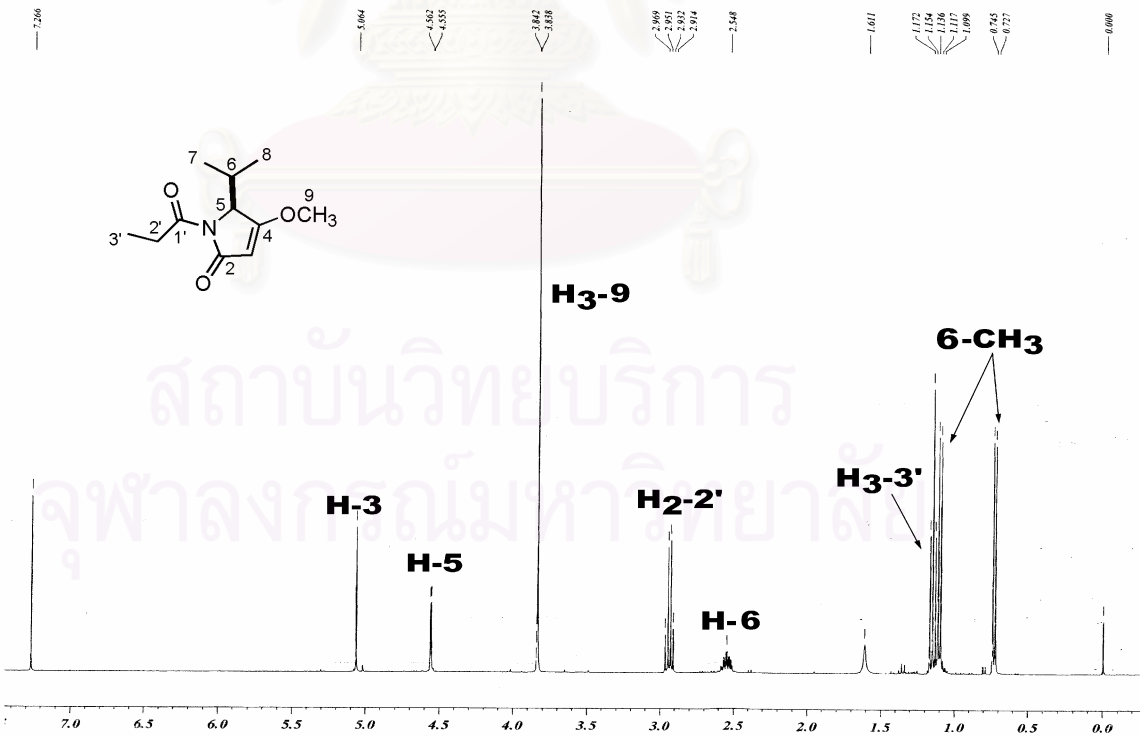

Figure 117. The 400 MHz ^{1}H NMR spectrum of 5(*S*)-isopropyl-4-methoxy-1-propionyl-Δ^3-pyrrolin-2-one [**M4**] in $CDCl_3$.

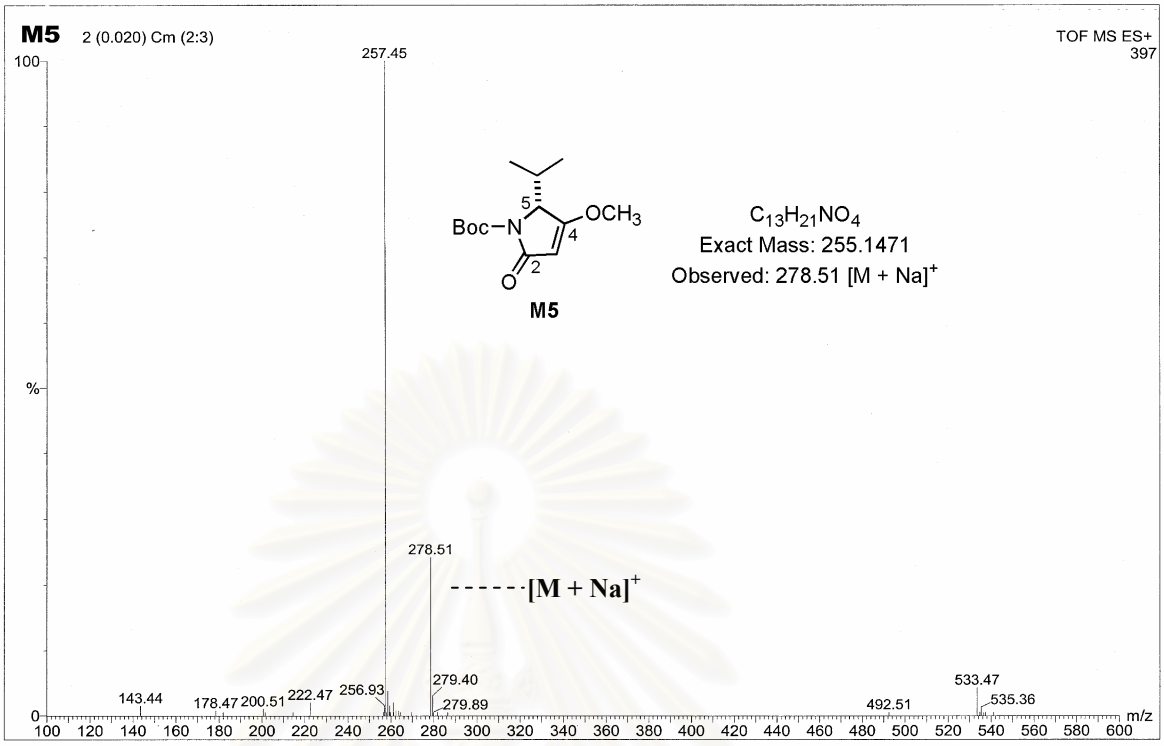

Figure 118. The ESITOF MS spectrum of *N*-Boc-5(*R*)-isopropyl-4-methoxy-Δ^3-pyrrolin-2-one [**M5**] in $CDCl_3$.

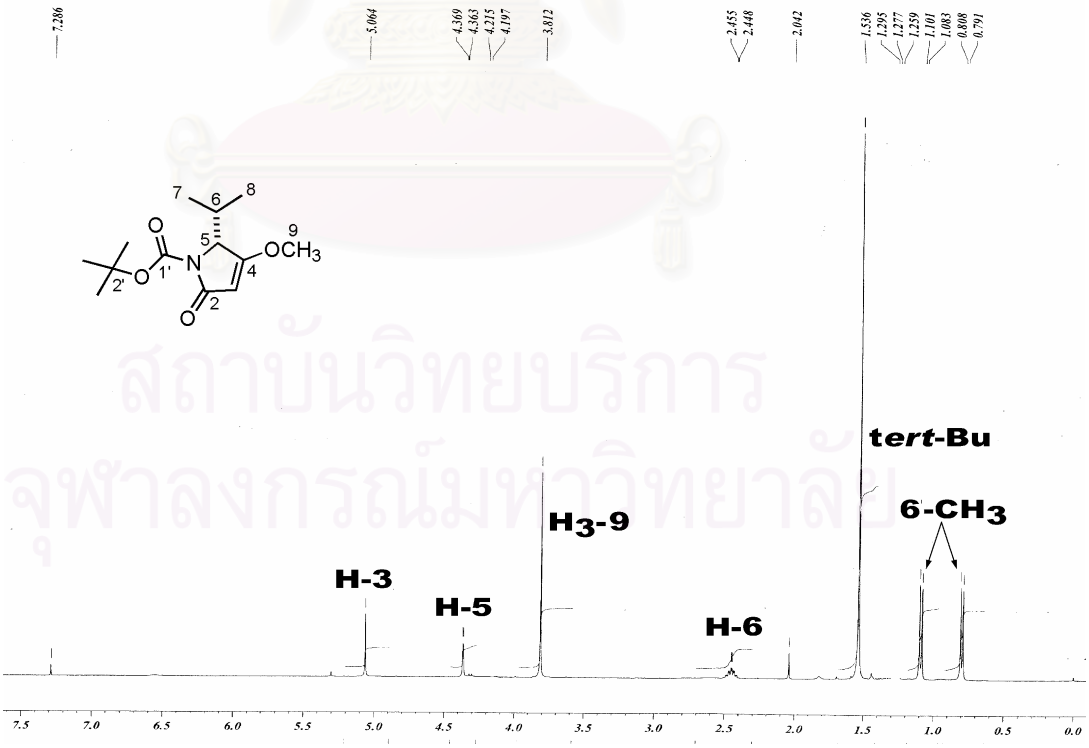

Figure 119. The 400 MHz ^{1}H NMR spectrum of *N*-Boc-5(*R*)-isopropyl-4-methoxy-Δ^3-pyrrolin-2-one [**M5**] in $CDCl_3$.

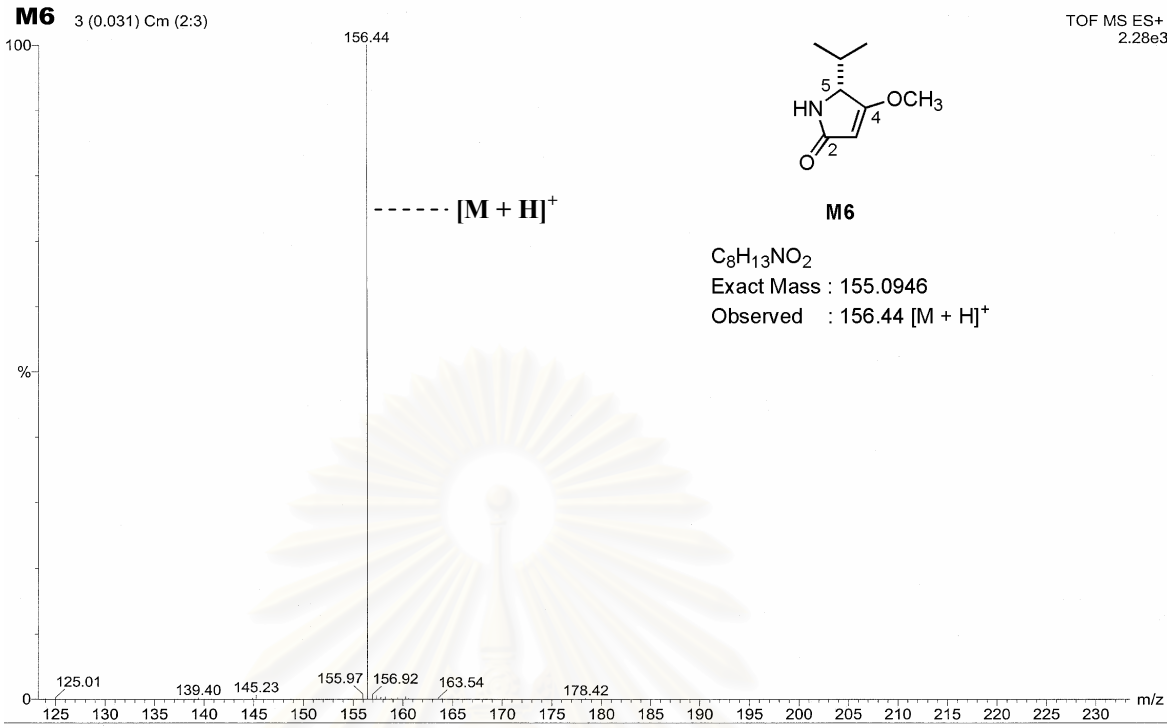

Figure 120. The ESITOF MS spectrum of 5(*R*)-isopropyl-4-methoxy-Δ^3-pyrrolin-2-one [**M6**] in $CDCl_3$.

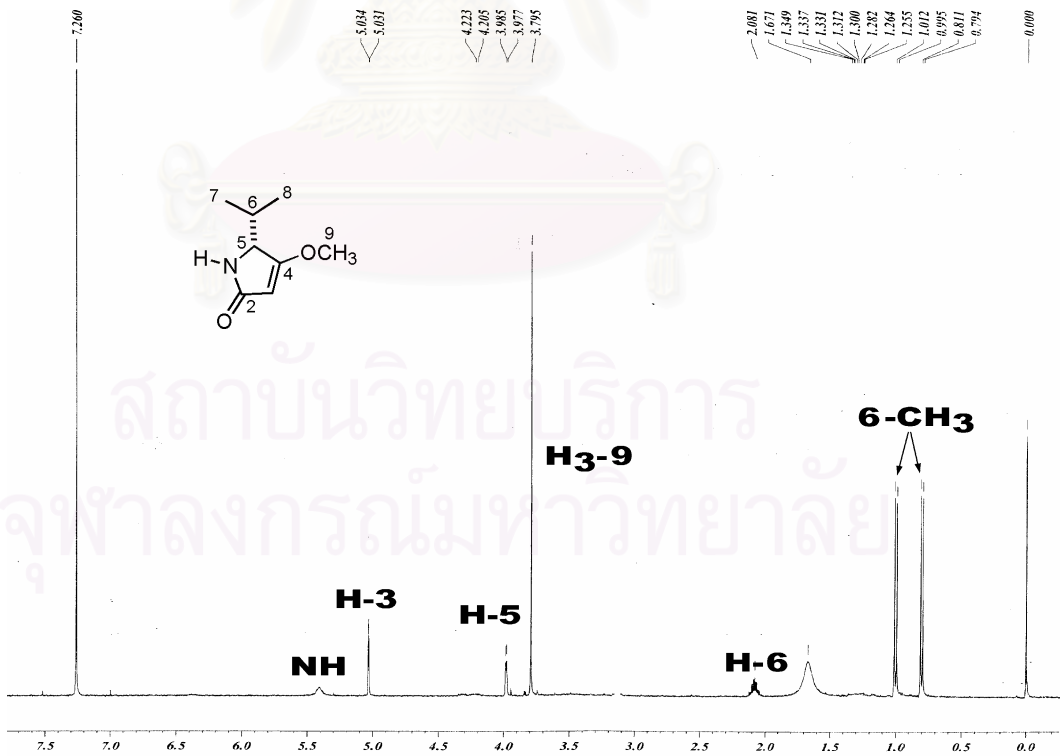

Figure 121. The 400 MHz ^{1}H NMR spectrum of 5(*R*)-isopropyl-4-methoxy-Δ^3-pyrrolin-2-one [**M6**] in $CDCl_3$.

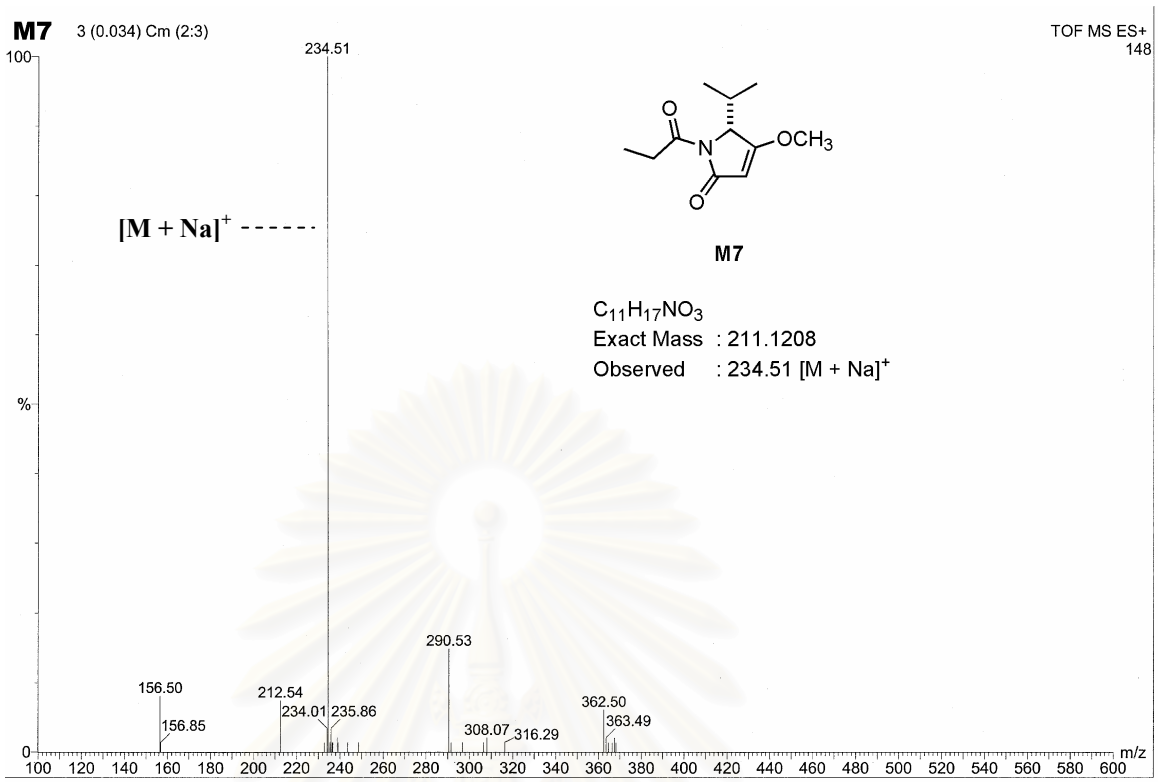

Figure 122. The ESITOF MS spectrum of 5(*R*)-isopropyl-4-methoxy-1-propionyl-Δ^3-pyrrolin-2-one [**M7**] in $CDCl_3$.

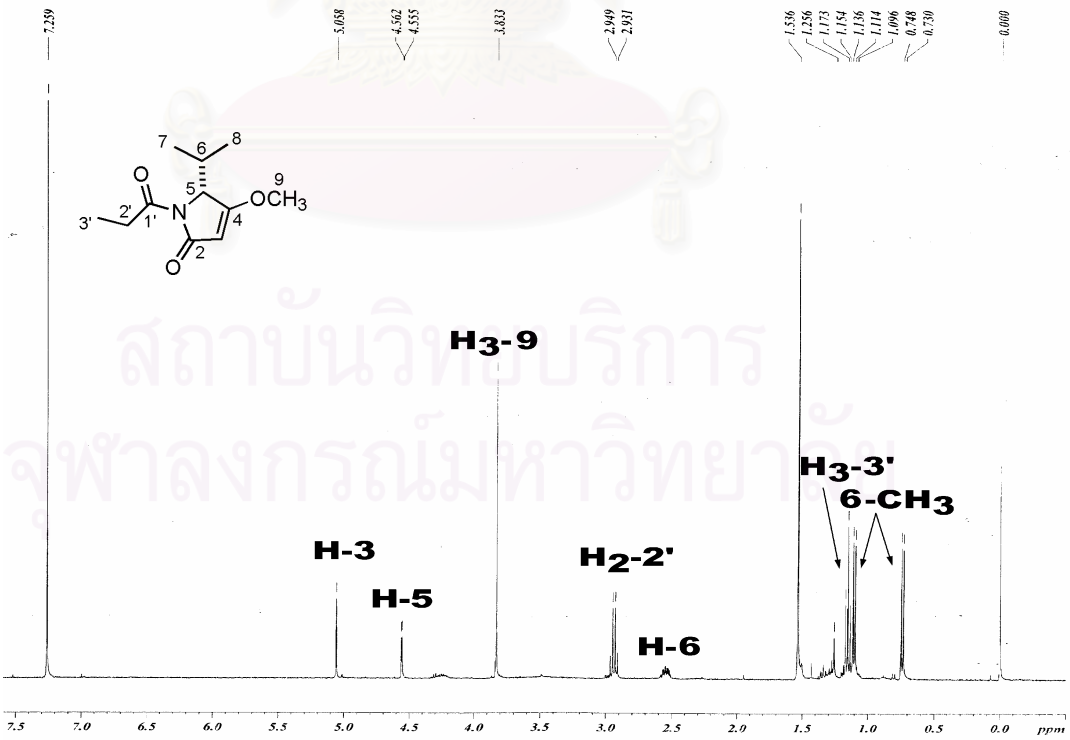

Figure 123. The 400 MHz ^{1}H NMR spectrum of 5(*R*)-isopropyl-4-methoxy-1-propionyl-Δ^3-pyrrolin-2-one [**M7**] in $CDCl_3$.

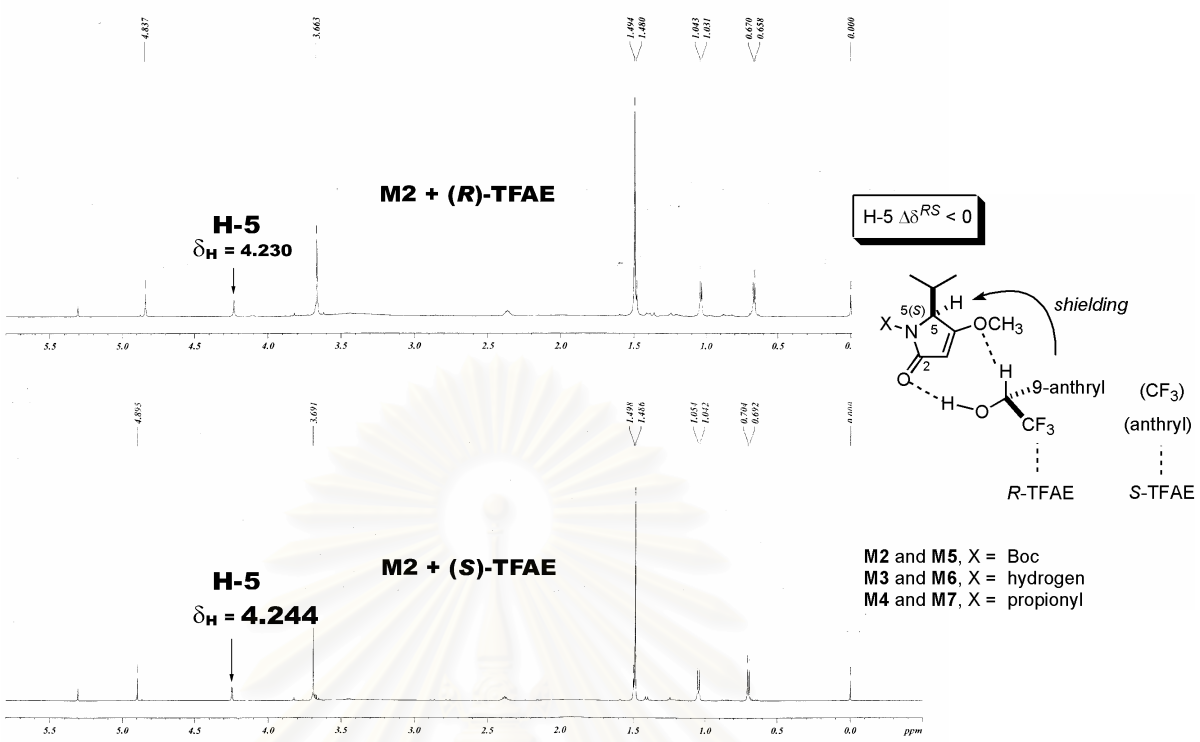

Figure 124. The 600 MHz ^{1}H NMR spectra of *N*-Boc-5(*S*)-isopropyl-4-methoxy-Δ^3-pyrrolin-2-one [**M2**] in the persence of 10 equiv. (*R*)-TFAE (upper) and (*S*)-TFAE (lower) in $CDCl_3$ at 274 °K.

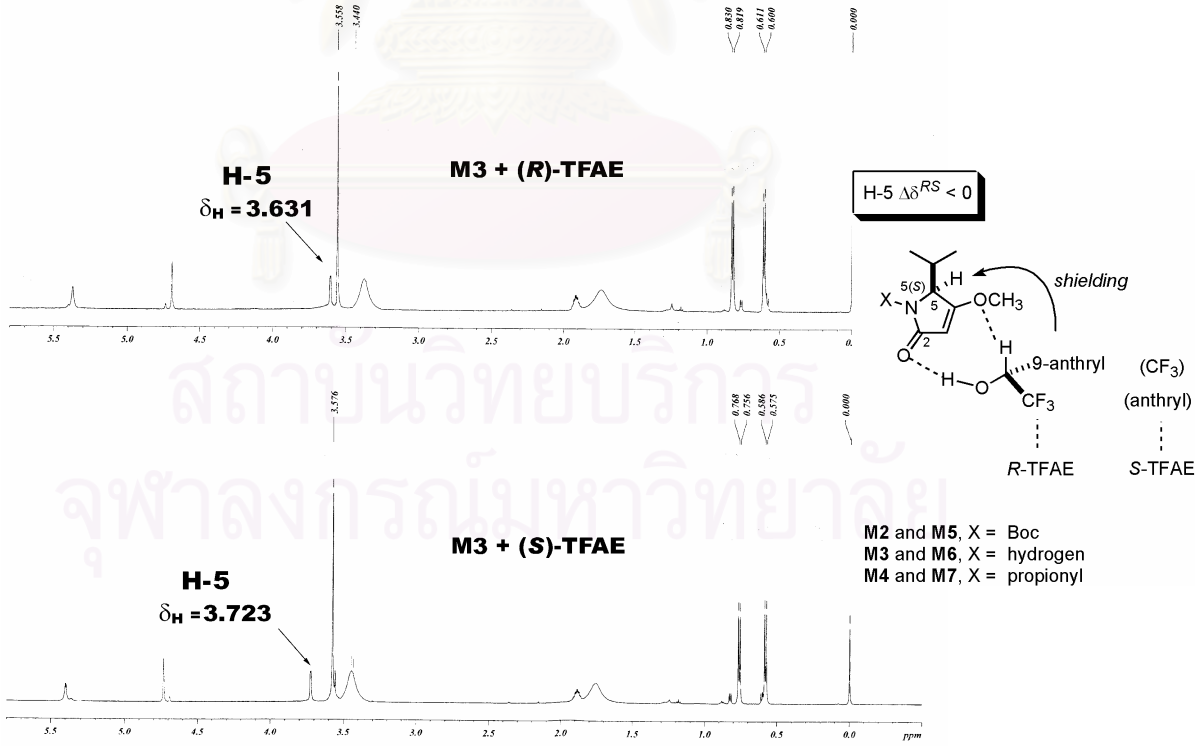

Figure 125. The 600 MHz ^{1}H NMR spectra of *N*-Boc-5(*S*)-isopropyl-4-methoxy-Δ^3-pyrrolin-2-one [**M3**] in the persence of 10 equiv. (*R*)-TFAE (upper) and (*S*)-TFAE (lower) in $CDCl_3$ at 274 °K.

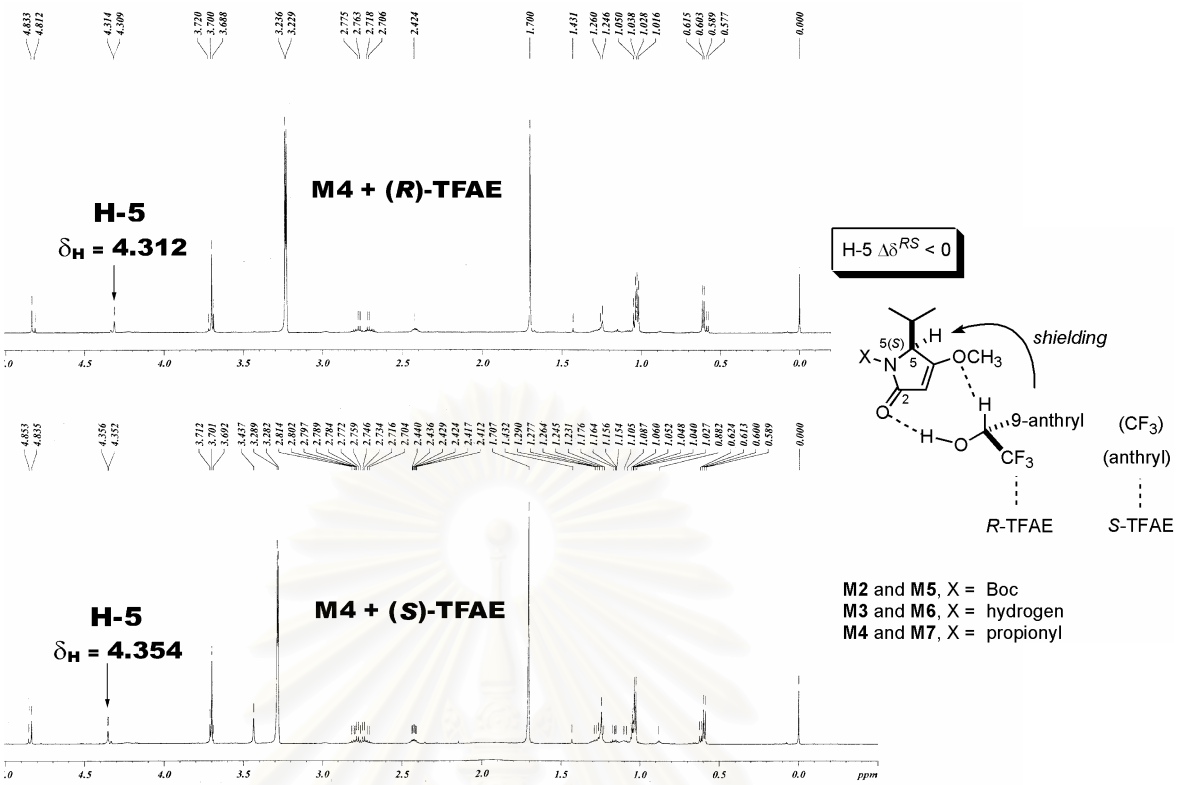

Figure 126. The 600 MHz ^{1}H NMR spectra of 5(*S*)-Isopropyl-4-methoxy-1-propionyl-Δ^3-pyrrolin-2-one [**M4**] in the presence of 10 equiv. (*R*)-TFAE (upper) and (*S*)-TFAE (lower) in $CDCl_3$ at 274 °K.

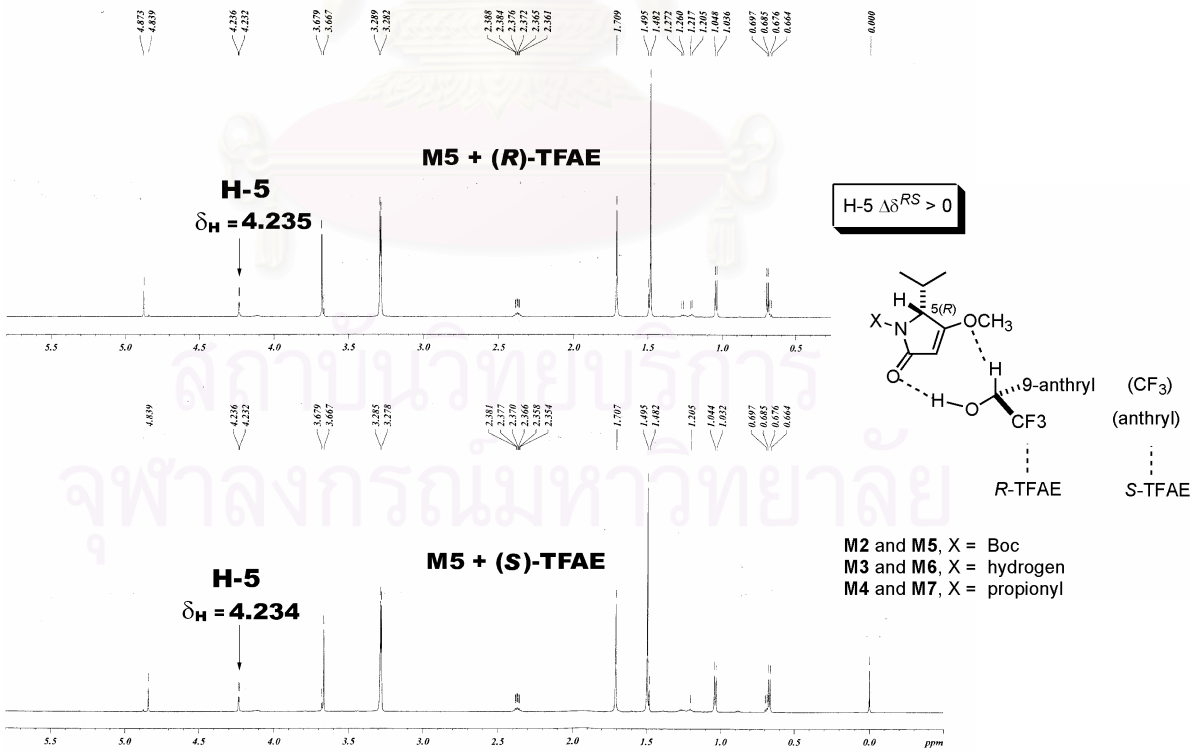

Figure 127. The 600 MHz ^{1}H NMR spectra of *N*-Boc-5(*R*)-isopropyl-4-methoxy-Δ^3-pyrrolin-2-one [**M5**] in the presence of 10 equiv. (*R*)-TFAE (upper) and (*S*)-TFAE (lower) in $CDCl_3$ at 274 °K.

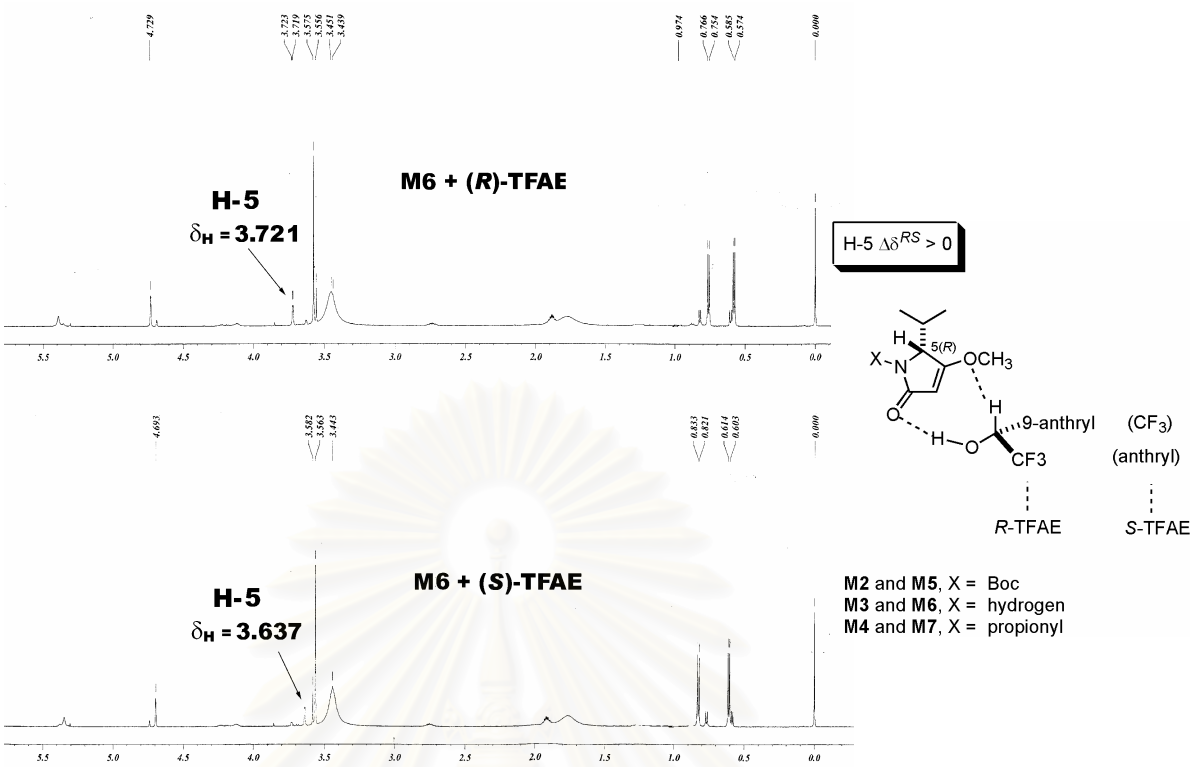

Figure 128. The 600 MHz ^{1}H NMR spectra of 5(*R*)-isopropyl-4-methoxy-Δ^3-pyrrolin-2-one [**M6**] in the presence of 10 equiv. (*R*)-TFAE (upper) and (*S*)-TFAE (lower) in $CDCl_3$ at 274 °K.

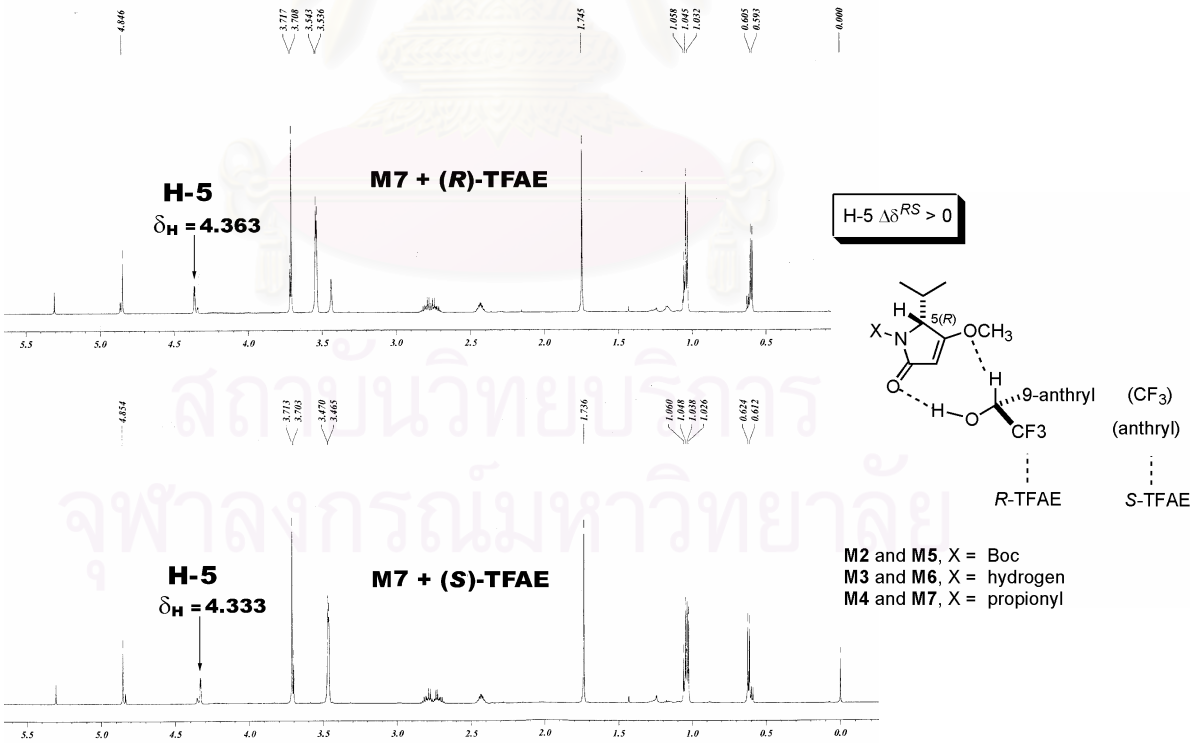

Figure 129. The 600 MHz ^{1}H NMR spectra of 5(*R*)-isopropyl-4-methoxy-1-propionyl-Δ^3-pyrrolin-2-one [**M7**] in the presence of 10 equiv. (*R*)-TFAE (upper) and (*S*)-TFAE (lower) in $CDCl_3$ at 274 °K.

VITA

Miss Suchada Suntornchashwej was born on April 13, 1972 in Samuth Sakorn, Thailand. She received her Bachelor of Science in Pharmacy from the Faculty of Pharmacy, Mahidol University in 1995 and Master of Science in Pharmacy (Pharmacognosy) from the Faculty of Pharmaceutical Sciences, Chulalongkorn University in 2000. She has been granted a 2000 Royal Golden Jubilee Ph.D. Scholarship from the Thailand Research Fund (TRF).

Publications

Suchada Suntornchashwej, Narongsak Chaichit, Minoru Isobe, and Khanit Suwanborirux. 2005. New Hectochlorin and Morpholine Derivatives from the Thai Sea Hare, *Bursatella leachii*. **J. Nat. Prod**. (in pressed)

Suchada Suntornchashwej, Kazushi Koga, Minoru Isobe, and Khanit Suwanborirux. Malyngamide X, the First Tripeptide Malyngamide from the Thai Sea Hare *Bursatella leachii*. (in preparation)

Suchada Suntornchashwej, Khanit Suwanborirux, and Minoru Isobe. Non-degradative determination of an isolated stereogenic center in the new malyngamide X. (in preparation)

Oral Presentation

Suchada Suntornchashwej, Minoru Isobe, and Khanit Suwanborirux. "Stereochemistry determination of malyngamide X from the Thai sea hare, *Bursatell leachii*" RGJ-Ph.D. Congress VI, April 28-30, 2005, Pattaya, Thailand. [Best Presentation Award in Chemistry]

Poster presentations

Suchada Suntornchashwej and Khanit Suwanborirux. "1-hydroxy-1-*nor*-methyl-resistomycin, a new derivative of the resistomycins produced by an estuarine *Streptomyces*" The 19th Annual Research Meeting in Pharmaceutical Sciences. December 4, 2002, Bangkok, Thailand.

Suchada Suntornchashwej and Khanit Suwanborirux. "Hectochlorin, potent cytotoxic metabolites from the Thai sea hare, *Bursatell leachii*" The 21th Annual Research Meeting in Pharmaceutical Sciences. December 23, 2004, Bangkok, Thailand.